Proteins that modulate trinucleotide repeat expansions in human cells

A thesis presented to the National University of Ireland for the degree of Doctor of Philosophy

By

Aisling Frizzell B.Sc.,
Discipline of Biochemistry, School of Natural Sciences, College of Sciences,
National University of Ireland, Galway

Head of School: Dr. Heinz-Peter Nasheuer
Head of Discipline: Dr. Michael Carty
Supervisor: Professor Robert S. Lahue

May 2012

Table of contents

Chapter 2: Materials and Methods

List of Figures

List of Tables

Abbreviations

°C	Degrees Celsius
ΔΔCt	Delta delta cycle threshold
AMP	Ampicillin
APC	adenomatous polyposis coli
Arg	Arginine
ARS	Autonomously replicating sequence
ASO	Antisense oligonucleotides
BER	Base excision repair
Can	Canavanine
CBP	CREB binding protein
CEN	Centromere
CHO	Chinese Hamster Ovary
DM1	Myotonic dystrophy
DMPK	dystrophia myotonica protein kinase
DMSO	Dimethyl sulfoxide
DNA	Deoxyribonucleic acid
DNMT1	DNA methyltransferase 1
DNTP	Deoxyribonucleic-5'-triphosphate
DSB	Double-strand break
DTT	Dithiothreitol
E. coli	*Escherichia Coli*
FACS	Fluorescence-activated cell sorting
FBH1	F-box helicase 1
FRAXA	Fragile X syndrome
FRDA	Friedreich's ataxia
FXN	Frataxin
HAT	Histone acetyltransferase
HD	Huntington's disease
HDAC	Histone deacetylase
HIS	Histidine
HLTF	Helicase-like transcription factor
HTT	Huntingtin
IDL	Insertion/deletion loops
Kb	Kilobases
mHTT	Mutant Huntingtin

MMR	Mismatch repair
OD	Optical density
Ori	Origin of replication
PBS	Phosphate buffered saline
PBS-T	PBS-Tween
PCAF	p300/CBP-associated factor
PCR	Polymerase chain reaction
PIP	PCNA-interacting domain
PKc	protein kinase, catalytic subunit
Polδ	Polymerase δ
RNA	Ribonucleic acid
RTEL1	Regulator of telomere length
RT-PCR	Reverse transcriptase PCR
S.cerevisiae	*Saccharomyces cerevisiae*
SC	Synthetic complete
SCA	Spinocerebellar ataxia
SDS	Sodium dodecyl sulphate
SEM	Standard error of the mean
SHPRH	Snf2 histone linker PHD RING helicase
siRNA	small interfering RNA
ssDNA	single-stranded DNA
SV40	Simian virus 40
Swi2/Snf2	SWItch/Sucrose nonfermentable
Ura	Uracil
UTR	Untranslated region
YPD	Yeast Extract Peptone Dextrose

Author Abstract

Expansions of trinucleotide repeats (TNRs) are the genetic cause of several inherited neurological diseases, such as Huntington's disease, myotonic dystrophy and fragile X syndrome. TNR diseases and their causal expansion mutations display several unique characteristics that distinguish them from other diseases and their associated genetic mutations. Such features include the ability of expandable repeats to form secondary structures such as hairpins, which are thought to be central to expansion mutagenesis and the occurrence of a threshold that demarcates stable and unstable alleles. The mechanisms by which TNRs expand are not well-defined. The mechanisms underlying expansions that cross the threshold length are largely uncharacterized, especially in human cells.

In order to gain some insight into this area, I used a selective genetic assay to determine the involvement of *trans*-acting factors in mediating CTG•CAG repeat instability near the threshold length in a human astrocytic cell line. RNA interference and/or small molecule inhibitors were used to interfere with proteins of interest to establish if they were relevant to instability in this system. This approach revealed novel mediators and shed some light on the mechanisms of repeat instability near the threshold. This study identified particular histone deacetylases (HDACs) and histone acetyltransferases (HATs) involved in instability. Specifically, HDAC3 and HDAC5 are proposed to promote expansions, while the evidence points towards HDAC9 having the contravening effect. Evidence suggests that the HATs, CBP and p300, function to inhibit expansions. Taken together with findings from the Lahue lab that specific HDAC complexes promote CTG•CAG repeat expansions in yeast, this represents a novel mechanism for repeat instability.

Further findings imply a direct role for the mismatch repair (MMR) complex MutSβ but not MutSα in promoting expansion of threshold-length CTG•CAG tracts. This observation led me to investigate whether certain HDACs might be mediating their expansion-promoting actions through MutSβ. Double knockdown analysis suggested that HDAC3 and MSH2 are acting through a common pathway to facilitate expansions. The nature of this functional interaction has not been identified. We determined that HDAC3 does not promote expansions by controlling access of MutSβ to the repeat tract, or by regulating MSH2 or MSH3 protein levels. Nevertheless, the identification of this linkage between HDACs and MMR represents an interesting mechanistic pathway.

Based on findings in yeast that the DNA helicase Srs2 inhibits expansions in concert with the postreplication repair (PRR) pathway, I investigated human orthologues of Srs2 and PRR factors with respect to TNR expansions. RTEL1, a proposed functional homologue of Srs2 was shown to prevent expansions in a common pathway with the PRR factors RAD18 and HLTF.

Acknowledgments

I firstly have to thank my project supervisor, Prof. Bob Lahue, for his wisdom, advice and guidance throughout my PhD. His infinite encouragement and support have been invaluable through tough times. I would like to thank all the members of the CCB. The weekly seminar series has proven a very useful pre-peer review procedure. I also wish to extend thanks to our collaborators including Simon Boulton and his research team, and Prof. Joel Gottesfeld.

To everybody in the Lahue lab, thanks for the help and guidance. I'll miss the tea-breaks and vigorous discussions about science and other important issues like what we are wearing to the Christmas party/upcoming social gathering. To Kim, Olive, Katherine and Maria I thoroughly enjoyed working with you and getting to know you. Thanks to Elaine for the many chats and delicious cakes and goodies you've made over the last few years. A special mention has to go to Claire, Anne-Marie and Lucy for their constant support and friendship, especially over the last few months. Claire, I've enjoyed our numerous chats about everything and nothing. I will miss our back-and-forth slanging matches but I know I've made a lifelong friend. Anne-Marie, your ultra-wise advice, when I have had the sense to heed it, has guided me in the right direction. Thanks for the laughs and head-clearing walks on the prom. Thanks to Lucy for being the lab events coordinator and keeping us all in check. I really appreciate all your help and advice.

A huge thanks to the brilliant friends I've made throughout my time in Galway, especially Christine, Nadine and Sarah. I have so many memories with you: nights out and in, tears, endless cups of tea, Florence and the Machine, the trash TV. You have made my time in Galway memorable and have always been there for me. To Aga and Ania, I'll never forget the singing in TC (and I've tried!) and the many pizza and beer nights in the college bar. Thanks to Rebecca for the many hilarious post-it notes and random conversations. Thanks to my friends from Sligo: Tara, Rhona, Niamh, Aileen and Kelly. Thanks for proving such a great distraction when I needed it most. The marathon catch-up chats, great nights out and phone calls have reminded me that there is life outside the lab.

I would like to sincerely thank my parents, Mary and Sean, and my brother, Vincent. Their support and belief in me throughout my whole life has been a constant comfort, especially during my PhD. I cannot thank you enough for everything you've done for me. Finally, I wish to thank my boyfriend Michael, who has always been there for me throughout my PhD. I am so grateful for your support and love.

CHAPTER 1

Introduction

1.1 Repeat instability overview

Trinucleotide repeats (TNRs) constitute the largest class of repetitive elements associated with disease. These tandem arrays of three base pairs are normally genetically stable, rarely undergoing significant length changes. However, some undergo very frequent expansion (increased length) mutations that are the sole genetic cause of at least 15 inherited neurological diseases including Huntington's disease (HD), myotonic dystrophy type 1 (DM1), Friedreich's ataxia (FRDA) and fragile X syndrome (FRAXA). I endeavour to describe the unique features of TNRs in this introduction and review some of the key molecular mechanisms proposed to underlie instability.

1.2 TNR diseases

TNR diseases predominantly exhibit autosomal dominant and X-linked inheritance patterns except for FRDA, which is autosomal recessive. While TNR diseases are all caused by a single type of mutation i.e. expansion of the relevant repeat tract, the clinical manifestations of disease vary greatly among this group of disorders (Orr and Zoghbi, 2007). TNR diseases can be divided into two broad categories based on whether the expanded TNR allele is located in a coding or noncoding region of the gene locus (Fig. 1.1). The first class of TNR diseases comprises those that have the expanded TNR located within the coding region. The expanded mutation generally arises within CAG tracts resulting in extraneous polyglutamine (PolyQ) tracts in the cognate protein. Many characterised polyQ proteins are involved in aspects of gene transcription suggesting a key function for these repeats (Butland et al., 2007). Increases in the length of these polyQ tracts are at the core of pathogenesis, leading to altered protein conformation and a dominant gain-of-function neurotoxicity (Orr and Zoghbi, 2007). Polyalanine-coding repeats have also been shown to undergo expansions. These polyalanine elongations are associated with at least nine human diseases, mostly early-onset developmental abnormalities (Messaed and Rouleau, 2009). Unlike many TNR expansions, polyalanine expansions contain tract interruptions, do not undergo somatic instability and are stably transmitted to the next generation (Messaed and Rouleau, 2009). The diseases of this class tend to exhibit shorter, less frequent expansions than those caused by mutation in non-coding regions (Pearson et al., 2005).

In the latter class of diseases, the TNR is not expressed in the cognate protein. With regard to genomic location, expandable repeats in this group of diseases can be situated at the 5'untranslated regions (5'-UTRs) or 3'-UTRs. These TNR disorders are typically characterized by much larger and more variable expansions than for polyglutamine diseases. For non-coding disorders, disease pathogenesis arises either due to a loss-of-function by the protein, e.g. FRDA, or a toxic gain-of-function for the respective RNA transcript e.g. DM1

(Cummings and Zoghbi, 2000). The causative expansion within the non-coding region of a TNR disease gene can induce multisystem pathogenic effects with several different tissues vulnerable to dysfunction or degeneration For example in DM1, symptoms include skeletal muscle wasting, myotonia, cardiac conduction impairment, gastrointestinal defects and other manifestations unrelated to muscular function such as hypersomnia, cataracts and learning difficulties (Day and Ranum, 2005).

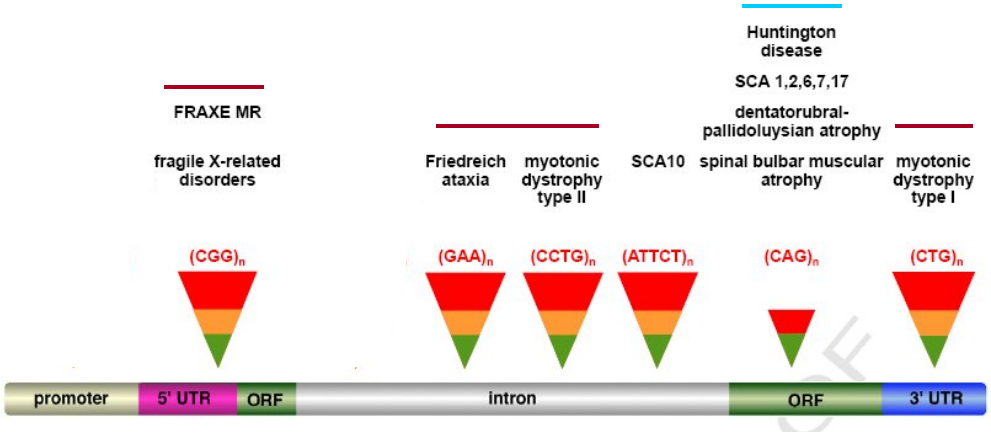

Figure 1.1 TNR diseases in humans. Polyglutamine diseases are demarcated by an aqua-blue line, while disorders of the non-coding variety are highlighted by a maroon line. Green represents normal length repeat alleles, yellow signifies carrier length and red denotes disease length. FRAXE: Fragile X E mental retardation, SCA: spinocerebellar ataxia Modified from (Kumari et al., 2012).

In unaffected individuals, the repeat tracts in the associated TNR disease gene are usually small (~5-35 repeats) and are generally stably transmitted to successive generations (Cleary and Pearson, 2003). For most TNR loci, repeat sequences display a polymorphic distribution with no apparent clinical significance within the general population. The transition between normal and disease state is demarcated by a clinical threshold length beyond which repeats are highly unstable and expand upon germline transmission resulting in the disease state. The defined clinical threshold varies among diseases but generally instability ensues when repeat length reaches 30-40 for diseases with repeats in the coding sequence, while for non-coding sequences unstable transmission initiates within the range of 55-200 repeats (Mirkin, 2007; McMurray, 2010). The spectrum of repeat lengths from stable and disease-length tracts can be defined based on the relative contribution to disease pathogenesis. At the HD locus, alleles of 26 or less CAG repeats are genetically stable with no clinical symptoms or instability during transmission observed (Semaka et al., 2006). Individuals harbouring 27-35 repeats are termed intermediate allele carriers. Carriers themselves do not develop HD,

although intermediate alleles exhibit *de novo* repeat instability during germline transmission so there is a risk, albeit small, of their offspring developing HD (Myers et al., 1993; Semaka et al., 2010). Individuals affected by HD have at least 36 repeats, although full disease penetrance has only been observed when tract length exceeds 39 repeats (Rubinsztein et al., 1993). Thus, a sharp threshold for disease governs HD; individuals with 35 or less repeats will remain unaffected while small increases in repeat length can deliver a transition to the pathogenic state.

1.3 Germline and somatic instability

It is important to differentiate between germline and somatic instability. Germline (arising during reproductive cell formation) instability is apparent for all TNR diseases. However some TNR diseases exhibit tissue-specific patterns of somatic instability, whereby tract length for a specific TNR locus varies between different tissues throughout development. The extent to which somatic instability contributes to TNR disease pathogenesis is debatable, although it appears to depend on the disorder. DM1 patients have much larger expansions in muscle cells, the primary affected tissue, than in unaffected tissues like blood (Thornton et al., 1994). For polyglutamine disorders, some of which also display somatic instability, the situation is not clear. In a knock-in mouse model of SCA1, no correlation was observed between somatic instability and the regions affected by disease pathogenesis (Watase et al., 2003). This group reported that instability was most prevalent in the striatum but less notable in areas vulnerable to pathogenesis such as the cerebellum. In support of the hypothesis that somatic expansion contributes to disease progression, a study that detailed somatic instability in the cortex region of the brain from HD individuals reported that instability was predictive of age of disease onset, with longer increases in repeat length associated with an earlier age of onset (Swami et al., 2009). Based on the observations that for DM1 and HD instability is most prominent in tissues that are the targets of pathogenesis, it has been proposed that somatic instability contributes to the progression of these TNR diseases during the lifetime of an individual. Thus factors that modify somatic instability represent useful therapeutic targets. The work described in this thesis models somatic expansions.

1.4 TNRs undergo dynamic mutations

One aspect that underscores TNR expansions as a unique form of mutation is their dynamic mutational mechanism. In many genetic diseases, the responsible mutation is retained in somatic tissues and exhibits a typical Mendelian pattern of inheritance; thus it is stable from generation to generation so all affected family members share the same inherited mutation. Examples of such static mutational events include point mutations, deletions and inversions.

In contrast to the static inheritance of these other single-gene mutations, the TNR mutation process is highly changeable, with products that continue to mutate across generations and within tissues so both germline and ongoing somatic instability is observed in some cases (Pearson et al., 2005). Thus, the products of a TNR expansion mutation have a greater predisposition to experience a successive mutation than their original substrate. These dynamic mutations are thus expansion-biased in a length-dependent manner. The dynamic nature of TNR instability is reflected in the genetic anticipation displayed by TNR diseases. Anticipation is the increase in the severity of disease with an earlier age of onset of symptoms in successive generations. This phenomenon had been reported as early as 1918 in DM1 but had often been dismissed as a statistical artefact (Howeler et al., 1989). It was not until the early 1990's when TNR instability was described that it was revealed to be a consequence of increase in TNR allele size with each consecutive generation (Fu et al., 1992; Mahadevan et al., 1992). Thus, anticipation is governed by the unusual characteristics of TNRs that determine their propensity to expand.

1.5 Unique characteristics of TNRs

While a wide range of pathogenic outcomes are triggered by TNR expansions, these mutations share several unique properties which reflect common dynamics and molecular mechanisms. One key feature of TNR diseases is that expansions are limited to only the TNR disease locus, which is in contrast to the genome-wide instability seen in HPNCC and sporadic colorectal cancers (Goellner et al., 1997). HNPCC-affected individuals have defects in one or more mismatch repair (MMR) proteins which are responsible for the observed multi-loci instability that manifests as small deletions and gains (Liu et al., 1996; Kwak and Chung, 2007). This is indicative of *cis*-elements internal to the repeat sequence influencing its mutability including the sequence of the repeat sequence, the length of the tract and the purity of the repeat tract, likely in concert with trans-acting factors involved in DNA metabolism. Other *cis*-elements proposed to regulate repeat instability are outside of the repeat tract itself and include flanking sequence, replication origins, CpG methylation and chromatin structure (Cleary and Pearson, 2003).

1.5.1 Threshold

One key feature of TNR instability is the occurrence of a genetic threshold, defined as the narrow part of the expansion mutation spectrum (~30-40 repeats in humans) that separates short stable repeats from longer, unstable disease-length repeats (McMurray, 2008). Work in the Lahue lab has focused on the infrequent expansions that demarcate short stable repeats, from longer unstable tracts. Studies in yeast have shown evidence of a threshold for

expansions of ~15 repeats based on the findings that an increase of the starting tract length from 10 to 20 CTG repeats leads to a 100-fold increase in expansion rates (Rolfsmeier et al., 2001). Expansion of a starting tract of 25 to 29-40 that crosses the predicted boundaries between normal, moderate, and disease-causing alleles for most (CAG)• (CTG) repeat disease genes, including HD was detected in a human astrocytic cell line (Claassen and Lahue, 2007).

Mutation (contractions and expansions) of the HD locus was analysed by measuring CAG length changes in single sperm from normal and unaffected individuals (Leeflang et al., 1995). Normal length alleles (15-18 repeats) underwent mutation at a rate of 0.6%. When the repeat tract increased to 30 or 36, the mutation frequency concomitantly rose to 11% and 53%, respectively. 92-99% of sperm carrying pathogenic alleles (38-51 repeats) showed alterations in length, with a strong bias towards expansions (Leeflang et al., 1995). Contractions were predominant up to 36 repeats, but a shift towards decreasing contractions was observed for longer alleles. The expansion bias is illustrated in figure 1.2.

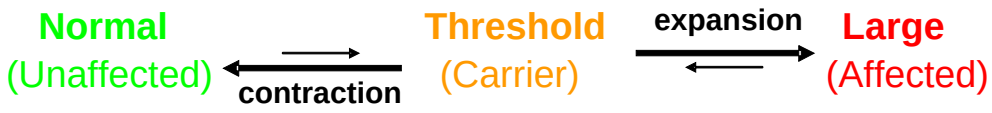

Figure 1.2 Instability bias above and below the TNR threshold. The thicker arrows reflect the bias towards either contraction or expansion. The thinner arrows reflect a lesser tendency to change length from one state to another.

The Lahue lab has identified several proteins involved in inhibiting TNR instability of sub-threshold length repeats in yeast (Bhattacharyya and Lahue, 2004; Daee et al., 2007; Razidlo and Lahue, 2008) and recently discovered that certain histone deacetylase components promote expansions in yeast (Debacker et al., 2012). Recent evidence from the Leffak lab, has provided an additional report of human proteins protecting short repeats from destabilisation, with the finding that knockdown of the replication fork stabilisation proteins Claspin, Timeless and Tipin led to increased contraction and expansion of a $(CTG)_{13}$• $(CAG)_{13}$ allele (Liu et al., 2012). However, in this study, it is difficult to determine if the instability observed following knockdown arose from the $(CTG)_{13}$• $(CAG)_{13}$ allele, as it is ambiguous whether events are contraction products from amplification of the expanded $(CTG)_{1000}$• $(CAG)_{1000}$ allele or expansions of the shorter, unexpanded allele. Nevertheless, very little information is currently available on what trans-acting factors influence the occurrence of the critical initiating expansions that cross the TNR threshold and lead to enhanced instability in higher organisms. To shed light on the rather, infrequent but important instability events that cross the threshold, I used a human astrocytic cell line and a

starting tract of 22 repeats, which is near the threshold (~30-40 repeats) for many human disorders, to identify proteins that modulate these events.

1.5.2 Sequence dependence

The sequence of the TNR repeat is proposed to be intrinsic in the governance of instability. The observation that only particular TNR sequences undergo instability might correspond to their ability to form of non-B sequence-specific structures, which are thought to be central to instability. Indeed, a common feature of TNRs that are prone to expand is their capacity to adopt secondary structures such as triplexes, quadruplexes, slipped strand structures and hairpins (Fig. 1.3), whereas TNR tracts that are not reported to expand have much lower propensity for secondary structure formation (Gacy et al., 1995; Zhao et al., 2010).
CNG repeats, where N is any nucleotide, can fold into intrastrand slipped structures or hairpins containing predominantly Watson-Crick (WC) and non-WC base-pairs. The inclination for CNG repeat tracts to form hairpins (Fig. 1.3A) is explicated by the stabilisation of a hairpin stem by GC doublets, which display strong base-stacking interactions (Petruska et al., 1996). The stability of these CNG hairpins is further governed by the identity of the associated mismatch (non-WC) such that the order of stability is as follows: CGG>CCG≈CTG>CAG (Gacy et al., 1995). CTG hairpins are more thermodynamically stable than CAG due to the smaller T-T mismatches being less bulky and thus less likely to interfere with normal base-stacking of GC and CG doublets than the A•A mismatches (Petruska et al., 1996) T-T mispairs actually form wobble pair with one H bond; slightly stabilizing the hairpin. The transient nature of non-B structures has made their detection *in vivo* difficult and this is borne out in the vast array of studies demonstrating their formation *in vitro* (Zhao et al., 2010). Recently, the formation of hairpin structures has been demonstrated *in vivo* in HeLa cells in an elegant study using zinc-finger nucleases that specifically cleaved CTG/CAG hairpins during replication (Liu et al., 2010).
Slipped-strand structures form when the TNR duplex denatures and renatures in a misaligned manner. This results in loop-outs on both strands (Fig. 1.3C) and the complexity of the structures formed were increased with the length of the repeat tracts reminiscent of the length-dependent instability effects observed in TNR disease (Pearson and Sinden, 1996; Pearson et al., 1998).

As well as hairpins, CGG repeats have been proposed to adopt a variety of structural conformations *in vitro* depending on repeat length and pH including G-quadruplexes (Fig. 1.3B) (Mitas et al., 1995; Fojtik and Vorlickova, 2001). The current dogma for instability encompasses secondary structures as crucial facilitators of instability. Thus, most models for instability predict that secondary structures formed by TNRs serve as mutagenic

intermediates, whose aberrant metabolism may lead to instability. GAA repeat tracts due to their asymmetric nature, have a tendency to form triplexes (Fig. 1.3D). The third strand of this structure can comprise of TTC repeats (pyrimidine:purine: pyrimidine) or GAA repeats (pyrimidine:purine:purine) (Gacy et al., 1998; Sakamoto et al., 1999). Furthermore, two GAA tracts on the same plasmid were shown to form 'sticky DNA', a composite triplex structure arising from the interaction of the two triplexes in the molecule (Gacy et al., 1998; Sakamoto et al., 1999; Vetcher et al., 2002).

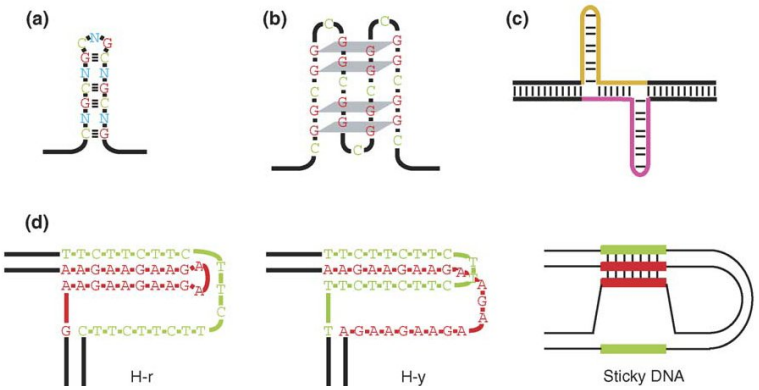

Figure 1.3 Secondary structures formed by TNR repeats. A. Hairpin formation of CNG repeats. **B.** Quadruplex formed by CGG repeats. **C.** Slip-stranded DNA. **D.** Triplex structures. From (Mirkin, 2006)

The working model for this study is centred on the formation of a hairpin intermediate as a key intermediate structure in the expansion process. Based on this assertion, it is proposed that TNR instability reflects the opposing actions of two sets of proteins, one inhibiting mutation and a second promoting it (Fig. 1.4). Several factors, mainly involved in replication and repair, have been implicated in either inhibiting or promoting expansions in various model systems. For example, the helicase Srs2 has been shown to unwind the TNR hairpin intermediate in yeast thereby preventing the occurrence of expansions (Savouret et al., 2003; Bhattacharyya and Lahue, 2004; Bhattacharyya and Lahue, 2005; Kerrest et al., 2009). Conversely, the mismatch repair factors MSH2/MSH3 are known to bind TNR hairpin substrates and studies in mice have shown that they promote expansions (Manley et al., 1999; van den Broek et al., 2002; Savouret et al., 2003; Wheeler et al., 2003; Owen et al., 2005; Foiry et al., 2006). The premise that certain proteins promote expansions and others prevent these mutations is a central rationale for the work described in the main body of the thesis. I will take a candidate-based approach to determining which factors are important in the control of expansion of repeats near the threshold in human cells.

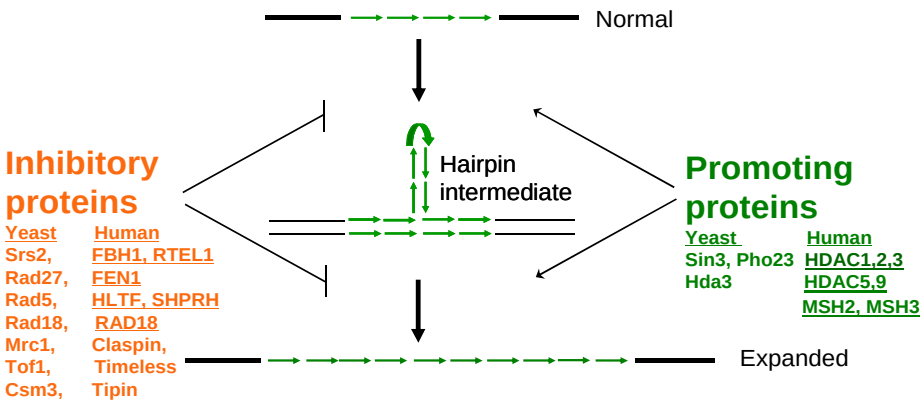

Figure 1.4 Proteins shown to inhibit or promote expansions in various model organisms. Of these, the proteins that are investigated in this study are underlined. In the case of the yeast factors, the human homologues or proposed functional orthologues are assessed.

1.5.3 Interruptions

Another feature of TNRs that influences instability is the purity of the repeat tract. Repeat tract interruptions are associated with TNR loci for a number of TNR diseases including SCA1, SCA2, SCA3, SCA8, DM1, FRDA and FRAXA (Lopez Castel et al., 2010). It is generally thought that interruptions reduce repeat instability as in many cases loss of interruptions is coincidental with expansion of the repeat tract. This is the case for FRAXA, whereby normal alleles have AGG interruptions in the CGG tract, while loss of a single interruption can confer repeat stability (Eichler et al., 1994). Additionally, in SCA1 patients, a CAG repeat tract containing as many as 39 repeats punctuated by a CAT interrupt was stable, while $(CAG)_{40}$ uninterrupted tract was unstable (Chong et al., 1995). More recent work has identified (CCG)• (CGG) interruptions at the 3' end of a (CTG)• (CAG) repeat at the DM1 locus, which likely contribute to the disease variability observed in such patients (Musova et al., 2009; Braida et al., 2010). It is thought that the instability associated with loss of interruptions is based on the propensity for TNR sequences to form secondary structures. CAT or AGG interruptions within CAG or CGG tracts result in fewer slipped DNA structures than pure, uninterrupted tracts (Pearson et al., 1998), which is linked with reduced instability. Interestingly, in yeast deficient in mismatch repair, there is an increased incidence in expansions of interrupted alleles (Rolfsmeier et al., 2000). Interruptions do not confer stability in all cases; expanded alleles of SCA8 contain interruptions, while normal alleles were reported to have no interruptions (Moseley et al., 2000).

1.6 Mechanisms of repeat instability

The mechanisms by which repeat instability occurs are relatively poorly understood.

However, the observation that expansion of TNR tracts inherently requires the synthesis of nascent DNA underlines the prerequisite for DNA metabolic processes such as replication, repair, recombination and transcription in mediating expansion. One salient commonality for the majority of proposed models of expansion, regardless of the metabolic source of instability, is that the unusual secondary structures formed by TNRs are thought to act as mutagenic intermediates during the instability process. Direct evidence for hairpin formation *in vivo* has recently been shown (Liu et al., 2010).

1.6.1 Replication

Many models for TNR expansions assume a replication-dependent mechanism. Evidence that supports a replication-induced mode of instability is gleaned from several model systems that require proliferation for instability (Schweitzer and Livingston, 1999; Cleary et al., 2002; Yang et al., 2003). Furthermore, pronounced instability is observed in DM1 patients in proliferative tissues such as the blood (Martorell et al., 1998) and during periods of rapid cell division including tumourgenesis and male germ cell (Jinnai et al., 1999; Leeflang et al., 1999). Studies have shown that TNRs cause replication fork stalling. (CAG)• (CTG) and (CGG)• (CCG) repeats have been shown to invoke replication fork stalling in yeast, primate and human cells (Pelletier et al., 2003; Voineagu et al., 2009; Liu et al., 2012). The proposed formation of secondary structures that can cause impediments for replication fork progression leading to instability is likely during lagging strand synthesis. This hypothesis was borne out of the observation that a region of the lagging strand template called the Okazaki initiation zone (OIZ) remains transiently single-stranded, thus TNR repeats could fold into secondary structures within this region.

Replication origin activity has been the focus of many studies. Origins of replication are common elements around several TNR repeat loci (Nenguke et al., 2003; Cleary et al., 2010; Liu et al., 2012). Studies in various model organisms suggest that TNR instability depends on repeat orientation relative to the origin of replication. This orientation bias is attributed to the propensity of the ability of the sequence to form thermodynamically stable hairpin structures. An increase in contractions occurs if the more structure-prone sequence is on the template strand, whereas expansions arise if the structure-prone TNR is on the nascent strand. Accordingly, studies in *E.coli*, yeast, HeLa cell extracts, simian cells and cultured astrocytes have demonstrated that contractions are more frequent when CTG comprised the lagging strand template (CAG on nascent lagging strand), whereas expansions were predominant when the CAG sequence was on the lagging strand template (CTG on nascent lagging strand) (Kang et al., 1995; Freudenreich et al., 1997; Miret et al., 1998; Cleary et al., 2002; Panigrahi et al., 2002). Additionally, the distance between the origin of replication and

the repeats is proposed to influence instability. In primate cells, this was supported by the finding that shifting the distance between $(CTG)_n$ repeats by as little as 130 bp caused a switch from predominantly expansions to contractions (Cleary et al., 2002). Studies in DM1 human fibroblasts and transgenic mice, containing a copy of the 45 kb human expanded (CTG_{300}) transgene, comparing origin activity at the DMPK locus have provided an insight into the complexity of the relationship between replication and instability (Cleary et al., 2010). Similar instability patterns were observed between human cells and mice (Lia et al., 1998) and human origins have been shown to be active when transferred to mouse cells (Aladjem et al., 1998). However, the origin activity at the DMPK locus between the two systems was markedly different; two origins were mapped upstream and downstream of the expanded repeat tract in DM1 fibroblasts, both of which were active, but only the downstream origin was active in mice (Cleary et al., 2010). This implies that the chromosomal integration site of the transgene and/or elements outside the transgene region might control origin activity, thereby influencing instability (Cleary et al., 2010).

Strong evidence for replication contributing to TNR instability is garnered from pharmacological interference studies. Exposure of DM1 fibroblasts to aphidicolin (inhibits lagging and leading strand replication) and emetine (hinders lagging strand replication), selectively increased the magnitude of CTG expansions for the expanded allele but did not affect the normal-length allele (Yang et al., 2003). Kidney cells from Dmt-D transgenic mice bearing $(CTG)_{160}$• $(CAG)_{160}$ repeats displayed increased expansions upon exposure of caffeine, which interferes with replication (Gomes-Pereira and Monckton, 2004). A similar increase in overall instability in a HeLa cell line containing 45 and 102 (CTG)• (CAG) repeat tracts following treatment of these cells with aphidicolin and emetine (Liu et al., 2010).

Two models for TNR expansion arising during lagging strand synthesis have been proposed. The first model involves polymerase slippage on the 3' end (Fig. 1.5). The DNA polymerase pauses or stalls while replicating across the TNR region leading to a transient dissociation of nascent DNA from its template. Reassociation of the strands results in misalignment leading to possible formation of a hairpin on the nascent strand. This loop-out can be incorporated into DNA during the next round of replication resulting in an expansion. Evidence for this model is derived from replication stalling at TNRs and also from the finding that Srs2 and post-replication repair (PRR) inhibit TNR expansions (Bhattacharyya and Lahue, 2004; Daee et al., 2007).

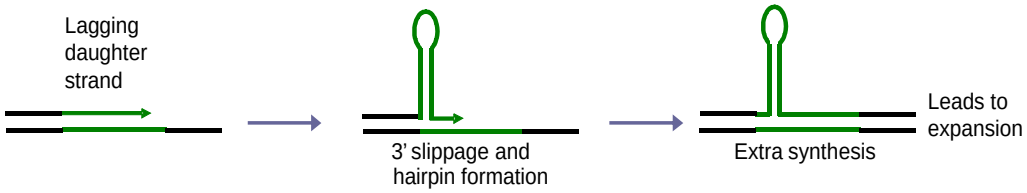

Figure 1.5 3' slippage model. Polymerase slippage at the 3' end of an Okazaki fragment occurs due to the repetitive nature of the TNR tract. This leads to hairpin formation and expansion of the tract. Green represents repeat tract.

Srs2, a 3'-5' helicase was identified in a yeast screen for trans-acting factors that inhibit TNR expansions (Bhattacharyya and Lahue, 2004). This yeast work and that described below provides the basis for the corresponding experiments in human cells, which are detailed in chapter in chapter 5. Srs2 suppresses homologous recombination to ensure HR takes place in an appropriate temporal and spatial manner and positively regulates PRR. Srs2 antirecombinase activity is evidenced by *srs2* mutants exhibiting a hyper-recombination phenotype (Aguilera and Klein, 1988). *In vitro* analysis demonstrated that Srs2 translocates on ssDNA and prevents Rad51-directed recombination by disrupting the Rad51 presynaptic filament (Krejci et al., 2003; Veaute et al., 2003). Srs2 was shown to be a potent inhibitor of expansions with increased expansion rates of CTG, CAG and CGG repeat tracts of up to 40-fold in *srs2* mutants. The phenotype of *srs2* mutants is selective for expansions; there is no effect of mutation of Srs2 on dinucleotide repeats, at unique sequences or on contractions. Biochemical analysis revealed that Srs2 selectively unwinds TNRs substrates that mimic the *in vivo* hairpin intermediates thought to contribute to instability (Dhar and Lahue, 2008). Further genetic analysis demonstrated that the protective role of Srs2 against expansions was independent of its role in homologous recombination rather via its capacity to direct PRR (Bhattacharyya and Lahue, 2004; Daee et al., 2007).

Srs2 acts as a molecular switch that favours processing of aberrant replication intermediates by PRR rather than homologous recombination. PRR ensures continuation of DNA synthesis in the presence of polymerase-blocking damage, deferring the engagement of conserved repair mechanisms that are in place, to faithfully repair DNA to its original sequence (Waters et al., 2009). Unlike DNA repair, PRR does not remove the replication-blocking lesion but facilitates bypassing of the damage allowing the replicative machinery to proceed. Because no repair as such occurs, PRR has often been referred to DNA damage tolerance (DDT) in many instances in the literature. PRR, which is best characterized in *S.cerevisiae*, has three main branches all directed by the Rad18-Rad6 ubiquitin-conjugating complex (Fig.

1.6) (Ulrich, 2005). Monoubiquitination of PCNA following damage at lysine 164 (K164) promotes the translesion synthesis (TLS) branch of PRR. This involves the use of specialized DNA polymerases that can use damaged DNA as a template permitting lesion bypass and continuation of replication. TLS is often error-prone due to the low fidelity of the polymerases that enable replication to proceed across damage but some TLS polymerases replicate past the lesion in an error-free manner. Rad6/Rad18-mediated monoubiquitination of PCNA is also required for the Rad5-dependent error-free branch of PRR. K63-linked polyubiquitination of PCNA at K164 residue is subsequently mediated by the physical interaction between Rad5's ubiquitin ligase domain and the ubiquitin-conjugating complex Mms2-Ubc13 (Ulrich and Jentsch, 2000). The mechanism of this pathway is not clearly defined. Genetic data in yeast has shown that Rad5's ATP-dependent 3'-5' helicase function, in addition to its ubiquitin ligase activity, is essential for its role in the replication of damaged DNA (Gangavarapu et al., 2006). This branch is thought to bypass DNA damage by using the undamaged sister duplex (template switching).

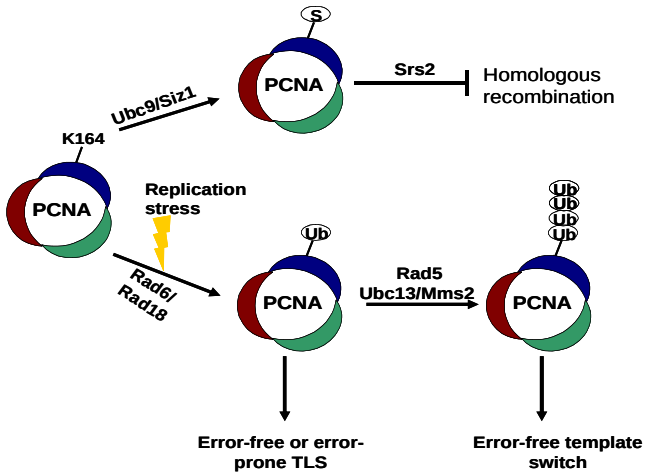

Figure 1.6 Postreplication repair pathways in yeast. In response to replication stress, PCNA is modified with ubiquitin (Ub) at K164. Monoubiquination, which is catalysed by the Rad6 Rad18 complex, is thought to promote TLS. Subsequent polyubiquitination at the same K164 residue by Mms2-Ubc13-Rad5 promotes the error-free branch. PCNA sumoylation (S) recruits Srs2 to the replication fork to prevent recombination

A study in yeast found that when the PRR pathway is disrupted by deletion of Rad18, Rad5 or Mms2 or by abolishing PCNA modification, there was a specific increase in expansions, but not contractions, of short repeats (Daee et al., 2007). Further analysis revealed that Srs2 and the PRR pathway concertedly act to inhibit TNR expansions (Daee et al., 2007). Functional human orthologues for Srs2 have been proposed such as FBH1, RTEL1 and, most recently, PARI (Chiolo et al., 2007; Barber et al., 2008; Moldovan et al., 2012). Additionally, two functional orthologues of Rad5 have been characterized HLTF and SHPRH (Motegi et al., 2006; Unk et al., 2006; Motegi et al., 2008; Unk et al., 2008).

Chapter 5 details efforts to determine if FBH1, RTEL1 or both recapitulate the expansion-protecting mechanism of Srs2. Members of the PRR pathway are also investigated to establish if they are involved in inhibiting expansions in human cells and to identify potential functional interactions between this pathway and Srs2 homologues.

The second model for expansions occurring during lagging strand synthesis involves TNRs folding to form hairpin structures in the 5' flap of the Okazaki fragment created during strand displacement (Fig. 1.7). It has been postulated that this hairpin prohibits flap processing by FEN1 (Gordenin et al., 1997), which is a flap endonuclease involved in removal of 5' flaps formed during Okazaki fragment maturation (Liu et al., 2004). The flaps can anneal with the adjacent Okazaki fragment leading to expansion. This provides the rationale for studying the role of FEN1 in expansions in human cells in chapter 5.

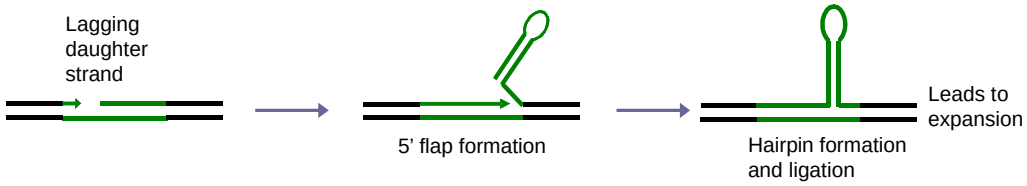

Figure 1.7 5' Flap model. A 5' flap is formed following displacement of the upstream Okazaki fragment. Persistence of this flap can lead to formation of a hairpin, which can be ligated into the downstream Okazaki fragment and result in extra repeats (expansion). Green represents repeat tract.

This model is supported by biochemical data and by yeast mutant analysis. In yeast, loss of the FEN1 homologue Rad27 resulted in an increase in the occurrence of CTG expansions (Freudenreich et al., 1998). This group reported that expansions were enhanced by approximately 30- and 60-fold, when the initial repeat tracts were $(CTG)_{40}$ and $(CTG)_{70}$, respectively. *rad27* yeast displayed an overall destabilisation of CAG repeat tracts with approximately 50% of the instability compromising expansions of one or more repeats (Schweitzer and Livingston, 1998). Haploinsufficiency of Rad27 in yeast was found to be sufficient in inducing length-dependent instability, with no change in tracts of 70 repeats, while $(CAG)_{155}$ tracts had substantially higher expansion frequencies (Freudenreich et al., 1998). Interestingly, double mutants of *rad27* and *rad18* revealed a synergistic increase in expansion rates of a $(CTG)_{13}$ relative to single mutants, implying that the two pathways act independently (presumably at the 5' and 3' ends, respectively) but synergize to prevent some expansion events (Daee et al., 2007). Thus in yeast, FEN1 is proposed to cleave a substantial

fraction of flaps prior to their folding in FEN1-resistant structures and thus preventing expansion.

However, this protective function has not been recapitulated in most of the human cell systems or transgenic mice models tested for TNR instability. FEN1 homozygous null mice die at an early stage of embryogenesis and this limitation restricts study of FEN1 to haploinsufficient Fen1 mice. Somatic cells of haploinsufficient Fen1 mice harbouring $(CAG)_{120}$• $(CTG)_{120}$ repeats at an ectopic HD locus did not undergo instability of this tract (Spiro and McMurray, 2003). In this study, an increase in intergenerational expansion frequency was reported although this was not statistically significant. No expansion of a $(CTG)_{110}$• $(CAG)_{110}$ tract was observed in a knock-in mouse model of DM1 (van den Broek et al., 2006) or a (CGG• $CCG)_{130}$ model of fragile X syndrome (Entezam et al., 2010). CAG repeats (13–27 repeat units) were stably maintained at the huntingtin gene locus in cells with FEN1 stably knocked down over 27 passages (Moe et al., 2008). Taken together, this implies that FEN1 does not play a role in repeat expansion but a caveat with the mouse studies is that reduction of FEN1 expression is only 50% of normal levels and the remaining levels of enzyme activity might be sufficient to inhibit expansions. In an attempt to shed some light on the role of FEN1 in TNR expansions in human cells, I used RNA interference to determine if loss of FEN1 has any impact on expansions near the threshold length (Chapter 5).

1.6.2 Repair

Despite the strong experimental evidence for replication-based TNR instability, it is not sufficient to explain the instability observed in non-dividing cells. The lack of correlation between the proliferative potential of transgenic mice tissues and repeat instability has highlighted the contribution of replication-independent mechanisms (Lia et al., 1998; Kennedy and Shelbourne, 2000; Seznec et al., 2000). Furthermore, postmitotic neurons from HD patient and HD mouse brains show expansions (Shelbourne et al., 2007; Gonitel et al., 2008).

Numerous studies have proposed that repair proteins play a role in inducing instability. The concept that the presence and not the absence of certain proteins promotes the occurrence of expansions is seemingly counterintuitive but these normally protective pathways have been hypothesised to have their normal biochemical functions replaced by mutagenic actions due to aberrant TNR-forming secondary structures. Evidence for the presence of such expansion-promoting factors includes the observation that disease-length alleles expand with almost 100% probability (Fu et al., 1991). The inherent site-specific nature of TNR expansions,

with no discernible effect on the rest of the genome (Goellner et al., 1997), supports the existence of proteins actively contributing to TNR instability. If defective repair was responsible for TNR instability, genome-wide instability would occur concurrently increasing cancer predisposition and no such susceptibility has been described.

Certain mismatch repair (MMR) proteins have been heralded for providing a mechanism for inducing CAG/CTG instability. MMR generally functions to maintain genomic instability by removing mismatches generated during replication (Li, 2008). In mammalian cells, the initiation of MMR via recognition of mismatches involves two heterodimeric complexes: MutSα (MSH2/MSH6) and MutSβ (MSH2/MSH3). MutSα preferentially binds base-base mismatches and small insertion/deletion loops (IDLs), while MutSβ favours larger IDLs. Msh2 has been shown promote instability in numerous transgenic mouse models. Loss of Msh2 leads to a decrease in somatic and germline expansions in DM1 mice (Savouret et al., 2003). Msh2 deficiency also promotes somatic and intergenerational expansions in various HD mouse models (Manley et al., 1999; Kovtun and McMurray, 2001; Wheeler et al., 2003). Further investigation of MSH2 interacting partners revealed that DM1 mice lacking Msh3 mimic the reduced somatic expansion phenotype of mice with an Msh2 deficiency, whereas loss of Msh6 resulted in an increase in expansions (van den Broek et al., 2002). $Msh6^{-/-}$ HD mice did not show any change in germline or somatic expansions, while an absence of Msh3 suppressed both (Owen et al., 2005). Thus MutSβ, not MutSα, seems to be the relevant MMR recognition complex for promoting expansions. It has been reported in several TNR disease mouse models that absence of Msh2 or Msh3 decreases the frequency of expansions in concert with an increase in contractions (Savouret et al., 2003; Wheeler et al., 2003; Foiry et al., 2006; Tome et al., 2009).

Interestingly, work in mice demonstrates that the effects of MMR on instability for GAA tracts are distinct to those reported for CAG/CTG TNRs. Mice expressing a YAC with the human FXN locus containing $(GAA)_{90\text{-}230}$ sequence were crossed with Msh2, Msh3, Msh6 and Pms2 knockout mice (Ezzatizadeh et al., 2012). The instability patterns observed suggest that MSH2 and MSH3 protect against contractions, but have no effect on expansions, while MSH6 protects against both expansions and contractions and PMS2 prevents expansions. Furthermore, MMR effects seem to differ between species for CNG repeats. In *E.coli*, defects in MMR result in a suppression of large (CTG)• (CAG) contractions, but an increase in small-scale expansions and contractions (Wells et al., 1998; Parniewski et al., 2000; Schmidt et al., 2000). In yeast, loss of MMR does not alter

expansions or contractions of CTG• CAG repeats (Schweitzer and Livingston, 1997; Miret et al., 1998; Rolfsmeier et al., 2000).

The mechanism through which MMR proteins mediate TNR instability has not yet been definitively identified. One commonly cited model proposes that MutSβ binds to (CAG)• (CTG) hairpins and stabilises the repeats instead of processing the "mismatches". This hypothesis is based on the observation that binding of MutSβ to $(CAG)_{13}$ or $(CTG)_{13}$ hairpins impaired its ATPase activity, altered both binding between the complex and DNA and its nucleotide affinity (Fig 1.8) (Owen et al., 2005; McMurray, 2008). This so-called "hijacking" model predicts that MutSβ recognizes and binds the mismatched base pairs in the stem of the TNR hairpin, but fails to successfully co-ordinate recognition/binding with downstream repair signalling. Inhibition of faithful DNA repair would lead to incorporation of unrepaired loops as expansions. Further support for this model was provided by recent single-molecule data demonstrating trapping of MutSβ by repair-resistant CAG loops implying that MutSβ binds hairpins but cannot elicit downstream repair signaling (Lang et al., 2011). However, this model has fallen out of favour due to a number of recent developments. An identical reduction in MutSβ ATPase activity was observed regardless of whether it was interacting with a $(CAG)_{13}$ hairpin, a $(CTG)_{13}$ hairpin, or its preferred substrate, an ID heteroduplex (Tian et al., 2009). Together with the finding that the catalytic efficiencies (kcat/Km) were similar for all three substrates, this suggests that the aberrant ATP hydrolysis is a general feature of MutSβ binding to DNA rather than being specific to TNR hairpins (Tian et al., 2009). Transgenic DM1 mice bearing >300 CTG repeats were crossed with *Msh2* ATPase-defective mice ($Msh2^{G674A}$ mice) to establish the importance of the ATPase activity in TNR expansions (Tome et al., 2009). The authors found that this mutation, which disrupts ATP binding and/or hydrolysis abrogated the incidence of both germline and somatic expansions and stimulated contractions in parent-to-offspring transmissions (Tome et al., 2009). In light of the finding that Pms2, which is involved subsequent to mismatch recognition, is partially required for TNR instability in DM1 mice (Gomes-Pereira et al., 2004), these data support to the hypothesis that functional MMR activity is required for expansions (Fig. 1.8). Taken together, these findings challenge the hypothesis the role of MMR in driving expansions is limited to the recognition of hairpins by MutSβ. If functional MMR is indeed required for expansions, targeting downstream members of the pathway should evoke similar findings as for MSH2, MSH3 and PMS2.

The mice used in the studies described above carry long TNR tracts, typically from 84 to >300 repeat units in length. An unanswered question, which I address in Chapter 4, is

whether the finding that MutSβ is an important promoter of expansions is applicable to short, sub-threshold alleles in human cells.

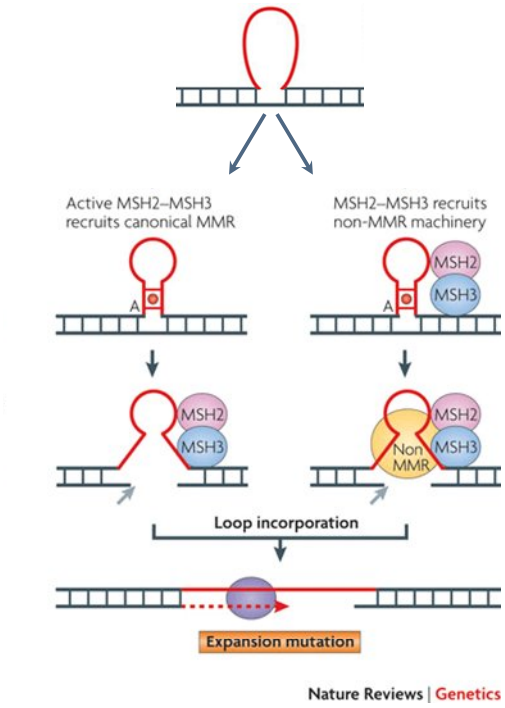

Figure 1.8 Proposed models for MMR involvement in TNR instability. Common to both models is a pre-formed hairpin and a nick on the strand opposite the hairpin. On the left-hand side, a model for active MMR is shown. In this model, MutSβ binds to the hairpin and signals to recruit downstream MMR factors resulting in a nick opposite the hairpin. Following gap-filling synthesis by a polymerase (purple), the hairpin becomes incorporated. Conversely, on the right-hand side, MutSβ binds to the hairpin and this binding prevents activation of downstream MMR events. This might result in recruitment of an alternative mechanism that leads to expansion. Adapted from McMurray, 2010

In addition to MMR, base excision repair (BER) has been proposed to cause somatic instability in mammals (Liu and Wilson, 2012). BER is the main DNA repair pathway involved in removal of damaged bases, such as oxidized bases (Robertson et al., 2009). Transgenic mice harbouring the HD $(CAG)_{135}$ repeat were crossed with mice lacking the BER DNA glycosylase OGG1 responsible for removal of 7,8-dihydro-8-oxoguanine (8-oxoG). Loss of OGG1, but not other glycosylases resulted in suppressed or delayed age-dependent somatic expansion *in vivo* (Kovtun et al., 2007). *In vitro* evidence further supports a requirement for BER for expansion with the finding that creation of a ssDNA break by OGG1 and APE1 during oxidative base removal in the context of CAG repeats, postulated to lead to hairpin formation, and subsequent extension by the BER polymerase, polβ leads to

repeat tract expansion (Kovtun et al., 2007; Liu et al., 2009). The hypothesis proposed is that the hairpin formed during oxidative repair of CAG repeats is refractory to FEN1 removal and thus becomes incorporated into the DNA forming an expansion. Because the damage is still present, it will be recognized by OGG1 and processed in the same way leading to cyclic expansions over time.

Based on *in vitr*o BER experiments, it has been suggested that mis-coordination between FEN1 and the BER polymerase polβ leads to CTG/CAG instability, as an increased FEN1 level resulted in increased expansion products (Liu et al., 2009). The authors suggested that increased FEN1 expression promotes expansion by facilitating ligation of hairpins by strand slippage (Liu et al., 2009). However, in HD transgenic mice, analysis of tissue-specific levels of BER proteins showed that low levels of FEN1 expression relative to polβ in the striatum correlates with high instability in this tissue, whereas a higher FEN1: polβ ratio was evident in the relatively stable cerebellum (Goula et al., 2009). Recent *in vitro* data showing that damage in CTG/CAG repeats are less efficiently repaired in BER reconstitution experiments mimicking the stoichiometry in the striatum than those reflecting the BER levels of the cerebellum provides support for the latter study (Goula et al., 2012).

The NER pathway is involved in the removal of bulky, helix-distorting lesions. Nucleotide excision repair (NER) has also been linked with instability but there is discordance between the findings of various studies. Mutation of *uvrA,* an excision nuclease involved in NER, increased contractions of transcribed repeats in *E.coli* (Parniewski et al., 1999). Conversely, depletion of several NER genes including CSB, ERCC1 and XPG, suppressed transcription-dependent CAG contractions in a human cell line (Lin et al., 2006; Lin and Wilson, 2007). The Wilson group showed that knocking down XPC, which is specific to the global genome NER (GG-NER) did not affect instability, implying that the other branch of NER, transcription-coupled repair (TC-NER), is the relevant pathway to instability (Lin and Wilson, 2007). Indeed, knockdown of CSB, which is involved specifically in TC-NER, suppressed expansions (Lin and Wilson, 2007). Use of transgenic mice to investigate a role for NER has led to conflicting results. Mice deficient in XPA bearing 145 CAG repeats at the SCA1 locus had reduced expansions in neuronal tissues but does not alter instability in the germline (Hubert et al., 2011), whereas HD mice deficient in CSB displayed increased germline repeat expansions but no major somatic instability in the brain (Kovtun et al., 2011). The authors of the SCA1 publication point out that this may be due to differences in experimental approaches or systems. Furthermore, XPA is only known to function in NER but CSB has been shown to have roles outside of NER including chromatin remodeling and transcription (Balajee et al., 1997; Citterio et al., 2000). It is also worth noting that while the

data from the SCA1 mouse model provides considerable evidence for a causative role for NER in somatic instability, it does not distinguish between TC-NER and GG-NER as XPA is a common component to both pathways. The premise that TC-NER is involved in inducing instability is based on evidence that transcription itself is involved. In a human cell contraction-based system, transcription increases contractions by around 15-fold (Lin et al., 2006). It has been postulated that hairpins arise during repair of R-loops (RNA• DNA hybrids), which form at transcribed TNRs leading to instability (Lin et al., 2010; Nakamori et al., 2011).

To the best of my knowledge, MSH2 and MSH3 are the only proteins that have been shown to be involved in promoting both germline and somatic CAG/CTG instability. Loss of XPA suppresses instability in neuronal tissues but does not affect germline transmission (Hubert et al., 2011), while OGG1 also specifically affects somatic instability (Kovtun et al., 2007). In contrast, CSB, DNA ligase I and the DNA methyltransferase DNMT1 are implicated only in germline instability (Dion et al., 2008; Kovtun et al., 2011; Tome et al., 2011). Because MSH2 and MSH3 are causative for both types of instability, it is possible that although differential mechanisms are involved in mediating these instability events, MutSβ is common to both.

1.7 Chromatin and TNRs

1.7.1 Expanded repeats are generally associated with heterochromatin

TNR expansions occur due to the interplay between DNA and modulating proteins. A crucial unknown is how chromatin structure affects these interactions. It has been well documented that expanded TNR alleles, unlike their corresponding normal-length alleles, display alterations in chromatin structure consistent with a heterochromatic environment (Dion and Wilson, 2009). At the DM1 locus, the chromatin surrounding expanded CTG repeats (>1000) contains an enrichment in the heterochromatic mark H3K9 trimethylation and a decrease in the euchromatin-associated H3K4 trimethylation, compared to the unexpanded counterpart (Cho et al., 2005). High levels of heterochromatic marks were detected at the disease locus in FRAXA patient cells, while marks typical of euchromatic regions were reduced (Coffee et al., 1999; Coffee et al., 2002). Additionally, expanded (GAA)• (TTC) repeats at the FRDA locus showed hypoacetylation of H3 and H4 and increased trimethylation of H3K9 (Herman et al., 2006). It is proposed that the heterochromatic environment of the expanded alleles contributes to the gene silencing associated with some TNR diseases.

1.7.2 Chromatin-modifying factors and TNRs

Interestingly, several studies investigating the mechanisms of TNR expansion have identified chromatin modifying proteins as key modulators of the mutagenic process. Many TNR genes have binding sites for the insulator protein CTCF (CCCTC-binding factor) either side of the repeat tracts (Filippova et al., 2001). In a SCA7 mouse model, inhibition of CTCF binding by methylation or mutation of CTCF binding sites near the SCA7 locus resulted in increased the incidence of contractions and expansions of a $(CAG)_{92}$ tract (Libby et al., 2008). CTCF binding at two CTCF sites which flank the CTG repeat at the DM1 locus act to restrict repeat-mediated heterochromatin to the immediate repeat region (Filippova et al., 2001). In contrast, the expanded DM1 allele in cells of congenital DM1 individuals displays abrogated CTCF binding coincident with spreading of heterochromatin to neighbouring genes and localised CpG methylation (Cho et al., 2005).The mechanism though which CTCF acts to prevent expansions is uncertain but a report from the same lab implies that CTCF positively regulates DNA replication near the repeat region, thereby acting to stabilise repeats (Cleary et al., 2010). Work in transgenic mice and mammalian cell lines has illustrated a role for the DNA methyltransferase that performs faithful maintenance of DNA methylation at CpG sites, DNMT1, in TNR instability. Chemical inhibition of DNMT1 activity and genome-wide methylation levels in CHO cells resulted in increases in contraction frequency as high as 1000-fold for (CTG)• (CAG) tracts of 61 and 95, while expansions were increased in DM1 patient fibroblasts (Gorbunova et al., 2004). Furthermore, germline but not somatic expansions of $(CAG)_{145}$ were enhanced in *Dnmt1*$^{+/-}$ SCA1 mice (Dion et al., 2008). The authors reported some subtle alterations in DNA methylation and local chromatin structure with increased DNA methylation and H3K9 methylation near the repeats indicative of heterochromatin but did not observe any corresponding change in histone acetylation. These data imply a role for methylation in TNR instability but no specific mechanisms have been identified.

Studies in fly and yeast have identified roles for HATs in repeat instability. Haploinsufficiency of the histone acetyltransferase (HAT), CBP, increased intergenerational $(CTG)_{78}$ repeat expansions in a SCA3 *Drosophila* model, whereas treatment with TSA resulted in a decrease in TNR expansions (Jung and Bonini, 2007). These data infer that CBP normally stabilises repeats, and some unknown HDAC(s) act in an opposing manner to promote expansions. Although global levels of histone H3 and H4 acetylation were found to be altered in this study, no changes were detected in the vicinity of the repeat, suggesting that the effects of histone acetylation on instability are likely direct. In yeast, loss of the HAT Rtt109 enhanced contractions of a CAG_{85} repeat tract by 3.3-fold with no detectable impact on expansions (Yang and Freudenreich, 2010). Double strand break (DSB) repair

was found to partially contribute to the generation of some contractions in *rtt109* mutants. The authors propose that Rtt109-catalysed H3K56 acetylation is important for proper nucleosome assembly at the replication fork to prevent aberrant secondary structures that might lead to contractions (Schneider et al., 2006). Repeat-localised measurements of histone acetylation status were not determined so it is unclear whether chromatin structure at the repeats is directly mediating the instability or the effects are wholly through an indirect mechanism. Although there is an increasing collection of evidence pointing toward proteins that influence chromatin structure being important in controlling TNR instability, no clear mechanisms have been described.

1.8 HDACs

In Chapter 3, investigations focus on the involvement of HDACs in instability so I provide some detail on these chromatin-modifiers here. Histone acetylation has been extensively studied since it was first discovered in 1964 that levels of histone acetylation correlated with gene activation (Allfrey et al., 1964). This status of this modification is controlled by the opposing action of HATs, which catalyse the addition of acetyl groups typically leading to an increase in gene transcription due to the resultant open chromatin structure, and HDACs, which mediate removal of acetyl groups often leading to gene expression silencing determined by the consequential closed chromatin structure. A dynamic balance between HAT and HDAC activities is proposed to govern gene expression. 18 HDACs have been identified in humans to date and they are grouped into four classes based on their homology to yeast HDACs (Fig 1.9) (de Ruijter et al., 2003; Yang and Seto, 2008; d'Ydewalle et al., 2012). Class I HDACs include HDAC1, 2, 3 and 8 and are most closely related to yeast Rpd3, the first HDAC described in yeast. HDAC1, 2 and 3 are ubiquitously expressed in most tissues, while HDAC8 expression is limited to smooth muscle (Waltregny et al., 2005). With the exception of HDAC3, all class I HDACs are predominantly localized to the nucleus due to the lack of a nuclear export signal (NES) (de Ruijter et al., 2003).

Class II HDACs have a more complex domain structure than class I HDACs, and are related to the yeast HDAC, Hda1. Unlike class I HDACs, expression of class II HDACs is tissue-restricted. Class IIa comprises HDAC4, HDAC5, HDAC7 and HDAC9, which shuttle between the cytoplasm and nucleus. It has been shown that the HDAC domains of HDAC4, HDAC5 and HDAC7 do not harbour enzymatic activity, but instead mediate HDAC activity by interacting with HDAC3 (Fischle et al., 2002). Furthermore, class IIa enzymes have been shown to bind acetyllysine peptides but fail to deacetylate acetyllysine (Bradner et al., 2010), implying that class IIa HDACs might bind acetyllysine residues and recruit HDAC3 to execute deacetylation. Class IIb includes HDAC6 and HDAC10, which are characterized by

two HDAC domains, although only one is known to be functional for HDAC10 (Guardiola and Yao, 2002). HDAC11 is the sole member of class IV. Little is known of its biological function and on the basis of lack of catalytic domain homology, it has not been classified as class I or II. Class I, II and IV HDACs contain a zinc molecule at the active site, which is critical for enzymatic acitivity. In contrast class III HDACs (sirtuins 1-7), which are homologous to yeast Sir2, do not depend on zinc, but instead catalyse deacetylation in a NAD^+-dependent manner (Yang and Seto, 2008).

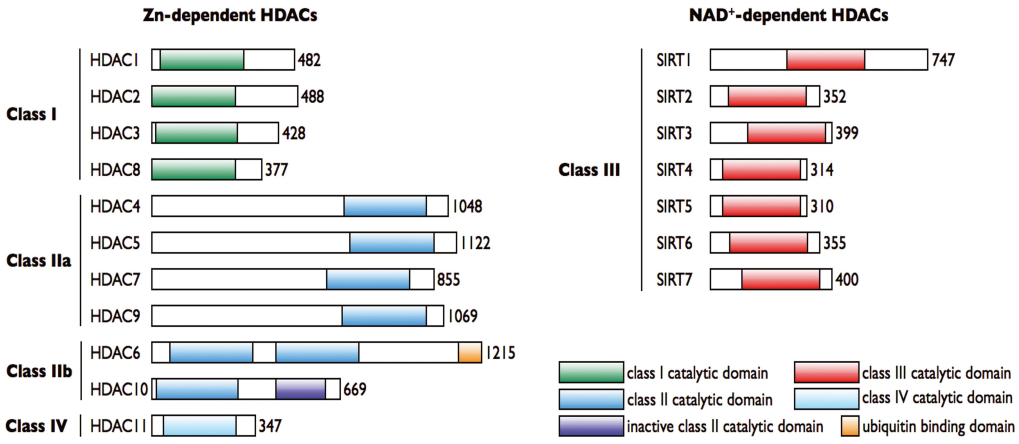

Figure 1.9 Classification of the 18 human HDACs. HDACs are grouped into classes I-IV based on their homology to yeast. HDACs sizes are shown in amino acid to the right of each HDAC. From (d'Ydewalle et al., 2012)

In addition to their role in histone-mediated chromatin remodeling, HDACs can deacetylate many non-histone proteins including transcription factors, chaperones, hormone receptors, signaling factors and cytoskeletal proteins (Yang and Seto, 2008). In fact, phylogenetic data from bacterial HDACs imply that histones evolved subsequent to HDAC evolution raising the possibility that histones may not be the primary targets of some HDACs (Gregoretti et al., 2004).

1.9 HDAC inhibitors as a potential treatment for TNR diseases

HDAC inhibitors are being investigated as potential therapeutic agents in the treatment of some TNR diseases by amelioration of the associated aberrant gene expression effects (Butler and Bates, 2006). Many TNR diseases are caused by down-regulation of normal transcription of one or more genes as a result of TNR expansion e.g. for Freidreich's ataxia, expansion of GAA repeats at the FRDA locus into the disease range results in formation of heterochromatin and a subsequent silencing of frataxin expression (Herman et al., 2006; De Biase et al., 2009). For HD, the transcriptional repercussions of pathologically relevant CAG

expansions are more indirect. The expanded polyglutamine sequence of mHTT sequesters a number of important transcription factors including the HAT and transcriptional co-activator, CBP, and thereby precludes their normal role in mediating gene expression (Fig. 1.10) (Kazantsev et al., 1999; McCampbell et al., 2000; Steffan et al., 2000). Furthermore, mHTT can alter posttranslational modifications of histones promoting the advent of heterochromatic structure (Steffan et al., 2001; Stack et al., 2007). Microarray studies of the brains of HD patients and R6/2 HD mice highlight the transcriptional dysfunction, with many genes being downregulated (Luthi-Carter et al., 2002; Hodges et al., 2006). In light of this transcriptional dysregulation, HDAC inhibitors seem like promising therapeutic candidates for treating these disorders.

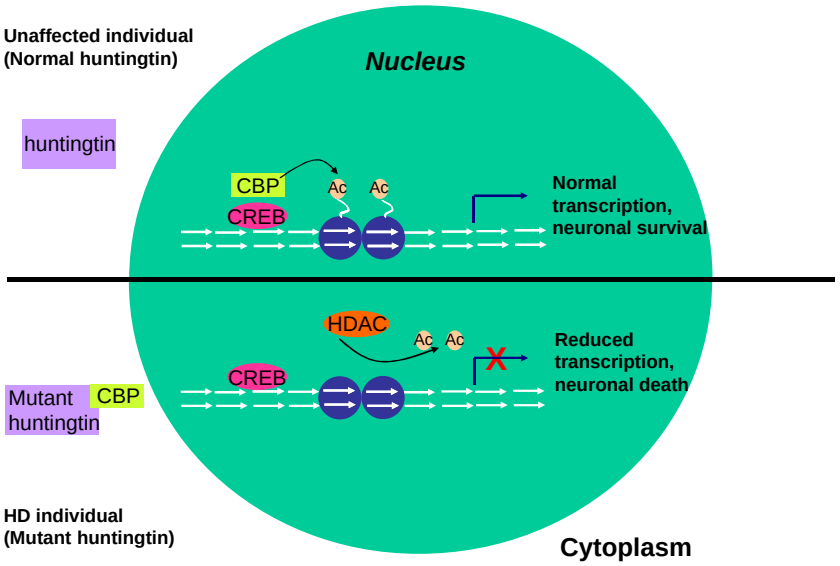

Figure 1.10 Transcription defects in HD. The wild type protein, which is predominantly located in the nucleus, does not interfere with the histone acetyltransferase CBP binding to CREB. CBP, increases basal transcription levels by interacting with transcription factors and acetylates histones of neuronal genes, which leads to higher levels of transcription overall. Thus, in normal individuals CBP acts to promote the transcription of key genes that facilitate neuronal health and survival. In cells affected by HD, the mutant huntingtin binds CBP and sequesters it into protein aggregates. This sequestered CBP is then redistributed away from its normal nuclear location. This results in an overall decrease in histone acetylation due to the balance being shifted in favour of HDACs, which leads to decreased transcription and eventual neurodegeneration. Image adapted from http://www.biocarta.com/pathfiles/h_huntingtonpathway.asp.

Various models of HD including *Drosophila* and mouse have been shown to respond beneficially to treatment with non-specific HDAC inhibitors. The class I and II HDAC inhibitors suberoylanilide hydroxamic acid (SAHA) and sodium butyrate suppressed

neuronal degeneration in a *Drosophila* model of HD (Steffan et al., 2001). In the R6/2 HD mouse model, administration of SAHA elevated histone acetylation levels in the brain and improved motor function (Hockly et al., 2003). Treatment of R6/2 mice with sodium butyrate improved motor performance, survival and increased histone H4 acetylation when administered presymptomatically (Ferrante et al., 2003). Phenylbutyrate, a class I and II inhibitor, attenuated brain atrophy and effected a increase in histone acetylation and a decrease in H3K9 methylation in N171-82Q HD mice (Gardian et al., 2005). In addition to HD, beneficial effects were reported in mouse models of spinobulbar muscular atropy, DRPLA and spinocerebellar ataxia type 3 following treatment with sodium butyrate (Minamiyama et al., 2004; Ying et al., 2006; Chou et al., 2011). While pan-HDAC inhibitors have proved useful, these compounds are often limited by their toxicity, probably resulting from their non-selective nature (Kazantsev and Thompson, 2008). Development of isoform-specific HDAC inhibitors has been ongoing in order to reduce toxicity and to perhaps avoid isoforms that are unrelated to disease, or even beneficial. A HDAC3-selective inhibitor, 4b, was found to delay weight loss, improve motor function and reduce brain atrophy in the R6/2 HD mouse model, with minimal cell cytotoxicity and apoptotic effects reported for this molecule at doses much higher than that required for effective enzyme inhibition (Thomas et al., 2008). In addition to ameliorating the disease phenotype, 4b reversed several transcriptional deficits and increased H3 acetylation in the brain. HDAC1- and HDAC3-specific inhibitors, including 4b, were effective in rescuing eye neurodegeneration in a *Drosophila* model of HD and improving metabolic defects associated with mHTT in immortalized cells from striatal tissue of *HdhQ111* knock-in mice (Jia et al., 2012). 4b was also shown to increase H3 and H4 acetylation in the frataxin gene upstream of the GAA repeats and to elevate frataxin mRNA levels 2.5-fold in FRDA primary lymphocytes, effects not recapitulated by the SAHA or Trichostatin A (TSA), pan-HDAC inhibitors (Herman et al., 2006). Recently it was shown that HDAC3$^{+/-}$ mice crossed with R6/2 HD mice did not show any improvement in behavioural and molecular phenotypes (Moumne et al., 2012). However, these mice retained 60% of HDAC3 protein level in the brain, which might not be sufficient to reveal HDAC3-dependent effects (Moumne et al., 2012).

It is evident that HDACs represent potential pharmacological targets in treatment of TNR diseases but whether specific HDACs have any effect on the process repeat instability is unknown. Intriguingly, a yeast screen performed in the Lahue lab to identify factors that promote expansion of (CTG)• (CAG) repeats near the threshold generated 3 of 11 hits as components of HDAC complexes, namely *SIN3*, *PHO23*, and *HDA3,* an enrichment of ~100-fold compared to random chance (Debacker et al., 2012). *SIN3* encodes a subunit of HDACs Rpd3L and Rpd3S, whereas the subunit encoded by *PHO23* is unique to Rpd3L.

HDA3 encodes a subunit of another HDAC, Hda1. Genetic mutation or chemical inhibition of yeast Rpd3L or Hda1 suppressed expansions by up to 90%. Considering this evidence and the growing body of evidence for chromatin modifying factors being implicated in instability, I decided to investigate the role of specific HDACs in promoting expansions near the threshold length in human cells (Chapter 3). To this end, isoform-specific HDAC inhibitors and HDAC-targeted siRNA were used to interfere with individual HDACs to identify relevant players. The small molecule HDAC inhibitors used were 4b, which I alluded to earlier, and compound 3, which is selective for HDAC1 (Fig 1.11).

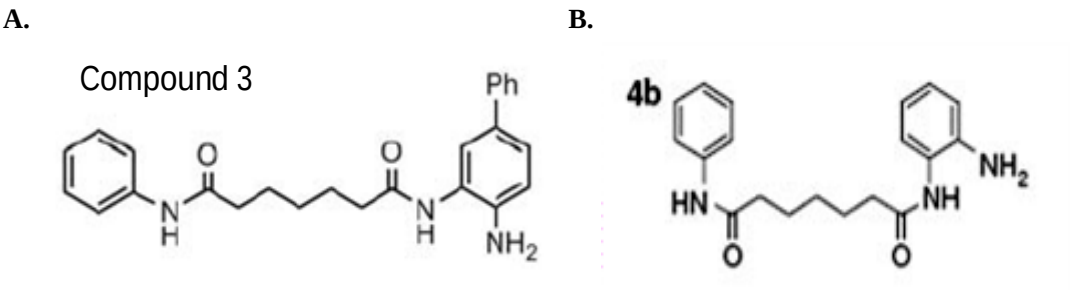

Figure 1.11 Chemical structure of small molecule HDAC inhibitors, compound 3 and 4b. A. HDAC1/2-specific inhibitor, compound 3 (Xu et al., 2009) B. HDAC3-specific inhibitor, 4b (Herman et al., 2006).

1.10 Using cultured human astrocytes as a model for instability

The cell line used in this study is an astrocytic cell line, SVG-A, derived from primary human glial cells, and immortalized by origin defective simian tumour virus 40 (Major et al., 1985). Astrocytes outnumber non-dividing neurons in the brain. Their functions are manifold and include promoting neuronal survival, elimination of glutamate and other toxic substances and regulation of the blood-brain barrier in the CNS (Hsiao and Chern, 2010). SVG-A cells are relevant to the study of instability as the brain is a major source of TNR instability. Several studies in humans and transgenic mice showing age-dependent increases in TNR length in the central nervous system (CNS) are based on evidence from terminally differentiated neurons (Kovtun et al., 2007; Shelbourne et al., 2007). Consequently, some of these studies suggest that non-replicative repair is the main mechanism for induction of TNR instability. However, the affected brain regions include neuronal cells and cells that maintain replicative capacity, such as astrocytes and microglia; the samples analysed contain non-neuronal cells also. Additionally, somatic expansions have been observed in glia in human and mouse HD brain tissue and it has been shown using laser capture microdissection that glia exhibit the greatest instability in DRPLA patients (Watanabe et al., 2000; Kovtun et al.,

2007). This indicates that instability in glial populations might contribute to TNR disease pathogenesis, particularly in light of the proposed role of astrocytes in HD.

Although neuronal death is considered to be the crucial event in HD pathogenesis, there is mounting evidence that glia also contribute to neuronal dysfunction in HD. Glial cells from HD patients have been shown to express mutant huntingtin (Singhrao et al., 1998; Shin et al., 2005), implying a role in HD neuropathology. Expression of mutant huntingtin (mHTT) in astrocytes of transgenic mice elicited age-dependent neurological symptoms (Bradford et al., 2009). Mice expressing mHTT in both neuronal and glial cells have an exacerbated disease phenotype than those expressing mHTT predominantly in neuronal cells (Bradford et al., 2010). The mechanism underlying the apparent role of astrocytes in HD pathogenesis is under investigation. It was found that glial mHTT resulted in an increased susceptibility of neurons to glutamate excitotoxicity (Lievens et al., 2001; Shin et al., 2005). Medium spiny neurons in the striatum, which are progressively lost in HD, are especially vulnerable to glutamate-induced cell-death due to being innervated by glutamatergic neurons. In addition, it has been shown that glial mHTT suppresses the transcription and release of the chemokine CCL5/RANTES in astrocytes of R6/2 mice (Chou et al., 2008). It is thought that decreased availability of this chemokine to neurons results in altered neuronal properties and impaired motor coordination (Hsiao and Chern, 2010). Brain-derived neurotrophic factor (BDNF) is proposed to protect striatal neurons from excitotoxicity, which contributes to their degeneration in HD (Perez-Navarro et al., 2000). Interestingly, primary astrocytes expressing mHTT secreted less BDNF than astrocytes expressing wild-type HTT, most likely due to disruptions in BDNF processing by the Golgi apparatus (Wang et al., 2012). This reduction of BDNF in astrocytes in the HD model might decrease its availability to neurons and may lead to neurodenegeration. Regardless of the underlying mechanism of astrocytes in HD pathogenesis, the evident biological relevance suggests that instability in glia is likely to be important in elucidating molecular mechanisms contributing to TNR disease pathogenesis. Thus, the SVG-A cell line can be considered a useful model for investigating disease-relevant instability.

SVG-A cells are amenable to routine cell culture techniques such as RNA interference and plasmid transfection and have been shown to exhibit instability, in the form of both contractions and expansions (Farrell and Lahue, 2006; Claassen and Lahue, 2007). The selective nature of the assay (Farrell and Lahue, 2006; Claassen and Lahue, 2007) (described in Chapter 2) facilitates measurement of length changes in short alleles. Transgenic mouse models for TNR instability typically use long alleles (~84-300 repeats). Assays to measure expansion in mice typically employ measurement of alleles by non-selective methods such

as PCR or Southern blot, which require frequent expansion to allow measurement due to a lack of sensitivity attributed to these methods. Additionally, although these mice tend to display a trend towards expansion, both somatically and inter-generationally, the threshold seems to be higher than for humans. For example, a transgenic mouse containing full-length human HD cDNA with 44 CAG repeats, (disease-length) did not exhibit any instability over several generations (Goldberg et al., 1996). A DM1 transgenic mouse model harbouring a 45-kb genomic segment with a $(CTG)_{55}$ tract showed mild somatic and germline instability, with changes in length being no more than +/-7 which is much lower than expected for the equivalent tract in humans (Gourdon et al., 1997) providing further evidence for mice having a higher threshold for instability than humans. Because mouse models fail to recapitulate a threshold for instability, this is suggestive of differential regulatory factors governing instability in humans and mice, underscoring the importance of human cells for studies on the stability of TNRs. Thus, transgenic mice are particularly useful for investigating the molecular mechanism that drive long, disease-causing alleles to become even longer but they are not applicable for measuring the infrequent expansions crossing the threshold are critical initiating mutations leading to further instability and disease. The SVG-A system has detected expansions in this region of the mutation spectrum (Claassen and Lahue, 2007).

A limitation in the field of TNR instability is the lack of human cell systems in existence to study expansions in cells that are biologically relevant to the incidence of disease. Several studies use fibroblast and lymphoblast cell lines derived from patients to model instability. The use of such cells where instability is typically very low in patients raises the issue of whether they are pathogenically relevant. For example, fibroblasts from HD patients are stable in culture (Kovtun et al., 2004). Additionally, CTG repeat tracts were stably maintained in cultured embryonic fibroblasts from DM1 mice (Gomes-Pereira et al., 2001). Additionally patient cell lines, like mice, often use long TNR tracts to ensure that instability is high enough to be detected by PCR or Southern blotting. While these physical methods are suitable when the mutation frequency is high, as in affected families (Fu et al., 1991), they do not provide sufficient sensitivity for the lower frequency events such as those near the threshold.

Use of SVG-A cells allows measurement of somatic instability. The magnitude of expansions observed using this system is more consistent with polyglutamine diseases rather than disorders of the non-coding class. Thus, it is a suitable model for investigating mechanisms underlying polyglutamine disorders but does not recapitulate large-scale expansions such as those observed in DM1. One major advantage of the shuttle vector assay in SVG-A cells is that it permits detection of single expansion events due to its genetic,

selective nature. This system is highly amenable to siRNA and plasmid transfection. Furthermore, it has been shown to recapitulate length- and sequence-dependence instability associated with TNR mutagenesis (Farrell and Lahue, 2006; Claassen and Lahue, 2007). The SVG-A system does have intrinsic shortcomings. Because SVG-A cells are SV40-transformed, certain DNA metabolic processes are altered, which might unduly influence repeat instability. The starting length of the repeat tract is limited to normal/near-threshold length so it is not applicable for analysis of disease length repeats. Additionally the non-chromosomal nature of the shuttle vector precludes examination of chromosomal, endogenous sequences flanking the repeat that might influence instability.

1.11 Thesis Objectives

In light of some the unanswered questions regarding TNR mutagenesis mentioned in this introduction, the study described in this thesis attempts to shed light on some key issues. Accordingly, the work presented addresses the role of candidate *trans*-acting factors and contribute to an understanding of the mechanisms underlying TNR instability.

1. HDACs and HATs contribute to the modulation TNR expansions

Yeast studies in the Lahue lab yeast work identified key HDAC components involved in facilitating expansions (Debacker et al., 2012). Chapter 3 describes experiments that investigate the role of numerous HDACs for a role in TNR instability in human cells. The results presented imply that certain HDACs, namely HDAC3 and HDAC5, promote expansions of repeat tracts near the threshold in human cells. The novel finding that acetylation is involved in TNR expansion is further supported by evidence for the HATs CBP and p300 acting to inhibit expansions. The involvement of specific HDACs in promoting expansions is consistent with preceding yeast data.

2. MutSβ and HDAC3 and HDAC5 appear to act in a shared pathway to promote expansions

MutSβ has been shown in several mouse models to promote expansions of disease-length repeats. As I discussed previously, it was unknown whether this would be applicable to expansion of shorter repeat tracts. Evidence presented in Chapter 4 implies that MutSβ also promotes this type of expansion. Additionally, I show a functional interaction between HDAC3 and MSH2 in promoting expansions. The nature of this interaction is addressed experimentally but remains unknown.

3. RTEL1 and PRR factors prevent expansions in a concerted manner

Work in the Lahue lab indicated that Srs2 works with PRR to inhibit expansions in yeast. A model for this suggests yeast Srs2 acts with PRR to target TNR hairpins for unwinding to prevent inhibiting expansions. Chapter 5 describes investigations of human orthologues of Srs2, namely RTEL1 and FBH1, and PRR proteins, SHPRH, HLTF and RAD18 with respect to TNR expansions. Interestingly, this work yielded results consistent with the idea that RTEL1, HLTF and RAD18 work together to inhibit expansions. Biochemical analysis of RTEL1 action by collaborators suggests that it unwinds TNR substrates predicted to form hairpins, similarly to Srs2. We suggest that RTEL1 might be targeted to the TNR hairpin where it resolves the structure preventing the occurrence of an expansion.

1.12 References

Aguilera, A. and H. L. Klein (1988). Genetic control of intrachromosomal recombination in Saccharomyces cerevisiae. I. Isolation and genetic characterization of hyper-recombination mutations. *Genetics* **119**(4): 779-90.

Aladjem, M. I., L. W. Rodewald, J. L. Kolman and G. M. Wahl (1998). Genetic dissection of a mammalian replicator in the human beta-globin locus. *Science* **281**(5379): 1005-9.

Allfrey, V. G., R. Faulkner and A. E. Mirsky (1964). Acetylation and Methylation of Histones and Their Possible Role in the Regulation of Rna Synthesis. *Proc Natl Acad Sci U S A* **51**: 786-94.

Balajee, A. S., A. May, G. L. Dianov, E. C. Friedberg and V. A. Bohr (1997). Reduced RNA polymerase II transcription in intact and permeabilized Cockayne syndrome group B cells. *Proc Natl Acad Sci U S A* **94**(9): 4306-11.

Barber, L. J., J. L. Youds, J. D. Ward, M. J. McIlwraith, N. J. O'Neil, M. I. Petalcorin, J. S. Martin, S. J. Collis, S. B. Cantor, M. Auclair, H. Tissenbaum, S. C. West, A. M. Rose and S. J. Boulton (2008). RTEL1 maintains genomic stability by suppressing homologous recombination. *Cell* **135**(2): 261-71.

Bhattacharyya, S. and R. S. Lahue (2004). Saccharomyces cerevisiae Srs2 DNA helicase selectively blocks expansions of trinucleotide repeats. *Mol Cell Biol* **24**(17): 7324-30.

Bhattacharyya, S. and R. S. Lahue (2005). Srs2 helicase of Saccharomyces cerevisiae selectively unwinds triplet repeat DNA. *J Biol Chem* **280**(39): 33311-7.

Bradford, J., J. Y. Shin, M. Roberts, C. E. Wang, X. J. Li and S. Li (2009). Expression of mutant huntingtin in mouse brain astrocytes causes age-dependent neurological symptoms. *Proc Natl Acad Sci U S A* **106**(52): 22480-5.

Bradford, J., J. Y. Shin, M. Roberts, C. E. Wang, G. Sheng, S. Li and X. J. Li (2010). Mutant huntingtin in glial cells exacerbates neurological symptoms of Huntington disease mice. *J Biol Chem* **285**(14): 10653-61.

Bradner, J. E., N. West, M. L. Grachan, E. F. Greenberg, S. J. Haggarty, T. Warnow and R. Mazitschek (2010). Chemical phylogenetics of histone deacetylases. *Nat Chem Biol* **6**(3): 238-243.

Braida, C., R. K. Stefanatos, B. Adam, N. Mahajan, H. J. Smeets, F. Niel, C. Goizet, B. Arveiler, M. Koenig, C. Lagier-Tourenne, J. L. Mandel, C. G. Faber, C. E. de Die-Smulders, F. Spaans and D. G. Monckton (2010). Variant CCG and GGC repeats within the CTG expansion dramatically modify mutational dynamics and likely contribute toward unusual symptoms in some myotonic dystrophy type 1 patients. *Hum Mol Genet* **19**(8): 1399-412.

Butland, S. L., R. S. Devon, Y. Huang, C. L. Mead, A. M. Meynert, S. J. Neal, S. S. Lee, A. Wilkinson, G. S. Yang, M. M. Yuen, M. R. Hayden, R. A. Holt, B. R. Leavitt and B. F. Ouellette (2007). CAG-encoded polyglutamine length polymorphism in the human genome. *BMC Genomics* **8**: 126.

Butler, R. and G. P. Bates (2006). Histone deacetylase inhibitors as therapeutics for polyglutamine disorders. *Nat Rev Neurosci* **7**(10): 784-96.

Chiolo, I., M. Saponaro, A. Baryshnikova, J. H. Kim, Y. S. Seo and G. Liberi (2007). The human F-Box DNA helicase FBH1 faces Saccharomyces cerevisiae Srs2 and postreplication repair pathway roles. *Mol Cell Biol* **27**(21): 7439-50.

Cho, D. H., C. P. Thienes, S. E. Mahoney, E. Analau, G. N. Filippova and S. J. Tapscott (2005). Antisense transcription and heterochromatin at the DM1 CTG repeats are constrained by CTCF. *Mol Cell* **20**(3): 483-9.

Chong, S. S., A. E. McCall, J. Cota, S. H. Subramony, H. T. Orr, M. R. Hughes and H. Y. Zoghbi (1995). Gametic and somatic tissue-specific heterogeneity of the expanded SCA1 CAG repeat in spinocerebellar ataxia type 1. *Nat Genet* **10**(3): 344-50.

Chou, A. H., S. Y. Chen, T. H. Yeh, Y. H. Weng and H. L. Wang (2011). HDAC inhibitor sodium butyrate reverses transcriptional downregulation and ameliorates ataxic symptoms in a transgenic mouse model of SCA3. *Neurobiol Dis* **41**(2): 481-8.

Chou, S. Y., J. Y. Weng, H. L. Lai, F. Liao, S. H. Sun, P. H. Tu, D. W. Dickson and Y. Chern (2008). Expanded-polyglutamine huntingtin protein suppresses the secretion and production of a chemokine (CCL5/RANTES) by astrocytes. *J Neurosci* **28**(13): 3277-90.

Citterio, E., V. Van Den Boom, G. Schnitzler, R. Kanaar, E. Bonte, R. E. Kingston, J. H. Hoeijmakers and W. Vermeulen (2000). ATP-dependent chromatin remodeling by the Cockayne syndrome B DNA repair-transcription-coupling factor. *Mol Cell Biol* **20**(20): 7643-53.

Claassen, D. A. and R. S. Lahue (2007). Expansions of CAG.CTG repeats in immortalized human astrocytes. *Hum Mol Genet* **16**(24): 3088-96.

Cleary, J. D., K. Nichol, Y. H. Wang and C. E. Pearson (2002). Evidence of cis-acting factors in replication-mediated trinucleotide repeat instability in primate cells. *Nat Genet* **31**(1): 37-46.

Cleary, J. D. and C. E. Pearson (2003). The contribution of cis-elements to disease-associated repeat instability: clinical and experimental evidence. *Cytogenet Genome Res* **100**(1-4): 25-55.

Cleary, J. D., S. Tome, A. Lopez Castel, G. B. Panigrahi, L. Foiry, K. A. Hagerman, H. Sroka, D. Chitayat, G. Gourdon and C. E. Pearson (2010). Tissue- and age-specific DNA replication patterns at the CTG/CAG-expanded human myotonic dystrophy type 1 locus. *Nat Struct Mol Biol* **17**(9): 1079-87.

Coffee, B., F. Zhang, S. Ceman, S. T. Warren and D. Reines (2002). Histone modifications depict an aberrantly heterochromatinized FMR1 gene in fragile x syndrome. *Am J Hum Genet* **71**(4): 923-32.

Coffee, B., F. Zhang, S. T. Warren and D. Reines (1999). Acetylated histones are associated with FMR1 in normal but not fragile X-syndrome cells. *Nat Genet* **22**(1): 98-101.

Cummings, C. J. and H. Y. Zoghbi (2000). Fourteen and counting: unraveling trinucleotide repeat diseases. *Hum Mol Genet* **9**(6): 909-16.

d'Ydewalle, C., E. Bogaert and L. Van Den Bosch (2012). HDAC6 at the Intersection of Neuroprotection and Neurodegeneration. *Traffic*.

Daee, D. L., T. Mertz and R. S. Lahue (2007). Postreplication repair inhibits CAG.CTG repeat expansions in Saccharomyces cerevisiae. *Mol Cell Biol* **27**(1): 102-10.

Day, J. W. and L. P. Ranum (2005). Genetics and molecular pathogenesis of the myotonic dystrophies. *Curr Neurol Neurosci Rep* **5**(1): 55-9.

De Biase, I., Y. K. Chutake, P. M. Rindler and S. I. Bidichandani (2009). Epigenetic silencing in Friedreich ataxia is associated with depletion of CTCF (CCCTC-binding factor) and antisense transcription. *PLoS One* **4**(11): e7914.

de Ruijter, A. J., A. H. van Gennip, H. N. Caron, S. Kemp and A. B. van Kuilenburg (2003). Histone deacetylases (HDACs): characterization of the classical HDAC family. *Biochem J* **370**(Pt 3): 737-49.

Debacker, K., A. Frizzell, O. Gleeson, L. Kirkham-McCarthy, T. Mertz and R. S. Lahue (2012). Histone deacetylase complexes promote trinucleotide repeat expansions. *PLoS Biol* **10**(2): e1001257.

Dhar, A. and R. S. Lahue (2008). Rapid unwinding of triplet repeat hairpins by Srs2 helicase of Saccharomyces cerevisiae. *Nucleic Acids Res* **36**(10): 3366-73.

Dion, V., Y. Lin, L. Hubert, Jr., R. A. Waterland and J. H. Wilson (2008). Dnmt1 deficiency promotes CAG repeat expansion in the mouse germline. *Hum Mol Genet* **17**(9): 1306-17.

Dion, V. and J. H. Wilson (2009). Instability and chromatin structure of expanded trinucleotide repeats. *Trends Genet* **25**(7): 288-97.

Eichler, E. E., J. J. Holden, B. W. Popovich, A. L. Reiss, K. Snow, S. N. Thibodeau, C. S. Richards, P. A. Ward and D. L. Nelson (1994). Length of uninterrupted CGG repeats determines instability in the FMR1 gene. *Nat Genet* **8**(1): 88-94.

Entezam, A., A. R. Lokanga, W. Le, G. Hoffman and K. Usdin (2010). Potassium bromate, a potent DNA oxidizing agent, exacerbates germline repeat expansion in a fragile X premutation mouse model. *Hum Mutat* **31**(5): 611-6.

Ezzatizadeh, V., R. M. Pinto, C. Sandi, M. Sandi, S. Al-Mahdawi, H. Te Riele and M. A. Pook (2012). The mismatch repair system protects against intergenerational GAA repeat instability in a Friedreich ataxia mouse model. *Neurobiol Dis* **46**(1): 165-71.

Farrell, B. T. and R. S. Lahue (2006). CAG*CTG repeat instability in cultured human astrocytes. *Nucleic Acids Res* **34**(16): 4495-505.

Ferrante, R. J., J. K. Kubilus, J. Lee, H. Ryu, A. Beesen, B. Zucker, K. Smith, N. W. Kowall, R. R. Ratan, R. Luthi-Carter and S. M. Hersch (2003). Histone deacetylase inhibition by sodium butyrate chemotherapy ameliorates the neurodegenerative phenotype in Huntington's disease mice. *J Neurosci* **23**(28): 9418-27.

Filippova, G. N., C. P. Thienes, B. H. Penn, D. H. Cho, Y. J. Hu, J. M. Moore, T. R. Klesert, V. V. Lobanenkov and S. J. Tapscott (2001). CTCF-binding sites flank CTG/CAG repeats and form a methylation-sensitive insulator at the DM1 locus. *Nat Genet* **28**(4): 335-43.

Fischle, W., F. Dequiedt, M. J. Hendzel, M. G. Guenther, M. A. Lazar, W. Voelter and E. Verdin (2002). Enzymatic activity associated with class II HDACs is dependent on a multiprotein complex containing HDAC3 and SMRT/N-CoR. *Mol Cell* **9**(1): 45-57.

Foiry, L., L. Dong, C. Savouret, L. Hubert, H. te Riele, C. Junien and G. Gourdon (2006). Msh3 is a limiting factor in the formation of intergenerational CTG expansions in DM1 transgenic mice. *Hum Genet* **119**(5): 520-6.

Fojtik, P. and M. Vorlickova (2001). The fragile X chromosome (GCC) repeat folds into a DNA tetraplex at neutral pH. *Nucleic Acids Res* **29**(22): 4684-90.

Freudenreich, C. H., S. M. Kantrow and V. A. Zakian (1998). Expansion and length-dependent fragility of CTG repeats in yeast. *Science* **279**(5352): 853-6.

Freudenreich, C. H., J. B. Stavenhagen and V. A. Zakian (1997). Stability of a CTG/CAG trinucleotide repeat in yeast is dependent on its orientation in the genome. *Mol Cell Biol* **17**(4): 2090-8.

Fu, Y. H., D. P. Kuhl, A. Pizzuti, M. Pieretti, J. S. Sutcliffe, S. Richards, A. J. Verkerk, J. J. Holden, R. G. Fenwick, Jr., S. T. Warren and et al. (1991). Variation of the CGG repeat at the fragile X site results in genetic instability: resolution of the Sherman paradox. *Cell* **67**(6): 1047-58.

Fu, Y. H., A. Pizzuti, R. G. Fenwick, Jr., J. King, S. Rajnarayan, P. W. Dunne, J. Dubel, G. A. Nasser, T. Ashizawa, P. de Jong and et al. (1992). An unstable triplet repeat in a gene related to myotonic muscular dystrophy. *Science* **255**(5049): 1256-8.

Gacy, A. M., G. Goellner, N. Juranic, S. Macura and C. T. McMurray (1995). Trinucleotide repeats that expand in human disease form hairpin structures in vitro. *Cell* **81**(4): 533-40.

Gacy, A. M., G. M. Goellner, C. Spiro, X. Chen, G. Gupta, E. M. Bradbury, R. B. Dyer, M. J. Mikesell, J. Z. Yao, A. J. Johnson, A. Richter, S. B. Melancon and C. T. McMurray (1998). GAA instability in Friedreich's Ataxia shares a common, DNA-directed and intraallelic mechanism with other trinucleotide diseases. *Mol Cell* **1**(4): 583-93.

Gangavarapu, V., L. Haracska, I. Unk, R. E. Johnson, S. Prakash and L. Prakash (2006). Mms2-Ubc13-dependent and -independent roles of Rad5 ubiquitin ligase in postreplication repair and translesion DNA synthesis in Saccharomyces cerevisiae. *Mol Cell Biol* **26**(20): 7783-90.

Gardian, G., S. E. Browne, D. K. Choi, P. Klivenyi, J. Gregorio, J. K. Kubilus, H. Ryu, B. Langley, R. R. Ratan, R. J. Ferrante and M. F. Beal (2005). Neuroprotective effects of phenylbutyrate in the N171-82Q transgenic mouse model of Huntington's disease. *J Biol Chem* **280**(1): 556-63.

Goellner, G. M., D. Tester, S. Thibodeau, E. Almqvist, Y. P. Goldberg, M. R. Hayden and C. T. McMurray (1997). Different mechanisms underlie DNA instability in Huntington disease and colorectal cancer. *Am J Hum Genet* **60**(4): 879-90.

Goldberg, Y. P., M. A. Kalchman, M. Metzler, J. Nasir, J. Zeisler, R. Graham, H. B. Koide, J. O'Kusky, A. H. Sharp, C. A. Ross, F. Jirik and M. R. Hayden (1996). Absence of disease phenotype and intergenerational stability of the CAG repeat in transgenic mice expressing the human Huntington disease transcript. *Hum Mol Genet* **5**(2): 177-85.

Gomes-Pereira, M., M. T. Fortune, L. Ingram, J. P. McAbney and D. G. Monckton (2004). Pms2 is a genetic enhancer of trinucleotide CAG.CTG repeat somatic mosaicism: implications for the mechanism of triplet repeat expansion. *Hum Mol Genet* **13**(16): 1815-25.

Gomes-Pereira, M., M. T. Fortune and D. G. Monckton (2001). Mouse tissue culture models of unstable triplet repeats: in vitro selection for larger alleles, mutational expansion bias and tissue specificity, but no association with cell division rates. *Hum Mol Genet* **10**(8): 845-54.

Gomes-Pereira, M. and D. G. Monckton (2004). Chemically induced increases and decreases in the rate of expansion of a CAG*CTG triplet repeat. *Nucleic Acids Res* **32**(9): 2865-72.

Gonitel, R., H. Moffitt, K. Sathasivam, B. Woodman, P. J. Detloff, R. L. Faull and G. P. Bates (2008). DNA instability in postmitotic neurons. *Proc Natl Acad Sci U S A* **105**(9): 3467-72.

Gorbunova, V., A. Seluanov, D. Mittelman and J. H. Wilson (2004). Genome-wide demethylation destabilizes CTG.CAG trinucleotide repeats in mammalian cells. *Hum Mol Genet* **13**(23): 2979-89.

Gordenin, D. A., T. A. Kunkel and M. A. Resnick (1997). Repeat expansion--all in a flap? *Nat Genet* **16**(2): 116-8.

Goula, A. V., B. R. Berquist, D. M. Wilson, 3rd, V. C. Wheeler, Y. Trottier and K. Merienne (2009). Stoichiometry of base excision repair proteins correlates with increased somatic CAG instability in striatum over cerebellum in Huntington's disease transgenic mice. *PLoS Genet* **5**(12): e1000749.

Goula, A. V., C. E. Pearson, J. Della Maria, Y. Trottier, A. E. Tomkinson, D. M. Wilson, 3rd and K. Merienne (2012). The Nucleotide Sequence, DNA Damage Location, and Protein Stoichiometry Influence the Base Excision Repair Outcome at CAG/CTG Repeats. *Biochemistry*.

Gourdon, G., F. Radvanyi, A. S. Lia, C. Duros, M. Blanche, M. Abitbol, C. Junien and H. Hofmann-Radvanyi (1997). Moderate intergenerational and somatic instability of a 55-CTG repeat in transgenic mice. *Nat Genet* **15**(2): 190-2.

Gregoretti, I. V., Y. M. Lee and H. V. Goodson (2004). Molecular evolution of the histone deacetylase family: functional implications of phylogenetic analysis. *J Mol Biol* **338**(1): 17-31.

Guardiola, A. R. and T. P. Yao (2002). Molecular cloning and characterization of a novel histone deacetylase HDAC10. *J Biol Chem* **277**(5): 3350-6.

Herman, D., K. Jenssen, R. Burnett, E. Soragni, S. L. Perlman and J. M. Gottesfeld (2006). Histone deacetylase inhibitors reverse gene silencing in Friedreich's ataxia. *Nat Chem Biol* **2**(10): 551-8.

Hockly, E., V. M. Richon, B. Woodman, D. L. Smith, X. Zhou, E. Rosa, K. Sathasivam, S. Ghazi-Noori, A. Mahal, P. A. Lowden, J. S. Steffan, J. L. Marsh, L. M. Thompson, C. M. Lewis, P. A. Marks and G. P. Bates (2003). Suberoylanilide hydroxamic acid, a histone deacetylase inhibitor, ameliorates motor deficits in a mouse model of Huntington's disease. *Proc Natl Acad Sci U S A* **100**(4): 2041-6.

Hodges, A., A. D. Strand, A. K. Aragaki, A. Kuhn, T. Sengstag, G. Hughes, L. A. Elliston, C. Hartog, D. R. Goldstein, D. Thu, Z. R. Hollingsworth, F. Collin, B. Synek, P. A. Holmans, A. B. Young, N. S. Wexler, M. Delorenzi, C. Kooperberg, S. J. Augood, R. L. Faull, J. M. Olson, L. Jones and R. Luthi-Carter (2006). Regional and cellular gene expression changes in human Huntington's disease brain. *Hum Mol Genet* **15**(6): 965-77.

Howeler, C. J., H. F. Busch, J. P. Geraedts, M. F. Niermeijer and A. Staal (1989). Anticipation in myotonic dystrophy: fact or fiction? *Brain* **112 (Pt 3)**: 779-97.

Hsiao, H. Y. and Y. Chern (2010). Targeting glial cells to elucidate the pathogenesis of Huntington's disease. *Mol Neurobiol* **41**(2-3): 248-55.

Hubert, L., Jr., Y. Lin, V. Dion and J. H. Wilson (2011). Xpa deficiency reduces CAG trinucleotide repeat instability in neuronal tissues in a mouse model of SCA1. *Hum Mol Genet* **20**(24): 4822-30.

Jia, H., J. Pallos, V. Jacques, A. Lau, B. Tang, A. Cooper, A. Syed, J. Purcell, Y. Chen, S. Sharma, G. R. Sangrey, S. B. Darnell, H. Plasterer, G. Sadri-Vakili, J. M. Gottesfeld, L. M. Thompson, J. R. Rusche, J. L. Marsh and E. A. Thomas (2012). Histone deacetylase (HDAC) inhibitors targeting HDAC3 and HDAC1 ameliorate polyglutamine-elicited phenotypes in model systems of Huntington's disease. *Neurobiology of Disease* **46**(2): 351-361.

Jinnai, K., T. Sugio, M. Mitani, K. Hashimoto and K. Takahashi (1999). Elongation of (CTG)n repeats in myotonic dystrophy protein kinase gene in tumors associated with myotonic dystrophy patients. *Muscle Nerve* **22**(9): 1271-4.

Jung, J. and N. Bonini (2007). CREB-binding protein modulates repeat instability in a Drosophila model for polyQ disease. *Science* **315**(5820): 1857-9.

Kang, S., A. Jaworski, K. Ohshima and R. D. Wells (1995). Expansion and deletion of CTG repeats from human disease genes are determined by the direction of replication in E. coli. *Nat Genet* **10**(2): 213-8.

Kazantsev, A., E. Preisinger, A. Dranovsky, D. Goldgaber and D. Housman (1999). Insoluble detergent-resistant aggregates form between pathological and nonpathological lengths of polyglutamine in mammalian cells. *Proc Natl Acad Sci U S A* **96**(20): 11404-9.

Kazantsev, A. G. and L. M. Thompson (2008). Therapeutic application of histone deacetylase inhibitors for central nervous system disorders. *Nat Rev Drug Discov* **7**(10): 854-68.

Kennedy, L. and P. F. Shelbourne (2000). Dramatic mutation instability in HD mouse striatum: does polyglutamine load contribute to cell-specific vulnerability in Huntington's disease? *Hum Mol Genet* **9**(17): 2539-44.

Kerrest, A., R. P. Anand, R. Sundararajan, R. Bermejo, G. Liberi, B. Dujon, C. H. Freudenreich and G. F. Richard (2009). SRS2 and SGS1 prevent chromosomal breaks and stabilize triplet repeats by restraining recombination. *Nat Struct Mol Biol* **16**(2): 159-67.

Kovtun, I. V., K. O. Johnson and C. T. McMurray (2011). Cockayne syndrome B protein antagonizes OGG1 in modulating CAG repeat length in vivo. *Aging (Albany NY)* **3**(5): 509-14.

Kovtun, I. V., Y. Liu, M. Bjoras, A. Klungland, S. H. Wilson and C. T. McMurray (2007). OGG1 initiates age-dependent CAG trinucleotide expansion in somatic cells. *Nature* **447**(7143): 447-52.

Kovtun, I. V. and C. T. McMurray (2001). Trinucleotide expansion in haploid germ cells by gap repair. *Nat Genet* **27**(4): 407-11.

Kovtun, I. V., A. R. Thornhill and C. T. McMurray (2004). Somatic deletion events occur during early embryonic development and modify the extent of CAG expansion in subsequent generations. *Hum Mol Genet* **13**(24): 3057-68.

Krejci, L., S. Van Komen, Y. Li, J. Villemain, M. S. Reddy, H. Klein, T. Ellenberger and P. Sung (2003). DNA helicase Srs2 disrupts the Rad51 presynaptic filament. *Nature* **423**(6937): 305-9.

Kumari, D., R. Lokanga, D. Yudkin, X. N. Zhao and K. Usdin (2012). Chromatin changes in the development and pathology of the Fragile X-associated disorders and Friedreich ataxia. *Biochim Biophys Acta*.

Kwak, E. L. and D. C. Chung (2007). Hereditary colorectal cancer syndromes: an overview. *Clin Colorectal Cancer* **6**(5): 340-4.

Lang, W. H., J. E. Coats, J. Majka, G. L. Hura, Y. Lin, I. Rasnik and C. T. McMurray (2011). Conformational trapping of mismatch recognition complex MSH2/MSH3 on repair-resistant DNA loops. *Proc Natl Acad Sci U S A* **108**(42): E837-44.

Leeflang, E. P., S. Tavare, P. Marjoram, C. O. Neal, J. Srinidhi, H. MacFarlane, M. E. MacDonald, J. F. Gusella, M. de Young, N. S. Wexler and N. Arnheim (1999). Analysis of germline mutation spectra at the Huntington's disease locus supports a mitotic mutation mechanism. *Hum Mol Genet* **8**(2): 173-83.

Leeflang, E. P., L. Zhang, S. Tavare, R. Hubert, J. Srinidhi, M. E. MacDonald, R. H. Myers, M. de Young, N. S. Wexler, J. F. Gusella and et al. (1995). Single sperm analysis of the trinucleotide repeats in the Huntington's disease gene: quantification of the mutation frequency spectrum. *Hum Mol Genet* **4**(9): 1519-26.

Li, G. M. (2008). Mechanisms and functions of DNA mismatch repair. *Cell Res* **18**(1): 85-98.

Lia, A. S., H. Seznec, H. Hofmann-Radvanyi, F. Radvanyi, C. Duros, C. Saquet, M. Blanche, C. Junien and G. Gourdon (1998). Somatic instability of the CTG repeat in mice transgenic for the myotonic dystrophy region is age dependent but not correlated to the relative intertissue transcription levels and proliferative capacities. *Hum Mol Genet* **7**(8): 1285-91.

Libby, R. T., K. A. Hagerman, V. V. Pineda, R. Lau, D. H. Cho, S. L. Baccam, M. M. Axford, J. D. Cleary, J. M. Moore, B. L. Sopher, S. J. Tapscott, G. N. Filippova, C. E. Pearson and A. R. La Spada (2008). CTCF cis-regulates trinucleotide repeat instability in an epigenetic manner: a novel basis for mutational hot spot determination. *PLoS Genet* **4**(11): e1000257.

Lievens, J. C., B. Woodman, A. Mahal, O. Spasic-Boscovic, D. Samuel, L. Kerkerian-Le Goff and G. P. Bates (2001). Impaired glutamate uptake in the R6 Huntington's disease transgenic mice. *Neurobiol Dis* **8**(5): 807-21.

Lin, Y., S. Y. Dent, J. H. Wilson, R. D. Wells and M. Napierala (2010). R loops stimulate genetic instability of CTG.CAG repeats. *Proc Natl Acad Sci U S A* **107**(2): 692-7.

Lin, Y., V. Dion and J. H. Wilson (2006). Transcription promotes contraction of CAG repeat tracts in human cells. *Nat Struct Mol Biol* **13**(2): 179-80.

Lin, Y. and J. H. Wilson (2007). Transcription-induced CAG repeat contraction in human cells is mediated in part by transcription-coupled nucleotide excision repair. *Mol Cell Biol* **27**(17): 6209-17.

Liu, B., R. Parsons, N. Papadopoulos, N. C. Nicolaides, H. T. Lynch, P. Watson, J. R. Jass, M. Dunlop, A. Wyllie, P. Peltomaki, A. de la Chapelle, S. R. Hamilton, B. Vogelstein and K. W. Kinzler (1996). Analysis of mismatch repair genes in hereditary non-polyposis colorectal cancer patients. *Nat Med* **2**(2): 169-74.

Liu, G., X. Chen, J. J. Bissler, R. R. Sinden and M. Leffak (2010). Replication-dependent instability at (CTG) x (CAG) repeat hairpins in human cells. *Nat Chem Biol* **6**(9): 652-9.

Liu, G., X. Chen, Y. Gao, T. Lewis, J. Barthelemy and M. Leffak (2012). Altered Replication in Human Cells Promotes DMPK (CTG)n {middle dot} (CAG)n Repeat Instability. *Mol Cell Biol* **32**(9): 1618-32.

Liu, Y., H. I. Kao and R. A. Bambara (2004). Flap endonuclease 1: a central component of DNA metabolism. *Annu Rev Biochem* **73**: 589-615.

Liu, Y., R. Prasad, W. A. Beard, E. W. Hou, J. K. Horton, C. T. McMurray and S. H. Wilson (2009). Coordination between polymerase beta and FEN1 can modulate CAG repeat expansion. *J Biol Chem* **284**(41): 28352-66.

Liu, Y. and S. H. Wilson (2012). DNA base excision repair: a mechanism of trinucleotide repeat expansion. *Trends Biochem Sci* **37**(4): 162-72.

Lopez Castel, A., J. D. Cleary and C. E. Pearson (2010). Repeat instability as the basis for human diseases and as a potential target for therapy. *Nat Rev Mol Cell Biol* **11**(3): 165-70.

Luthi-Carter, R., S. A. Hanson, A. D. Strand, D. A. Bergstrom, W. Chun, N. L. Peters, A. M. Woods, E. Y. Chan, C. Kooperberg, D. Krainc, A. B. Young, S. J. Tapscott and J.

M. Olson (2002). Dysregulation of gene expression in the R6/2 model of polyglutamine disease: parallel changes in muscle and brain. *Hum Mol Genet* **11**(17): 1911-26.

Mahadevan, M., C. Tsilfidis, L. Sabourin, G. Shutler, C. Amemiya, G. Jansen, C. Neville, M. Narang, J. Barcelo, K. O'Hoy and et al. (1992). Myotonic dystrophy mutation: an unstable CTG repeat in the 3' untranslated region of the gene. *Science* **255**(5049): 1253-5.

Major, E. O., A. E. Miller, P. Mourrain, R. G. Traub, E. de Widt and J. Sever (1985). Establishment of a line of human fetal glial cells that supports JC virus multiplication. *Proc Natl Acad Sci U S A* **82**(4): 1257-61.

Manley, K., T. L. Shirley, L. Flaherty and A. Messer (1999). Msh2 deficiency prevents in vivo somatic instability of the CAG repeat in Huntington disease transgenic mice. *Nat Genet* **23**(4): 471-3.

Martorell, L., D. G. Monckton, J. Gamez, K. J. Johnson, I. Gich, A. Lopez de Munain and M. Baiget (1998). Progression of somatic CTG repeat length heterogeneity in the blood cells of myotonic dystrophy patients. *Hum Mol Genet* **7**(2): 307-12.

McCampbell, A., J. P. Taylor, A. A. Taye, J. Robitschek, M. Li, J. Walcott, D. Merry, Y. Chai, H. Paulson, G. Sobue and K. H. Fischbeck (2000). CREB-binding protein sequestration by expanded polyglutamine. *Hum Mol Genet* **9**(14): 2197-202.

McMurray, C. T. (2008). Hijacking of the mismatch repair system to cause CAG expansion and cell death in neurodegenerative disease. *DNA Repair (Amst)* **7**(7): 1121-34.

McMurray, C. T. (2010). Mechanisms of trinucleotide repeat instability during human development. *Nat Rev Genet* **11**(11): 786-99.

Messaed, C. and G. A. Rouleau (2009). Molecular mechanisms underlying polyalanine diseases. *Neurobiol Dis* **34**(3): 397-405.

Minamiyama, M., M. Katsuno, H. Adachi, M. Waza, C. Sang, Y. Kobayashi, F. Tanaka, M. Doyu, A. Inukai and G. Sobue (2004). Sodium butyrate ameliorates phenotypic expression in a transgenic mouse model of spinal and bulbar muscular atrophy. *Hum Mol Genet* **13**(11): 1183-92.

Miret, J. J., L. Pessoa-Brandao and R. S. Lahue (1998). Orientation-dependent and sequence-specific expansions of CTG/CAG trinucleotide repeats in Saccharomyces cerevisiae. *Proc Natl Acad Sci U S A* **95**(21): 12438-43.

Mirkin, S. M. (2006). DNA structures, repeat expansions and human hereditary disorders. *Curr Opin Struct Biol* **16**(3): 351-8.

Mirkin, S. M. (2007). Expandable DNA repeats and human disease. *Nature* **447**(7147): 932-40.

Mitas, M., A. Yu, J. Dill, T. J. Kamp, E. J. Chambers and I. S. Haworth (1995). Hairpin properties of single-stranded DNA containing a GC-rich triplet repeat: (CTG)15. *Nucleic Acids Res* **23**(6): 1050-9.

Moe, S. E., J. G. Sorbo and T. Holen (2008). Huntingtin triplet-repeat locus is stable under long-term Fen1 knockdown in human cells. *J Neurosci Methods* **171**(2): 233-8.

Moldovan, G. L., D. Dejsuphong, M. I. Petalcorin, K. Hofmann, S. Takeda, S. J. Boulton and A. D. D'Andrea (2012). Inhibition of homologous recombination by the PCNA-interacting protein PARI. *Mol Cell* **45**(1): 75-86.

Moseley, M. L., L. J. Schut, T. D. Bird, M. D. Koob, J. W. Day and L. P. Ranum (2000). SCA8 CTG repeat: en masse contractions in sperm and intergenerational sequence changes may play a role in reduced penetrance. *Hum Mol Genet* **9**(14): 2125-30.

Motegi, A., H. J. Liaw, K. Y. Lee, H. P. Roest, A. Maas, X. Wu, H. Moinova, S. D. Markowitz, H. Ding, J. H. Hoeijmakers and K. Myung (2008). Polyubiquitination of proliferating cell nuclear antigen by HLTF and SHPRH prevents genomic instability from stalled replication forks. *Proc Natl Acad Sci U S A* **105**(34): 12411-6.

Motegi, A., R. Sood, H. Moinova, S. D. Markowitz, P. P. Liu and K. Myung (2006). Human SHPRH suppresses genomic instability through proliferating cell nuclear antigen polyubiquitination. *J Cell Biol* **175**(5): 703-8.

Moumne, L., K. Campbell, D. Howland, Y. Ouyang and G. P. Bates (2012). Genetic knock-down of HDAC3 does not modify disease-related phenotypes in a mouse model of Huntington's disease. *PLoS One* **7**(2): e31080.

Musova, Z., R. Mazanec, A. Krepelova, E. Ehler, J. Vales, R. Jaklova, T. Prochazka, P. Koukal, T. Marikova, J. Kraus, M. Havlovicova and Z. Sedlacek (2009). Highly unstable sequence interruptions of the CTG repeat in the myotonic dystrophy gene. *Am J Med Genet A* **149A**(7): 1365-74.

Myers, R. H., M. E. MacDonald, W. J. Koroshetz, M. P. Duyao, C. M. Ambrose, S. A. Taylor, G. Barnes, J. Srinidhi, C. S. Lin, W. L. Whaley and et al. (1993). De novo expansion of a (CAG)n repeat in sporadic Huntington's disease. *Nat Genet* **5**(2): 168-73.

Nakamori, M., C. E. Pearson and C. A. Thornton (2011). Bidirectional transcription stimulates expansion and contraction of expanded (CTG)*(CAG) repeats. *Hum Mol Genet* **20**(3): 580-8.

Nenguke, T., M. I. Aladjem, J. F. Gusella, N. S. Wexler and N. Arnheim (2003). Candidate DNA replication initiation regions at human trinucleotide repeat disease loci. *Hum Mol Genet* **12**(9): 1021-8.

Orr, H. T. and H. Y. Zoghbi (2007). Trinucleotide repeat disorders. *Annu Rev Neurosci* **30**: 575-621.

Owen, B. A., Z. Yang, M. Lai, M. Gajec, J. D. Badger, 2nd, J. J. Hayes, W. Edelmann, R. Kucherlapati, T. M. Wilson and C. T. McMurray (2005). (CAG)(n)-hairpin DNA binds to Msh2-Msh3 and changes properties of mismatch recognition. *Nat Struct Mol Biol* **12**(8): 663-70.

Panigrahi, G. B., J. D. Cleary and C. E. Pearson (2002). In vitro (CTG)*(CAG) expansions and deletions by human cell extracts. *J Biol Chem* **277**(16): 13926-34.

Parniewski, P., A. Bacolla, A. Jaworski and R. D. Wells (1999). Nucleotide excision repair affects the stability of long transcribed (CTG*CAG) tracts in an orientation-dependent manner in Escherichia coli. *Nucleic Acids Res* **27**(2): 616-23.

Parniewski, P., A. Jaworski, R. D. Wells and R. P. Bowater (2000). Length of CTG.CAG repeats determines the influence of mismatch repair on genetic instability. *J Mol Biol* **299**(4): 865-74.

Pearson, C. E., K. Nichol Edamura and J. D. Cleary (2005). Repeat instability: mechanisms of dynamic mutations. *Nat Rev Genet* **6**(10): 729-42.

Pearson, C. E. and R. R. Sinden (1996). Alternative structures in duplex DNA formed within the trinucleotide repeats of the myotonic dystrophy and fragile X loci. *Biochemistry* **35**(15): 5041-53.

Pearson, C. E., Y. H. Wang, J. D. Griffith and R. R. Sinden (1998). Structural analysis of slipped-strand DNA (S-DNA) formed in (CTG)n. (CAG)n repeats from the myotonic dystrophy locus. *Nucleic Acids Res* **26**(3): 816-23.

Pelletier, R., M. M. Krasilnikova, G. M. Samadashwily, R. Lahue and S. M. Mirkin (2003). Replication and expansion of trinucleotide repeats in yeast. *Mol Cell Biol* **23**(4): 1349-57.

Perez-Navarro, E., A. M. Canudas, P. Akerund, J. Alberch and E. Arenas (2000). Brain-derived neurotrophic factor, neurotrophin-3, and neurotrophin-4/5 prevent the death of striatal projection neurons in a rodent model of Huntington's disease. *J Neurochem* **75**(5): 2190-9.

Petruska, J., N. Arnheim and M. F. Goodman (1996). Stability of intrastrand hairpin structures formed by the CAG/CTG class of DNA triplet repeats associated with neurological diseases. *Nucleic Acids Res* **24**(11): 1992-8.

Razidlo, D. F. and R. S. Lahue (2008). Mrc1, Tof1 and Csm3 inhibit CAG.CTG repeat instability by at least two mechanisms. *DNA Repair (Amst)* **7**(4): 633-40.

Robertson, A. B., A. Klungland, T. Rognes and I. Leiros (2009). DNA repair in mammalian cells: Base excision repair: the long and short of it. *Cell Mol Life Sci* **66**(6): 981-93.

Rolfsmeier, M. L., M. J. Dixon and R. S. Lahue (2000). Mismatch repair blocks expansions of interrupted trinucleotide repeats in yeast. *Mol Cell* **6**(6): 1501-7.

Rolfsmeier, M. L., M. J. Dixon, L. Pessoa-Brandao, R. Pelletier, J. J. Miret and R. S. Lahue (2001). Cis-elements governing trinucleotide repeat instability in Saccharomyces cerevisiae. *Genetics* **157**(4): 1569-79.

Rubinsztein, D. C., J. Leggo, D. E. Barton and M. A. Ferguson-Smith (1993). Site of (CCG) polymorphism in the HD gene. *Nat Genet* **5**(3): 214-5.

Sakamoto, N., P. D. Chastain, P. Parniewski, K. Ohshima, M. Pandolfo, J. D. Griffith and R. D. Wells (1999). Sticky DNA: self-association properties of long GAA.TTC repeats in R.R.Y triplex structures from Friedreich's ataxia. *Mol Cell* **3**(4): 465-75.

Savouret, C., E. Brisson, J. Essers, R. Kanaar, A. Pastink, H. te Riele, C. Junien and G. Gourdon (2003). CTG repeat instability and size variation timing in DNA repair-deficient mice. *Embo J* **22**(9): 2264-73.

Schmidt, K. H., C. M. Abbott and D. R. Leach (2000). Two opposing effects of mismatch repair on CTG repeat instability in Escherichia coli. *Mol Microbiol* **35**(2): 463-71.

Schneider, J., P. Bajwa, F. C. Johnson, S. R. Bhaumik and A. Shilatifard (2006). Rtt109 is required for proper H3K56 acetylation: a chromatin mark associated with the elongating RNA polymerase II. *J Biol Chem* **281**(49): 37270-4.

Schweitzer, J. K. and D. M. Livingston (1997). Destabilization of CAG trinucleotide repeat tracts by mismatch repair mutations in yeast. *Hum Mol Genet* **6**(3): 349-55.

Schweitzer, J. K. and D. M. Livingston (1998). Expansions of CAG repeat tracts are frequent in a yeast mutant defective in Okazaki fragment maturation. *Hum Mol Genet* **7**(1): 69-74.

Schweitzer, J. K. and D. M. Livingston (1999). The effect of DNA replication mutations on CAG tract stability in yeast. *Genetics* **152**(3): 953-63.

Semaka, A., J. A. Collins and M. R. Hayden (2010). Unstable familial transmissions of Huntington disease alleles with 27-35 CAG repeats (intermediate alleles). *Am J Med Genet B Neuropsychiatr Genet* **153B**(1): 314-20.

Semaka, A., S. Creighton, S. Warby and M. R. Hayden (2006). Predictive testing for Huntington disease: interpretation and significance of intermediate alleles. *Clin Genet* **70**(4): 283-94.

Seznec, H., A. S. Lia-Baldini, C. Duros, C. Fouquet, C. Lacroix, H. Hofmann-Radvanyi, C. Junien and G. Gourdon (2000). Transgenic mice carrying large human genomic sequences with expanded CTG repeat mimic closely the DM CTG repeat intergenerational and somatic instability. *Hum Mol Genet* **9**(8): 1185-94.

Shelbourne, P. F., C. Keller-McGandy, W. L. Bi, S. R. Yoon, L. Dubeau, N. J. Veitch, J. P. Vonsattel, N. S. Wexler, N. Arnheim and S. J. Augood (2007). Triplet repeat mutation length gains correlate with cell-type specific vulnerability in Huntington disease brain. *Hum Mol Genet* **16**(10): 1133-42.

Shin, J. Y., Z. H. Fang, Z. X. Yu, C. E. Wang, S. H. Li and X. J. Li (2005). Expression of mutant huntingtin in glial cells contributes to neuronal excitotoxicity. *J Cell Biol* **171**(6): 1001-12.

Singhrao, S. K., P. Thomas, J. D. Wood, J. C. MacMillan, J. W. Neal, P. S. Harper and A. L. Jones (1998). Huntingtin protein colocalizes with lesions of neurodegenerative diseases: An investigation in Huntington's, Alzheimer's, and Pick's diseases. *Exp Neurol* **150**(2): 213-22.

Spiro, C. and C. T. McMurray (2003). Nuclease-deficient FEN-1 blocks Rad51/BRCA1-mediated repair and causes trinucleotide repeat instability. *Mol Cell Biol* **23**(17): 6063-74.

Stack, E. C., S. J. Del Signore, R. Luthi-Carter, B. Y. Soh, D. R. Goldstein, S. Matson, S. Goodrich, A. L. Markey, K. Cormier, S. W. Hagerty, K. Smith, H. Ryu and R. J. Ferrante (2007). Modulation of nucleosome dynamics in Huntington's disease. *Hum Mol Genet* **16**(10): 1164-75.

Steffan, J. S., L. Bodai, J. Pallos, M. Poelman, A. McCampbell, B. L. Apostol, A. Kazantsev, E. Schmidt, Y. Z. Zhu, M. Greenwald, R. Kurokawa, D. E. Housman, G. R. Jackson, J. L. Marsh and L. M. Thompson (2001). Histone deacetylase inhibitors

arrest polyglutamine-dependent neurodegeneration in Drosophila. *Nature* **413**(6857): 739-43.

Steffan, J. S., A. Kazantsev, O. Spasic-Boskovic, M. Greenwald, Y. Z. Zhu, H. Gohler, E. E. Wanker, G. P. Bates, D. E. Housman and L. M. Thompson (2000). The Huntington's disease protein interacts with p53 and CREB-binding protein and represses transcription. *Proc Natl Acad Sci U S A* **97**(12): 6763-8.

Swami, M., A. E. Hendricks, T. Gillis, T. Massood, J. Mysore, R. H. Myers and V. C. Wheeler (2009). Somatic expansion of the Huntington's disease CAG repeat in the brain is associated with an earlier age of disease onset. *Hum Mol Genet* **18**(16): 3039-47.

Thomas, E. A., G. Coppola, P. A. Desplats, B. Tang, E. Soragni, R. Burnett, F. Gao, K. M. Fitzgerald, J. F. Borok, D. Herman, D. H. Geschwind and J. M. Gottesfeld (2008). The HDAC inhibitor 4b ameliorates the disease phenotype and transcriptional abnormalities in Huntington's disease transgenic mice. *Proc Natl Acad Sci U S A* **105**(40): 15564-9.

Thornton, C. A., K. Johnson and R. T. Moxley, 3rd (1994). Myotonic dystrophy patients have larger CTG expansions in skeletal muscle than in leukocytes. *Ann Neurol* **35**(1): 104-7.

Tian, L., C. Hou, K. Tian, N. C. Holcomb, L. Gu and G. M. Li (2009). Mismatch recognition protein MutSbeta does not hijack (CAG)n hairpin repair in vitro. *J Biol Chem* **284**(31): 20452-6.

Tome, S., I. Holt, W. Edelmann, G. E. Morris, A. Munnich, C. E. Pearson and G. Gourdon (2009). MSH2 ATPase domain mutation affects CTG*CAG repeat instability in transgenic mice. *PLoS Genet* **5**(5): e1000482.

Tome, S., G. B. Panigrahi, A. Lopez Castel, L. Foiry, D. W. Melton, G. Gourdon and C. E. Pearson (2011). Maternal germline-specific effect of DNA ligase I on CTG/CAG instability. *Hum Mol Genet* **20**(11): 2131-43.

Ulrich, H. D. (2005). Mutual interactions between the SUMO and ubiquitin systems: a plea of no contest. *Trends Cell Biol* **15**(10): 525-32.

Ulrich, H. D. and S. Jentsch (2000). Two RING finger proteins mediate cooperation between ubiquitin-conjugating enzymes in DNA repair. *Embo J* **19**(13): 3388-97.

Unk, I., I. Hajdu, K. Fatyol, J. Hurwitz, J. H. Yoon, L. Prakash, S. Prakash and L. Haracska (2008). Human HLTF functions as a ubiquitin ligase for proliferating cell nuclear antigen polyubiquitination. *Proc Natl Acad Sci U S A* **105**(10): 3768-73.

Unk, I., I. Hajdu, K. Fatyol, B. Szakal, A. Blastyak, V. Bermudez, J. Hurwitz, L. Prakash, S. Prakash and L. Haracska (2006). Human SHPRH is a ubiquitin ligase for Mms2-Ubc13-dependent polyubiquitylation of proliferating cell nuclear antigen. *Proc Natl Acad Sci U S A* **103**(48): 18107-12.

van den Broek, W. J., M. R. Nelen, G. W. van der Heijden, D. G. Wansink and B. Wieringa (2006). Fen1 does not control somatic hypermutability of the (CTG)(n)*(CAG)(n) repeat in a knock-in mouse model for DM1. *FEBS Lett* **580**(22): 5208-14.

van den Broek, W. J., M. R. Nelen, D. G. Wansink, M. M. Coerwinkel, H. te Riele, P. J. Groenen and B. Wieringa (2002). Somatic expansion behaviour of the (CTG)n repeat in myotonic dystrophy knock-in mice is differentially affected by Msh3 and Msh6 mismatch-repair proteins. *Hum Mol Genet* **11**(2): 191-8.

Veaute, X., J. Jeusset, C. Soustelle, S. C. Kowalczykowski, E. Le Cam and F. Fabre (2003). The Srs2 helicase prevents recombination by disrupting Rad51 nucleoprotein filaments. *Nature* **423**(6937): 309-12.

Vetcher, A. A., M. Napierala, R. R. Iyer, P. D. Chastain, J. D. Griffith and R. D. Wells (2002). Sticky DNA, a long GAA.GAA.TTC triplex that is formed intramolecularly, in the sequence of intron 1 of the frataxin gene. *J Biol Chem* **277**(42): 39217-27.

Voineagu, I., C. F. Surka, A. A. Shishkin, M. M. Krasilnikova and S. M. Mirkin (2009). Replisome stalling and stabilization at CGG repeats, which are responsible for chromosomal fragility. *Nat Struct Mol Biol* **16**(2): 226-8.

Waltregny, D., W. Glenisson, S. L. Tran, B. J. North, E. Verdin, A. Colige and V. Castronovo (2005). Histone deacetylase HDAC8 associates with smooth muscle alpha-actin and is essential for smooth muscle cell contractility. *Faseb J* **19**(8): 966-8.

Wang, L., F. Lin, J. Wang, J. Wu, R. Han, L. Zhu, M. Difiglia and Z. Qin (2012). Expression of mutant N-terminal huntingtin fragment (htt552-100Q) in astrocytes suppresses the secretion of BDNF. *Brain Res* **1449**: 69-82.

Watanabe, H., F. Tanaka, M. Doyu, S. Riku, M. Yoshida, Y. Hashizume and G. Sobue (2000). Differential somatic CAG repeat instability in variable brain cell lineage in dentatorubral pallidoluysian atrophy (DRPLA): a laser-captured microdissection (LCM)-based analysis. *Hum Genet* **107**(5): 452-7.

Watase, K., K. J. Venken, Y. Sun, H. T. Orr and H. Y. Zoghbi (2003). Regional differences of somatic CAG repeat instability do not account for selective neuronal vulnerability in a knock-in mouse model of SCA1. *Hum Mol Genet* **12**(21): 2789-95.

Waters, L. S., B. K. Minesinger, M. E. Wiltrout, S. D'Souza, R. V. Woodruff and G. C. Walker (2009). Eukaryotic translesion polymerases and their roles and regulation in DNA damage tolerance. *Microbiol Mol Biol Rev* **73**(1): 134-54.

Wells, R. D., P. Parniewski, A. Pluciennik, A. Bacolla, R. Gellibolian and A. Jaworski (1998). Small slipped register genetic instabilities in Escherichia coli in triplet repeat sequences associated with hereditary neurological diseases. *J Biol Chem* **273**(31): 19532-41.

Wheeler, V. C., L. A. Lebel, V. Vrbanac, A. Teed, H. te Riele and M. E. MacDonald (2003). Mismatch repair gene Msh2 modifies the timing of early disease in Hdh(Q111) striatum. *Hum Mol Genet* **12**(3): 273-81.

Xu, C., E. Soragni, C. J. Chou, D. Herman, H. L. Plasterer, J. R. Rusche and J. M. Gottesfeld (2009). Chemical probes identify a role for histone deacetylase 3 in Friedreich's ataxia gene silencing. *Chem Biol* **16**(9): 980-9.

Yang, J. H. and C. H. Freudenreich (2010). The Rtt109 histone acetyltransferase facilitates error-free replication to prevent CAG/CTG repeat contractions. *DNA Repair (Amst)* **9**(4): 414-20.

Yang, X. J. and E. Seto (2008). The Rpd3/Hda1 family of lysine deacetylases: from bacteria and yeast to mice and men. *Nat Rev Mol Cell Biol* **9**(3): 206-18.

Yang, Z., R. Lau, J. L. Marcadier, D. Chitayat and C. E. Pearson (2003). Replication inhibitors modulate instability of an expanded trinucleotide repeat at the myotonic dystrophy type 1 disease locus in human cells. *Am J Hum Genet* **73**(5): 1092-105.

Ying, M., R. Xu, X. Wu, H. Zhu, Y. Zhuang, M. Han and T. Xu (2006). Sodium butyrate ameliorates histone hypoacetylation and neurodegenerative phenotypes in a mouse model for DRPLA. *J Biol Chem* **281**(18): 12580-6.

Zhao, J., A. Bacolla, G. Wang and K. M. Vasquez (2010). Non-B DNA structure-induced genetic instability and evolution. *Cell Mol Life Sci* **67**(1): 43-62.

CHAPTER 2

Materials and Methods

2.1 General reagents and consumables

Unless otherwise indicated, all chemical and molecular reagents were obtained from Fisher Scientific (Ballycoolin, Dublin), Sigma Aldrich (Arklow, Co. Wicklow, Ireland), Formedium (Hunstanton, Norfolk, U.K.), New England Biolabs (ISIS Ltd., Unit 1 & 2, Ballywaltrim Business Centre, Boghall Road, Bray, Co. Wicklow, Ireland). All primers for PCR analysis were acquired from Eurofins MWG Operon (Anzingerstr. 7a, 85560 Ebersberg, Germany). All plastics and consumables were purchased from Sarstedt (Sinnottstown Lane, Drinnagh, Co. Wexford) or Fisher Scientific. All sterile plastic-ware for cell culture was from Sarstedt.

2.2 Shuttle vector assay overview

The shuttle vector assay utilizes yeast as a biosensor for measuring expansion and contraction events that occur in mammalian tissue culture cells (Pelletier et al., 2005; Farrell and Lahue, 2006; Claassen and Lahue, 2007). The benefits of this assay are numerous; it is a sensitive and selective genetic assay for examination of instability events that occur in human cell culture. This assay system has been demonstrated to recapitulate numerous aspects of CTG•CAG repeat instability including threshold effects, sequence-dependence and orientation of replication (Farrell and Lahue, 2006; Claassen and Lahue, 2007). Additonally, sizes of the instability events can be measured by PCR and expansion sizes in SVG-A cells were shown to overlap with in vivo somatic expansions in polyglutamine diseases (Claassen and Lahue, 2007). A limitation of the assay is the number of repeats that can be used. The assay does not allow evaluation of expansions for tracts longer than ~26 repeats because tracts above this size turn off the *CAN1* gene so expansions could be identified because of a lack of selection. This precludes its applicability from the study of disease-length repeat instability. One of the key features of this assay is the shuttle vector itself. The shuttle vector harbours numerous genetic elements that facilitate its propagation in bacterial, yeast and mammalian cells. The plasmid is capable of replication in SVG-A and other mammalian cells expressing the SV40 large T antigen by means of the SV40 origin of replication. The presence of the *ARS* and *CEN* elements allow for low-copy plasmid replication in yeast. The *HIS3* gene identifies yeast transformants. The promoter-TNR-*CAN1* reporter cassette allows for selection of expansions, while the promoter-TNR-*URA3* enables selection of contractions. For all expansion analyses in this thesis, the shuttle vector had $(CTG)_{22}$ repeats comprising the Okazaki fragment (Fig 2.1), while the shuttle vector used for contractions had $(CAG)_{33}$ on the lagging strand template. The *E.coli* ori and ampicillin (Amp) resistance gene are required for plasmid propagation and selection to produce experimental-scale quantities. The amp resistance gene served an additional purpose in this study (see modifications made; section 2.2).

This assay was performed as described in Claassen and Lahue, 2007 but with the additional element of RNAi or small molecule inhibitors to determine what proteins are important for TNR instability. Also some technical modifications have been made (see modifications made). An overview schematic for the assay steps is presented in Fig. 2.2A. The shuttle vector is transfected into SVG-A cells treated with siRNA against a gene of interest or a small molecule inhibitor. The plasmid is allowed to propagate in cell culture for 2 days, isolated by an alkaline lysis procedure and transformed into yeast whereby genetic selection allows for measurement of the expansion or contraction frequency which has occurred during replication in cell culture. PCR amplification of selective yeast colonies facilitates visualisation of changes in length repeat length.

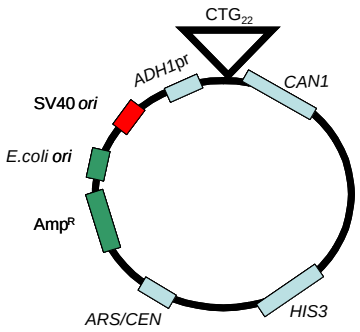

Figure 2.1 Shuttle vector for expansions. There are genetic elements on the plasmid (plasmid size: ~9 kb) that facilitate their propagation in bacterial (green components), yeast (blue components) and mammalian cells (red component).

The selection for changes in TNR length is based on reporter gene expression, driven by the *S. pombe adh1* promoter, being dependent on correct spacing between the TATA box and the preferred transcription initiation site (denoted *I* in fig 2.2B and C). Starting TNR lengths of 22 facilitates expression of the *CAN1* reporter gene allowing uptake of the toxic arginine analogue, canavanine (Can) (Debacker et al., 2012). Thus, cells transformed with an unexpanded molecule will be sensitive to canavanine-containing media. Expansions of ≥4 repeats alter transcription initiation, incorporating the out-of-frame ATG codon that blocks translation of *CAN1* and canavanine resistance ensues. For contractions, starting lengths of 33 positioned between the TATA and *I*, inhibit expression of the *URA3* reporter gene causing the cells to become Ura^-. Contraction of the repeat tract to ≤28 re-establishes expression of *URA3* and cells will grow on media lacking uracil.

<u>Modifications made to shuttle vector assay compared with that described by Claassen and Lahue, 2007:</u>

- Use of canavanine reporter system for detection of expansions instead of 5FOA (section 2.3)
- Replica plating from SC-His to SC-His-Arg+Can instead of plating directly onto selective plates (section 2.16)
- Transformation of shuttle vector into *E.coli* to obtain total transformant number rather than number of His^+ colonies (section 2.16)

A.

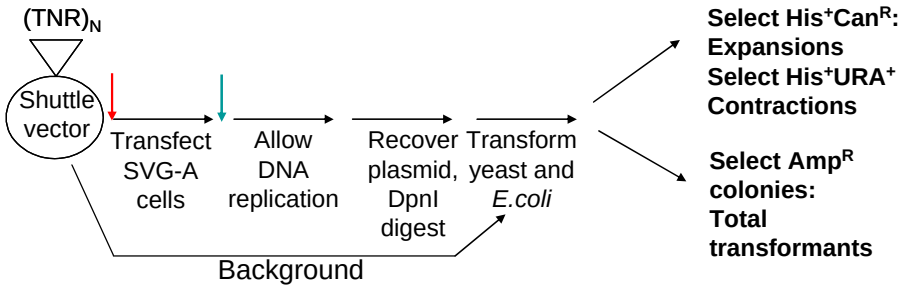

B.

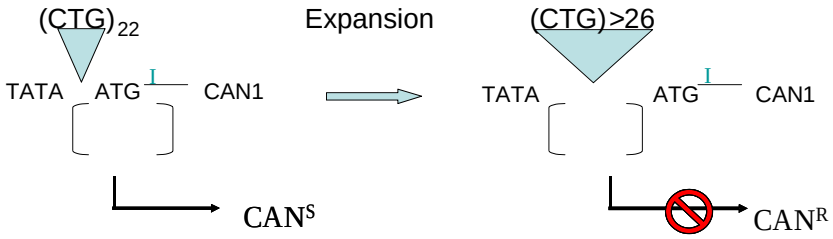

C.

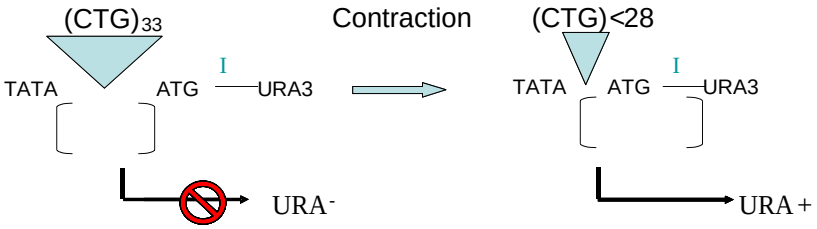

Figure 2.2 Shuttle vector assay. A. Timeline of siRNA or small-molecule inhibitor treatment. The schematic shows transfection of a TNR-containing shuttle vector into SVG-A cells and use of yeast as a biosensor for expansions and contractions that occurred during SVG-A cell culture. The coloured arrows indicate time-course for additional elements of the basic assay system e.g. siRNA transfection (red arrow) or drug addition (green arrow). **B.** Selection for expansions using *CAN1* reporter system. Expansion of the starting tract to 26 or more repeats causes an out-of-frame ATG to be encoded in the *CAN1* gene leading to canavanine-resistance. **C.** Selection for contractions using *URA3* reporter system. Contraction of the starting repeat tract to 28 or less leads to a functional *URA3* gene product and a Ura^+ phenotype.

2.3 Construction of shuttle vectors with *CAN1* reporter

All shuttle vectors used were originally constructed by Brian Farrell and David Claassen (Farrell and Lahue, 2006; Claassen and Lahue, 2007). These plasmids contained a P_{adh1}

promoter-TNR-*URA3* reporter constructs, which require 5FOA for selection. The shuttle vector backbone had the SV40 origin of replication subcloned into the blunted *ApaI* site of pRS313. For the purposes of this study, it was decided to use *CAN1* as the reporter gene as it has been adopted by the lab for fluctuation analysis in yeast and has proved a robust selection system. In order to create derivatives of these vectors with *CAN1* as the reporter gene instead of *URA3*, a fragment swapping approach was used. The 3kb P_{adh1} promoter-$(CTG)_{22}$-*CAN1* reporter construct from pBL272 were isolated by restriction digest with BamHI and XhoI. The backbone of shuttle vector pBL252 (5 kb) (Claassen and Lahue, 2007) containing the SV40 ori was digested with BamHI and XhoI (New England Biolabs). The digested products were separated by agarose gel electrophoresis. The relevant fragments were then excised from the gel and purified using the QIAquick Gel Extraction Kit (Qiagen, Crawley, West Sussex, UK). The P_{adh1} promoter-$(CTG)_{22}$-*CAN1* reporter construct was then subcloned into the corresponding restriction sites of the shuttle vector backbone to produce pBL302. This plasmid was used for all expansion analyses described in this study. 50% glycerol stocks of LB+amp cultures of *E.coli* expressing this plasmid were prepared and stored at -80°C.

2.4 Plasmid DNA preparation

Maxi prep plasmid preparations were performed using a Qiagen EndoFree Plasmid Maxi Kit) or a Nucleobond Xtra Maxi EF kit (Machery-Nagel). Briefly, 400 ml or 600 ml LB supplemented with 75 μg/ml ampicillin was inoculated with a single colony of *E.coli* expressing the relevant plasmid from a freshly-streaked LB+amp plate. The flask was incubated with shaking at 200 rpm at 37°C overnight. Care was taken to ensure that the culture did not reach stationary phase by measuring OD at 600 nm (OD >1: stationary phase) using a spectrophotometer and harvesting cells when OD value was 0.5-1. This precaution is taken as it has previously been shown that TNRs in *E.coli* undergo high frequencies of contractions as the cells proceed through stationary phase (Bowater et al., 1996).

2.5 Cell culture conditions for SVG-A cells

SVG-A cells were maintained in Dulbecco's modified Eagle's medium supplemented with 10% FBS**,** Pen/Strep and Amphotericin B in a humidified 5% CO2 atmosphere at 37°C.

2.6 Confirmation of glial nature of SVG-A cells

SVG-A cells are an astrocytic subclone of the original SVG human glial cell line created by transformation of human foetal glial cells with an origin-defective simian virus 40 (SV40) (Major et al., 1985). In order to confirm that SVG-A cells were glial in nature, cells were examined for expression of GFAP, a glial-specific intermediate filament that acts as a

marker of mature astrocytes. Attempts to detect GFAP expression in SVG-A cells and a control cell line that should not express GFAP (HT1080) by immunofluorescent microscopy were uninformative as HT1080 cells stained positive in addition to SVG-A cells. This was the outcome for two different antibodies. Western blotting using lysates from SVG-A, HT1080 and HeLa cells indicated that the antibodies used for IF were not specific for GFAP. As an alternative strategy, pGFAP-lacZ, a plasmid that contained the *E.coli lacZ* coding sequence under the control of the human GFAP promoter, was used (kindly provided by Dr. Lang Zhuo, (Maubach et al., 2006). HeLa cells were transiently transfected with 1 μg of plasmid using Lipofectamine 2000 in 6-well dishes. SVG-A cells were stably transfected with 1 μg of SalI-linearised plasmid. Six hr after transfection, media was removed and replaced with DMEM+10% FBS. HeLa cells were stained for β-galactosidase activity 2-3 days post-transfection. 2 days after transfection, SVG-A cells were trypsinised and reseeded into 10 cm dishes containing DMEM+10% FBS supplemented with 500 μg/ml Zeocin to allow selection of positive clones. After 4 weeks, Zeo^R colonies were trypsinised and individually propagated in 6-well dishes for 3 days before staining for β-galactosidase activity.

β-galactosidase activity was used a read-out for positive clones and was performed in the tissue culture vessel. Media was aspirated from the cells and they were washed twice with PBS. Cells were fixed by addition of 2 ml of 0.5% glutaraldehyde (in PBS) for 5 min and washed thrice with PBS. Thereafter, 2 ml of staining mixture (5 mM potassium ferrocyanide, 5 mM potassium ferricyanide, 1.5 mM magnesium chloride, 1 mg/ml X-gal (in DMSO) in PBS) was added to each well. The cells were incubated at 37°C for 30 min-overnight after which time staining of the blue end product was measured. Staining was recorded using a DSLR-A200 digital camera (Sony) attached to an inverted bright field microscope. For HeLa cells, as expected no blue staining was observed (Fig 2.3). Of ten SVG-A clones selected for SVG-A cells, three stained positive for GFAP expression (Fig 2.3) providing evidence to confirm the glial nature of SVG-A cells. Evidently, a more stringent comparison should have been done whereby HeLa cells were stably transfected also. However, transient transfection of SVG-A cells also induced blue staining but not as intensely as for the stable transfectants. Furthermore, stably-transfected HeLa cell lines did not stain positive for β-galactosidase activity (Maubach et al., 2006). To summarise, though this is quite a crude assessment and needs to be repeated with the proper controls as outlined above, it does give an indication that the SVG-A cell line is glial in character.

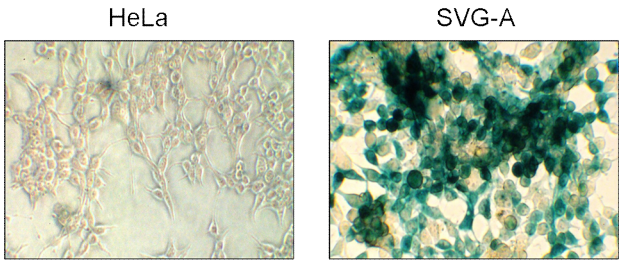

Figure 2.3. X-gal staining of HeLa and SVG-A cells transfected with pGFAP-lacZ. Representative images from transient transfection of HeLa and one of three positive SVG-A stable transfectants.

2.7 Determination of SVG-A transfection efficiency

Since the SVG-A transfection of the shuttle vectors is transient and without selection, it is important to obtain a high efficiency. To this end, SVG-A cells were transfected with 6 μg of a plasmid expressing the lacZ gene driven by the CMV promoter. 48 hours after transfection, cells were fixed and stained to determine β-galactosidase activity as described in section 2.6. In order to quantitate transfection efficiency, the number of total cells and blue cells was estimated. For each well 5 fields were counted; transfection efficiency percentage was calculated as: blue cell #/total cell # x 100. The average transfection efficiency from three independent experiments was 88% (± 7).

siRNA transfection efficiency was not determined using fluorescently-labelled siRNAs. However, densiometric analysis revealed a reduction in levels of 87% for HLTF and RAD18 (Chapter 5) indicating that siRNA transfection of SVG-A was sufficient.

2.8 Shuttle vector transfection and small molecule inhibitors

For shuttle vector transfection and drug treatment of SVG-A cells, SVG-A cells were transfected with shuttle vector DNA using Lipofectamine 2000 according to manufacturer's instructions (Invitrogen Corporation, Paisley UK). Briefly, SVG-A cells were seeded at a density of 300,000 cells in DMEM+10% FBS with no antibiotics in 60 mm tissue culture dishes and transfected 24 hr later. 10 μl of Lipofectamine and 5 μg of plasmid DNA were diluted to a final volume of 100 μl with DMEM in separate 1.5 ml tubes. Five minutes later, the tubes were combined and incubated at room temperature for 20 min. The transfection reaction (final volume of 200 μl) was added to the dishes containing 1.6 ml DMEM. After six hours, the transfection media (DMEM) was replaced by 4 ml DMEM media supplemented with 10% FBS containing the HDAC inhibitor 4b or compound 3 (both kindly provided by Joel Gottesfeld, The Scripps Research Institute (Herman et al., 2006; Xu et al., 2009) or DMSO only. Cells were incubated for an additional 48 hours and samples were taken for either expansion assay or histone analysis.

2.9 siRNA resuspension

All siRNas used in this study were purchased from Dharmacon. A full list of siRNAs used in this study is provided in Table 2.1. ON-TARGET plus, siGenome SMARTpool, individual siRNAs or scrambled non-targeting siRNA (D-001810) was diluted to 20 μM stock solutions with 1x siRNA buffer. This buffer was prepared from a 5X siRNA buffer (Dharmacon) using HyClone® HyPure RNase-free H_2O (Fisher Scientific). Aliquots were prepared and stored at -80°C.

Table 2.1 siRNAs used in this study

Target gene	Catalogue Number/Reference	siRNA type
HDAC3	L-003496	ON-TARGETplus SMARTpool
HDAC3	M-003496	siGenome SMARTpool
HDAC1	M-003493	siGenome SMARTpool
CBP	L-003477	ON-TARGETplus SMARTpool
p300	L-003486	ON-TARGETplus SMARTpool
CtIP	(Yu and Chen, 2004)	Customised individual siRNAs
Mre11	M-009271	siGenome SMARTpool
HDAC5	M-003498	siGenome SMARTpool
HDAC5	MU-003498	siGenome set of 4 indivdual siRNAs
HDAC9	M-005241	siGenome SMARTpool
MSH2	L-003909	ON-TARGETplus SMARTpool
MSH3	L-019665	ON-TARGETplus SMARTpool
MSH6	L-019287	ON-TARGETplus SMARTpool
FEN1	L-010344	ON-TARGETplus SMARTpool
FBH1	L-017404	ON-TARGETplus SMARTpool
RTEL1	LQ-013379-00	ON-TARGETplus set of 4 indivdual siRNAs (pooled)
RTEL1	LQ-013379-01	ON-TARGETplus set of 4 indivdual siRNAs
HLTF	L-006448	ON-TARGETplus SMARTpool
SHPRH	L-007167	ON-TARGETplus SMARTpool
Rad18	L-004591	ON-TARGETplus SMARTpool
Polβ	L-005164	ON-TARGETplus SMARTpool

2.10 Combined siRNA and shuttle vector transfections

RNA interference experiments were performed as described for section 2.8 but with minor variations. SVG-A cells were seeded at a density of 200,000 cells in DMEM+10% FBS with no antibiotics in 60 mm tissue culture dishes. Briefly, cells were transfected with the appropriate siRNAs; from Dharmacon using DharmaFECT 1 24 hours later. 10 μl siRNA was diluted with 190 μl DMEM. For double knockdowns, the total dosage of siRNAs was the same as that in single knockdowns (100 nM), i.e., the concentration of each contributing siRNA was reduced by half. In a separate 1.5 ml tube, 8μl of Dharmafect 1 was diluted to a final volume of 200 μl. Five minutes later, the tubes were combined and incubated at room

temperature for 20 min. The transfection reaction (final volume of 200 µl) was added to the dishes containing 1.6 ml DMEM+10% FBS. After 48 hours, cells were transfected with 7 µg of shuttle vector and also re-transfected with siRNAs using Lipofectamine 2000. After another two days, expansion frequencies were prepared as above, in parallel with immunoblot analysis of whole cell lysates or reverse transcription (RT) real-time PCR.

2.11 Cell viability assessment by Nigrosin exclusion assay

Cell viability following small molecule or siRNA treatment was determined by nigrosin. Subsequent to harvesting, an aliquot of cell suspension was removed and an equal volume of 0.2% nigrosin (in PBS) was added. Cells were counted on a haemocytometer. Cell viability was calculated as the number of viable cells (unstained) divided by the total number of cells (stained and unstained). Relative cell growth was calculated as total number of cells for inhibitor/siRNA treated/total number of cells treated with DMSO/scrambled siRNA. Both values were expressed as percentages.

2.12 Plasmid isolation from SVG-A cells and DpnI digestion of recovered plasmids

To measure expansions, plasmid DNA was extracted from SVG-A cells by Hirt's alkaline lysis (Hirt 1967). Briefly, medium was aspirated from cells and cells were washed gently with PBS. 1 ml of Hirt's lysis buffer (SDS 0.6%, 0.01 M EDTA, 0.01 M Tris-HCl, pH 7.4) was added to the dish, with gentle agitation of the dish. The lysate was decanted into a 1.5 ml tube, 250 µl 5M NaCl was added, inverted several times and stored at 4°C overnight. Thereafter, the lysate was centrifuged at 13000 rpm at 4°C for 40 min. The supernatant was decanted to a new 1.5 ml tube and incubated with proteinase K to a final concentration of 100 µg/ml at 50°C for 2 hr. The lysate was transferred to an Amicon Ultra 50K centrifugal filter units (Millipore, Tullagreen, Carrigtwohill, Co. Cork) and centrifuged at 5000 rpm at 4°C for 10 min. The centrifugal unit was inverted into a new vial and centrifuged at 3000 rpm at 4°C for 5 min to recover the retentate. The retentate was transferred to a new 1.5 ml tube and precipitated with two volumes of 100% ethanol overnight at -20°C. The sample was centrifuged at 13000 rpm at 4°C for 15 min. The resultant pellet was air-dried and resuspended in 100 µl TE buffer.

50 µl of the purified plasmid DNA was digested with 1 µl RNase A (10 mg/ml) and 3 µl DpnI (60 units), along with 6 µl 10X buffer 4 .The digest reaction was incubated at 37°C for 1 -3 hr and subsequently heat-inactivated at 75 °C for 10 min. The purpose of this digestion is to eliminate any plasmids that did not undergo replication in SVG-A cells. Plasmids replicated in *E.coli* are methylated at their adenine residues, while those replicated in human

cells are not. DpnI cleaves the sequence GATC only when the A residue is methylated, thus is useful for distinguishing between plasmids replicated in humans and those that have not. $1/10^{th}$ of the undigested and DpnI-digested recovered shuttle vector were subjected to agarose gel electrophoresis to examine DpnI resistance. A representative gel is shown in fig 2.4. As expected DpnI digestion of the stock plasmid, which was prepared in *E.coli*, resulted in digestion to completion. Digestion of the recovered shuttle vector prep does not yield any visible DpnI-sensitive material, indicating that the vast majority of the recovered DNA is plasmid that has replicated at least once in SVG-A cells. Following DpnI digestion, the recovered prep was then transformed into *S. cerevisiae* for measurement of expansions by selection for canavanine resistance or into *E.coli* for analysis of total plasmid numbers as measured by ampicillin-resistant colonies.

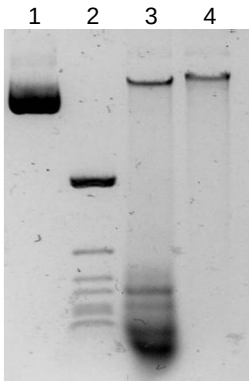

Figure 2.4. Agarose gel electrophoresis of DpnI-digested shuttle vector. Lane 1 represents the uncut stock plasmid used for the transfection and digested with DpnI in lane 2. Lane 3 contains uncut shuttle vector recovered from SVG-A cells and in lane 4, it has been DpnI-digested.

2.13 Identification of TNR expansions and contractions

To confirm changes in TNR length and to determine the size of the expansion or contraction, cell samples from single canavanine-resistant (expansion) or Ura^+ (contractions) yeast colonies were lysed in 100 µl of 50mM DTT with 0.5% Triton X-100, incubated at 37°C for 30 min and 95°C for 8 min . Samples were kept on ice thereafter PCR was performed with Cy5-labeled primers that flank the triplet repeat tract for 30 cycles (1 min at 95°C, 1 min at 60°C and 1 min at 72°C), with a final extension at 72°C for 5 min. For detection of expansions and contractions the following forward primer was used oBL251 (CY5-AGTAGCAGCACGTTCCTTATATGTAGCTTT-3'). The reverse primer varied depending on whether expansions (*CAN1*-reverse (CY5-TGCTTCTCCTCTATGTCGGCGTCT-3') or contractions oBL252 (CY5-AGTAGCAGCACGTTCCTTATATGTAGCTTT-3') were being examined. PCR products were analyzed on a denaturing 6% polyacrylamide gel. Product sizes were

determined by comparison of the reaction products with standards containing repeats of known size. Repeat lengths are estimated to within ±2 repeats. An example of this is shown in Fig 2.5.

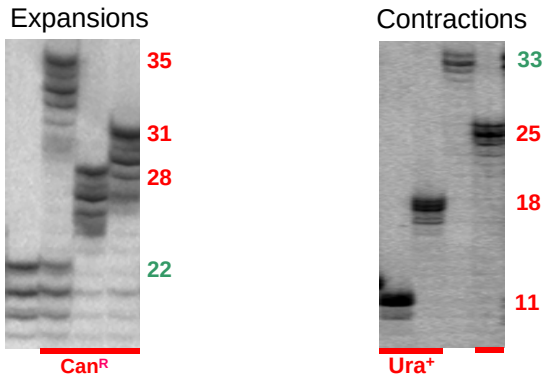

Figure 2.5. Analysis of expansions and contractions in SVG-A cells. PCR products of His^+Can^R (expansions) or His^+Ura^+ (contractions) colonies ran on a denaturing 6% polyacrylamide gel. The numbers in red denote changes in length from the original starting tract (green; the starting sizes are located in the first lane on expansion gel and in the third lane on contraction gel) estimated to within ±2 repeats.

The weighted average of expansion/contraction sizes was calculated by the determining the sum of the number of repeats added by the number of events for each repeat unit divided by the total number of expansion events analysed. A sample calculation is shown in section 2.17. The observed expansion frequency per 100,000 events was calculated as number of His^+Can^R colonies / number of total transformants (Amp^R colonies) x 100,000**.** The observed contraction frequency per 100,000 events was calculated as number of His^+Ura^+ colonies / number of total transformants (Amp^R colonies) x 100,000**.** The final corrected expansion or contraction frequency per 100,000 events was calculated by multiplying the fraction of plasmids harbouring real, genetically independent changes in TNR tract length by the observed frequency. For each data set, expansion/contraction frequencies were normalized for transformation efficiencies of yeast and *E.coli* defined as His^+colonies/ng control plasmid (pRS313) and Amp^R colonies/ ng control plasmid (pUC19), respectively. A sample calculation is described in section 2.17.

Determination of the background expansion frequency was performed to measure the basal level of expansions that could occur in *E. coli* during preparation of stock plasmid, or in yeast before selection became effective. This was done by transforming stock plasmid directly into yeast and *E.coli.* 625 ng was transformed directly into yeast and $1/50^{th}$-$1/200^{th}$ was plated onto -His. For *E.coli,* 1/1000 dilutions of the prep were made, the approximate concentration checked by UV absorption and 3 µl of this was transformed. $1/10^{th}$-$1/20^{th}$ was

plated onto LB+Amp. Appropriate corrections for dilution factors to ascertain the number of His^+Can^R colonies and Amp^R colonies for transformation of 625 ng were made. Background frequencies were calculated from a minimum of three independent measurements for each maxi-prep of plasmid used throughout the study and corrected background frequencies were determined using PCR data.

2.14 Preparation of $CaCl_2$ Competent *Escherichia coli*

A single colony of *E. coli* DH5α high efficiency competent cells (C2992H, NEB; Genotype: *F′ proA+B+ lacIq Δ(lacZ)M15 zzf::Tn10 (TetR) / fhuA2Δ(argF-lacZ)U169 phoA glnV44 Φ80Δ(lacZ)M15 gyrA96 recA1 endA1 thi-1 hsdR17)* was inoculated into 5 ml LB. Cells were incubated overnight at 37°C with shaking (200 rpm). Thereafter, the 5 ml culture was transferred to LB (250 ml) and incubated at 37 ^oC with shaking (200 rpm) until an OD_{600} of 0.4-0.6 was reached (~2-3 h). The culture was then placed on ice for 20 min followed by centrifugation at 4 ^oC at 5300 rpm for 10 min. The cell pellet was resuspended in 500 µl 0.1M $CaCl_2$/ml of culture and incubated on ice for 30 min. The cells were centrifuged at 4 ^oC at 5300 rpm for 10 min and the cell pellet was resuspended in 0.1M $CaCl_2$ containing 15% glycerol (100 µl per ml of original culture). The $CaCl_2$ competent cells were aliquoted and snap- frozen in liquid nitrogen before being stored at -80 ^oC.

2.15 *E.coli* transformation

E. coli competent cells were thawed on ice. Recovered shuttle vector prep was diluted 1/5 in ddH_2O and 3 µl was added to 50 µl cells. For maxi-preps, generally a 1/1000 dilution was prepared and 3 µl was added to 50 µl cells. 140 pg of pUC19 control plasmid was included each time to provide a consistent measure of transformation efficiency. Cells were incubated on ice for 30 min, heat-shocked in a 42°C water bath for 30 sec and incubated on ice for 5 min. Cells were incubated at 37°C for 1-2 hr shaking at 200 rpm subsequent to spreading a proportion of the cell suspension onto LB plates containing ampicillin (75 µg/ml). Plates were incubated overnight in an inverted position in a 37°C incubator. Total transformant number was evaluated as Amp^R colony number rather than number of His^+ colonies as previously described (Pelletier et al., 2005; Farrell and Lahue, 2006; Claassen and Lahue, 2007). This modification was made in order to increase the sensitivity of the assay due to *E.coli* being more amenable to transformation than yeast.

2.16 Yeast transformation

BL1435 (***MATa*** *leu2-3 leu2-112 his3- Δ trp1-289 ura3-52 Δcan1::KanMX*) was used for transformation of shuttle vector preps recovered from SVG-A cells. A small amount of the frozen glycerol stock was streaked onto a YPD plate and incubated at 30°C for two days. A high efficiency PEG/LiAC transformation protocol was used (Gietz and Woods, 2002). A single colony from a plate was used to inoculate 5 ml of YPD medium. The liquid culture was subsequently incubated at 30°C for 16–18 hr with shaking at 200 rpm. 1.5-2 ml of the overnight culture was added to 50 ml YPD in a 250 ml conical flask and this culture was incubated at 30°C until the OD_{600} reached 0.7-1.0 (3-4 hr) with shaking at 200 rpm. The yeast culture was then centrifuged at 1,500 x g for 5 min and washed twice with ddH_2O. Cells were resuspended in 1 ml ddH_2O and aliquoted into 100 µl volumes. Cells were centrifuged at 10,000 x g for 1 min and pellets were resuspended in 326 µl transformation mix (240 µl filter-sterile 50% w/v polyethylene glycol 3500, 36 µl 1M filter-sterilized lithium acetate and 50 µl boiled salmon sperm carrier DNA per transformation). For each transformation up to 34 µl of recovered shuttle vector was added to the cells and transformation mix; if less than 34 µl of DNA transformed, ddH_2O was added to make up to 34 µl. For transformation of stock plasmid for background measurement or pRS313, which was used throughout to determine transformation efficiency, 625 ng of the plasmid was transformed. The tubes were vortexed vigorously and then incubated in a 42°C water bath for 40 min. The yeast cells were then pelleted by centrifugation at 10,000 x g for 1 min. The transformed cells were suspended in 200 µl of ddH_2O and plated onto the appropriate selection medium i.e. SC-His or SC-His+Ura. For recovered shuttle vector-transformed cells, all of the cell suspension was plated. For stock plasmid preps, $1/50^{th}$ -$1/200^{th}$ was plated. Plates were incubated in an inverted position in a 42°C incubator. After two days, colonies from -His plates were replica-plated onto SC-His-Arg+Can (100 µg/ml) plates using three waste plates in between. The plates were incubated at 30°C for a further five days. The replica plating was performed in order to correct for any phenotypic lag. It was found that without replica plating, a high incidence of false positive expansions was regularly observed when plating the cell suspension directly onto SC-His+Can (60 µg/ml). For contraction assays, SC-His+Ura plates were incubated at 30°C for five days. Subsequent to this incubation period, colonies were counted and changes in repeat length was analysed by PCR.

2.17 Sample calculation of expansion frequency

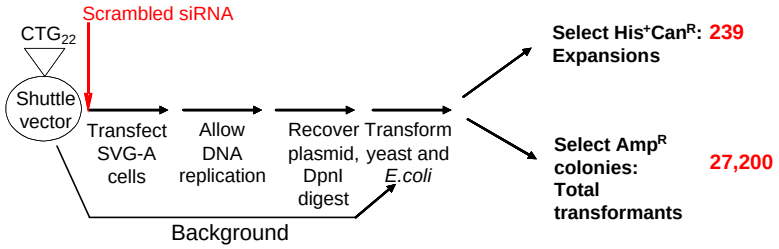

Figure 2.6. Sample calculation to determine expansion frequency. SVG-A cells were transfected with scrambled siRNA and shuttle vector. Following plasmid recovery and DpnI digestion, transformation into yeast and *E.coli* was performed yielding 239 $His^{+}Can^{R}$ colonies and 27,200 amp^{R} colonies (in red; all dilution factors accounted for).

1. Experimental details (fig 2.6):

Yeast transformation:

34 µl pBL302 transformed into BL1435 recovered following scrambled siRNA/shuttle vector transfection. Resuspended cells in 200 µl H_2O and plated all on SC-His; then replica-plated to SC-His-Arg+Can

E.coli transformation:

3 µl of a 1:5 dilution of pBL302 transformed into DH5α recovered following scrambled siRNA/shuttle vector transfection

Plated 200 µl of the cell suspension (total 1000 µl) onto LB+amp

2. Dilution and plating factors:

Yeast transformation: not applicable

E.coli transformation: = dilution fold of recovered DNA x plating dilution/volume of diluted DNA transformed x volume of prep transformed into yeast

= 5 x 5 / 3 x 34

E.coli transformation: = 96 x 5 x 5 / 3 x 34 = 27,200 = total transformant number

3. Calculate expansion frequency:

Observed expansion frequency = number of $His^{+C}an^{R}$ colonies / number of total transformants (amp^{R}colonies) x 100,000

For scrambled siRNA: 239 / 27,200 x 100,000 = 880

Corrected expansion frequency = observed expansion frequency x fraction of real genetically independent expansions

PCR analysis (as per Fig. 2.5) determined that there were 5 genetically independent bona fide expansions, while 14 samples were false positives

For scrambled siRNA: 880 x (5/19) = 232

The same calculation was applied for HDAC5 siRNA and the corrected expansion frequency was determined to be 112.

Changes in expansion frequency were expressed as fold change over scrambled siRNA: 112/232 = 0.48, where scrambled siRNA is arbitrarily defined as 1.

Corrected background expansion frequency for the plasmid maxi-prep was determined to be ~2% compared to that of scrambled siRNA.

Background expansion frequencies for the maxi-preps used are summarised in table 2.2 in comparison to the values for all DMSO/scrambled siRNA-treated cells for the corresponding maxi-prep. On average, ~10% of expansions were found to have occurred outside SVG-A.

4. Normalising for yeast and *E.coli* transformation efficiencies: For statistical analysis between data sets

Normalised His^+Can^R: Number of His^+can^R colonies / Yeast transformation efficiency
for scrambled siRNA: 239/334 = 0.72
for HDAC5 siRNA: 293/334 = 0.88

Normalised ampR: Number of amp^R colonies / *E.coli* transformation efficiency
for scrambled siRNA: 27,200/20,000 = 1.36
for HDAC5 siRNA: 39,100/20,000 = 1.96

Normalised observed expansion frequency: Normalised His^+Can^R/ Normalised amp^R
for scrambled siRNA: 0.72/1.36 = 0.53
for HDAC5 siRNA: 0.88/1.96 = 0.45

Normalised corrected expansion frequency: Normalised observed expansion frequency x fraction of real genetically independent expansions
for scrambled siRNA: 0.53 x (5/19) = 0.14
for HDAC5 siRNA = 0.45 x (3/20) = 0.07

This was done for each set of data due to the absolute corrected expansion frequency tending to vary from set to set, likely as a result of the many elements and different stages to the assay e.g. transformation efficiencies, variance in plasmid yield from experiment to experiment. In order to control for this variation in so far as possible, the above calculation was performed and "normalized corrected expansion frequencies" were used for statistical analysis.

Table 2.2 Background expansion frequencies of maxi-preps used in this study

Maxi prep number	Average background corrected expansion frequency/ 10^5	Average relative background/ Scrambled siRNA or DMSO control	SEM
1	1.9	0.08	0.064
2	0.3	0.02	0.004
3	6.6	0.27	0.114
4	2.1	0.02	0.02 (Range)
5	17.2	0.13	0.041
6	13.5	0.11	0.053
7	10.9	0.11	0.003
8	7.2	0.04	0.006
Average		**0.10**	

2.18 Calculation of weighted average increase in expansion size

To evaluate the increase in expansion sizes, the average weighted increase was determined. Shown below is a sample calculation.

Table 2.3 Expansion sizes as determined by PCR across the repeat tract and resolution of products on a denaturing 6% polyacrylamide gel.

Number of CTG repeats added	Incidence/Number of expansion events
5	1
6	2
7	2
8	5
9	1
10	5
11	1
12	3
13	3
14	1
15	1
16	1
17	2
18	1
19	1
20	1
Total number of expansions	31

Average weighted increase in expansion size = SUM (Number of repeats added x Incidence)/Total number of expansion events

Average weighted increase in expansion size for the example above

= SUM (5*1, 6*2, 7*2, 8*5, 9*1, 10*5, 11*1, 12*3, 13*3, 14*1, 15*1, 16*1, 17*2, 18*1, 19*1, 20*1)/31

= **10.1**

2.19 Harvesting SVG-A cells for whole cell extracts or RNA isolation

Subsequent to siRNA transfection, medium was aspirated from 60 mm dishes. Cells were washed with PBS, scraped on ice or trypsinised and centrifuged at 2000 rpm for 5 min. The supernatant was removed and the cell pellet was resuspended in 1 ml PBS, followed by centrifugation at 4^{o}C at 2000 rpm for 5 min. The resultant pellet was then stored at -80°C until required or used immediately for preparation of whole cell extracts or RNA isolation (section 2.20 and 2.21).

2.20 Preparation of whole cell extracts

Following cell harvesting, the resultant pellets were resuspended in RIPA lysis buffer (0.1% SDS, 0.1% Triton X-100, 0 1% sodium deoxylcholate; filter-sterilised and supplemented with 100X protease inhibitor cocktail III from Fisher Scientific immediately before use) and placed on ice for 30 min. Lysates were sonicated in a waterbath sonicator to minimize viscosity. Lysates were centrifuged at 4^{o}C at 13000 rpm for 30 min. The supernatant was transferred to a new tube and stored at –20°C as whole cell extract.

2.21 RNA isolation and cDNA synthesis

To assess siRNA knockdown in SVG-A cells by real-time RT-PCR, cells were treated as described in assay section. RNA was isolated using a Qiagen RNeasy Kit. All tips and tubes used in this procedure were treated with Diethylpyrocarbonate (DEPC) to inactivate RNases and subsequently autoclaved. Cell pellets were lysed by Buffer RLT and viscosity was reduced by homogenisation using Qiashredder columns. On-column DNase digestion was performed by addition of RNase-free DNase to eliminate DNA contamination (Qiagen). RNA was eluted in 30 µl RNase-free water. The concentration of RNA was determined by UV absorption. RNA samples were stored at -80°C. cDNA synthesis was performed using Precision nanoScript Reverse Transcription kit (Primer Design, Southampton, UK). 1 µg of RNA was added to 1 µl of random nonamer primers, primer annealing was performed at 65°C for 5 min and samples were placed on ice thereafter. 2 µl of qScript 10X buffer, 1 µl of dNTP mix (10 mM of each), 2 µl of DTT (100 mM), 2 µl of RNAse/DNase-free water and 1 µl of qScript enzyme was added to the annealed mixture. The mixture was then incubated at 25°C for 5 min, then at 55°C for 20 min, followed by heat inactivation 75°C for 15 min. cDNA samples were stored at -20°C.

2.22 Real-time RT-PCR

For real-time PCR analysis of transcript levels, cDNA was analysed using SYBR GreenMaster Mix (Applied Biosystems, ABI, Foster City, CA) on the 7500 fast Real-time

PCR system (Applied Biosystems). Each sample was assayed in triplicate for every run. All primers used were resuspended in RNase/DNase-free water. Primer efficiencies were validated by performing a relative standard curve with a 2-fold serial dilution series for cDNA samples. Primer sequences are listed in table 2.4. All primers were used at a concentration of 300 nM. Normalization for cDNA quantity was performed with HPRT control primers for each template and absolute abundance numbers were adjusted to yield an arbitrary value of 1 for scrambled siRNA control templates using the ΔΔCt method (Livak and Schmittgen, 2001). Abundance values were expressed relative to scrambled siRNA, which was arbitrarily defined as 100%.

Table 2.4 Primers used for real-time RT-PCR

Gene	Forward primer	Reverse primer	Accesion number/Reference
HPRT	TGACACTGGCAAAACAATGCA	GGTCCTTTTCACCAGCAAGCT	(Baelde et al., 2007)
HDAC3	CTGGCTTCTGCTATGTCAAC	ACATATTCAACGCATTCCCCA	(Atsumi et al., 2006)
HDAC5	GTCTCGGCTCTGCTCAGTGTAGA	GGCCACTGCGTTGATGTTG	(Milde et al., 2010)
HDAC9	CAGGCTGCTTTTATGCAACA	TTTCTTGCAGTCGTGACCAG	(Choi and Kang, 2011)
FBH1	CGGTGGGATGGAGTTTCTAA	ATCTTGGTCGGTTTCACCAG	NM_032807.3, NM_178150.1
RTEL1	GCCAGGGAGCTACATCTTTG	CCCTTGGTCTGAAACGTGAT	NM_016434.2, NM_032957.3

2.23 Preparation of histone extracts

Medium was aspirated from 60 mm dishes. Cells were washed with ice-cold PBS, harvested by trypsinisation and centrifuged at 4 ^{o}C at 2000 rpm for 5 min. Cells were washed twice with ice-cold PBS. Cells were resuspended in Triton Extraction Buffer (TEB: PBS containing 0.5% Triton X 100 (v/v), 2 mM phenylmethylsulfonyl fluoride (PMSF), 0.02% (w/v) NaN_3 : 10^7 cells per ml buffer). Cells were resuspended in half the volume of TEB and centrifuged at 4 ^{o}C at 2000 rpm for 5 min. Histones were extracted in 0.2N HCl (50µl / 2 x 10^6 cells) at 4 ^{o}C overnight.

2.24 Protein quantification

Protein content of WCEs and histone extracts was determined by DC assay, a modified Lowry-based protein assay (Bio-Rad). Bovine serum albumin (BSA) was used as a standard at concentrations of 0 µg/µl to 1 µg/µl diluted in RIPA buffer (for WCEs) or PBS (for histone extracts). 5 µl was added in duplicate to wells of a 96-well plate. 5 µl of sample diluted 1:5 in RIPA buffer (for WCEs) or PBS (for histone extracts) was added to duplicate wells. 25 µl of reagent A and 200 µl of reagent B was added to each well. The samples were

incubated at room temperature for 15 min and absorbances were read at 490 nm using a WALLAC Victor™ Multi-label microtitre plate-reader. Protein concentration was determined by interpolation of the standard curve.

2.25 SDS polyacrylamide gel electrophoresis (SDS-PAGE) and transfer to PVDF membrane

Proteins were resolved by SDS-PAGE according to standard methodology (Sambrook et al., 1989). The percentage of acrylamide in the resolving gel was 8%, 10% or 15% depending on the size of the protein of interest. The resolving gel was overlaid with a stacking gel 5% acrylamide. For detection of CBP and p300 (approx 300 kDa), pre-cast SDS-PAGE gels (4-20%) were used (Bio-Rad). Running buffer (0.3% Tris base, 1.44% glycine and 0.1% SDS) was added to the inner and outer chambers of the Mini PROTEAN III Cell electrophoresis unit (Bio-Rad). Before loading, 4x Laemmli buffer was added to each sample and boiled for 5 min. 7 µl of SeeBlue Plus2 standard (Invitrogen) was used as a molecular marker. Following sample loading, electrophoresis was performed at 100V until the bromophenol blue dye front had reached the bottom of the gel.

Subsequent to electrophoresis, the SDS-PAGE gels were removed from the gel apparatus and transferred to PVDF membrane (Millipore). Transfer was performed TRANS-BLOT™ transfer unit along with an ice block and magnetic stir bar. The tank was filled with transfer buffer (25 mM Tris; 193 mM glycine; 20 % methanol) and transfer was performed at 100V for 120-150 min, depending on the size of the protein of interest. Following transfer, the membrane was stained with Ponceau S (0.1% (w/v) in 5% acetic acid) to verify effective transfer of proteins. Thereafter, the membrane was destained with dH_2O and subjected to western blot analysis.

2.26 Western blotting

PVDF membranes were blocked in 5% non-fat milk PBS-T (PBS; 0.05% Tween®-20), or 5% BSA PBS-T at room temperature for 1 hr or at 4°C overnight on a rotating platform depending on the protein of interest: All antibodies except for H4 and AcH4 were diluted in 5% milk PBS-T with the preceding block being 5% milk PBS-T. For the anti-H4 and AcH4 antibodies, the membranes were blocked in 5% BSA PBS-T and the primary and secondary antibodies were diluted in 1% BSA PBS-T. The membrane was incubated with an appropriate dilution of primary antibody in blocking solution as described in Table 2.5 at 4°C (room temperature for incubations that were not overnight) for a suitable period of time. The membrane was washed with three times with PBS-T for 5 min. The membrane was incubated with the appropriate HRP-conjugated secondary antibody diluted 1/10,000 in the

same solution as the primary antibody at room temperature for 1 hour. Secondary antibodies conjugated to horseradish-peroxidase were donkey anti-rabbit (711-035-152), goat anti-mouse (115-035-003) and donkey anti-goat (705-035-147) from Jackson ImmunoResearch Laboratories (West Grove, PA, USA). Bands were detected using chemiluminescence reagents (Western Lightning Plus-ECL, PerkinElmer) by exposure to X-ray film (Kodak) using a CP1000 Automatic Film processor with Devalex X Ray Developer and FixaPlus X Ray Fixer and/or by a G-Box imager (Syngene). The intensity of immunoreactive bands was measured using Image J software (http://rsb.info.nih.gov/ij/). Densitometry was calculated as the mean intensity normalized to the loading control (Actin).

2.27 Statistical Analyses

All *P* values were determined by two-tailed Student's t-test assuming unequal variances. *P* values for each data set are reported in the text body. *n* values for each data set are specified in the figure legend unless stated within the text body.

Table 2.5 Primary antibodies used in this study

Protein	Source	Cat number	Raised in	Dilution used	Incubation time	Band size (kDa)
FEN1	Abcam	Ab17993	Rabbit	1/2500	Overnight	47
MSH2	Calbiochem	NA26	Mouse	1/100	Overnight	100
HDAC1	CHDI repository	CH00218	Rabbit	1/1000	Overnight	60
HDAC3	Santa Cruz	sc-11417	Rabbit	1/200	Overnight	50 (often doublet)
HDAC5	Abcam	ab1439	Rabbit	1/1000	Overnight	105
HDAC5	CHDI repository	CH00150	Rabbit	1/100	Overnight	105
HDAC9	CHDI repository	CH00172	Rabbit	1/1000	Overnight	110
HDAC9	Abcam	ab18970	Rabbit	1/1000	Overnight	110
ACTIN	Sigma	2066	Rabbit	1/500	Overnight/ 3 hr	42
MSH3	BD Transduction Laboratories	611390	Mouse	1/100	Overnight	127
MSH3	(Holt et al., 2011)	N/A	Mouse	1/25	Overnight	130
MSH6	BD Transduction Laboratories	610919	Mouse	1/1000	Overnight	130
PMS2	Calbiochem	NA30	Mouse	1/250	Overnight	100
Polβ	Abcam	ab3181	Mouse	1/200	Overnight	39
Histone H4	Abcam	ab31830	Mouse	1/500	Overnight	14
Acetyl Histone H4	Millipore	06-866	Rabbit	1/10000	30-60 min	14
p53	R&D systems	HAF1355	Goat	1/1000	Overnight	53
Acetyl p52 (Lys 382)	Cell Signaling	2525	Rabbit	1/1000	Overnight	53
CBP	Santa Cruz	sc-583	Rabbit	1/200	Overnight	300
p300	Santa Cruz	sc-585	Rabbit	1/200	Overnight	300
CtIP	Richard Baer (Yu and Baer, 2000)	N/A	Mouse	1/40	Overnight	110
Mre11	Santa Cruz	sc-5859	Goat	1/200	Overnight	76
Rad18	Abcam	ab57447	Mouse	1/500	Overnight	75/80 (sometimes doublet)
HLTF	Bethyl Laboratories	A300-230A	Rabbit	1/1000	Overnight	117
SHPRH	Origene	TA501443	Mouse	1/1000	Overnight	170

2.28 References

Atsumi, A., A. Tomita, H. Kiyoi and T. Naoe (2006). Histone deacetylase 3 (HDAC3) is recruited to target promoters by PML-RARalpha as a component of the N-CoR co-repressor complex to repress transcription in vivo. *Biochem Biophys Res Commun* **345**(4): 1471-80.

Baelde, H. J., M. Eikmans, D. W. Lappin, P. P. Doran, D. Hohenadel, P. T. Brinkkoetter, F. J. van der Woude, R. Waldherr, T. J. Rabelink, E. de Heer and J. A. Bruijn (2007). Reduction of VEGF-A and CTGF expression in diabetic nephropathy is associated with podocyte loss. *Kidney Int* **71**(7): 637-45.

Choi, D. and S. Kang (2011). Identification and characterization of RNF2 response elements in human kidney cells. *Mol Cells* **31**(3): 247-53.

Claassen, D. A. and R. S. Lahue (2007). Expansions of CAG.CTG repeats in immortalized human astrocytes. *Hum Mol Genet* **16**(24): 3088-96.

Debacker, K., A. Frizzell, O. Gleeson, L. Kirkham-McCarthy, T. Mertz and R. S. Lahue (2012). Histone deacetylase complexes promote trinucleotide repeat expansions. *PLoS Biol* **10**(2): e1001257.

Farrell, B. T. and R. S. Lahue (2006). CAG*CTG repeat instability in cultured human astrocytes. *Nucleic Acids Res* **34**(16): 4495-505.

Gietz, R. D. and R. A. Woods (2002). Transformation of yeast by lithium acetate/single-stranded carrier DNA/polyethylene glycol method. *Methods Enzymol* **350**: 87-96.

Herman, D., K. Jenssen, R. Burnett, E. Soragni, S. L. Perlman and J. M. Gottesfeld (2006). Histone deacetylase inhibitors reverse gene silencing in Friedreich's ataxia. *Nat Chem Biol* **2**(10): 551-8.

Holt, I., L. Thanh Lam, S. Tome, D. G. Wansink, H. Te Riele, G. Gourdon and G. E. Morris (2011). The mouse mismatch repair protein, MSH3, is a nucleoplasmic protein that aggregates into denser nuclear bodies under conditions of stress. *J Cell Biochem* **112**(6): 1612-21.

Livak, K. J. and T. D. Schmittgen (2001). Analysis of relative gene expression data using real-time quantitative PCR and the 2(-Delta Delta C(T)) Method. *Methods* **25**(4): 402-8.

Major, E. O., A. E. Miller, P. Mourrain, R. G. Traub, E. de Widt and J. Sever (1985). Establishment of a line of human fetal glial cells that supports JC virus multiplication. *Proc Natl Acad Sci U S A* **82**(4): 1257-61.

Maubach, G., M. C. Lim, C. Y. Zhang and L. Zhuo (2006). GFAP promoter directs lacZ expression specifically in a rat hepatic stellate cell line. *World J Gastroenterol* **12**(5): 723-30.

Milde, T., I. Oehme, A. Korshunov, A. Kopp-Schneider, M. Remke, P. Northcott, H. E. Deubzer, M. Lodrini, M. D. Taylor, A. von Deimling, S. Pfister and O. Witt (2010). HDAC5 and HDAC9 in medulloblastoma: novel markers for risk stratification and role in tumor cell growth. *Clin Cancer Res* **16**(12): 3240-52.

Pelletier, R., B. T. Farrell, J. J. Miret and R. S. Lahue (2005). Mechanistic features of CAG*CTG repeat contractions in cultured cells revealed by a novel genetic assay. *Nucleic Acids Res* **33**(17): 5667-76.

Sambrook, J., T. Maniatis and E. F. Fritsch (1989). Molecular cloning : a laboratory manual. Cold Spring Harbor, N.Y., Cold Spring Harbor Laboratory Press.

Xu, C., E. Soragni, C. J. Chou, D. Herman, H. L. Plasterer, J. R. Rusche and J. M. Gottesfeld (2009). Chemical probes identify a role for histone deacetylase 3 in Friedreich's ataxia gene silencing. *Chem Biol* **16**(9): 980-9.

Yu, X. and R. Baer (2000). Nuclear localization and cell cycle-specific expression of CtIP, a protein that associates with the BRCA1 tumor suppressor. *J Biol Chem* **275**(24): 18541-9.

Yu, X. and J. Chen (2004). DNA damage-induced cell cycle checkpoint control requires CtIP, a phosphorylation-dependent binding partner of BRCA1 C-terminal domains. *Mol Cell Biol* **24**(21): 9478-86.

CHAPTER 3

Role of histone deacetylases and histone acetyltransferases in trinucleotide repeat instability

Some of the material presented in this chapter was published in the following article:

"Histone Deacetylase Complexes Promote Trinucleotide Repeat Expansions"
PLoS Biology 2012 10(2): e1001257

Kim Debacker*, Aisling Frizzell*, Olive Gleeson, Lucy Kirkham-McCarthy, Tony Mertz and Robert Lahue

*: Equal contributions

3.1 Summary

The results presented in this chapter describe the roles of various HDACs and HATs in TNR instability. Yeast data show that specific class I and class II HDACs promote expansions. I hypothesized that expansions in human cells would also be promoted by specific HDACs. I found that the class I HDAC3 promotes threshold-length CTG repeat expansions in SVG-A cells. Chemical inhibition of HDAC3 resulted in a decrease in expansions by up to 77%. In contrast, treatment with a HDAC1/HDAC2-specific inhibitor did not affect expansion frequency. These observations were validated by siRNA depletion of HDAC1 and HDAC3. Knockdown of HDAC1 had no effect on expansions, while decreased HDAC3 expression showed a similar reduction of expansions as for the HDAC3 inhibitor. Thus, HDAC3 is the specific class I HDAC involved in promoting expansions. Knockdown of HDAC3, did not impact on contractions, implying specificity for expansions. Investigation of the involvement of class II HDACs, HDAC5 and HDAC9, in expansions revealed HDAC5 to accelerate expansions, while HDAC9 was shown to inhibit their occurrence. Double knockdown of HDAC3 and HDAC5 resulted in a similar decrease in expansions as for single knockdowns of HDAC3 and HDAC5 implying that they are acting through the same mechanism to promote expansions. Treatment of SVG-A cells with siRNA against the HATs CBP/p300 effected a stimulation in expansions. This further confirms a role for chromatin-modifying enzymes in modulating TNR expansions. In yeast, stability of the repair protein Sae2 has been shown to be controlled its acetylation status. Sae2 and Mre11 have been implicated as downstream factors Rpd3L and Hda1 in promoting expansions in yeast. The respective human homologues, CtIP and MRE11, do not affect expansions in SVG-A cells. The data presented identify HDACs as novel modulators of TNR expansions.

3.2 Introduction

One of the most intriguing aspects of TNR instability is that TNRs expand due to the presence, not the lack of certain proteins, most likely due to corruption of their normal biochemical activities by the repetitive nature of the DNA (Mirkin, 2007; McMurray, 2010). Therein lies an opportunity to target the root-cause of TNR disease by identification of specific expansion-promoting factors that are amenable to therapeutic intervention. Thus, detection of factors that accelerate TNR expansions and subsequent elucidation of their mode of action is warranted in order to provide new therapeutic and mechanistic insights to understanding and controlling these mutations. To this end, a blind screen was performed in yeast by the Lahue lab for mutants that reduced the rate of expansions near the threshold. The screen comprised cells with a genomically integrated $(CTG)_{20}$-*CAN1* reporter randomly mutagenised using a gene disruption library with ~50% coverage of the non-essential genes. This screen revealed 3 of 11 hits as constituent members of the Rpd3L or Hda1 HDAC complexes (Debacker et al., 2012). Single mutants of *sin3, pho23* and *hda3* had reduced expansion rates of up to 90%. Double mutants of HDACs from the two complexes had a more pronounced effect with almost complete ablation of expansions. This was a highly novel finding, providing the first direct link between specific HDACs and the somatic expansion process. Although the identification of particular HDACs that are causal for expansions was unprecedented, it was not an entirely surprising discovery as the TNR literature contains several reports implying connections between expansions and chromatin remodeling/epigenetic factors as discussed in chapter one.

Interestingly, HDAC inhibition is currently being developed as a potential therapeutic strategy to alleviate symptoms of TNR diseases. The rationale behind use of HDAC inhibitors in this context stems from the fact that transcriptional deregulation is central to disease etiology for many of these disorders. While there have been extensive investigations into the effect of HDAC inhibition on transcription levels in TNR diseases, little has been done to establish the impact of specific HDACs/HATs on TNR instability. Moreover, most of the studies showing a role for chromatin-modifying enzymes in instability employ long TNR tracts corresponding to the disease state in affected individuals and thus are useful for gleaning information on the further expansion of disease-length alleles. As a result, there is a distinct lack of information regarding what is happening at the threshold.

Work in the Lahue lab has revealed novel factors contributing to instability with the identification of certain HDAC components as proteins that accelerate expansions at the threshold in yeast (Debacker et al., 2012). In addition to strengthening support for chromatin-modifying enzymes modulating instability, these findings provided candidate

proteins to test for a role in promoting expansions in higher model systems. Bolstered by the fact that HDACs are highly conserved from yeast to humans, this led us to address their participation in modulating expansions near the threshold in human cells. If the finding that HDACs promote expansions in yeast translates to humans, then chemical inhibition and/or siRNA knockdown of one or more HDACs should suppress expansions. In yeast, members of the Rpd3L and Hda1 complexes were shown to be mediators of expansions while the sirtuin Sir2 did not have any effect on expansions (Debacker et al., 2012). Thus, the experimental focus was narrowed to targeting specific class I (homologous to Rpd3L) and class II HDACs (homologous to Hda1) in human cells to ascertain their influence on expansions (Fig. 3.1).

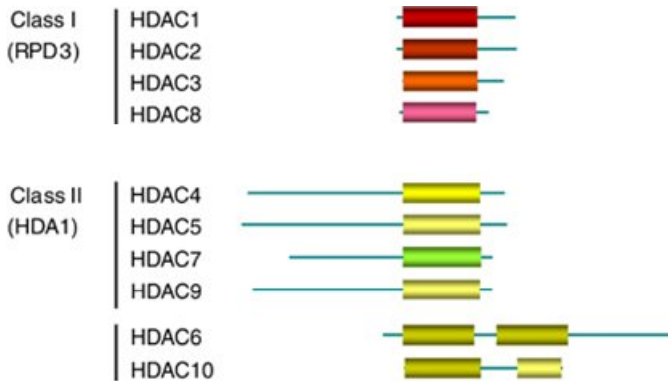

Figure 3.1 Schematic of the organization of class I and II human HDACs with respect to their homology to yeast. From (Richon, 2006). Coloured, shaded regions represent the catalytic domains.

3.3 Results

3.3.1 Effect of small-molecule inhibitors of HDAC3 and HDAC1/2 on TNR expansions in SVG-A cells.

In light of the finding in yeast that Rpd3 promotes expansions, I focussed on the human homologues, class I HDACs. To search for relevant HDACs that might have similar functions in modulating expansions, I used isoform-specific HDAC inhibitors. The small molecule inhibitor 4b is selective for the class I enzyme HDAC3 but has some specificity for HDAC1 (Herman et al., 2006; Jia et al., 2012). 4b has been shown to reverse FXN gene silencing in primary lymphocytes from FRDA patients (Herman et al., 2006). Furthermore, it has been shown to alleviate disease phenotype and reduce transcriptional abnormalities in transgenic HD mice (Thomas et al., 2008). Compound 3 is a HDAC1/2 specific inhibitor and failed to upregulate FXN mRNA levels in patient lymphocytes (Xu et al., 2009).

Treatment of cells with either HDAC inhibitor was performed using three concentrations; 5 μM, 10 μM and 20 μM. 4b efficiently suppressed TNR expansions in SVG-A cells at doses that are well tolerated. Treatment with 4b reduced expansion frequencies in a dose-dependent manner. Treatment of cells with the lowest dose of 4b, 5 μM did not change expansion frequencies when compared with the DMSO-only control. In contrast, expansion frequencies were suppressed 70% and 77% by 4b at 10 μM and 20 μM, respectively (Fig. 3.2A). Modest increases in expansion frequency were observed for 5 μM and 10 μM compound 3 (1.33- and 1.63-fold over DMSO only control), while 20 μM compound 3 resulted in an expansion frequency similar to that of DMSO only (0.89 vs 1) (Fig. 3.2B). None of the doses of compound 3 elicited statistically significant alterations in expansion frequency thereby suggesting that unlike HDAC3, HDAC1 and HDAC2 are not involved in modulating expansions in SVG-A cells.

Chemical inhibition of HDAC1/2 and HDAC3 revealed that specifically targeting HDAC3 resulted in a suppression of expansions, while impairing HDAC1/2 activity did not affect the frequency of expansions. It was hypothesized that HDAC3 might also alter the spectrum of expansion sizes by elimination of certain sizes of expansions, or all sizes of expansions were equally affected. To assess this possibility, expansion sizes were determined. The weighted average expansion sizes are +10.5 repeats for the DMSO-only control and +8.8 repeats for the 4b-treated cells (Fig. 3.2C). The similarity in sizes implies that 4b does not affect expansion sizes. Thus, treatment with 4b gives fewer expansions of similar sizes, thus inhibition of HDAC3, impacted on the frequency of expansions, not the size of the expansions. Perhaps if HDAC1/2 were involved in TNR expansions in human cells, specific

inhibition of these may skew the sizes of expansions occurring during SVG-A culture. However, there was no change in the spectrum of expansions upon compound 3 treatment with weighted average expansion increases of 8.6 for DMSO-treated and 9.9 for compound 3-treated cells (Fig. 3.2D).

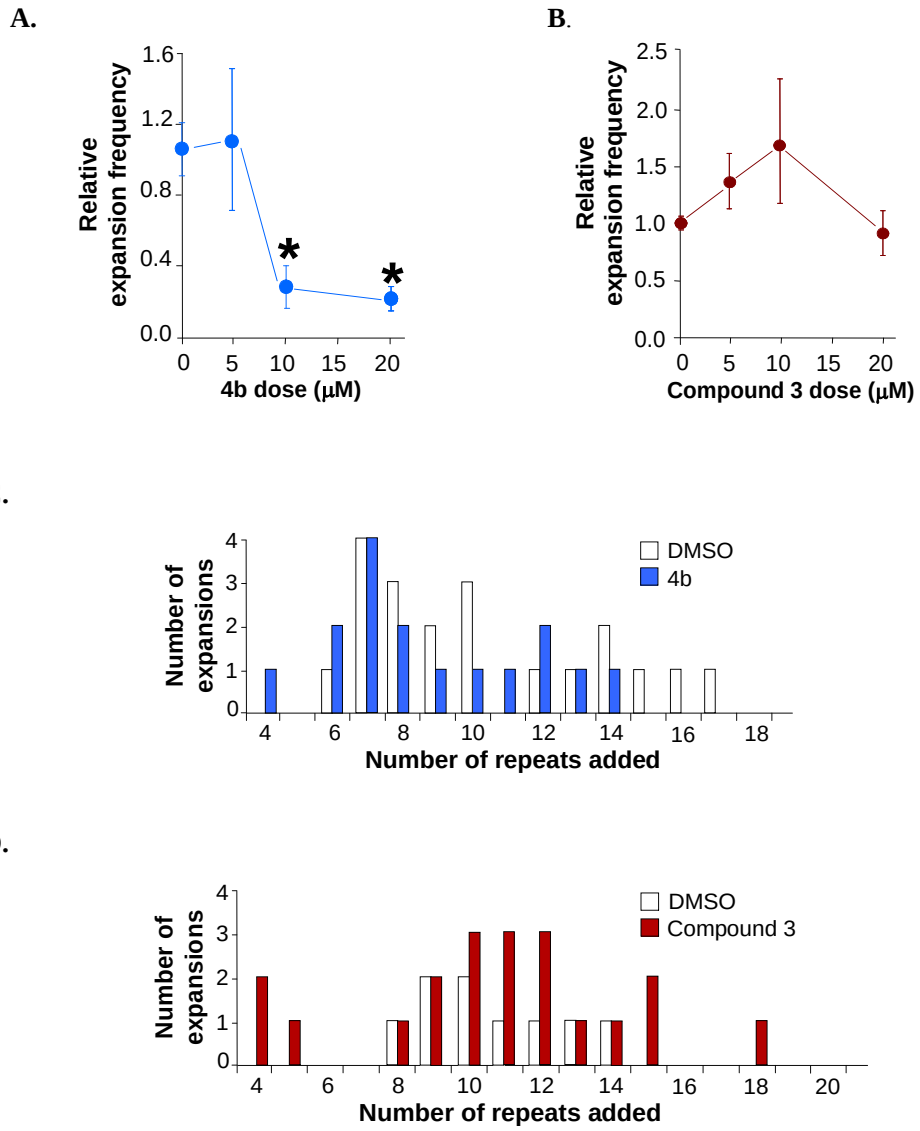

Figure 3.2 Expansion data for 4b- and compound 3-treated SVG-A cells. Expansion frequencies for **A.** 4b-treated cells; n= 5 (*P*=0.93 for 5 μM, *P*=0.009 for 10 μM, *P*=0.003 for 20 μM) and for **B.** compound 3-treated cells; n=3. (*P*=0.17 for 5 μM, *P*=0.31 for 10 μM, *P*=0.65 for 20 μM) Error bars denote ± one SEM; *, *P*<0.05 compared to DMSO control. Expansion sizes for **C.** 4b-treated cells: 21 genetically independent expansions for DMSO, 16 for 4b (data from 10 μM and 20 μM treatments) and for **D.** compound 3-treated cells: 9 genetically independent expansions for DMSO, 20 for compound 3 (data from 10 μM and 20 μM treatments).

To exclude the possibility that the suppression of expansions in 4b-treated cells is due to cytotoxic effects of the drug, cell viability was measured. The reduced number of expansions upon 4b treatment could not attributed to increased cell death, because the SVG-A cells retained ≥83% viability, relative to DMSO-only control, even at the highest dose of inhibitor (Fig. 3.3A). Furthermore, treatment with the same doses of compound 3, which did not impact on expansion frequencies, had similar effects cell viability. Although, treatment with 4b or compound 3 did not have any major undesirable effects on cell viability, a dose-dependent reduction in cell growth was observed. Upon treatment with the highest dose of 4b, 20 μM, the cells are still dividing but at two-fold slower rate than DMSO-only treated cells (Fig. 3.3B) Notably, no cell-static effects were reported for lymphoblast cells following treatment of 4b at concentrations <20 μM (Thomas et al., 2008). This difference is might be due to the combinatorial impact of lipofectin-mediated transfection and 4b treatment in SVG-A cells or may be due to cell-specific effects.

A.

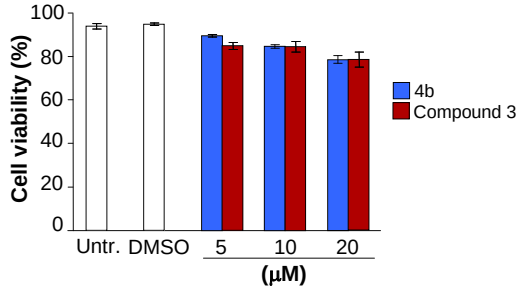

B.

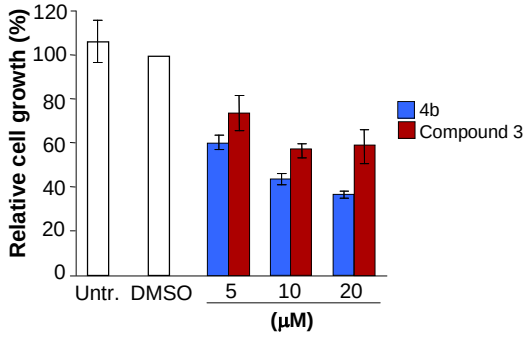

Figure 3.3 Cell viability and growth for 4b- and compound 3-treated SVG-A cells. A. Cell viability was measured by nigrosin-exclusion assay following treatment of SVG-A cells with 4b and compound 3. Viability is expressed as number of viable cells/total number of cells n = 5 for untreated, DMSO and 4b, n= 3 for compound 3. **B.** Growth of 4b- and compound 3-treated cells. Total cell counts are expressed relative to DMSO-treated cells. n = 5 for untreated, DMSO and 4b, n= 3 for compound 3. Error bars denote ± one SEM.

To confirm that 4b is inhibiting HDAC activity in SVG-A cells, acetylation of histone H4 was examined by western blotting. Figure 3.4A. shows the AcH4 accumulation in response to 4b treatment. There is a dose-dependent increase in histone H4 acetylation with the

anticipated increase in acetylated H4, up to approximately 10-fold, when cells were treated with 4b (Fig. 3.4B)**.** In order to verify that HDAC1 is specifically being inhibited by compound 3 exposure, p53 acetylation following treatment was measured. HDAC1 has been shown to deacetylate p53 at all known acetylated lysines *in vivo* (Ito et al., 2002). To this end, western blotting analysis for p53 acetylation at lysine 382 was examined for samples from compound 3-treated cells and 4b-treated cells. 4b-treated cells were used as a negative control as many studies have eliminated a role for HDAC3 in p53 acetylation. In some western blots, there appeared to be an increase in acetylated p53 for compound 3-treated cells, most predominantly for the two higher concentrations, 10 μM and 20 μM. However, this analysis did not prove a tractable means of definitively determining that HDAC1 was inhibited, with levels of acetylation varying from experiment to experiment. In some cases, total levels of p53 were decreased for the compound 3-treated cells with a concordant increase in p53 acetylation (Fig. 3.4C).Samples from 4b-treated cells not showing this effect. Similar observations have been reported in various human cancer cell lines whereby TSA and sodium butyrate reduced total p53 levels, while p53 acetylation was elevated (Suzuki et al., 2000; Bandyopadhyay et al., 2004). The reasons behind this occurrence have not yet been elucidated. The concentrations of compound 3 used in this experiment were chosen based on the observation that the treatment with 10 μM compound 3 resulted in increased acetylation of histone H3 in FRDA patient lymphoblasts (Xu et al., 2009).

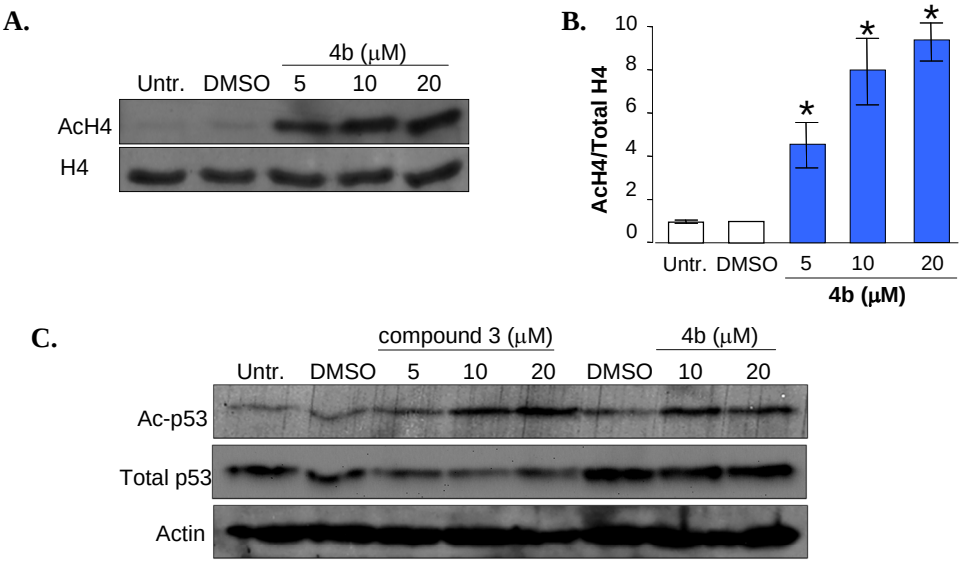

Figure 3.4 Acetylation status of histone H4 and p53 upon treatment of SVG-A cells with HDAC inhibitors. A. Representative western blot analysis of acetylated histone H4 (AcH4) and total H4 upon treatment with 4b. **B.** AcH4/Total H4 ratio normalized to the DMSO-only. These results are from 4 independent measurements of AcH4 and total H4 by immunoblot. Error bars denote ± one SEM. *, $P<0.05$ compared to DMSO-only.**C.** Representative western blot analysis of acetylated p53 (Ac-53), total p53 and Actin upon treatment with compound 3 and 4b.

It was observed that both 4b- and compound 3-treatment of SVG-A cells results in an increased yield of transfected plasmid compared with that recovered from DMSO-only cells. The increase in the number of total transformants (*E.coli* transformants) is shown in tables 3.1 and 3.2. Total transformant numbers for cells treated with 5-, 10- and 20 μM 4b show a 4.8-, 10.2- and 12.5-fold increase, respectively over DMSO. A similar but less dramatic trend is observed for compound 3, with cells treated with 5-, 10- and 20 μM compound 3 showing increases of 3.2-, 4.6- and 7.1-fold, respectively.

Table 3.1 Total transformant numbers from 4b-treated SVG-A cells

μM 4b	**Fold change in total transformant number relative to DMSO only control**	**+/- SEM**
DMSO	1.0	0.0
5	4.8	1.5
10	10.2	2.6
20	12.5	2.3

Table 3.2 Total transformant numbers from compound 3-treated SVG-A cells

μM compound 3	**Fold change in total transformant number relative to DMSO only control**	**+/- SEM**
DMSO	1.0	0.0
5	3.2	0.7
10	4.7	1.2
20	7.2	3.1

This is suggestive of increased shuttle vector upon chemical inhibition of HDACs. SVG-A large T antigen has been shown to be acetylated by CBP (Poulin et al., 2004; Borger and DeCaprio, 2006). The purpose of T antigen acetylation is unclear; one report found acetylated T antigen to be degraded, while another study proposed that acetylation is required for its stabilisation (Shimazu et al., 2006; Valls et al., 2007). Inhibition of specific HDACs might result in T antigen stability, then this could explain the increase in plasmid yield perhaps due to increased binding to the SV40 ori and thus an increase in SV40-driven replication. Hyperacetylation of histones, or loss of histone tails, has been shown to

facilitate the elongation step of SV40 DNA replication (Quintini et al., 1996; Alexiadis et al., 1997). Perhaps the minichromosomes of SV40 are hyperacetylated upon treatment with 4b and compound 3 enhancing SV40 replication resulting in augmentation of shuttle vector replication. However increased plasmid yields were not observed following HDAC1 or HDAC3 siRNA knockdown (section 3.3.2; data not shown). It is difficult to reconcile the discrepancies between the plasmid yields for drug versus siRNA. Perhaps the level of drug-induced inhibition of specific HDACs was more potent than that of siRNA. The level effected by the siRNAs may not have enough to bring about sufficient decreases in HDAC activity. HDAC1 and HDAC3 protein levels were reduced to approximately 25% and this low level of HDAC expression may have been enough to retain at least some gene silencing action. Another possibility is that the HDAC inhibitors are exacting off-target effects that are not applicable for the siRNA treatments. It appears that plasmid replication is enhanced following treatment with 4b and compound 3**.** Nevertheless, the perceived increase in plasmid replication does not appear to correlate with the observed reduced expansion phenotype as both chemical inhibition and siRNA depletion of HDAC3 had a similar decrease in expansion phenotype.

3.3.2 Characterisation of TNR expansions in human cells following depletion of HDAC1 and HDAC3 in SVG-A cells

HDAC3 appears to be the relevant class I HDAC involved in promoting expansions, based on the observation that chemical inhibition of HDAC3 suppressed expansion frequencies while HDAC1 and HDAC2-inhibiton did not reduce expansions. In order to further corroborate that HDAC3 is the relevant target, SVG-A cells were subjected to RNAi knockdown of HDAC1 and HDAC3. HDAC1 siRNA-treated cells did not demonstrate any significant changes in expansion frequency, when compared to scrambled siRNA control cells (P=0.66) (Fig. 3.5A). In contrast, treatment of SVG-A cells with HDAC3 siRNA resulted in a decrease in expansion frequency of approximately 76%, a similar extent of suppression observed with 4b treatment (P=0.025) (Fig. 3.5B). The spectra of expansion events in cells with reduced HDAC1 expression overlaps with that of cells treated with scrambled siRNA with +10.3 and +10.6 average increases in repeat tract length, respectively (Fig 3.5C). This indicates that events are of similar sizes in HDAC1 siRNA-and scrambled siRNA-treated cells, as well as occurring at comparable frequencies. Similarly, expansion sizes in HDAC3 siRNA-treated cells and scrambled siRNA-treated cells are comparable with weighted average expansion increases of +10.8 and +11.3, respectively (Fig. 3.5D).These data in combination with the HDAC inhibitor results imply a role for HDAC3 but not HDAC1 in promoting expansions in SVG-A cells.

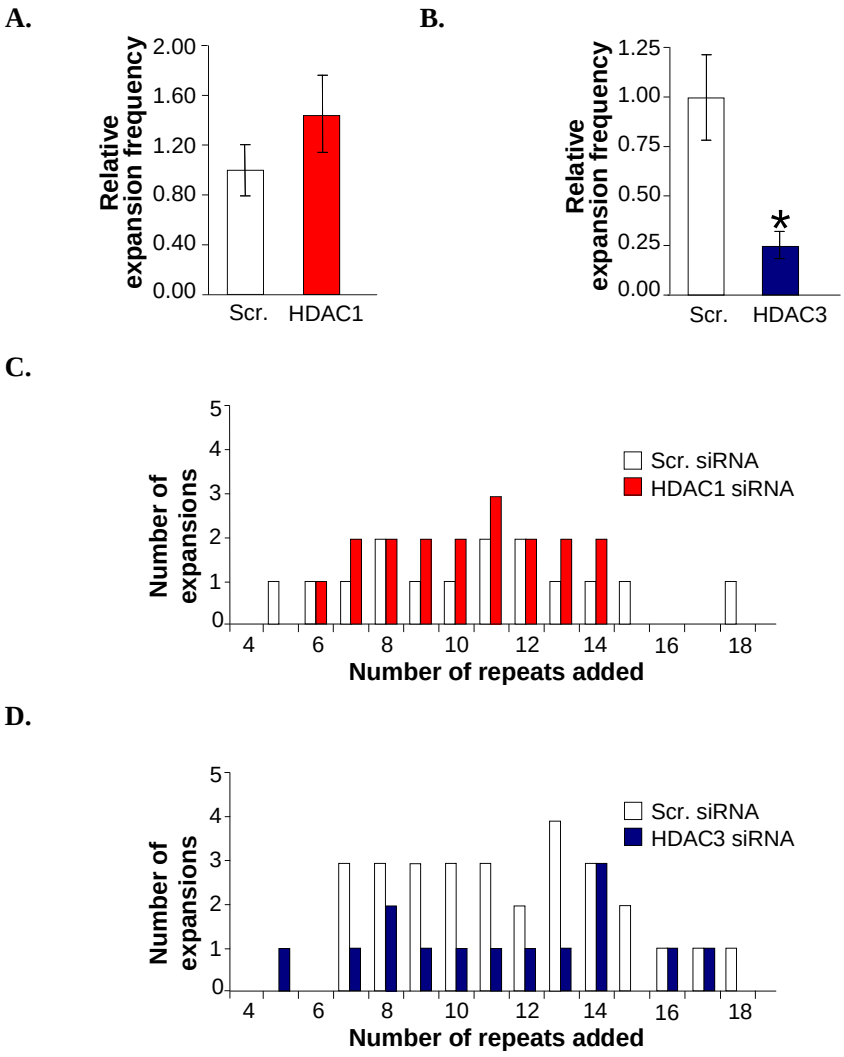

Figure 3.5 Expansion data for HDAC1 and HDAC3 siRNA-treated SVG-A cells. Expansion frequencies for **A.** HDAC1 siRNA; n= 3 and **B.** HDAC3 siRNA; n=3. Error bars denote ± one SEM; *, $P<0.05$ compared to scrambled siRNA control. Expansion sizes for **C.** HDAC1 siRNA: 15 genetically independent expansions for scrambled siRNA, 18 for HDAC1 siRNA and for **D.** HDAC3 siRNA: 28 genetically independent expansions for scrambled siRNA, 13 for HDAC3 siRNA

Following treatment with the relevant siRNAs, HDAC1 and HDAC3 proteins levels were reduced by 76% (± 2) and 76% (± 8) respectively as determined by western blot analysis (Fig. 3.6A-D). Assessment of HDAC3 expression via western blot analysis typically resulted in two bands around 50 kDa, (predicted size of HDAC3) presumably representing the two reported isoforms of HDAC3 (Yang et al., 1997). Throughout all experiments, consistent knockdown of the top band was observed following HDAC3 siRNA treatment, however, levels of the bottom band varied between experiments. In some western blots, the bottom band was not present. Quantitation of HDAC3 knockdown was performed by densitometric analysis of the top band only.

Because chemical inhibition of HDAC1 and HDAC3 in SVG-A (section 3.3.1) has no detectable effect on cell viability but resulted in a decrease in cell growth, these outcomes were examined following siRNA depletion of HDAC1 and HDAC3 to establish if similar outcomes were observed. Cells with reduced HDAC1 or HDAC3 levels did not exhibit diminishment in cellular viability compared with the scrambled siRNA control cells (Fig. 3.6E) an observation in line with the HDAC inhibitor experiments. No substantial alteration in cell growth was observed upon HDAC3 knockdown compared with the scrambled siRNA control cells (Fig. 3.6F). However, cells treated with HDAC1 siRNA exhibited 50% (± 2) lower total cell count than scrambled siRNA. This is similar to the trend observed in compound 3-treated cells. The key finding from these experiments is confirmation of HDAC3 being the relevant class I HDAC with regard to promoting expansions.

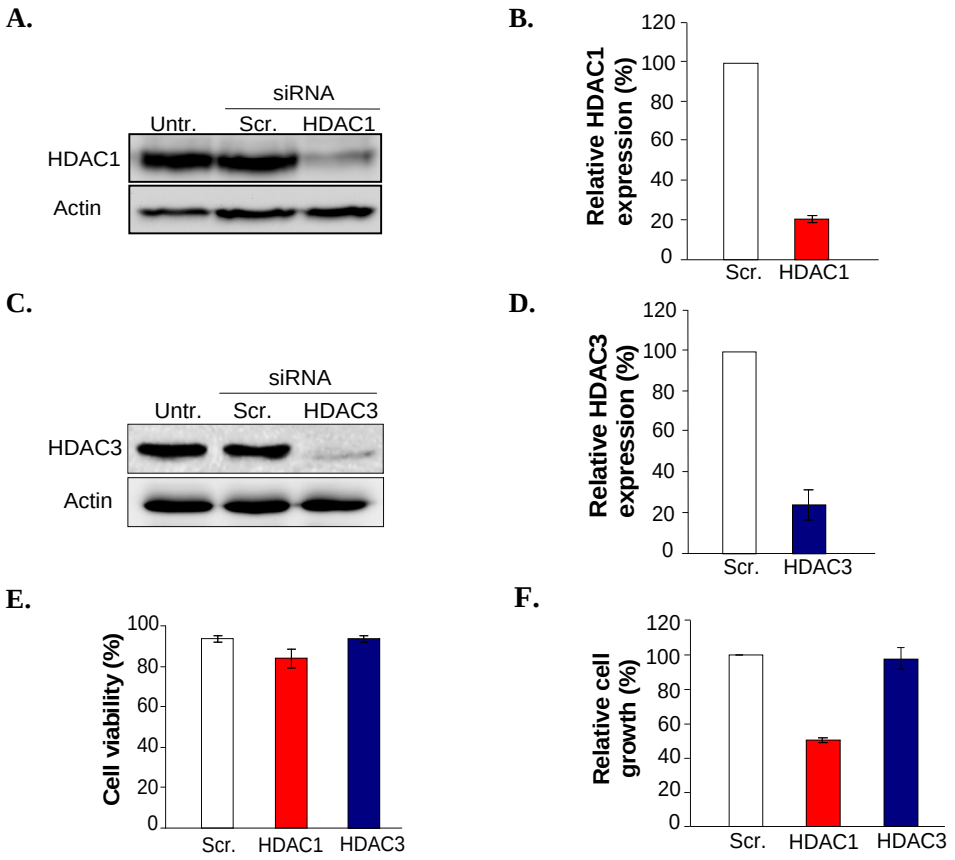

Figure 3.6 Knockdown of HDAC1 and HDAC3 in SVG-A cells. A. Representative western blot of HDAC1 and **C** HDAC3 knockdown. Actin was used as a loading control. **B.** Expression levels of HDAC3 and **D** HDAC1 both normalized to Actin and to scrambled siRNA. These results are from 3 independent measurements of HDAC1 and HDAC3 by immunoblot. Error bars denote ± one SEM. **E.** Cell viability was measured by nigrosin-exclusion assay. n =3. **F.** Cell growth. Total cell counts are expressed relative to scrambled siRNA-treated cells. n = 3. Error bars denote ± one SEM.

3.3.3 Role of HDAC3 in TNR contractions in SVG-A cells

The evidence presented in sections 3.3.1 and 3.3.2 provides evidence for a key role for HDAC3 in promoting expansions. In terms of targeting HDAC3 in a therapeutic context, a highly favourable scenario would be that HDAC3 inhibition leads to suppression of expansions with an enhancement of contractions to offset expansions. If HDAC3 is normally acting to suppress contractions, I would expect an increase in contraction frequency when HDAC3 is depleted by RNAi. The shuttle vector used to assess this was pBL247, which contains the reporter construct P_{adh1} promoter-$(CTG)_{33}$-*URA3* with the shuttle vector backbone to enable replication in human cells (Farrell and Lahue, 2006). SVG-A cells were treated with siRNA directed against HDAC3 and contraction frequencies were evaluated thereafter.

Knockdown of HDAC3 did not have any effects on contractions, with the frequency comparable to that of scrambled siRNA-treated cells (Fig. 3.7A, P= 0.64). This suggests that HDAC3 does not have any role in modulating the frequency of contractions in this system. Measurement of the sizes of the contractions was unchanged in HDAC3 knockdown cells compared with scrambled siRNA-treated cells (Fig. 3.7B). These data eliminate a role for HDAC3 in TNR contractions in SVG-A cells.

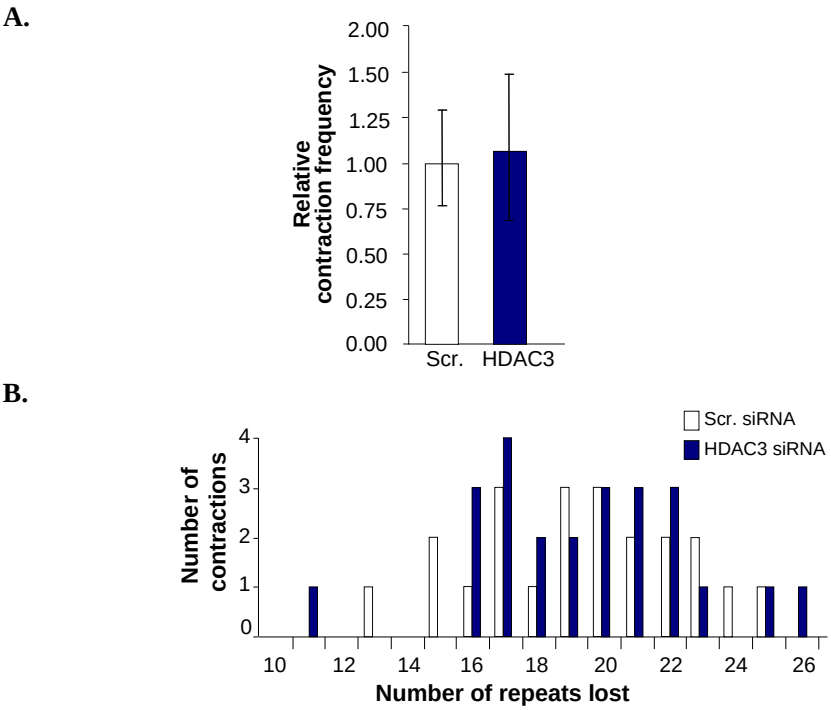

Figure 3.7 Contractions in HDAC3 siRNA-treated cells. A. Contraction frequency of HDAC3 siRNA-treated cells relative to scrambled siRNA control. n = 4. Error bars denote ± one SEM **B.** Contraction sizes for HDAC3 siRNA-treated cells: 22 genetically independent contractions for scrambled siRNA, 24 for HDAC3 siRNA.

3.3.4 Expansions in SVG-A cells treated with siRNA against the histone acetyltransferases CBP and/or p300

If, as the results in sections 3.3.1 and 3.3.2 imply, specific HDACs can cause expansions, then the corollary is that certain HATs would inhibit expansions. To test this hypothesis, CBP and its closely-related homologue p300 were examined for a role in TNR expansions. These two proteins were promising candidates as transgenic *Drosophila* heterozygous for CBP demonstrated an elevation in CTG expansions (no p300 homologue in *Drosophila*) (Jung and Bonini, 2007). If these HATs do oppose the expansion-promoting action of HDACs, then an increase in expansions would be the predicted outcome when these proteins are depleted by RNAi. In addition to individual knockdowns of CBP and p300, simultaneous knockdowns were performed as although they are highly homologous enzymes and often exhibit shared functional properties, there is evidence for CBP and p300 having unique functions also. For instance, both CBP and p300 knockout mice are embryonic lethal but only p300 null embryos displayed abnormal heart development, while an elevated frequency of hematological malignancies was only reported in CBP knockout mice (Yao et al., 1998; Kung et al., 2000).

Knockdown of CBP resulted in a 3.6-fold in increase in expansion frequency, while cells deficient in p300 had a 6.3-fold enhanced expansion frequency relative to scrambled siRNA control-treated cells (Fig. 3.8A)**.** The increase observed for CBP siRNA-treated was not quite statistically significant (P=0.06) but depletion of p300 resulted in a statistically significant enhancement of expansions (P=0.01). A 9.1-fold increase in expansions was observed following concurrent knockdown of both CBP and p300 (P=0.02). Evaluation of expansion sizes for individual CBP, p300 and double knockdowns did not reveal any shift in the expansion size spectrum with weighted average changes in tract length for scrambled siRNA, CBP siRNA, p300 siRNA and CBP+p300 siRNA of +11.6, +10.4, +11 and +10, respectively (Fig. 3.8B). siRNA-mediated single knockdowns of CBP and p300 resulted in 76% and 80% decrease in expression of CBP and p300, respectively (Fig. 3.8C and D). Double knockdown of CBP and p300 resulted in a 79% reduction of CBP expression, while p300 levels were depleted by 88% (Fig. 3.8C and D). These data provide evidence for a role for CBP and p300 in suppressing expansions in by reducing the incidence of expansions but not affecting the sizes. Thus, as hypothesised CBP and p300 appear to counteract the expansion-inducing action of HDACs.

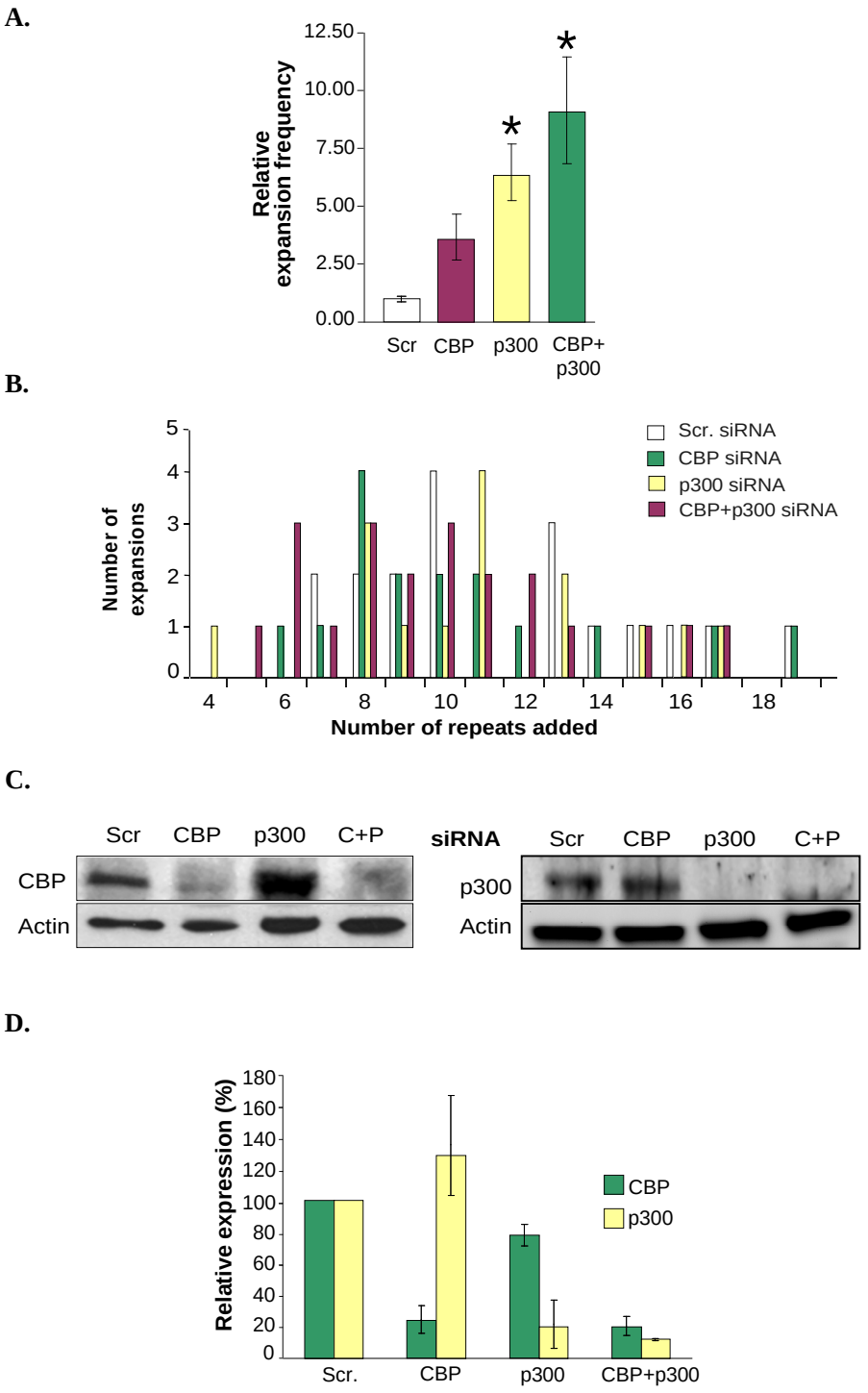

Figure 3.8 CBP and p300 siRNA experiments. A. Expansion frequencies following siRNA treatment against CBP and p300. All frequencies were normalized to scrambled siRNA. n = 3. (**P*<0.05) **B.** Expansion sizes measured subsequent to CBP and p300 siRNA depletion. 18 genetically independent expansions for scrambled siRNA, 16 for CBP siRNA, 15 for p300 siRNA and 21 for double CBP/p300 siRNA. **C.** Representative western blot of WCEs from cells treated with CBP and p300 siRNA **D.** Graph summarising knockdown efficiency following siRNA treatment, protein levels were normalized to that of scrambled siRNA and Actin; n=2. Error bars denote ± one SEM for A and range for D.

3.3.5 Does HDAC3 promote expansions through CtIP and MRE11?

A pressing question is how is HDAC3 acting to promote expansions? Yeast experiments performed by members of the Lahue lab were indicative that HDACs most likely promote expansions *in trans*, perhaps by controlling the expression or stability of factors that expand the TNR (Debacker et al., 2012). The yeast nuclease Sae2 was identified as a potential downstream target of the HDACs because it has been shown to be stabilized by deacetylation in a Rpd3L- and Hda1-dependent manner (Robert et al., 2011). Furthermore, Sae2 functions with Mre11 (in the context of the Mre11/Rad50/Xrs2 complex) to promote opening and resectioning of hairpins *in vitro* (Lengsfeld et al., 2007). Results from the Lahue lab suggest that Rpd3L and Hda1 positively regulate Sae2, which then acts with Mre11 to promote expansions. Specifically, mutation of sae2 or mre11 suppressed expansions, and *mre11 sin3* double mutants showed no further reduction in expansion rates than either single mutant (Debacker et al., 2012). These findings prompted us to investigate if the human homologue of Sae2 CtIP, would also promote expansions, and if so is it through HDACs as in yeast. Although Mre11 has not been reported to be deacetylated in yeast or humans, this enzyme was evaluated for a role in expansions due to its close association with CtIP (part of MRE11-RAD50-NBS1 (MRN) complex) and based on the observation that *mre11* and *sin3 mre11* yeast mutants exhibited a decrease in expansions.

Expansion frequencies in CtIP knockdown cells were unchanged with respective 1.6- and 1.2-fold increases for CtIP siRNAs #1 and #2 over scrambled siRNA (P=0.82 for siRNA #1, P=0.72 for siRNA #2) (Fig. 3.9A). Likewise, a 1.3-fold upward shift in expansion frequency relative to scrambled siRNA was observed when MRE11 was knocked down (P=0.51) (Fig. 3.9B). Furthermore, treatment of SVG-A cells with siRNAs targeting CtIP does not affect the sizes of expansions with weighted average expansion tract increases of +10.2, +11 and +9.6 for scrambled siRNA, CtIP siRNA #1 and CtIP siRNA #2, respectively (Fig. 3.9C). For the MRE11 siRNA data set, the weighted average increase in size for scrambled siRNA was +11.1 and +10.1 for MRE11 siRNA-treated cells (Fig. 3.9D). Taken together, these findings seem to a role for CtIP or MRE11 in the induction of expansions in SVG-A cells. However, we cannot rule out the possibility that there might be functional redundancy or that the knockdown level was not sufficient to cause an expansion phenotype.

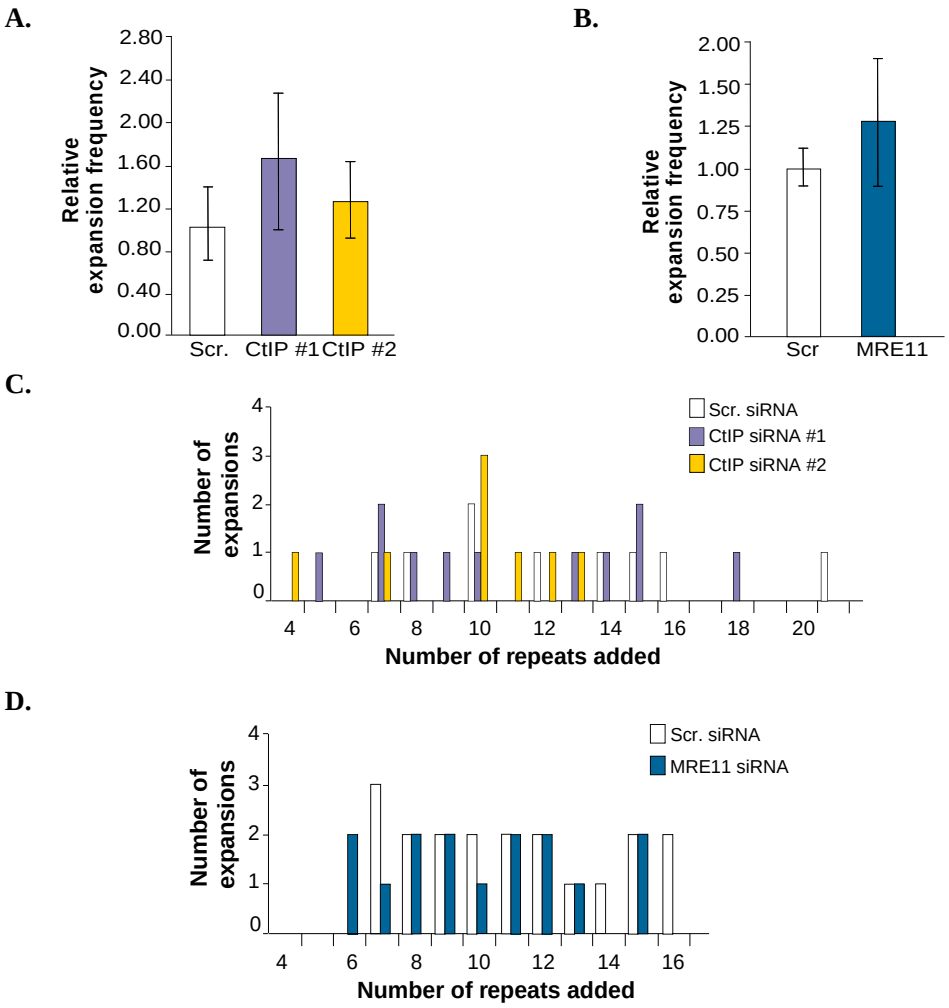

Figure 3.9 Expansion frequencies and sizes for SVG-A cells treated with CtIP or MRE11 siRNA. Expansion frequencies subsequent to treatment with **A.** CtIP individual siRNAs denoted #1 and #2 and **B.** MRE11 siRNA. n=3 Error bars denote ± one SEM; *, $P<0.05$ compared to scrambled siRNA control. Expansion sizes for **C.** CtIP siRNA: 9 genetically independent expansions for scrambled siRNA, 11 for CtIP siRNA #1 and 8 for CtIP siRNA #2. and for **D.** MRE11 siRNA: 19 genetically independent expansions for scrambled siRNA, 15 for MRE11 siRNA

Knockdown of CtIP and MRE11 was confirmed by western blotting. Treatment of cells with individual CtIP siRNAs #1 and #2 resulted in a decrease in CtIP protein levels of 65% (± 14) and 77% (± 14), while knockdown of MRE11 reduced MRE11 levels by 75% (± 6) (Fig. 3.10A-D). Similar levels of knockdown led to measurable phenotypes in other studies. For example, knockdown of CtIP to comparable levels as shown here reduced the ability of its interacting protein AdE1A to transactivate a luciferase reporter (Bruton et al., 2007)**.** Additionally, knockdown of MRE11 to similar levels sensitised human adenocarcinoma cells to ionising radiation (Xu et al., 2004). This indicates that it is unlikely that the absence

of a phenotype in our system is due to residual levels of expression following siRNA knockdown.

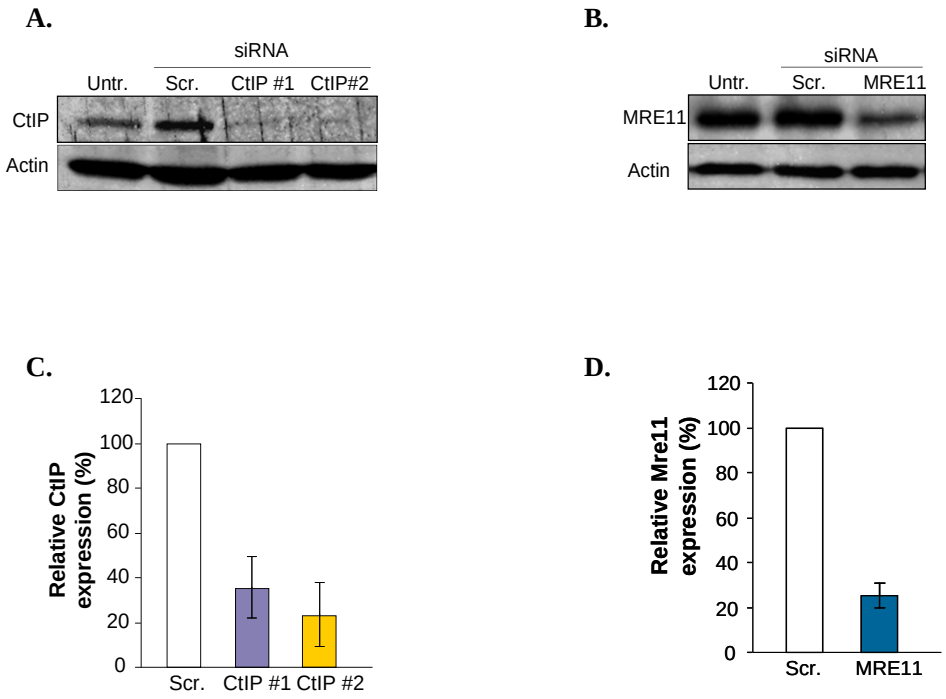

Figure 3.10 Knockdown of CtIP and MRE11. Representative western blots of SVG-A cells treated with **A.** individual CtIP siRNAs denoted #1 and #2 and **B.** MRE11 siRNA. Expression levels of **C.** CtIP and **D** MRE11 both normalized to Actin and to scrambled siRNA. Results are from immunoblots. n=3 for CtIP and Mre11. Error bars denote ± one SEM.

3.3.6. Expansions in SVG-A cells treated with siRNA against HDAC5

The results shown thus far indicate that a specific class I HDAC is involved in accelerating the occurrence of expansions. Yeast studies from the Lahue lab showed that Hda1 as well as Rpd3L promotes expansions. Class II HDACs in humans have been shown to be homologous to Hda1 (Grozinger et al., 1999). In order to determine if class II HDACs play a role in modulating expansions in human cells, RNAi was used to interfere with the expression of HDAC5 and HDAC9 and expansions were then evaluated. HDAC5 was chosen as it is highly enriched in the brain and may be pertinent to instability therein (Hoshino et al., 2003; Broide et al., 2007). Reported HDAC9 levels in the brain have varied from undetectable to high among different expression analysis studies (Zhou et al., 2001; Broide et al., 2007; Lucio-Eterovic et al., 2008).

Evaluation of expansion frequencies showed that depletion of HDAC5 resulted in a 3-fold decrease in expansions implying that it promotes expansions (P=0.008; Fig. 3.11A). This

agrees with yeast data that class II HDACs can cause expansions, as well as class I HDACs. Treatment of SVG-A cells with SMARTpool HDAC5 siRNA did not result in any detectable reduction in protein levels (Fig. 13.11E). 62% (± 12) knockdown of HDAC5 mRNA was observed following real-time RT-PCR (Fig. 13.11F). Perhaps both HDAC5 antibodies used in our study were not specific enough and the band assumed to be HDAC5 is a non-specific band. Nevertheless, the data presented in section 3.3.6 implies that like HDAC3, HDAC5 acts to promote expansions.

Because no HDAC5 knockdown at the protein level had been observed, two individual HDAC5 siRNAs, denoted #5 and #7, were used to confirm that the reduced expansion phenotype was not due to off-target effects of the pooled siRNA. Again, no reduction in HDAC5 protein levels was seen but HDAC5 mRNA levels were reduced by 52% (± 3) for siRNA #5 and 53% (± 3) for siRNA #7. (Fig. 3.11F). Following HDAC5 knockdown, expansion frequencies were significantly reduced by ~4-fold for both siRNAs (Fig. 3.11B)**.** This provides further evidence for a role for HDAC5 in promoting expansions. No change in expansion sizes was detected for HDAC5 knockdown compared to control cells with weighted average increases in size ranging from 10.5-11.6 (Fig. 3.11C and D) implying that HDAC5 promotes the occurrence of expansions but does not affect their sizes.

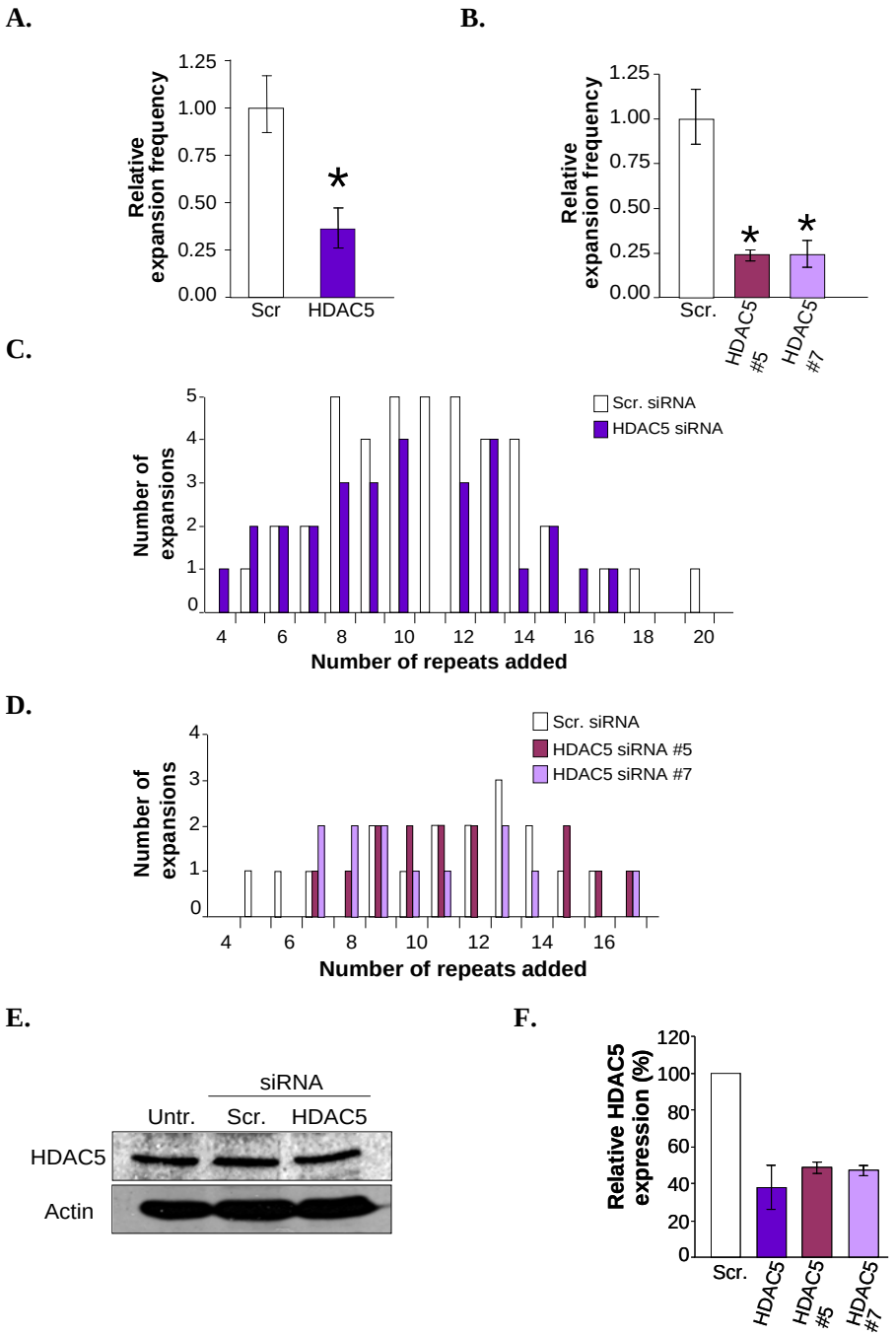

Figure 3.11 Expansions in cells treated with HDAC5 siRNA. Expansion frequencies subsequent to treatment with **A.** HDAC5 SMARTpool siRNA n=6 and **B.** individual HDAC5 siRNAs denoted #5 and #7. n=3 *, $P<0.05$ compared to scrambled siRNA control. Expansion sizes for **C.** HDAC5 SMARTpool siRNA: 42 genetically independent expansions for scrambled siRNA, 29 for HDAC5 SMARTpool siRNA. and for **D.** HDAC5 siRNA #5 and #7: 17 genetically independent expansions for scrambled siRNA, 14 for HDAC5 siRNA #5 and 12 for HDAC5 siRNA #7. **E.** Representative western blot of HDAC5 expression subsequent to treatment with HDAC5 siRNA (SMARTpool). **F.** Expression levels of HDAC5 determined by real-time RT-PCR for SMARTpool and individual siRNAs normalised to scrambled siRNA and HPRT levels. n= 3 for HDAC5 SMARTpool n=2 for HDAC5 siRNAs #5 and HDAC #7. Error bars denote ± one SEM for **A** and **B**, and represent range for **F**.

3.3.7. Expansions in SVG-A cells treated with siRNA against HDAC9

The data in section 3.3.6 suggests a role for HDAC5 in promoting expansions in SVG-A cells. We decided to investigate if another class II HDAC, HDAC9, had a similar function in promoting expansions or does this function this only pertain to specific HDACs. Interestingly**,** a statistically significant enhancement in the frequency of expansions was observed in cells treated with HDAC9 siRNA compared with the scrambled siRNA control (4.5-fold increase; *P*=0.025) (Fig. 13.12A). This implies that HDAC9 normally acts to inhibit expansions in SVG-A cells, in contrast to HDAC5 suggesting that specific HDACs have differential roles in control of instability. HDAC9 does not influence expansion sizes as weighted average expansion sizes from HDAC9 siRNA-treated cells were comparable to control cells: 11.3 and 10.1 respectively. (Fig. 13.12B)

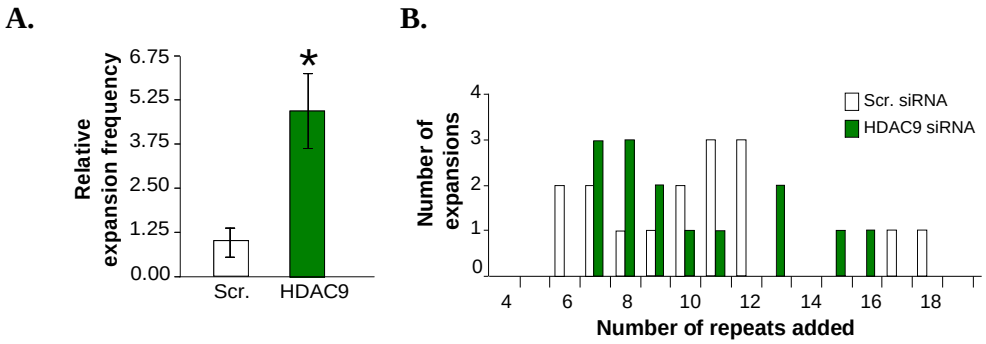

Figure 3.12 Effect of HDAC9 siRNA treatment on expansions A. Expansion frequencies Expansion frequencies following siRNA treatment against HDAC9 normalized to scrambled siRNA. n = 3. (**P*<0.05). **B.** Expansion sizes measured subsequent to siRNA transfection. 16 genetically independent expansions for scrambled siRNA, 14 for HDAC9 siRNA.

Similarly to the case of HDAC5, no decrease in HDAC9 protein levels were observed following HDAC9 siRNA (Fig. 3.13A) but HDAC9 mRNA levels were depleted by 75% (± 6) (Fig. 3.13B). As with exposure of SVG-A cells to HDAC1 siRNA and the small-molecule HDAC inhibitors, HDAC9 siRNA-treated cells grew 54% slower than the control cells, despite minimal adverse effects on viability (Fig. 13.3C and 13.3D). In contrast to HDAC3 and HDAC5, the findings documented in this section suggest that HDAC9 acts to inhibit expansions.

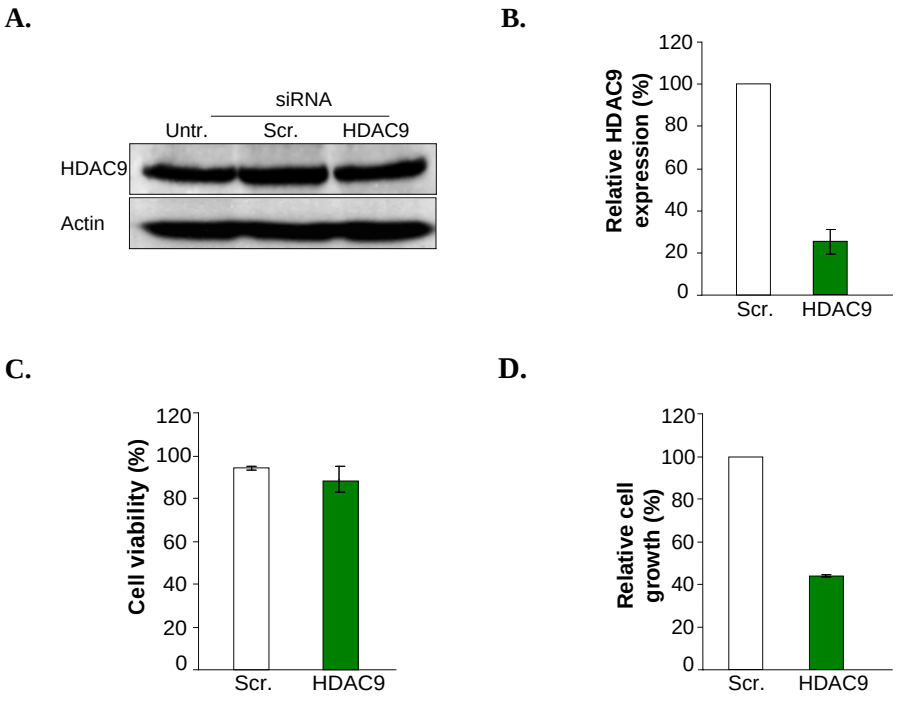

Figure 3.13 HDAC9 siRNA in SVG-A cells. A. Representative western blot showing HDAC9 expression. **B.** Graph summarising mRNA levels following siRNA treatment, mRNA levels were normalized to that of scrambled siRNA and HPRT; n=3.**C.** Cell viability was measured by nigrosin-exclusion assay. n =3. **D.** Cell growth. Total cell counts are expressed relative to scrambled siRNA-treated cells. n = 3. Error bars denote ± one SEM.

3.3.8 Effect of double knockdown of HDAC3 and HDAC5 on expansions

In yeast, double mutants of Rpd3L and Hda1 decreases in expansion rates were always more potent than for single mutants implying that these HDACs are contributing to the promotion of expansions independent of each other (Debacker et al., 2012). If this were the case in human cells, we would expect that combinatorial knockdown of a class I and class II HDAC would result in a decrease in expansions greater than the sum of the fold difference of the two individual knockdowns. To examine this scenario in SVG-A cells, concurrent knockdown of HDAC3 and HDAC5 was performed in conjunction with the expansion assay.

Simultaneous knockdown of HDAC3 and HDAC5 resulted in a significant decrease in expansions to a comparable extent as HDAC3 and HDAC5 relative to scrambled siRNA in SVG-A cells, with respective 3-, 4- and 2.3- fold decreases observed (P = 0.0008, 0.03,and 0.001, respectively) (Fig. 13.14A). In contrast to yeast, no significant differences were observed between HDAC3 and HDAC5 single knockdowns compared with the double knockdown (P=0.32 and 0.54, respectively). These data imply that HDAC3 and HDAC5 are acting in the same pathway to promote expansions. No detectable shift in expansion size

spectra was observed for this experiment. Tract length increases ranged from +8.8 to +10.7 (Fig. 13.14B).

Knockdown was measured by real-time RT-PCR and western blotting. Following HDAC3 and double siRNA treatment, HDAC3 mRNA levels were reduced by 31% and 41%, respectively (Fig. 13.14D). HDAC5 siRNA decreased HDAC5 mRNA levels to 50 % while double siRNA treatment resulted in 36% (±11) HDAC5 mRNA compared to scrambled siRNA. As noted previously, no knockdown of HDAC5 was observed at the protein level, while HDAC3 protein levels were reduced to 22 % (± 0.3) and 37 % (± 3) when treated with HDAC3 siRNA and HDAC3+5 siRNA, respectively (Fig. 13.14C). Because double knockdown of HDAC3 and HDAC5 resulted in a similar decrease in expansions as for the single knockdowns, one can surmise that they act together to promote expansions, unlike the synergistic interactions between class I and II HDACs in yeast (Debacker et al., 2012).

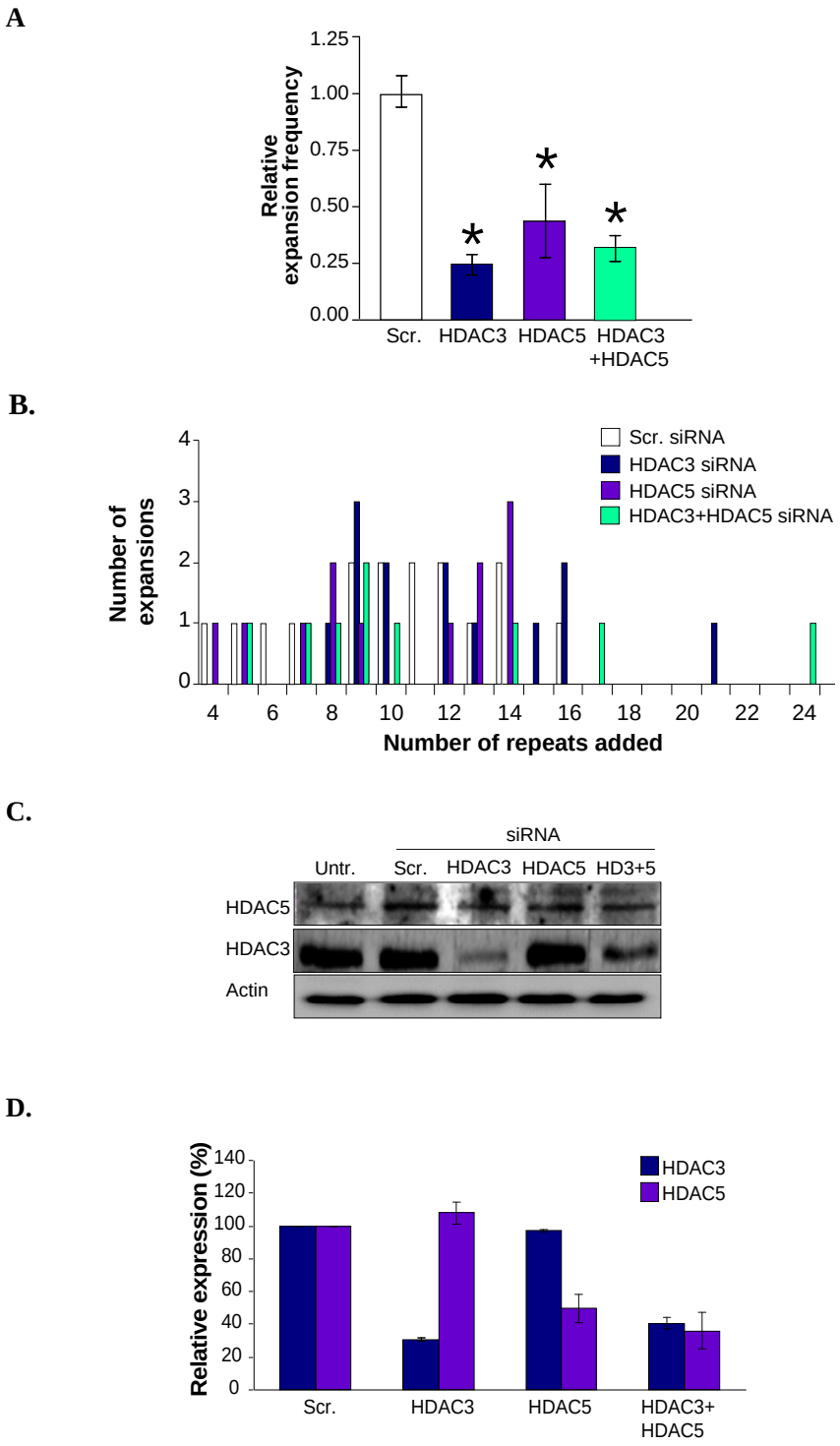

Figure 3.14 HDAC3 and HDAC5 siRNA double knockdowns. A. Expansion frequencies following siRNA treatments. All frequencies were normalized to scrambled siRNA. n = 3. (**P*<0.05). **B.** Expansion sizes measured subsequent to siRNA treatment. 16 genetically independent expansions for scrambled siRNA, 13 for HDAC3 siRNA, 12 for HDAC5 siRNA and 9 for double HDAC3+HDAC5 siRNA. **C.** Representative western blot showing HDAC3 and HDAC5 expression. **D.** Graph summarising mRNA levels following siRNA treatment, mRNA levels were normalized to that of scrambled siRNA and HPRT; n=2. Error bars denote ± one SEM for A and range for D.

3.4 Discussion

The data presented in this chapter identifies specific HDACs as key factors that mediate expansions TNR expansions, which is in agreement with the observations in yeast that Rpd3L and Hda1 promote expansions of threshold-length repeats (Debacker et al., 2012). Modulation of HDAC3 function by a small molecule inhibitor or depletion by siRNA knockdown resulted in an elimination of 70-80% of expansions, while interfering with HDAC1 and HDAC2 did not influence expansions. This implies that specific class I HDACs act to promote expansions in human cells. Although, HDAC3 involvement in mediating instability in SVG-A cells encompasses expansions, it does not extend to contractions as ascertained by siRNA depletion of HDAC3 having no impact on contraction frequency. Conversely, the HATs CBP and p300 were found to stabilise repeats, which complements a previous study in *Drosophila* whereby CBP was shown to circumvent the occurrence of $(CTG)_{78}$ expansions (Jung and Bonini, 2007). With regard to class II HDACs, HDAC5, like HDAC3, was shown to promote expansions, perhaps through the same pathway. In contrast HDAC9 appears to inhibit expansions. The identification of specific HDACs as proteins that promote expansions and HATs as inhibitory factors, taken together with the findings in yeast that HDACs act to promote expansions, demonstrates a key link between acetylation and deacetylation in controlling TNR instability. This observation is in line with a growing body of evidence in transgenic mouse models and human cells implicating a number of chromatin-modifying/epigenetic factors in repeat instability including DNMT1, HDACs, CBP and CTCF (Gorbunova et al., 2004; Jung and Bonini, 2007; Dion et al., 2008; Libby et al., 2008). Importantly, the work described in this chapter in combination with the yeast data is the first report identifying individual HDACs acting to promote TNR expansion, as the only other experiment to identify a role for HDACs was in a *Drosophila* model of SCA3 whereby a ~3-fold reduction in expansions was observed using TSA, a pan inhibitor for class I and II HDACs (Jung and Bonini, 2007). Furthermore, the work reported here and in the yeast experiments is the first to decipher a role for chromatin modifying enzymes in mediating expansions near the threshold.

The parallels in the data from human cells and yeast compound evidence for specific HDAC being causative for expansions though it appears that not all aspects of expansion modulation are shared between yeast and humans. In yeast, double mutants for Rpd3 and Hda1 revealed highly additive effects contributed by these two HDAC complexes in the process of promoting expansions. However, this does not seem to be the case in SVG-A cells with HDAC3 and HDAC5 knockdown resulting in a similar extent suppression of expansions as for single knockdowns. Given the reasonably conserved expansion-promoting action of HDACs in yeast and humans, how can we reconcile these seemingly conflicting

results? One possibility is that the detection limit of the expansion assay does not allow measurement of expansions in SVG-A cells below this point, thereby masking any dramatic expansion phenotypes. However, measurement of the background expansion frequency of the plasmid used in this experimental set revealed that technically expansion frequencies as low as 0.6% compared with scrambled siRNA could be detected, whereas 25% was the lowest frequency measured for the HDAC3 and 5 siRNA experiment. Moreover, in some individual experiments expansion frequencies as low ~10% of that of scrambled siRNA-treated cells were recorded. Thus, it is improbable that a saturation of the detection capacity of the expansion assay can be attributed to the lack of synergy observed for HDAC3 and HDAC5. Another explanation for the discrepancy between the yeast and human cells is that perhaps the levels of proteins remaining following double knockdown is sufficient to at least partially promote expansions, thus the expansion phenotype is not fully revealed under these conditions. This is an inherent issue with using RNAi as a method of modulating proteins. Indeed, simultaneous treatment with HDAC3 and HDAC5 did show less stringent knockdown of HDAC3 compared with single siRNA. However, it might not explain the disparity as it is doubtful that the quite modest difference in levels would be sufficient to cause variations in phenotype. Furthermore, treatment of SVG-A cells with individual HDAC5 siRNAs (#5 and 7) only decreased HDAC5 mRNA levels to ~50%, which was adequate to cause a decrease in expansions.

An alternative reason why additive effects are not observed for HDAC3 and HDAC5 in promoting expansions is that they are in fact acting in the same pathway. However, the evidence for this is not clear-cut. This notion is supported by evidence for HDAC5 binding to HDAC3 (Fischle et al., 2002). It has been proposed that all of the class IIa enzymes (HDAC4, 5, 7 and 9) have intrinsically low deacetylase activity on acetyl-lysine substrates due to the presence of a His residue at amino acid 298 in the binding pocket instead of a Tyr residue for class I HDACs (Lahm et al., 2007). One school of thought is that class IIa enzymes may act to direct deacetylase activity at acetylated lysines by recruiting HDAC3 (Fischle et al., 2002). It has been shown that HDAC4/5 recruit HDAC3, which deacetylates and thereby activates FOXO transcription factors required for expression of gluconeogenic genes (Mihaylova et al., 2011). However in the case of promoting expansions, loss of either HDAC3 or HDAC5 suppresses expansions indicating that if HDAC3 and HDAC5 act in a complex to execute this function, one HDAC can compensate for the other. Such an interaction has not been described in the literature but the well-established interactions between HDAC3 and HDAC5 suggest the potential for overlap of functions between these two proteins.

A somewhat unanticipated finding from the results presented in this chapter was the observation that knockdown of HDAC9 increases expansions indicative of a protective role for expansions. Taken together with the findings that HDAC3 and HDAC5 promote expansions, this indicates that specific HDACs, even members of the same family, have directly opposing actions in expansion mutagenesis. Studies have shown that HDACs can mediate contrasting effects on related biological processes, with numerous cases reported for neuronal survival in various species. In a *C.elegans* HD model, loss of the homologue of HDAC1 resulted in a potentiation of neurodegeneration, while knockdown of the HDAC3 homologue suppressed neurotoxocity (Bates et al., 2006). In mammalian systems, HDAC3 and HDAC5 appear to contribute to neuronal degeneration (Linseman et al., 2003; Bardai and D'Mello, 2011), while HDAC7 and HDRP, a truncated HDAC9 isoform lacking the catalytic domain, have been proposed to be neuroprotective (Morrison et al., 2006; Ma and D'Mello, 2011). Given the precedent that specific HDACs contribute differential effects in certain process, it seems plausible that expansions are governed by specific HDACs in different ways i.e. preventing and causing expansions.

The observation that HDAC9 acts in an antagonistic manner to HDAC3/5, while HDAC1 and possibly HDAC2 do not affect expansions implies that only specific HDACs contribute to the control of expansions. Bearing this in mind, it might be informative to identify which if any of the remaining untested HDACs affect expansions to determine what the key expansion mediators and protectors are in this group of enzymes. The observation that HDACs can have distinct and often opposing roles in expansions, in addition to the other biological processes mentioned above, illustrates the importance of targeting individual HDACs to clearly determine their contributions rather than using broad-spectrum pan HDAC inhibitors. In light of the findings presented in this chapter, a study performed in CHO cells treated with sodium butyrate, a pan HDAC inhibitor where no effects on TNR instability were reported might not be wholly informative (Gorbunova et al., 2004).

Cell growth was greatly reduced in cells treated with compound 3, 4b, HDAC1- and HDAC9-specific siRNAs. This observation concurs with the well documented cell cycle arrest resulting from HDAC inhibition or depletion (Ungerstedt et al., 2005; Wilson et al., 2006). While the cell viability data combined with total cell counts suggests that a decrease in cell proliferation is at play, analysis of cell cycle progression would confirm this. This decreased propagation did not appear to have major impact on expansion frequency as both chemical inhibition and siRNA-mediated knockdown of HDAC3 gave similar decreases in expansions, despite the slow cell growth only being detected in 4b-treated cells. The variation of drug versus siRNA treatments in the cells in the case of HDAC3 siRNA and 4b

might be attributable to off-target effects that are not applicable for the siRNA treatments. Notably, no cell-static effects were reported for lymphoblast cells following treatment of 4b at concentrations <20 μM (Thomas et al., 2008). This difference is likely due to the combinatorial impact of lipofectin-mediated transfection and 4b treatment in SVG-A cells.

HDAC1/2 do not seem to be required for modulating expansions in SVG-A cells. This finding helps to tentatively rule out a protective role for HDAC1/2 against expansions by promoting non-homologous end-joining (NHEJ) shown in yeast to prevent instability arising from DSBs (Sundararajan et al., 2010). It has been shown that inhibition of HDAC1 and HDAC2 leads to defective NHEJ (Miller et al., 2010). These HDACs are recruited to DNA damage sites to promote deacetylation of H3K56 thereby regulating binding of NHEJ factors to DSB sites (Miller et al., 2010). No change in expansion frequency was observed when HDAC1 and HDAC2 were inhibited by compound 3 or when HDAC1 levels were depleted by siRNA. This may indicate that NHEJ does not play a role in modulating expansions at the threshold in SVG-A cells, although this evidence is indirect as a role for NHEJ was not directly assessed in this study. Indeed, NHEJ is unlikely to be mechanistically applicable to threshold length repeats as DSBs are less frequent in shorter alleles (Callahan et al., 2003). This provisional finding correlates with the observation that DM1 mice (>300 CTG repeats) crossed with mice knockout for the NHEJ gene DNA PKcs did not affect intergenerational repeat instability (Savouret et al., 2003).

A key question arising from the novel finding that certain HDACs promote expansions is how do these enzymes play a causal role in TNR instability. This chapter is devoted mainly to reporting the identification of particular HDACs as novel factors that accelerate expansions with mechanistic avenues only being briefly explored. What can be stated is that it is distinctly improbable that HDACs are acting in a previously uncharacterised capacity to directly add repeats within a TNR tract so the effect is likely mediated through their acetylation activities to influence factors that promote expansions. Two broad models for this HDAC action in directing expansions can be proposed: (i) HDACs influence the chromatin structure surrounding the TNR tract thereby regulating access of proteins that promote and inhibit expansions (ii) HDACs are acting indirectly or at a distance to control the expression, stability and/or activity of trans-acting expansion-promoting proteins. Endeavours to elucidate the mechanism for HDACs' role in favouring the occurrence of expansions have shown that it is unlikely that TNR chromatin acetylation status controls TNR expansions (Debacker et al., 2012). The data in yeast imply that Rpd3L and Hda1 are mediating their influence on expansions through distant effects.

The possibility that deacetylation of non-histone proteins that then act *in trans* to promote expansions was tested in yeast. This led to the Lahue lab proposing that Rpd3L and Hda1 promote expansions at least in part through the hairpin-processing actions of Sae2, likely by catalysing its deacetylation and consequent stabilisation (Debacker et al., 2012). In a separate study, *sae2* and *mre11* yeast mutants with longer repeats $(CAG)_{70}$ exhibited increased expansion frequencies likely due to increased breakage of these alleles engaging Sae2 and Mre11 end-joining action in the context of DSB repair (Freudenreich et al., 1998; Sundararajan et al., 2010). In yeast with shorter repeat tracts, Sae2 and Mre11 promote expansions possibly via processing of hairpin substrates, offering a explanation for the different expansion outcomes for these proteins. However, this attractive nuclease model is not applicable to explaining how HDACs act to effect expansions in SVG-A cells. Knockdown of the Sae2 human homologue, CtIP or MRE11 did not mediate any reduction in the incidence of expansions in SVG-A cells suggesting that HDACs are not promoting expansions via these proteins in human cells. A probable explanation for this outcome is that CtIP is deacetylated by the class III HDAC, SIRT6, which results in stimulation of its DNA resectioning activity, with no reported activity for class I or II HDACs (Kaidi et al., 2010). Kaidi et al., 2010 observed no impairment in camptothecin-induced DNA damage response upon treatment with sodium butyrate and as a result did not examine the contribution of individual class I or II HDACs to CtIP activity. Class III HDACs were not examined for a role in expansions in our study. The work presented in this study rules out any involvement of a pathway involving CtIP being regulated by SIRT6 in the control of TNR expansions. In order to conclusively determine any contribution of class III HDACs to instability, more direct investigations are required such as using the pan-class III inhibitor nicotinamide and/or siRNA directed against individual sirtuins. In yeast, specific sirtuins were ruled out as factors that control expansions (Debacker et al., 2012).

This study revealed HDAC3 and HDAC5 to be key players in expansion causation, whereas the HATs CBP/p300 were found have the contravening effect of suppressing expansions congruent with their opposing enzymatic roles in regulation of acetylation status. Interestingly, CBP/p300 and these HDACs share many of the same non-histone substrates. Acetylation of the male sex determining protein SRY by p300 results in its nuclear localisation and augments its DNA binding ability; deacetylation by HDAC3 reverses this (Thevenet et al., 2004). Furthermore, the transcription factor glial cell missing (GCMa), which is important in development, is deacetylated by HDAC3 and acetylated by p300 and p300/CBP-associated factor (PCAF) (Chuang et al., 2006). HDAC3-mediated deacetylation of myocyte enhancer factor 2 suppresses its transcription factor activity, while p300 and PCAF catalyse its acetylation thereby enhancing its DNA binding and transcriptional ability

(Ma et al., 2005; Gregoire et al., 2007). A striking finding in the latter two examples was that HDAC3 deacetylated the relevant antagonistic HATs, inhibiting their functions in the aforementioned pathways (Chuang et al., 2006; Gregoire et al., 2007). HDAC5 was also identified to be involved in promoting expansions in SVG-A cells in this study. Overexpression of HDAC5 reduced NFATc1 acetylation, a transcription factor involved in immune response and osteoclastogenesis (Kim et al., 2011). The same group demonstrated that NFATc1 is stabilised by acetylation by PCAF, which is enhanced by p300 acetylation of PCAF. These observations coupled with the finding that HDAC3/5 and p300/CBP have opposing actions in the modulation of TNR expansions in SVG-A cells provides some evidence that these chromatin-modifying enzymes might act on one or more as of yet unknown and/or unidentified non-histone targets, which in turn control the occurrence of expansions. In other words, the balance of HATs and HDACs enzymatic activities may influence the activity, stability or expression of key proteins that are proposed to be involved in controlling TNR mutagenesis. There is no immediately apparent candidate protein that fits this description.

In summary, the results presented in this chapter propose a role for specific class I and II HDACs in controlling somatic instability. While HDAC3 and HDAC5 were identified as novel promoters of expansions, HDAC9 acts to inhibit expansions suggesting a complex interplay underlies control of expansions by HDACs. Furthermore, the HATs CBP and p300 were found to prevent expansions. There is no clear mechanism for how these acetylation-controlling enzymes are involved in controlling expansions, a complexity underpinned by their many roles throughout the cell (Spange et al., 2009). Two general models for how HDACs promote expansions are based on whether HDAC activity is localised to or distant from the repeat region. These models may not be mutually exclusive. Direct testing of aspects these models is addressed in chapter 4. The key findings presented in this chapter are that the acetylation/deacetylation activities of specific HDACs and HATs are crucial to determining TNR expansion outcomes.

References

Alexiadis, V., L. Halmer and C. Gruss (1997). Influence of core histone acetylation on SV40 minichromosome replication in vitro. *Chromosoma* **105**(6): 324-31.

Bandyopadhyay, D., A. Mishra and E. E. Medrano (2004). Overexpression of histone deacetylase 1 confers resistance to sodium butyrate-mediated apoptosis in melanoma cells through a p53-mediated pathway. *Cancer Res* **64**(21): 7706-10.

Bardai, F. H. and S. R. D'Mello (2011). Selective toxicity by HDAC3 in neurons: regulation by Akt and GSK3beta. *J Neurosci* **31**(5): 1746-51.

Bates, E. A., M. Victor, A. K. Jones, Y. Shi and A. C. Hart (2006). Differential contributions of Caenorhabditis elegans histone deacetylases to huntingtin polyglutamine toxicity. *J Neurosci* **26**(10): 2830-8.

Borger, D. R. and J. A. DeCaprio (2006). Targeting of p300/CREB binding protein coactivators by simian virus 40 is mediated through p53. *J Virol* **80**(9): 4292-303.

Broide, R. S., J. M. Redwine, N. Aftahi, W. Young, F. E. Bloom and C. J. Winrow (2007). Distribution of histone deacetylases 1-11 in the rat brain. *J Mol Neurosci* **31**(1): 47-58.

Bruton, R. K., M. Rasti, K. L. Mapp, N. Young, R. Z. Carter, I. A. Abramowicz, G. G. Sedgwick, D. F. Onion, M. Shuen, J. S. Mymryk, A. S. Turnell and R. J. Grand (2007). C-terminal-binding protein interacting protein binds directly to adenovirus early region 1A through its N-terminal region and conserved region 3. *Oncogene* **26**(53): 7467-79.

Callahan, J. L., K. J. Andrews, V. A. Zakian and C. H. Freudenreich (2003). Mutations in yeast replication proteins that increase CAG/CTG expansions also increase repeat fragility. *Mol Cell Biol* **23**(21): 7849-60.

Chuang, H. C., C. W. Chang, G. D. Chang, T. P. Yao and H. Chen (2006). Histone deacetylase 3 binds to and regulates the GCMa transcription factor. *Nucleic Acids Res* **34**(5): 1459-69.

Debacker, K., A. Frizzell, O. Gleeson, L. Kirkham-McCarthy, T. Mertz and R. S. Lahue (2012). Histone deacetylase complexes promote trinucleotide repeat expansions. *PLoS Biol* **10**(2): e1001257.

Dion, V., Y. Lin, L. Hubert, Jr., R. A. Waterland and J. H. Wilson (2008). Dnmt1 deficiency promotes CAG repeat expansion in the mouse germline. *Hum Mol Genet* **17**(9): 1306-17.

Farrell, B. T. and R. S. Lahue (2006). CAG*CTG repeat instability in cultured human astrocytes. *Nucleic Acids Res* **34**(16): 4495-505.

Fischle, W., F. Dequiedt, M. J. Hendzel, M. G. Guenther, M. A. Lazar, W. Voelter and E. Verdin (2002). Enzymatic activity associated with class II HDACs is dependent on a multiprotein complex containing HDAC3 and SMRT/N-CoR. *Mol Cell* **9**(1): 45-57.

Freudenreich, C. H., S. M. Kantrow and V. A. Zakian (1998). Expansion and length-dependent fragility of CTG repeats in yeast. *Science* **279**(5352): 853-6.

Gorbunova, V., A. Seluanov, D. Mittelman and J. H. Wilson (2004). Genome-wide demethylation destabilizes CTG.CAG trinucleotide repeats in mammalian cells. *Hum Mol Genet* **13**(23): 2979-89.

Gregoire, S., L. Xiao, J. Nie, X. Zhang, M. Xu, J. Li, J. Wong, E. Seto and X. J. Yang (2007). Histone deacetylase 3 interacts with and deacetylates myocyte enhancer factor 2. *Mol Cell Biol* **27**(4): 1280-95.

Grozinger, C. M., C. A. Hassig and S. L. Schreiber (1999). Three proteins define a class of human histone deacetylases related to yeast Hda1p. *Proc Natl Acad Sci U S A* **96**(9): 4868-73.

Herman, D., K. Jenssen, R. Burnett, E. Soragni, S. L. Perlman and J. M. Gottesfeld (2006). Histone deacetylase inhibitors reverse gene silencing in Friedreich's ataxia. *Nat Chem Biol* **2**(10): 551-8.

Hoshino, M., K. Tagawa, T. Okuda, M. Murata, K. Oyanagi, N. Arai, T. Mizutani, I. Kanazawa, E. E. Wanker and H. Okazawa (2003). Histone deacetylase activity is retained in primary neurons expressing mutant huntingtin protein. *J Neurochem* **87**(1): 257-67.

Ito, A., Y. Kawaguchi, C. H. Lai, J. J. Kovacs, Y. Higashimoto, E. Appella and T. P. Yao (2002). MDM2-HDAC1-mediated deacetylation of p53 is required for its degradation. *Embo J* **21**(22): 6236-45.

Jia, H., J. Pallos, V. Jacques, A. Lau, B. Tang, A. Cooper, A. Syed, J. Purcell, Y. Chen, S. Sharma, G. R. Sangrey, S. B. Darnell, H. Plasterer, G. Sadri-Vakili, J. M. Gottesfeld, L. M. Thompson, J. R. Rusche, J. L. Marsh and E. A. Thomas (2012). Histone deacetylase (HDAC) inhibitors targeting HDAC3 and HDAC1 ameliorate polyglutamine-elicited phenotypes in model systems of Huntington's disease. *Neurobiology of Disease* **46**(2): 351-361.

Jung, J. and N. Bonini (2007). CREB-binding protein modulates repeat instability in a Drosophila model for polyQ disease. *Science* **315**(5820): 1857-9.

Kaidi, A., B. T. Weinert, C. Choudhary and S. P. Jackson (2010). Human SIRT6 promotes DNA end resection through CtIP deacetylation. *Science* **329**(5997): 1348-53.

Kim, J. H., K. Kim, B. U. Youn, H. M. Jin, J. Y. Kim, J. B. Moon, A. Ko, S. B. Seo, K. Y. Lee and N. Kim (2011). RANKL induces NFATc1 acetylation and stability via histone acetyltransferases during osteoclast differentiation. *Biochem J* **436**(2): 253-62.

Kung, A. L., V. I. Rebel, R. T. Bronson, L. E. Ch'ng, C. A. Sieff, D. M. Livingston and T. P. Yao (2000). Gene dose-dependent control of hematopoiesis and hematologic tumor suppression by CBP. *Genes Dev* **14**(3): 272-7.

Lahm, A., C. Paolini, M. Pallaoro, M. C. Nardi, P. Jones, P. Neddermann, S. Sambucini, M. J. Bottomley, P. Lo Surdo, A. Carfi, U. Koch, R. De Francesco, C. Steinkuhler and P. Gallinari (2007). Unraveling the hidden catalytic activity of vertebrate class IIa histone deacetylases. *Proc Natl Acad Sci U S A* **104**(44): 17335-40.

Lengsfeld, B. M., A. J. Rattray, V. Bhaskara, R. Ghirlando and T. T. Paull (2007). Sae2 is an endonuclease that processes hairpin DNA cooperatively with the Mre11/Rad50/Xrs2 complex. *Mol Cell* **28**(4): 638-51.

Libby, R. T., K. A. Hagerman, V. V. Pineda, R. Lau, D. H. Cho, S. L. Baccam, M. M. Axford, J. D. Cleary, J. M. Moore, B. L. Sopher, S. J. Tapscott, G. N. Filippova, C. E. Pearson and A. R. La Spada (2008). CTCF cis-regulates trinucleotide repeat instability in an epigenetic manner: a novel basis for mutational hot spot determination. *PLoS Genet* **4**(11): e1000257.

Linseman, D. A., C. M. Bartley, S. S. Le, T. A. Laessig, R. J. Bouchard, M. K. Meintzer, M. Li and K. A. Heidenreich (2003). Inactivation of the myocyte enhancer factor-2 repressor histone deacetylase-5 by endogenous Ca(2+) //calmodulin-dependent kinase II promotes depolarization-mediated cerebellar granule neuron survival. *J Biol Chem* **278**(42): 41472-81.

Lucio-Eterovic, A. K., M. A. Cortez, E. T. Valera, F. J. Motta, R. G. Queiroz, H. R. Machado, C. G. Carlotti, Jr., L. Neder, C. A. Scrideli and L. G. Tone (2008). Differential expression of 12 histone deacetylase (HDAC) genes in astrocytomas and normal brain tissue: class II and IV are hypoexpressed in glioblastomas. *BMC Cancer* **8**: 243.

Ma, C. and S. R. D'Mello (2011). Neuroprotection by histone deacetylase-7 (HDAC7) occurs by inhibition of c-jun expression through a deacetylase-independent mechanism. *J Biol Chem* **286**(6): 4819-28.

Ma, K., J. K. Chan, G. Zhu and Z. Wu (2005). Myocyte enhancer factor 2 acetylation by p300 enhances its DNA binding activity, transcriptional activity, and myogenic differentiation. *Mol Cell Biol* **25**(9): 3575-82.

McMurray, C. T. (2010). Mechanisms of trinucleotide repeat instability during human development. *Nat Rev Genet* **11**(11): 786-99.

Mihaylova, M. M., D. S. Vasquez, K. Ravnskjaer, P. D. Denechaud, R. T. Yu, J. G. Alvarez, M. Downes, R. M. Evans, M. Montminy and R. J. Shaw (2011). Class IIa histone deacetylases are hormone-activated regulators of FOXO and mammalian glucose homeostasis. *Cell* **145**(4): 607-21.

Miller, K. M., J. V. Tjeertes, J. Coates, G. Legube, S. E. Polo, S. Britton and S. P. Jackson (2010). Human HDAC1 and HDAC2 function in the DNA-damage response to promote DNA nonhomologous end-joining. *Nat Struct Mol Biol* **17**(9): 1144-51.

Mirkin, S. M. (2007). Expandable DNA repeats and human disease. *Nature* **447**(7147): 932-40.

Morrison, B. E., N. Majdzadeh, X. Zhang, A. Lyles, R. Bassel-Duby, E. N. Olson and S. R. D'Mello (2006). Neuroprotection by histone deacetylase-related protein. *Mol Cell Biol* **26**(9): 3550-64.

Poulin, D. L., A. L. Kung and J. A. DeCaprio (2004). p53 targets simian virus 40 large T antigen for acetylation by CBP. *J Virol* **78**(15): 8245-53.

Quintini, G., K. Treuner, C. Gruss and R. Knippers (1996). Role of amino-terminal histone domains in chromatin replication. *Mol Cell Biol* **16**(6): 2888-97.

Richon, V. M. (2006). Cancer biology: mechanism of antitumour action of vorinostat (suberoylanilide hydroxamic acid), a novel histone deacetylase inhibitor. *Br J Cancer* **95** (Suppl. 1): S2-6.

Robert, T., F. Vanoli, I. Chiolo, G. Shubassi, K. A. Bernstein, R. Rothstein, O. A. Botrugno, D. Parazzoli, A. Oldani, S. Minucci and M. Foiani (2011). HDACs link the DNA damage response, processing of double-strand breaks and autophagy. *Nature* **471**(7336): 74-9.

Savouret, C., E. Brisson, J. Essers, R. Kanaar, A. Pastink, H. te Riele, C. Junien and G. Gourdon (2003). CTG repeat instability and size variation timing in DNA repair-deficient mice. *Embo J* **22**(9): 2264-73.

Shimazu, T., Y. Komatsu, K. I. Nakayama, H. Fukazawa, S. Horinouchi and M. Yoshida (2006). Regulation of SV40 large T-antigen stability by reversible acetylation. *Oncogene* **25**(56): 7391-400.

Spange, S., T. Wagner, T. Heinzel and O. H. Kramer (2009). Acetylation of non-histone proteins modulates cellular signalling at multiple levels. *Int J Biochem Cell Biol* **41**(1): 185-98.

Sundararajan, R., L. Gellon, R. M. Zunder and C. H. Freudenreich (2010). Double-strand break repair pathways protect against CAG/CTG repeat expansions, contractions and repeat-mediated chromosomal fragility in Saccharomyces cerevisiae. *Genetics* **184**(1): 65-77.

Suzuki, T., H. Yokozaki, H. Kuniyasu, K. Hayashi, K. Naka, S. Ono, T. Ishikawa, E. Tahara and W. Yasui (2000). Effect of trichostatin A on cell growth and expression of cell cycle- and apoptosis-related molecules in human gastric and oral carcinoma cell lines. *Int J Cancer* **88**(6): 992-7.

Thevenet, L., C. Mejean, B. Moniot, N. Bonneaud, N. Galeotti, G. Aldrian-Herrada, F. Poulat, P. Berta, M. Benkirane and B. Boizet-Bonhoure (2004). Regulation of human SRY subcellular distribution by its acetylation/deacetylation. *Embo J* **23**(16): 3336-45.

Thomas, E. A., G. Coppola, P. A. Desplats, B. Tang, E. Soragni, R. Burnett, F. Gao, K. M. Fitzgerald, J. F. Borok, D. Herman, D. H. Geschwind and J. M. Gottesfeld (2008). The HDAC inhibitor 4b ameliorates the disease phenotype and transcriptional abnormalities in Huntington's disease transgenic mice. *Proc Natl Acad Sci U S A* **105**(40): 15564-9.

Ungerstedt, J. S., Y. Sowa, W. S. Xu, Y. Shao, M. Dokmanovic, G. Perez, L. Ngo, A. Holmgren, X. Jiang and P. A. Marks (2005). Role of thioredoxin in the response of normal and transformed cells to histone deacetylase inhibitors. *Proc Natl Acad Sci U S A* **102**(3): 673-8.

Valls, E., N. Blanco-Garcia, N. Aquizu, D. Piedra, C. Estaras, X. de la Cruz and M. A. Martinez-Balbas (2007). Involvement of chromatin and histone deacetylation in SV40 T antigen transcription regulation. *Nucleic Acids Res* **35**(6): 1958-68.

Wilson, A. J., D. S. Byun, N. Popova, L. B. Murray, K. L'Italien, Y. Sowa, D. Arango, A. Velcich, L. H. Augenlicht and J. M. Mariadason (2006). Histone deacetylase 3 (HDAC3) and other class I HDACs regulate colon cell maturation and p21 expression and are deregulated in human colon cancer. *J Biol Chem* **281**(19): 13548-58.

Xu, C., E. Soragni, C. J. Chou, D. Herman, H. L. Plasterer, J. R. Rusche and J. M. Gottesfeld (2009). Chemical probes identify a role for histone deacetylase 3 in Friedreich's ataxia gene silencing. *Chem Biol* **16**(9): 980-9.

Xu, M., R. J. Myerson, C. Hunt, S. Kumar, E. G. Moros, W. L. Straube and J. L. Roti Roti (2004). Transfection of human tumour cells with Mre11 siRNA and the increase in radiation sensitivity and the reduction in heat-induced radiosensitization. *Int J Hyperthermia* **20**(2): 157-62.

Yang, W. M., Y. L. Yao, J. M. Sun, J. R. Davie and E. Seto (1997). Isolation and characterization of cDNAs corresponding to an additional member of the human histone deacetylase gene family. *J Biol Chem* **272**(44): 28001-7.

Yao, T. P., S. P. Oh, M. Fuchs, N. D. Zhou, L. E. Ch'ng, D. Newsome, R. T. Bronson, E. Li, D. M. Livingston and R. Eckner (1998). Gene dosage-dependent embryonic development and proliferation defects in mice lacking the transcriptional integrator p300. *Cell* **93**(3): 361-72.

Zhou, X., P. A. Marks, R. A. Rifkind and V. M. Richon (2001). Cloning and characterization of a histone deacetylase, HDAC9. *Proc Natl Acad Sci U S A* **98**(19): 10572-7.

CHAPTER 4

Role of mismatch repair proteins in TNR expansion

Some of the material presented in this chapter was presented in the following article:

"MutSβ and histone deacetylase complexes promote expansions of trinucleotide repeats in human cells"

Submitted to Nucleic Acid Research

Anne-Marie Gannon*, Aisling Frizzell*, Evan Healy and Robert Lahue

*: Equal contributions

4.1 Summary

Mismatch repair (MMR) proteins, specifically MutSβ, have been implicated in driving expansions in several transgenic mouse models. While the requirement for MMR proteins for promoting expansion of long, disease-causing alleles is well established, it is unknown if this mutational mechanism is applicable to shorter repeats.

siRNA knockdown of the MutSβ subunits MSH2 and MSH3 suppressed expansions of threshold-length repeats, while depletion of the MutSα subunit MSH6 had no effect. These findings imply a direct role for MutSβ in promoting expansion of threshold-length CTG•CAG tracts. To test for a functional interaction between HDAC3, which was previously shown to promote expansions, and the MMR factor MSH2, double knockdowns of HDAC3 and MSH2 were performed. Simultaneous knockdown of HDAC3 and MSH2 led to an expansion phenotype that was indistinguishable from knockdown of either MSH2 or HDAC3 alone. This finding implies that HDAC3 and MutSβ are working to promote expansions of CTG•CAG repeats in SVG-A cells through a shared pathway. Expression levels of MSH2 and MSH3 were unchanged in HDAC3 knockdown cells and modestly decreased in cells treated with the HDAC3 inhibitor 4b, suggesting that HDAC3 does not promote expansions by altering transcription or protein turnover of MSH2 or MSH3.

4.2 Introduction

Although MMR normally functions to detect and repair mismatches, the counterintuitive notion that proteins involved in this process are implicated in inducing expansions is well supported. A large body of evidence from several mouse models indicates that MutSβ is a facilitator of expansions of disease-length CTG alleles in transgenic mouse models of TNR diseases as reviewed in chapter 1 (Manley et al., 1999; Kovtun and McMurray, 2001; van den Broek et al., 2002; Savouret et al., 2003; Wheeler et al., 2003). It is unknown whether there are mechanistic differences between expansions of long repeat tracts and short, near-threshold alleles, or whether the same factors promote expansions of both. In support of the idea that MutSβ could promote expansion of repeats near the threshold, biochemical studies using human cell extracts indicate that MutSβ is required for repair of small CTG slip-outs (Panigrahi et al., 2010), while purified MutSβ also binds short $(CAG)_n$ and $(CTG)_n$ hairpins *in vitro* (Owen et al., 2005; Tian et al., 2009; Lang et al., 2011). Nevertheless, it is possible that MMR functions differently at shorter repeats, as indicated by work in yeast. Studies in yeast have eliminated a role for MMR in contributing to TNR instability for repeats near the threshold. $(CAG)_{25}$• $(CTG)_{25}$ expansion rates in *msh2, msh3* and *pms1* mutants were comparable with the wild-type strain (Miret et al., 1998; Rolfsmeier et al., 2000). Strikingly, MMR was shown to be a major force in the stabilisation of interrupted alleles in yeast (Rolfsmeier et al., 2000). However, *msh2, msh3* and *pms2* mutants did not influence larger contractions or expansions in tracts of $(CAG)_{50}$• $(CTG)_{50}$ or $(CTG)_{64\text{-}92}$• $(CAG)_{64\text{-}92}$ (Miret et al., 1997; Schweitzer and Livingston, 1997). These findings were largely in contrast with data from the mouse studies. In light of this contradiction, the incongruence between yeast and mice studies may reflect different instability mechanisms among species. I decided to investigate what involvement they have for expansions near the threshold length in human cells to clarify this issue.

In addition to establishing whether MMR plays a role in expansion of repeats near the threshold in SVG-A cells, this chapter focuses on identification of potential mechanistic links between HDACs and effectors of expansions. The findings presented in chapter 3 infer a role for specific HDACs in promoting TNR expansions. Because HDACs are implicated in a wide range of biological processes, this complicates the question of how they facilitating the occurrence of expansions. Despite this complexity, the mechanism in yeast has been at least partially established with the finding that Sae2, which is protected from autophagic degradation by Rpd3 and Hda1, and Mre11 promote expansions (Debacker et al., 2012). However, the human homologue of Sae2, CtIP did not affect expansions in SVG-A cells (Chapter 3) likely due to its deacetylation being directed by SIRT6, rather than class I or II

HDACs (Kaidi et al., 2010). This candidate-based approach to investigating a mechanistic hypothesis for HDACs was extended to factors that are known to promote expansions in different model systems. Candidates that were tested included specific MMR repair proteins. Firstly, however, a role for these proteins in promoting expansions in SVG-A cells had to be established.

A similar approach to address the involvement of MMR in expansions was used as for most of Chapter 3. Specifically, siRNA knockdown of MSH2, MSH3 and MSH6 was performed to identify which, if any, of the MMR recognition complexes were relevant for expansions in SVG-A cells. Also, a mechanistic association between HDAC3 and MSH2 in the promotion of expansions was investigated.

4.3 Results

4.3.1 Role of MSH2 and MSH3 in TNR expansions

To determine if specific MMR factors contribute to TNR expansion of repeats approaching the threshold range in human cells, components of MutSβ and MutSα were investigated. If MMR factors do indeed promote expansion of shorter TNRs in a similar manner to the longer disease-length alleles tested in mice, then using RNAi to reduce expression levels of MSH2 and MSH3 ought to result in a decrease in expansions.

To this end, SVG-A cells were treated with MSH2 and MSH3 siRNA and then utilized for the shuttle vector expansion assay. Depletion of MSH2 resulted in a significant reduction in expansion frequency of 2.9-fold relative to scrambled siRNA (P=0.02; Fig 4.1A). This implies a role for MSH2 in promoting expansions in SVG-A cells, indicating that expansion of shorter repeats is governed at least in part by a similar mechanism as for longer disease-length repeats. Analysis in HeLa and HL-60 cells demonstrated that the MutSα complex is 6-10-fold more abundant than MutSβ, thus the majority of MSH2 is in the form of MutSα (Genschel et al., 1998). Despite being lower in abundance, evidence suggests that MutSβ is the relevant MMR complex in promoting expansions. In DM1 transgenic mice, loss of one MSH3 allele was sufficient to decrease the frequency of germline expansions, suggesting that MSH3 is a limiting factor in mediating TNR expansions (Foiry et al., 2006). This finding was corroborated in HD knock-in mice crossed with mice deficient in MMR genes, whereby striatal instability was significantly decreased in $Msh3^{+/-}$ mice but not in $Msh2^{+/-}$ mice (Dragileva et al., 2009). In light of the importance of MSH3 in mediating instability in mice, the effect of siRNA knockdown of MSH3 on TNR expansions was evaluated. Knockdown of MSH3 resulted in a similar extent of expansion suppression (~2.6-fold) (P=0.03; Fig 4.1B) as for MSH2 (2.9-fold). The observed decrease in expansions following MSH2 and MSH3 depletion suggests that they normally act to promote expansions in this system.

Analysis of the spectra of expansions in MSH2 and MSH3 knockdown cells did not reveal any notable differences compared with scrambled siRNA control cells (Fig. 4.1C&D) The weighted average increase in expansions was calculated as +10.8 and +9.4 for scrambled and MSH2 siRNA, respectively. Similarly there was no change in the spectrum of expansions upon MSH3 knockdown with weighted average expansion increases of +9.9 and +10.5 for scrambled and MSH2 siRNA, respectively. The uniformity across the mutation spectra is

consistent with lower incidences of expansions rather than knockdown precluding the disappearance of a certain size class.

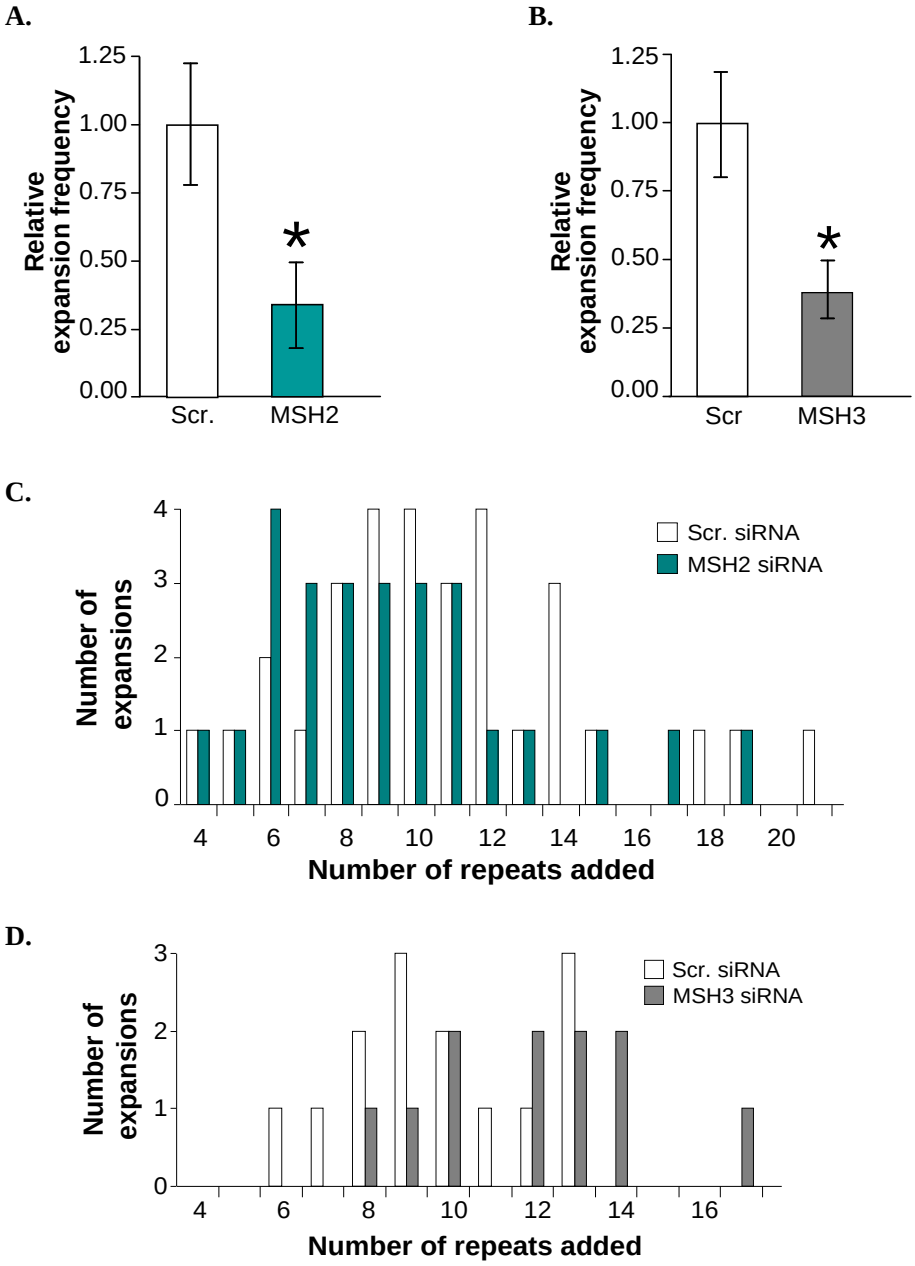

Figure 4.1 Role of mismatch repair proteins MSH2 and MSH3 in expansions. Expansion frequencies following siRNA treatment against **A.** MSH2 and **B.** MSH3. All frequencies were normalized to scrambled siRNA. n = 4 for MSH2 siRNA, n= 3 for MSH3 siRNA (**P*<0.05) Error bars denote ± one SEM. Expansion sizes for **C.** MSH2 experiments; 31 genetically independent expansions for scrambled siRNA, 26 for MSH2 siRNA and for **D**. MSH3 experiments; 14 for scrambled siRNA and 11 for MSH3 siRNA.

To confirm knockdown of MSH2 and MSH3 by siRNA, western blotting was performed. MSH2 levels were reduced by 72% (± 4) in cells transfected with MSH2 siRNA, while

siRNA directed against MSH3 depleted cognate protein expression by 79 % (± 4) (Fig. 4.2A-D).

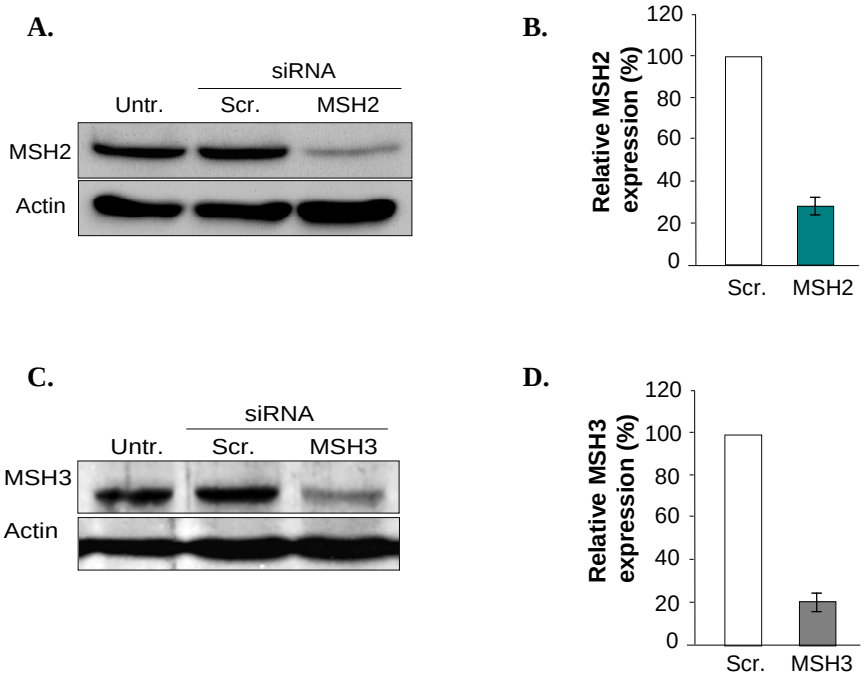

Figure 4.2 Expression of MSH2 and MSH3 following siRNA depletion. Representative western blots of **A.** MSH2 expression in SVG-A cells treated with MSH2 siRNA and **C.** MSH3 expression following MSH3 siRNA treatment. Quantification of **B.** MSH2 and **D.** MSH3 protein levels after knockdown, normalised to actin and to the scrambled siRNA control. Error bars denote ± one SEM; n= 3.

4.3.2 Knockdown of MSH6 does not influence expansions

The findings presented in section 4.3.1 imply that MutSβ promotes expansions. In order to determine if MutSα is involved in modulating expansions in SVG-A cells, knockdown of the MutSα-specific subunit MSH6 was performed. Based on work in transgenic mice, the prediction inferred is that MSH6 does not play a similar role to MSH2 and MSH3 in promoting TNR expansion. However, indirect effects of MSH6 deficiencies have been reported in transgenic mice. A possible outcome was that knockdown of MSH6 might result in an increase in expansions, as was observed for DM1 mice bearing a $(CTG)_{84}$ repeat tract deficient in MSH6 (van den Broek et al., 2002). This effect was ascribed to the competition between MSH3 and MSH6 for binding to MSH2 being shifted in favour of MSH3. Furthermore, for maternal transmissions in an $MSH6^{-/-}$ DM1 mouse, expansions were decreased likely due to the observation that ovaries deficient in MSH6 had significantly lower amounts of MSH2 and MSH3 (Foiry et al., 2006). No indirect effects that were

reported for MSH6 were borne out in our system, with depletion of MSH6 in SVG-A cells not showing any change in expansion frequency (Fig 4.3A). Specifically, compared with scrambled siRNA-treated cells, cells deficient in MSH6 showed a 1.1 fold increase in expansion frequency ($P = 0.76$). The observation that loss of MSH6 does not impact on expansions, whereas knockdown of MSH2 and MSH3 evokes a diminishment in expansions, compounds evidence for MutSβ being the relevant MMR complex in promoting expansions in SVG-A cells.

The expansion mutation spectra in MSH6-deficient and scrambled siRNA-treated cells overlapped, indicating that MSH6, in addition to not playing a role in influencing the frequency of expansions, does not influence the size of expansions (Fig 4.3B). This was further borne out by determination of weighted average increase in size of expansions, which was +10.6 for scrambled siRNA and +10.4 for MSH6 siRNA. Overall, this data excludes a role for MSH6 in modulating expansions.

Knockdown of MSH6 was verified by western blot, showing a 69% reduction in MSH6 levels following siRNA transfection (Fig. 4.3C&D). Stable knockdown of MSH6 to a relatively similar level in another study led to suppression of MMR-induced double strand breaks following chromium treatment, indicating that the absence of a phenotype in our system is not likely to be due to residual expression of MSH6 following siRNA knockdown (Zecevic et al., 2009).

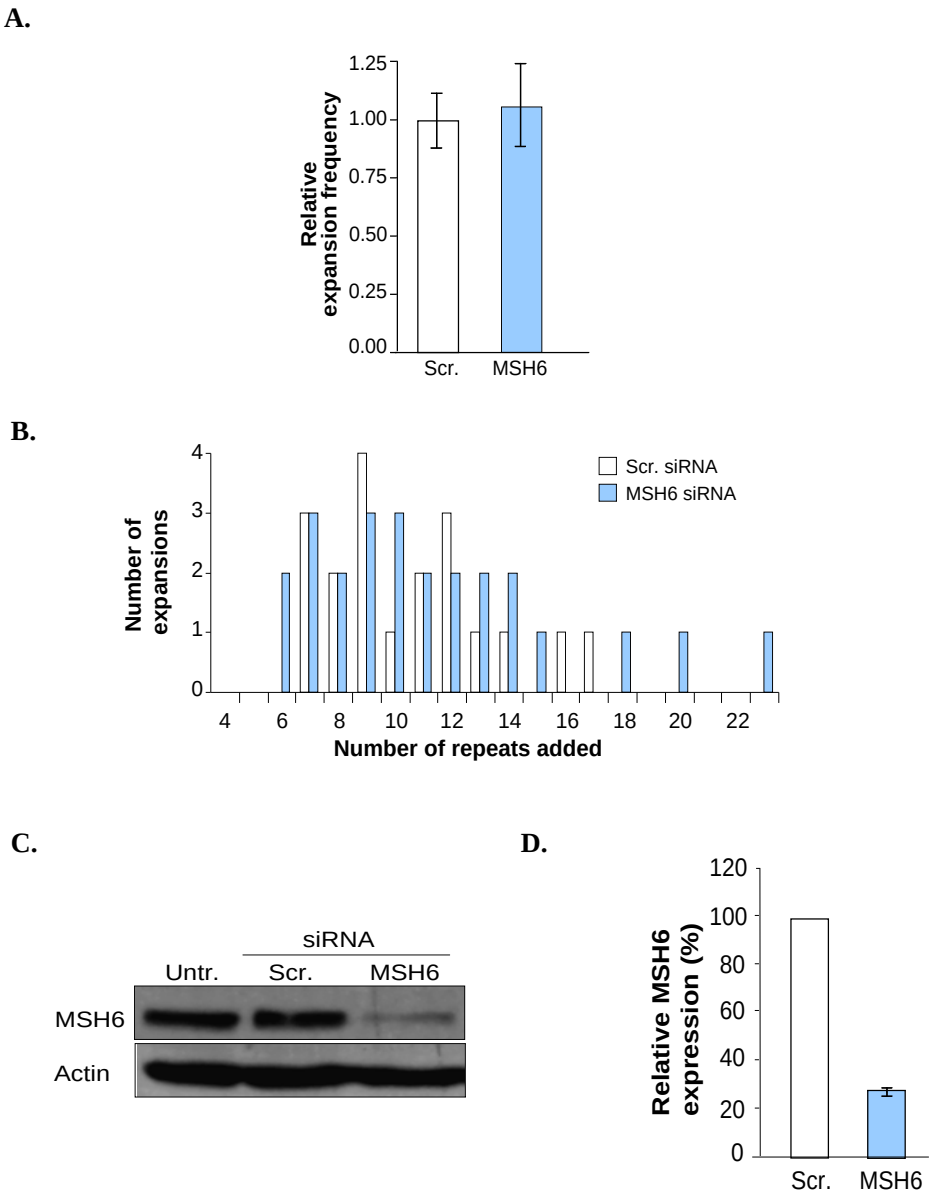

Figure 4.3 Expansions in SVG-A cells treated with MSH6 siRNA.
A. Expansion frequencies subsequent to treatment with MSH6 siRNA. All frequencies are normalised to scrambled siRNA. Error bars denote ± one SEM; *, $p<0.05$ compared to scrambled siRNA control; n= 3. **B.** Expansion sizes for MSH6 siRNA-treated cells: 19 genetically independent contractions for scrambled siRNA, 25 for MSH6 siRNA. **C.** Representative western blots confirming knockdown of MSH6. **D.** Quantification of MSH6 proteins levels normalised to actin and to the scrambled siRNA control cell levels. Error bars denote ± one SEM; n = 3.

4.3.3 Effect of double knockdown of HDAC3 and MSH2 on expansions

Following the observation that the majority of expansions in SVG-A cells are at least in part mediated by the MMR complex MutSβ, we wondered whether a link between these promoting factors and HDAC3 existed. We tested whether HDAC3 is acting through MMR to generate instability for a number of reasons. Firstly, the extent of suppression of expansions was similar upon inhibition of HDAC3 by 4b (3.3 to 4.3-fold, Chapter 3), knockdown of HDAC3 (4.2-fold, Chapter 3) or siRNA knockdown of MSH2 (2.9-fold) or MSH3 (2.6-fold). Secondly, a recent study showed that down-regulated MMR expression was coincidental with reduced instability upon differentiation of myotonic dystrophy stem cells, consistent with reduced expansion frequencies observed in knock-out mice of these proteins (Seriola et al., 2010). In light of the well-established functions of HDACs in control of gene expression, it seemed reasonable to envisage that HDAC3 might regulate MSH2 and MSH3 expression, thereby influencing their role in promoting expansions. Another rational possibility for the concerted action of HDACs and MMR proteins is that perhaps HDAC3 favours access of MutSβ to the repeat tract through modification of TNR chromatin, where it acts to incite expansion. Taking this into consideration, it was decided to perform double knockdowns of HDAC3 and MSH2 to test the possibility of these proteins working together to stimulate expansions.

Combinatorial knockdown of MSH2 and HDAC3 in SVG-A cells resulted in a statistically significant 3.2-fold reduction in expansion frequency compared to scrambled siRNA-treated cells ($P = 0.009$; Fig. 4.4A). Notably, this decrease is in line with that observed for the single HDAC3 and MSH2 knockdowns performed alongside, which were calculated to be 4.5-fold and 3.6-fold, respectively ($P = 0.006$ and 0.008, respectively; Fig. 4.4A). Furthermore, statistical analysis revealed no significant differences between the single knockdowns and the double (P vs HDAC3 = 0.22 and P vs MSH2 = 0.32) inferring that HDAC3 is acting in a shared pathway with MSH2 to promote expansions. Examination of the expansion sizes did not identify any differences between the expansion spectra for the different siRNA treatments (Fig. 4.4B). Confirmation of specific, efficacious knockdown is shown in Figure. 4.5. In cells transfected with MSH2 and HDAC3+MSH2 siRNA, MSH2 levels were decreased by 79% (± 3) and 83% (± 1), respectively (Fig. 4.5A and B). HDAC3 levels were reduced by 81% for single HDAC3 siRNA- and double siRNA-treated cells (Fig. 4.5A and B).

A.

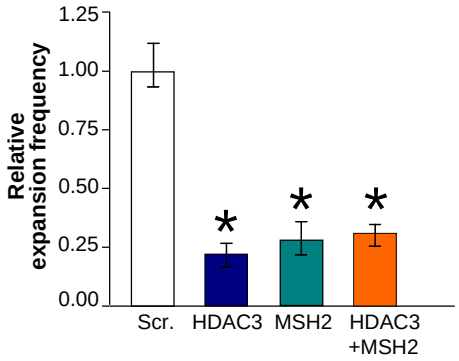

B.

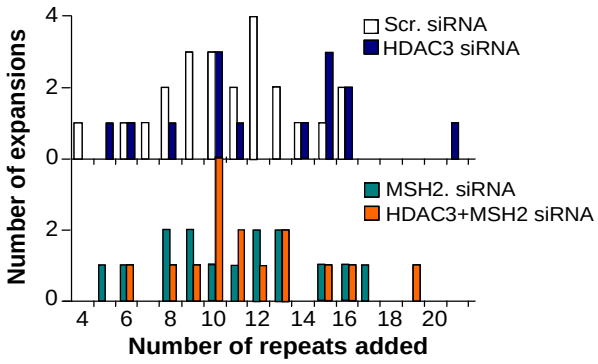

Figure 4.4 Effect of double knockdown of HDAC3 and MSH2 on expansions. A. Expansion frequencies following separate siRNA treatments against HDAC3 and MSH2 and a simultaneous HDAC3+MSH2 siRNA treatment. All frequencies were normalized to scrambled siRNA. n = 3 (**P*<0.05) Error bars denote ± one SEM. **B.** Expansion sizes, derived from PCR analysis. 23 genetically independent expansions for scrambled siRNA, 14 for HDAC3 siRNA, 15 for MSH2 siRNA and 15 for HDAC3+MSH2 siRNA.

Since HDAC3 and MutSβ seem to act through a common pathway that promotes expansions of CTG•CAG repeats in SVG-A cells, my attention shifted to identifying the mechanism of this connection. One possibility alluded to at the beginning of section 4.3.3 is that expression of MSH2/MSH3 is enhanced by HDAC3. Upon impairment of HDAC3, it might be expected that expression of these factors is downregulated either through transcription or by affecting stability of the proteins. Furthermore, direct deacetylation of proteins can influence their stability. HDAC1 has been reported to deacetylate DNMT1, protecting it from proteasomal degradation (Du et al., 2010). Furthermore, Sae2 is stabilised in a manner dependent on Rpd3 and Hda1 (Robert et al., 2011). If HDAC3 positively regulates the expression or stability of MMR repair proteins, then this might explain why double knockdowns of HDAC3 and MSH2 suppress expansions to the same extent as the respective single knockdowns.

I tested MSH2 protein levels following treatment of SVG-A cells with siRNA and/or the HDAC3 inhibitor, 4b. Quantitation of proteins levels from three independent experiments showed that depletion of HDAC3 by siRNA did not effect any change in MSH2 expression as determined by western blotting (Fig. 4.5A and B). Thus, while specific knockdown was achieved, no change in protein expression of MSH2 following depletion of HDAC3 was observed.

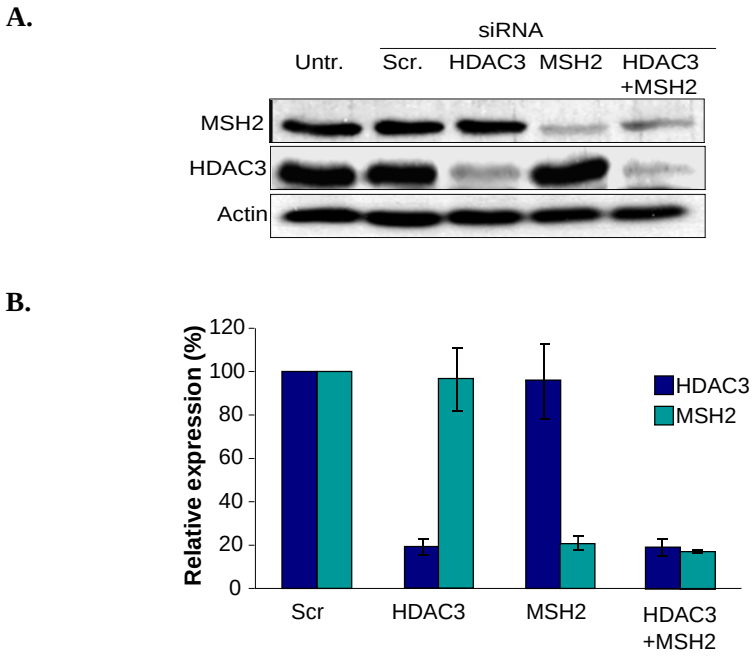

Figure 4.5 Expression levels of HDAC3 and MSH2 following single and double knockdown. A. Representative western blot analysis confirming knockdown of HDAC3 and MSH2 expression following siRNA treatments. β-actin was used as a loading control. **B.** Quantification of HDAC3 and MSH2 protein levels normalised to actin and to the scrambled siRNA control cell levels. n= 3; Error bars denote ± one SEM.

4.3.4 Expression of MMR proteins in 4b-treated SVG-A cells

Based on the observation that HDAC3 knockdown did not alter MSH2 levels in SVG-A cells, a similar outcome might be expected upon treatment by the small molecule inhibitor 4b. SVG-A cells were treated with 10 and 20 μM 4b for 48 hr and subsequently analysed for changes in expression of MSH2 and MSH3 by western blotting. MSH2 levels were reduced to a modest but statistically significant 58% in cells treated with 20 μM 4b compared to cells treated with DMSO ($P = 0.01$; Fig. 4.6A and B). This is in contrast to what was observed for HDAC3 siRNA-treated cells, but is in line with microarray studies using a colon cancer cell line SW480 where shRNA knockdown of HDAC3 led to a similar decrease in expression of MSH2 (Godman et al., 2008). MSH3 levels were reduced to 70% in cells treated with 20 μM

4b ($P = 0.2$). PMS2 was also included in these analyses. Pms2-null mice were shown to have a 50% reduction in somatic expansions (Gomes-Pereira et al., 2004). PMS2 levels were doubled in cells treated with 20 μM 4b ($P = 0.03$; Fig. 4.6A and B). Again these are in line with microarray data (Godman et al., 2008) but knockdown of HDAC3 by siRNA in SVG-A cells did not alter MSH2 or MSH3 levels (Fig 4.5A-B;(Gannon et al., Submitted). Despite the inconsistency between siRNA and inhibitor studies, it is unlikely that the modest changes in MSH2 and MSH3 expression in 4b-treated cells are sufficient to explain a functional connection between HDAC3 and MSH2/3 in facilitating expansions as discussed in section 4.4.

A.

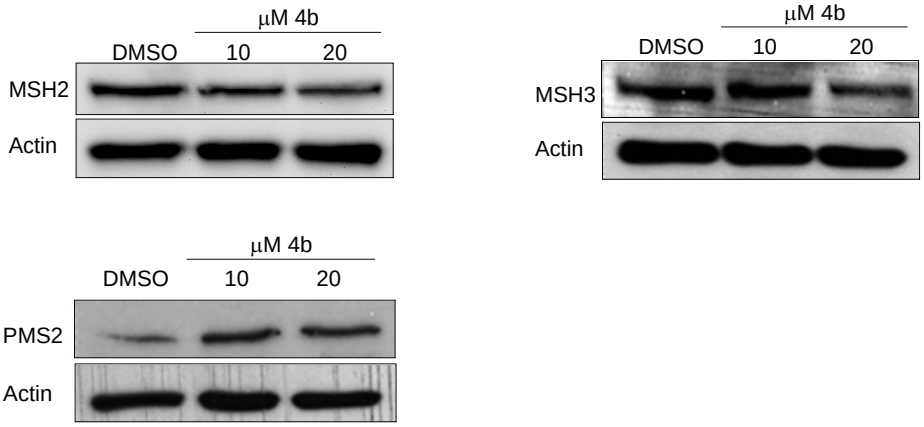

B.

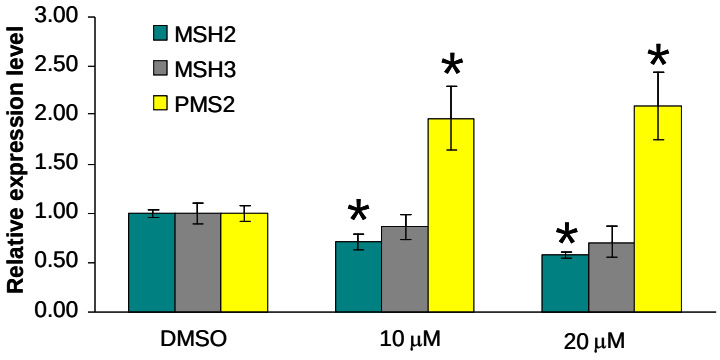

Figure 4.6 Expression of MSH2, MSH3 and PMS2 in 4b-treated SVG-A cells.
A. Western blot analysis of MSH2, MSH3 and PMS2 levels in SVG-A cells treated with DMSO, 10 and 20 μM 4b. β-actin was used as a loading control. **B.** Quantification of MSH2, MSH3 and PMS2 levels normalised to actin and to the DMSO-treated cell levels. n= 3 (*P<0.05 vs DMSO control) Error bars denote ± one SEM.

4.4. Discussion

The data presented in this chapter provide further insights into the mechanisms of TNR instability. While it has been well documented that MMR plays a role in mediating TNR instability in transgenic mice bearing disease-length repeats, little data was available on whether this action is restricted to pathogenic repeats or whether it is applicable for shorter, threshold-length repeats. Using siRNA silencing in conjunction with the shuttle vector expansion assay, it was determined that MSH2 and MSH3 promote TNR expansions in SVG-A cells, as knockdown of the MutSβ subunits impeded expansions. In contrast, depletion of MSH6 did not exert any alterations in the frequency of expansions, implying the relevance of MSH2/MSH3 dimers rather than MSH2/MSH6. Intriguingly, HDAC3 appears to be mediating its stimulatory effect on expansions through a mechanism involving MSH2.

The inference that MutSβ is the relevant MMR complex involved in mediating TNR expansions for near-threshold repeat lengths is in agreement with data from transgenic mouse models harbouring long alleles (van den Broek et al., 2002; Savouret et al., 2003; Foiry et al., 2006; Dragileva et al., 2009). MutSβ is thought to exert its influence on expansions through direct interaction with the TNR, since the complex binds CAG and CTG hairpins *in vitro* (Owen et al., 2005; Lang et al., 2011). Furthermore, ChIP experiments indicated that both MSH2 and MSH3, but not MSH6, were enriched immediately downstream of a long GAA repeat tract in induced pluripotent stem cells (iPSCs) derived from FRDA fibroblasts compared to control iPSCs derived from normal fibroblasts (Ku et al., 2010). To determine if MutSβ is enriched at the TNR region in SVG-A cells, cells were transfected with shuttle vector containing a $(CTG)_{22}$ tract or a randomised $(C,T,G)_{22}$ tract that is not prone to forming secondary structure and occupancy of MMR factors was determined by ChIP (Gannon et al., Submitted). This analysis revealed that MSH2 and MSH3, but not MSH6, were enhanced at the repeat region compared to the control tract. This finding supports the concept that expansions detected in SVG-A cells are at least partially generated by a mechanism involving MSH2 and MSH3, which is congruent with mouse model data.

One of the key findings is that HDAC3 and MSH2 promote expansions through a common pathway in SVG-A cells. What is the mechanistic link between these two proteins in facilitating expansions of CTG•CAG repeat tracts near the threshold? Various models are presented in figure 4.7 and discussed below. One manner in which HDACs might control expansions through MMR is in *cis* through deacetylation actions on histones near the repeat (Fig. 4.7A). The locus-specific nature of TNR mutability implies the importance of *cis*-

elements in these events, thus HDACs mediating their effects on expansions *in cis* would help explain this site specificity (Goellner et al., 1997). A role for chromatin modification by HDACs of histones near the TNR in instability is further supported by the observation that tracts with similar length and sequence composition exhibit different levels of instability for different loci (La Spada et al., 1992; Leeflang et al., 1995; Richards, 2001). A potential scenario is that deacetylation favours access of MMR proteins that promote expansions and/or precludes access of proteins that inhibit expansions, thus redressing the balance towards expansions. In support of this hypothesis, close examination of ChIP experiments at expanded FXN alleles reported in FRDA iPSCs reveals a correlation between heterochromatic histone marks and MutSβ occupancy (Ku et al., 2010), although MSH3 has been shown to be excluded from heterochromatin in *msh3*-null MEFs (Holt et al., 2011). In an effort to address the possibility that HDAC3 action on TNR chromatin promotes recruitment of MMR proteins, ChIP experiments to assess changes in occupancy of MMR proteins at the repeat tract in HDAC3 siRNA-treated SVG-A cells were performed. If HDAC3 acts to promote access of MSH2 and MSH3 to the repeat tract, then knockdown of HDAC3 should lead to a decrease in occupancy of these proteins. No change in occupancy of MSH2, MSH3 or MSH6 was observed in HDAC3 siRNA-treated cells compared with scrambled siRNA implying HDAC3 does not influence expansions by favouring occupancy (Gannon et al., Submitted). Thus the mechanism of action might be indirect, similar to yeast (Debacker et al., 2012) and *Drosophila* where loss of CBP increased expansions but changes in acetylation were not observed near the repeat (Jung and Bonini, 2007). In yeast, evidence suggests that expansions are minimally affected whether the TNR is integrated at different loci that are sensitive or insensitive to the effects of *sin3* mutation on transcription and local histone acetylation (Debacker et al., 2012). However, the ChIP data in SVG-A cells do not rule out the possibility that other factors might functionally interact with MSH2 and MSH3 to promote expansions. Downstream repair proteins might be the target of alterations in chromatin composition at the tract.

In an effort to elucidate if HDAC3 influences the expression of MMR proteins (Fig. 4.7B), steady-state protein levels were monitored following HDAC3 knockdown and inhibition. The observation that a decrease in MSH2 expression, albeit modest, followed treatment of SVG-A cells with the 4b inhibitor but not when HDAC3 is knocked down by siRNA might reflect a HDAC3-independent effect. The inhibitor is reported to be effective against HDAC1, although not as potently as for HDAC3 (Jia et al., 2012), so perhaps the discrepancy between the inhibitor and HDAC3 siRNA expression data can be explained by HDAC1 involvement. However, similar changes in expression as observed in 4b-treated cells were reported in a microarray study using a colon cancer cell line SW480 with shRNA

knockdown of HDAC3 (Godman et al., 2008). Nevertheless the changes in expression levels in 4b-treated cells are mild for MSH2 and MSH3, and would be unlikely to account for the suppression of expansions. Mice hetereozygous for Msh2 displayed similar levels of expansions as wild-type, implying that one copy (50% of protein level) of Msh2 is not sufficient (Savouret et al., 2003). Furthermore, MSH3 levels were mildly decreased in 4b-treated cells. MSH3 has been identified as a limiting factor in mediating TNR expansions with $Msh3^{+/-}$ transgenic mice displaying decreased instability (Foiry et al., 2006; Dragileva et al., 2009). However, the level remaining after 4b treatment in SVG-A is unlikely to be low enough for such an effect. Taken with the observation that no change in steady-state MSH3 levels was observed in SVG-A cells with HDAC3 knocked down (Fig 4.5, (Gannon et al., Submitted), this implies that HDAC3 does not strongly influence MSH3 expression. Thus, it can be concluded that HDAC3 is not promoting expansions by regulating MSH2 and MSH3 protein levels.

Therefore, the possibility that HDAC3 promotes CTG•CAG expansions by regulating MSH2 or MSH3 protein expression, or by controlling access of MutSβ to the repeat tract has been excluded. Acetylation sites have been identified on MSH2 but the function of this modification has not been elucidated (Choudhary et al., 2009). MSH2 acetylation sites were identified by mass spectrometry and are located at lysine 555 and lysine 635 (Choudhary et al., 2009), which are situated within the MSH3/MSH6 binding domain. Although the relevant HDAC(s) have not been identified and the consequences of this acetylation on MSH2 activity, expression or localisation have not been determined, it could be speculated that perhaps HDAC3 catalyses deacetylation of one or both of these lysines, which influences the ability of MSH2 to stimulate expansions. The ChIP data revealed that MSH2 and MSH3 enrichment at the TNR is not impaired in the absence of HDAC3 so we can speculate that this acetylation, if important in determining expansion, does not impair binding to the TNR tract (Gannon et al., Submitted). One possibility is that increased acetylation of MSH2 might negatively regulate its ATPase activity (Fig. 4.7C), which was previously shown to be required for TNR expansions in a DM1 mouse model (Tome et al., 2009). Whether ATPase activity is required for expansions in the SVG-A system has yet to be established. Additonally, this concept requires that HDAC3 deacetylates MSH2 and that the ATPase function is regulated through this acetylation, neither of which has been described.

An alternative scenario is that HDAC3 knockdown influences expression, TNR occupancy or activity of another unidentified factor that functionally interacts with MutSβ in promoting

expansions. Support for a functional MMR system in mediating expansion is garnered from the finding in DM1 mice that the ATPase activity of MSH2 is necessary for expansions (Tome et al., 2009). Moreover, mice lacking the MutL homologue PMS2, which forms a heterodimer (MutLα) with MLH1 and interacts with mismatches identified by MutSα or MutSβ to initiate excision and resynthesis, displayed a 50% decrease in somatic expansions in DM1 mice (Gomes-Pereira et al., 2004). Additionally MLH1 can form a heterodimer with PMS1 (MutLβ) or MLH3 (MutLγ). If any of the MutL proteins are involved in driving expansions downstream of MutSβ, then they might represent the actual targets of HDAC3. MLH1/PMS2 is thought to be the major MutL component of MMR but PMS2 is thought to be partially redundant with MLH3 (Korhonen et al., 2007), which may also contribute to instability. 4b treatment of SVG-A cells resulted in a 2-fold increase in PMS2 expression. If HDAC3 inhibition serves to augment expression of the predicted promoting factor PMS2, then it is not clear how it acts in concert to promote expansions. However, this increase in expression has not been confirmed in cells treated with HDAC3 siRNA and may be an off-target effect of the small molecule inhibitor. Further investigations are required to establish the mode of action through which MMR is promoting expansion of short tracts in SVG-A cells.

In Chapter 3, I presented evidence for HDAC3 and HDAC5 working together to promote expansions. While the role of HDAC5 has not been addressed directly in this work, it is supposed that it is acting in the same pathway described for HDAC3. In light of biochemical analyses showing that HDAC3 interacts with HDAC5 (Fischle et al., 2002), and that class IIa HDACs exhibit little or no deacetylase activity on acetyllysine residues (Lahm et al., 2007; Bottomley et al., 2008), perhaps HDAC5 recruits HDAC3 to the relevant acetylation residue to effect deacetylation. Further investigations are required to elucidate the relationship between HDAC3, HDAC5 and MMR.

The findings presented in this chapter have answered a key question regarding the involvement of MMR in expansions of CTG•CAG tracts near the threshold length. Studies in yeast had previously shown that expansion of threshold length repeats did not involve MMR (Miret et al., 1998; Rolfsmeier et al., 2000). Based on the observation that long repeat tracts were also largely unchanged in yeast (Schweitzer and Livingston, 1997), and the finding that MutSβ drives expansions of sub-threshold CTG•CAG repeats in human cells, it is likely that some mechanistic differences regarding MMR involvement in TNR instability may exist between yeast and mammalian systems. In further support of MutSβ promoting expansions, MSH2 and MSH3 were shown to be enriched at the repeat region in SVG-A

cells. HDAC3 and MSH2 appear to be working in the same pathway to promote expansions but the nature of this mechanism has yet to be determined.

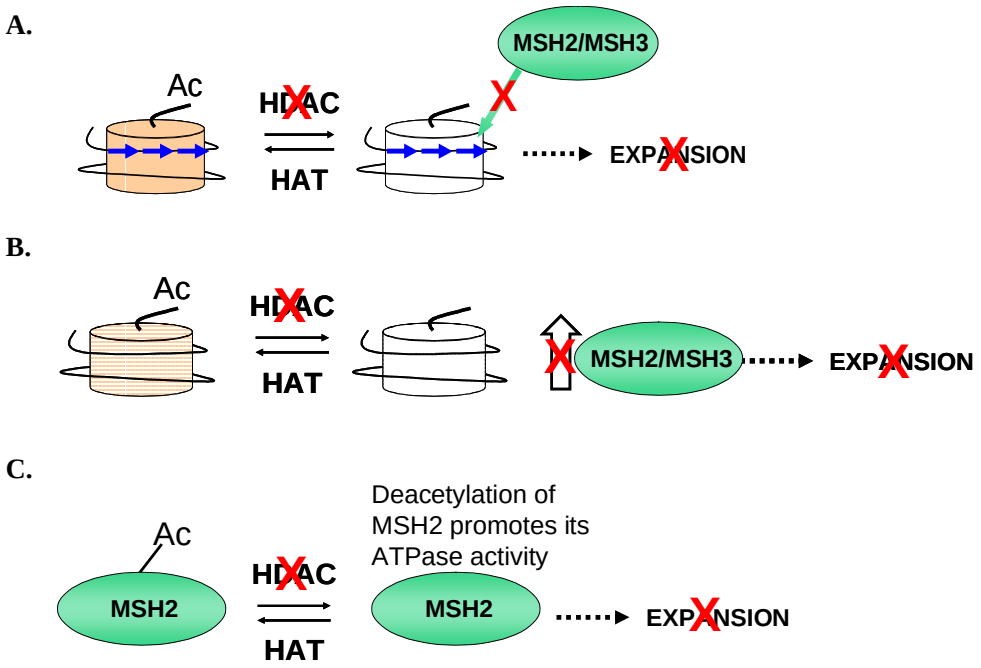

Figure 4.7. Models for concerted action of HDAC3 and MSH2/3. A. Histone acetylation near the TNR tracts is altered leading to enhanced DNA access by MSH2 and MSH3 resulting in an increase in expansions. When HDAC3 is depleted or inhibited, access is limited and leads to a suppression of expansions. ChIP experiments have eliminated this model with no detectable difference in MutSβ binding to the $(CTG)_{22}$ tract upon HDAC3 knockdown. **B.** HDAC3 acts to promote the transcription or stability of MSH2 and MSH3. When HDAC3 is depleted or inhibited, MSH2/3 expression is depleted and expansions are reduced. **C.** HDAC3 directly deacetylates MSH2, enhancing its ATPase activity, which has been shown to be required for expansions in DM1 mice (Tome et al., 2009). This possibility is speculative and has not been tested. Other scenarios can be imagined wherein a factor that functionally interacts with MutSβ to promote expansions might be the target of HDAC3 action.

4.5 References

Bottomley, M. J., P. Lo Surdo, P. Di Giovine, A. Cirillo, R. Scarpelli, F. Ferrigno, P. Jones, P. Neddermann, R. De Francesco, C. Steinkuhler, P. Gallinari and A. Carfi (2008). Structural and functional analysis of the human HDAC4 catalytic domain reveals a regulatory structural zinc-binding domain. *J Biol Chem* **283**(39): 26694-704.

Choudhary, C., C. Kumar, F. Gnad, M. L. Nielsen, M. Rehman, T. C. Walther, J. V. Olsen and M. Mann (2009). Lysine acetylation targets protein complexes and co-regulates major cellular functions. *Science* **325**(5942): 834-40.

Debacker, K., A. Frizzell, O. Gleeson, L. Kirkham-McCarthy, T. Mertz and R. S. Lahue (2012). Histone deacetylase complexes promote trinucleotide repeat expansions. *PLoS Biol* **10**(2): e1001257.

Dragileva, E., A. Hendricks, A. Teed, T. Gillis, E. T. Lopez, E. C. Friedberg, R. Kucherlapati, W. Edelmann, K. L. Lunetta, M. E. MacDonald and V. C. Wheeler (2009). Intergenerational and striatal CAG repeat instability in Huntington's disease knock-in mice involve different DNA repair genes. *Neurobiol Dis* **33**(1): 37-47.

Du, Z., J. Song, Y. Wang, Y. Zhao, K. Guda, S. Yang, H. Y. Kao, Y. Xu, J. Willis, S. D. Markowitz, D. Sedwick, R. M. Ewing and Z. Wang (2010). DNMT1 stability is regulated by proteins coordinating deubiquitination and acetylation-driven ubiquitination. *Sci Signal* **3**(146): ra80.

Fischle, W., F. Dequiedt, M. J. Hendzel, M. G. Guenther, M. A. Lazar, W. Voelter and E. Verdin (2002). Enzymatic activity associated with class II HDACs is dependent on a multiprotein complex containing HDAC3 and SMRT/N-CoR. *Mol Cell* **9**(1): 45-57.

Foiry, L., L. Dong, C. Savouret, L. Hubert, H. te Riele, C. Junien and G. Gourdon (2006). Msh3 is a limiting factor in the formation of intergenerational CTG expansions in DM1 transgenic mice. *Hum Genet* **119**(5): 520-6.

Gannon, A., A. Frizzell, E. Healy and R. S. Lahue (Submitted). MutSβ and histone deacetylase complexes promote expansions of trinucleotide repeats in human cells.

Genschel, J., S. J. Littman, J. T. Drummond and P. Modrich (1998). Isolation of MutSbeta from human cells and comparison of the mismatch repair specificities of MutSbeta and MutSalpha. *J Biol Chem* **273**(31): 19895-901.

Godman, C. A., R. Joshi, B. R. Tierney, E. Greenspan, T. P. Rasmussen, H. W. Wang, D. G. Shin, D. W. Rosenberg and C. Giardina (2008). HDAC3 impacts multiple oncogenic pathways in colon cancer cells with effects on Wnt and vitamin D signaling. *Cancer Biol Ther* **7**(10): 1570-80.

Goellner, G. M., D. Tester, S. Thibodeau, E. Almqvist, Y. P. Goldberg, M. R. Hayden and C. T. McMurray (1997). Different mechanisms underlie DNA instability in Huntington disease and colorectal cancer. *Am J Hum Genet* **60**(4): 879-90.

Gomes-Pereira, M., M. T. Fortune, L. Ingram, J. P. McAbney and D. G. Monckton (2004). Pms2 is a genetic enhancer of trinucleotide CAG.CTG repeat somatic mosaicism: implications for the mechanism of triplet repeat expansion. *Hum Mol Genet* **13**(16): 1815-25.

Holt, I., L. Thanh Lam, S. Tome, D. G. Wansink, H. Te Riele, G. Gourdon and G. E. Morris (2011). The mouse mismatch repair protein, MSH3, is a nucleoplasmic protein that aggregates into denser nuclear bodies under conditions of stress. *J Cell Biochem* **112**(6): 1612-21.

Jia, H., J. Pallos, V. Jacques, A. Lau, B. Tang, A. Cooper, A. Syed, J. Purcell, Y. Chen, S. Sharma, G. R. Sangrey, S. B. Darnell, H. Plasterer, G. Sadri-Vakili, J. M. Gottesfeld, L. M. Thompson, J. R. Rusche, J. L. Marsh and E. A. Thomas (2012). Histone deacetylase (HDAC) inhibitors targeting HDAC3 and HDAC1 ameliorate polyglutamine-elicited phenotypes in model systems of Huntington's disease. *Neurobiology of Disease* **46**(2): 351-361.

Jung, J. and N. Bonini (2007). CREB-binding protein modulates repeat instability in a Drosophila model for polyQ disease. *Science* **315**(5820): 1857-9.

Kaidi, A., B. T. Weinert, C. Choudhary and S. P. Jackson (2010). Human SIRT6 promotes DNA end resection through CtIP deacetylation. *Science* **329**(5997): 1348-53.

Korhonen, M. K., T. E. Raevaara, H. Lohi and M. Nystrom (2007). Conditional nuclear localization of hMLH3 suggests a minor activity in mismatch repair and supports its role as a low-risk gene in HNPCC. *Oncol Rep* **17**(2): 351-4.

Kovtun, I. V. and C. T. McMurray (2001). Trinucleotide expansion in haploid germ cells by gap repair. *Nat Genet* **27**(4): 407-11.

Ku, S., E. Soragni, E. Campau, E. A. Thomas, G. Altun, L. C. Laurent, J. F. Loring, M. Napierala and J. M. Gottesfeld (2010). Friedreich's ataxia induced pluripotent stem cells model intergenerational GAATTC triplet repeat instability. *Cell Stem Cell* **7**(5): 631-7.

La Spada, A. R., D. B. Roling, A. E. Harding, C. L. Warner, R. Spiegel, I. Hausmanowa-Petrusewicz, W. C. Yee and K. H. Fischbeck (1992). Meiotic stability and genotype-phenotype correlation of the trinucleotide repeat in X-linked spinal and bulbar muscular atrophy. *Nat Genet* **2**(4): 301-4.

Lahm, A., C. Paolini, M. Pallaoro, M. C. Nardi, P. Jones, P. Neddermann, S. Sambucini, M. J. Bottomley, P. Lo Surdo, A. Carfi, U. Koch, R. De Francesco, C. Steinkuhler and P. Gallinari (2007). Unraveling the hidden catalytic activity of vertebrate class IIa histone deacetylases. *Proc Natl Acad Sci U S A* **104**(44): 17335-40.

Lang, W. H., J. E. Coats, J. Majka, G. L. Hura, Y. Lin, I. Rasnik and C. T. McMurray (2011). Conformational trapping of mismatch recognition complex MSH2/MSH3 on repair-resistant DNA loops *Proc Natl Acad Sci U S A* **108**(42): E837-44.

Leeflang, E. P., L. Zhang, S. Tavare, R. Hubert, J. Srinidhi, M. E. MacDonald, R. H. Myers, M. de Young, N. S. Wexler, J. F. Gusella and et al. (1995). Single sperm analysis of the trinucleotide repeats in the Huntington's disease gene: quantification of the mutation frequency spectrum. *Hum Mol Genet* **4**(9): 1519-26.

Manley, K., T. L. Shirley, L. Flaherty and A. Messer (1999). Msh2 deficiency prevents in vivo somatic instability of the CAG repeat in Huntington disease transgenic mice. *Nat Genet* **23**(4): 471-3.

Miret, J. J., L. Pessoa-Brandao and R. S. Lahue (1997). Instability of CAG and CTG trinucleotide repeats in Saccharomyces cerevisiae. *Mol Cell Biol* **17**(6): 3382-7.

Miret, J. J., L. Pessoa-Brandao and R. S. Lahue (1998). Orientation-dependent and sequence-specific expansions of CTG/CAG trinucleotide repeats in Saccharomyces cerevisiae. *Proc Natl Acad Sci U S A* **95**(21): 12438-43.

Owen, B. A., Z. Yang, M. Lai, M. Gajec, J. D. Badger, 2nd, J. J. Hayes, W. Edelmann, R. Kucherlapati, T. M. Wilson and C. T. McMurray (2005). (CAG)(n)-hairpin DNA binds to Msh2-Msh3 and changes properties of mismatch recognition. *Nat Struct Mol Biol* **12**(8): 663-70.

Panigrahi, G. B., M. M. Slean, J. P. Simard, O. Gileadi and C. E. Pearson (2010). Isolated short CTG/CAG DNA slip-outs are repaired efficiently by hMutSbeta, but clustered slip-outs are poorly repaired. *Proc Natl Acad Sci U S A* **107**(28): 12593-8.

Richards, R. I. (2001). Dynamic mutations: a decade of unstable expanded repeats in human genetic disease. *Hum Mol Genet* **10**(20): 2187-94.

Robert, T., F. Vanoli, I. Chiolo, G. Shubassi, K. A. Bernstein, R. Rothstein, O. A. Botrugno, D. Parazzoli, A. Oldani, S. Minucci and M. Foiani (2011). HDACs link the DNA damage response, processing of double-strand breaks and autophagy. *Nature* **471**(7336): 74-9.

Rolfsmeier, M. L., M. J. Dixon and R. S. Lahue (2000). Mismatch repair blocks expansions of interrupted trinucleotide repeats in yeast. *Mol Cell* **6**(6): 1501-7.

Savouret, C., E. Brisson, J. Essers, R. Kanaar, A. Pastink, H. te Riele, C. Junien and G. Gourdon (2003). CTG repeat instability and size variation timing in DNA repair-deficient mice. *Embo J* **22**(9): 2264-73.

Schweitzer, J. K. and D. M. Livingston (1997). Destabilization of CAG trinucleotide repeat tracts by mismatch repair mutations in yeast. *Hum Mol Genet* **6**(3): 349-55.

Seriola, A., C. Spits, J. P. Simard, P. Hilven, P. Haentjens, C. E. Pearson and K. Sermon (2010). Huntington's and myotonic dystrophy hESCs: down-regulated trinucleotide repeat instability and mismatch repair machinery expression upon differentiation. *Hum Mol Genet* **20**(1): 176-85.

Tian, L., C. Hou, K. Tian, N. C. Holcomb, L. Gu and G. M. Li (2009). Mismatch recognition protein MutSbeta does not hijack (CAG)n hairpin repair in vitro. *J Biol Chem* **284**(31): 20452-6.

Tome, S., I. Holt, W. Edelmann, G. E. Morris, A. Munnich, C. E. Pearson and G. Gourdon (2009). MSH2 ATPase domain mutation affects CTG*CAG repeat instability in transgenic mice. *PLoS Genet* **5**(5): e1000482.

van den Broek, W. J., M. R. Nelen, D. G. Wansink, M. M. Coerwinkel, H. te Riele, P. J. Groenen and B. Wieringa (2002). Somatic expansion behaviour of the (CTG)n repeat in myotonic dystrophy knock-in mice is differentially affected by Msh3 and Msh6 mismatch-repair proteins. *Hum Mol Genet* **11**(2): 191-8.

Wheeler, V. C., L. A. Lebel, V. Vrbanac, A. Teed, H. te Riele and M. E. MacDonald (2003). Mismatch repair gene Msh2 modifies the timing of early disease in Hdh(Q111) striatum. *Hum Mol Genet* **12**(3): 273-81.

Zecevic, A., H. Menard, V. Gurel, E. Hagan, R. DeCaro and A. Zhitkovich (2009). WRN helicase promotes repair of DNA double-strand breaks caused by aberrant mismatch repair of chromium-DNA adducts. *Cell Cycle* **8**(17): 2769-78.

CHAPTER 5

Factors proposed to protect TNRs from expansion

5.1 Summary

This chapter investigates if mechanisms proposed to protect against repeat expansion in yeast also play a similar role in SVG-A cells. Previous studies in the Lahue lab and others identified a role for the yeast helicase Srs2 in blocking expansions. One study indicated that this anti-expansion function of Srs2 also requires the error-free branch of the post-replication repair (PRR) pathway, including the Rad18 and Rad5 proteins. I used RNA interference in SVG-A cells to test human homologues of Srs2, Rad18 and Rad5 proteins as expansion-blocking factors. The prediction is that loss of a protective factor would increase expansion frequencies. Of the two proposed orthologues of Srs2, RTEL1 inhibits expansions, while FBH1 does not seem to be involved. Specifically, knockdown of RTEL1 in SVG-A cells resulted in a ~4.5-fold increase in expansions compared to cells treated with scrambled siRNA, while knockdown of FBH1 did not alter expansion outcomes. A role for PRR in moderating expansions was also established. Knockdown of hRAD18 and the human Rad5 orthologue, HLTF resulted in increased expansion frequencies. In contrast, siRNA depletion of a distinct Rad5 orthologue, SHPRH, did not alter expansions. To determine if RTEL1 acts in concert with PRR to inhibit expansions, double knockdowns of RTEL1 and RAD18 or RTEL1 and HLTF were performed. Double knockdowns stimulated expansions to a similar extent as the single knockdowns indicating that they are acting in a shared pathway to reduce expansions. In addition to Srs2 and PRR, several yeast and biochemical studies have demonstrated the importance of the flap endonuclease activity of Rad27 (FEN1) in preventing expansions. However, whether a corresponding function for FEN1 exists in higher organisms is unclear due to conflicting reports. In SVG-A cells, reduction of FEN1 expression by siRNA did not affect the frequency of expansions. I conclude that RTEL1, RAD18, and HLTF protect TNRs in human cells from expansions; that the three proteins likely work together in this capacity; and that the other candidate proteins FBH1, SHPRH and FEN1 are not relevant in my experimental system.

5.2 Introduction

The data presented in chapters 3 and 4 focused largely on factors that are involved in promoting expansions. This chapter will see attention shift to those proposed to be involved in inhibiting expansions. Studies in budding yeast provided compelling evidence for a novel pathway involving the DNA helicase Srs2 in the inhibition of TNR expansions. Mutants lacking Srs2 show a high expansion rate compared to wild type controls (Bhattacharyya and Lahue, 2004). Biochemical analysis revealed that Srs2 selectively unwinds TNR substrates that mimic the *in vivo* hairpin intermediates thought to contribute to instability (Bhattacharyya and Lahue, 2005; Dhar and Lahue, 2008). Further genetic analysis demonstrated that the protective role of Srs2 against expansions was independent of its role in homologous recombination but was instead due to its capacity to direct post-replication repair (PRR) (Bhattacharyya and Lahue, 2004; Daee et al., 2007). PRR ensures continuation of DNA synthesis in the presence of polymerase-blocking damage, deferring the engagement of conserved repair mechanisms that are in place, to faithfully repair DNA to its original sequence as described in Chapter 1 (Waters et al., 2009). Interestingly, there is also an increased rate of expansions in mutants of the PRR pathway, such as *rad18* and *rad5* (Daee et al., 2007). Furthermore, the observation that double mutants deficient for both Srs2 and PRR exhibited an epistatic relationship was interpreted as Srs2 acting in concert with PRR to block expansions. Another point in favor of this model is that srs2 mutants and pol30K164R (PCNA) mutants both share the unusual mutator signature whereby expansions are the only type of mutation that is enhanced in these backgrounds. Since Rad18 and Rad5 proteins are required for ubiquitylating PCNA at K164R, these findings are consistent with a protective role for PRR in preventing TNR expansions. In light of the finding that Srs2 efficiently unwinds triplet repeat DNA *in vitro*, it was postulated that in response to aberrant DNA replication at the TNR tract, PRR acts together with Srs2 to inhibit TNR expansions by targeting resolution of resultant hairpins. This provided evidence for a 3' slippage model (Fig. 5.1) as PRR processing is proposed to be recruited to the 3' end of intermediates formed at sites of stalled replication (Ulrich, 2005).

The connotations of these findings for regulation of expansions in human cells are unknown. However, given that proteins involved in PRR are generally well-conserved from yeast to humans and due to the relatively recent identification of candidate Srs2 human orthologues, testing the translation of these findings to human cells is now feasible.

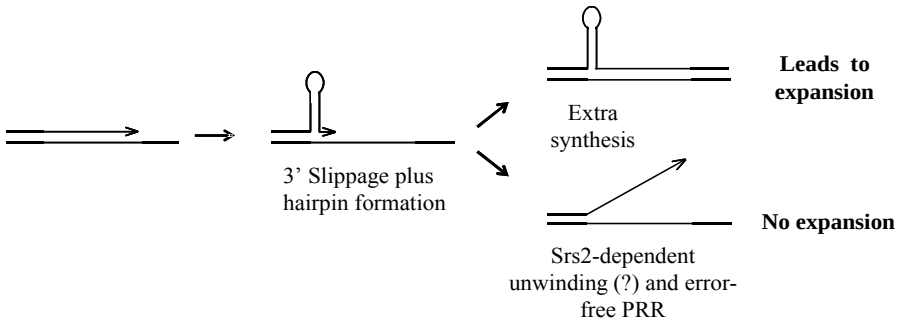

Figure 5.1 Model for prevention of TNR expansions arising from the 3' end of an Okazaki fragment during lagging strand synthesis. DNA polymerase stalling at the TNR tract can result in 3' slippage and possible hairpin formation. Resolution of this replicative stress by the unwinding action of Srs2 and by PRR prevents expansions. From Daee et al., 2007.

In addition to the proposed protective action of Srs2 and PRR on expansions occurring by polymerase stalling and subsequent 3' slippage, there is considerable evidence for a corresponding mechanism for prevention of expansions originating from the 5' end of DNA being synthesized (Fig 5.2). In this model of TNR instability, expansions can occur due to improper processing of 5' flaps created during Okazaki fragment maturation (Gordenin et al., 1997). This 5' flap model is supported by the findings that loss of the yeast flap endonuclease, Rad27 results in large increases in expansion rates and expansion sizes (Freudenreich et al., 1998; Henricksen et al., 2000; Callahan et al., 2003; Liu and Bambara, 2003; Liu et al., 2004) It is likely that Rad27 cleaves these single-stranded flap substrates, thereby averting their folding into hairpins that would otherwise inhibit FEN1 cleavage and introduce extraneous DNA into the nascent strand.

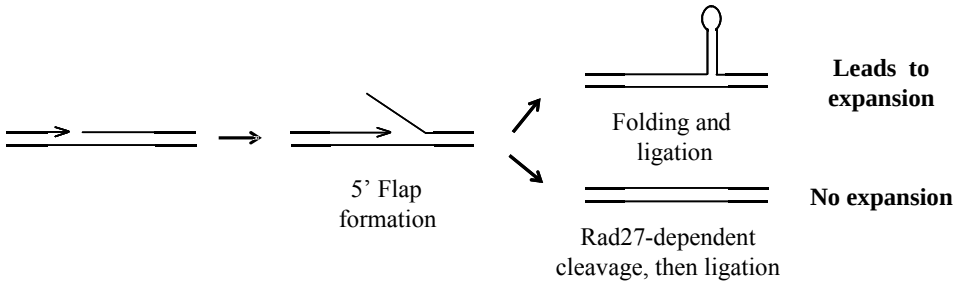

Figure 5.2 Model for prevention of TNR expansions arising from the 5' end of an Okazaki fragment during lagging strand synthesis. In this model, strand displacement creates a 5' TNR flap that is cleaved by Rad27 before it becomes long enough to form a stable hairpin. If left intact, the flap forms stable hairpins that are refractory to Rad27 cleavage and can be ligated with the upstream Okazaki fragament resulting in an addition of repeats and thus expansion. From Daee et al., 2007.

Double mutants of *rad27* with *rad18* showed synergistic increases over either single mutant, indicating the existence of largely independent pathways for preventing expansion of TNR tracts, whereby expansions arising from the 5' and 3' ends, respectively, of an Okazaki fragment are dealt with by separate mechanisms (Daee et al., 2007). The inference from yeast is that the flap processing activity of Rad27 provides an effective mechanism to prevent TNR mutations. Whether FEN1 plays an equivalent role in higher organisms is not yet clear, with some studies in mice and human cells suggesting that FEN1 is not involved (Spiro and McMurray, 2003; van den Broek et al., 2006; Moe et al., 2008; Entezam et al., 2010).

This chapter investigates the involvement of the Srs2 orthologues, FBH1 and RTEL1, and members of the PRR pathway, RAD18, HLTF and SHPRH in TNR expansions in SVG-A cells. The rationale behind this study was derived from the findings in yeast outlined above and further compelled by the relatively recent identification of human counterparts of some of these factors e.g. RTEL1, SHPRH and HLTF. Additionally, the influence of FEN1 on TNR expansions was addressed in SVG-A cells. The experimental approach taken for this study involved knocking down the proteins of interest by siRNA and evaluating the expansion phenotype through the shuttle vector expansion assay.

5.3 Results

5.3.1 Role of FBH1 in TNR expansions

The human F-box DNA helicase FBH1 is a proposed Srs2 homologue in humans. FBH1 contains an active UvrD helicase domain and human U2OS cells overexpressing FBH1 showed inhibition of Rad51 accumulation, thus suppressing HR (Fugger et al., 2009). Furthermore, expression of hFBH1 in *srs2Δ* cells rescued the MMS sensitivity of PRR mutants (Chiolo et al., 2007). However, loss of FBH1 in DT40 cells did not lead to increased recombination (Kohzaki et al., 2007). Thus, conflicting results have led to uncertainty over the degree to which FBH1 acts as an antirecombinase *in vivo* like Srs2. In order to determine if its functional homology to Srs2 extends to modulating expansions, knockdown of FBH1 by siRNA was performed in SVG-A cells and expansion frequencies were measured by the shuttle vector expansion assay. If FBH1 acts to influence expansions in a similar manner to Srs2 (i.e. inhibition), then it would be expected that knockdown of FBH1 would result in an increase in expansions due to impairment of its protective function.

A significant effect of FBH1 depletion on expansion frequency was not observed, with only an 8% decrease in expansion frequency compared with scrambled siRNA ($P = 0.82$) suggesting that FBH1 does not recapitulate the role of yeast Srs2 in mediating protection against expansions (Fig. 5.3A). Efficiency of FBH1 knockdown was measured by real-time RT-PCR. Western blotting was not attempted due to the recognised lack of viable FBH1 antibodies (Laulier et al., 2010). Real-time RT-PCR analysis showed that levels of FBH1 mRNA were reduced by 68% (± 1) (Fig. 5.3C). It could be claimed that the knockdown of FBH1 was insufficient to reveal an expansion phenotype, with adequate expression remaining to execute its functions in preventing TNR instability. This possibility is unlikely given the observations of a previous lab member that 90% knockdown of FBH1 mRNA levels did not result in any change in expansion frequency (Claassen, 2009). This evidence against a role for FBH1 in inhibiting expansions strengthens the case for my findings. Measurement of expansion sizes in FBH1-deficient and scrambled siRNA-treated SVG-A cells did reveal any considerable changes in the spectrum of expansions, with average increases in tract length of +10.1 and +9.6, respectively (Fig. 5.3B).

This data, in combination with previous work in the Lahue lab, leads me to conclude that FBH1 is unlikely to be involved in stabilising TNR tracts in my experimental system. Thus, while this helicase possesses functions in PRR and recombination that partly overlap with Srs2, its functional similarity to Srs2 does not encompass a role in maintenance of TNR stability.

A.

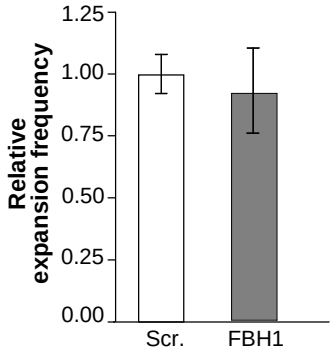

B.

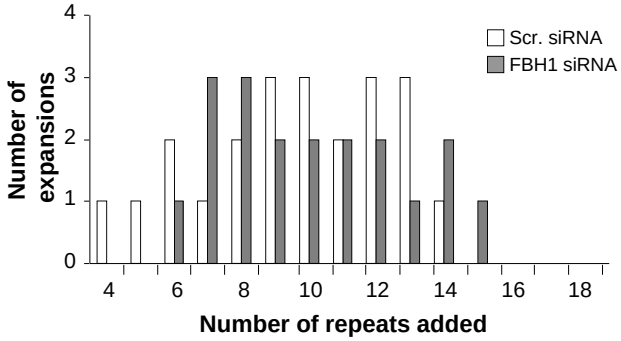

C.

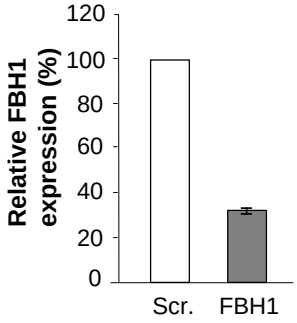

Figure 5.3 FBH1 siRNA experiments. A. Expansion frequencies following siRNA treatment against FBH1. All frequencies were normalized to scrambled siRNA. n = 3. (**P*<0.05). **B.** Expansion sizes for FBH1 siRNA. 22 genetically independent expansions for scrambled siRNA, 19 for FBH1 siRNA. **C.** Expression levels of FBH1 determined by real-time RT-PCR for FBH1 siRNA normalised to scrambled siRNA and HPRT levels. n = 3.

5.3.2 Expansions in SVG-A cells treated with siRNA against RTEL1

The Rad3-like helicase RTEL1 was identified in a screen for functional analogues of Srs2 in *C. elegans.* RTEL1 has been shown to share many phenotypes with Srs2 based on repair and recombination studies in *C. elegans* and human cell culture (Barber et al., 2008). In *C. elegans*, loss of RTEL1 resulted in an increase in meiotic recombination and elevated sensitivity to DNA-damaging agents that impede replication fork progression, which was observed in RTEL1 knockdown human cells also. siRNA knockdown of RTEL1 in HeLa cells resulted in a 4-fold increase in homologous recombination. Thus, like Srs2 in yeast, RTEL1 has antirecombinase activity. Unlike Srs2, *in vitro* studies showed that purified human RTEL1 is unable to dissociate Rad51 nucleoprotein filaments but the nature of its antirecombinase function is through disassembly of the later-stage D-loop recombination intermediates (Barber et al., 2008). Thus RTEL1 shares some but not all functions of Srs2.

Since knockdown of FBH1 did not show any expansion phenotype, it was reasoned instead that RTEL1 in SVG-A cells might fulfil a protective function against TNR expansion similar to Srs2 in yeast. To test this hypothesis, RTEL1 was knocked down using siRNA and the effect on expansion frequency was measured relative to scrambled siRNA control cells. RTEL1 siRNA-treated SVG-A cells showed a 4.6-fold elevation in expansion frequency compared to cells transfected with non-targeting siRNA ($P = 0.005$, Fig. 5.4A). This finding is suggestive of RTEL1 normally acting to prevent expansions in SVG-A cells. As was the case for FBH1, quantitation of knockdown was performed by real-time RT-PCR instead of western blotting. It has been well documented that RTEL1 expression is very low in mice and human cells thus limiting the likelihood of sufficient detection, especially in knockdown cells, by western blotting (Ding et al., 2004; Barber et al., 2008). Delivery of pooled RTEL1 siRNA to SVG-A cells decreased RTEL1 mRNA levels by 55% (± 4) indicative of rather inefficacious targeting (Fig. 5.4E). A study in HeLa cells using RTEL1 siRNA observed higher levels of knockdown as determined by real-time RT-PCR (~90%) (Barber et al., 2008). Nonetheless, the pooled RTEL1 siRNA produced a substantial expansion phenotype.

Because considerable levels of RTEL1 remained after siRNA transfection, an independent verification of the increased expansion phenotype was sought to rule out off-targeting effects. This was borne out by utilisation of an individual RTEL1 siRNA (RTEL1 siRNA #9) that was not a constituent of the pooled siRNA used above. Following treatment with RTEL1 siRNA #9, RTEL1 mRNA levels were reduced by 69% (± 13), an improvement over the pooled siRNA but with greater variability among individual measurements (Fig. 5.4E). The expansion frequency was again increased for cells with reduced expression of RTEL1 ($P = 0.008$, Fig. 5.4B). Interestingly, almost exactly the same magnitude of expansion

frequency augmentation was observed for the individual siRNA as for the pooled siRNA experiments (4.4- and 4.6-fold increases, respectively over scrambled siRNA control). This finding corroborates a role for RTEL1 in inhibiting expansions in SVG-A cells. Perhaps surprisingly, cells with approximately half of RTEL1 mRNA present exhibited the increase in expansions. Taken together with the lack of phenotypic amplification in cells with increased knockdown, it could be proposed that because RTEL1 is already low in abundance in cells, even depletion of half of the cell's supply is adequate to negate its physiological role in curtailing instability. Once this threshold level of RTEL1 expression has been reached, further depletion may be ineffective with respect to the impact on expansions. Notably, the extent of the elevation in expansion frequencies in SVG-A cells treated with RTEL1 is quite comparable to the equivalent *srs2* yeast mutant. RTEL1 siRNA knockdowns augmented expansions by ~4.5-fold, while *srs2* mutant yeast harbouring $(CTG)_{25}$ and $(CAG)_{25}$ tracts exhibited respective 4.9-fold and 10-fold increases in expansion rates (Bhattacharyya and Lahue, 2004; Daee et al., 2007). For *srs2* mutants bearing shorter $(CTG)_{13}$ tracts, more dramatic increases in expansion rates were reported, in the range of 10-40-fold over wild-type (Bhattacharyya and Lahue, 2004; Daee et al., 2007).

During analysis of the raw data for RTEL1 siRNA experiments, a consistent observation was seen whereby the number of $His^{+}Can^{R}$ colonies and total number of transformants were always lower than that of scrambled siRNA. This implies that the yield of plasmid from RTEL1 knockdown cells was lower. Although the degree of variation between the colony numbers for scrambled siRNA and RTEL1 siRNA differed between experiments, this trend was omnipresent. It is unlikely that the increased expansion phenotype can be solely attributed to discrepancies between transformant numbers because the number of canavanine-resistant colonies was typically proportionally higher for RTEL1 knockdown cells than for scrambled control cells.

Expansion sizes of CTG tracts were measured in RTEL1-deficient and scrambled siRNA cells (Fig 5.4C and D). For the RTEL1 siRNA pool experiments, the weighted average change in the size of expansion alleles was +9.8 for scrambled siRNA and +10.3 for RTEL1 siRNA. Weighted average expansion sizes for the RTEL1 siRNA #9 experiments were +9.8 for scrambled siRNA and +10.3 for RTEL1 siRNA. The overlapping mutational spectra for control and RTEL1-targeted cells infer that the incidence of expansions, rather than their size, is responsible for the hyperexpansion phenotype observed in RTEL1 siRNA-treated cells. Thus, of the proposed Srs2 human homologues tested in this study, it is RTEL1 rather than FBH1 that performs an analogous function in preventing expansions. Whether it is doing so in a similar manner to Srs2 in yeast or in a different capacity is of great interest.

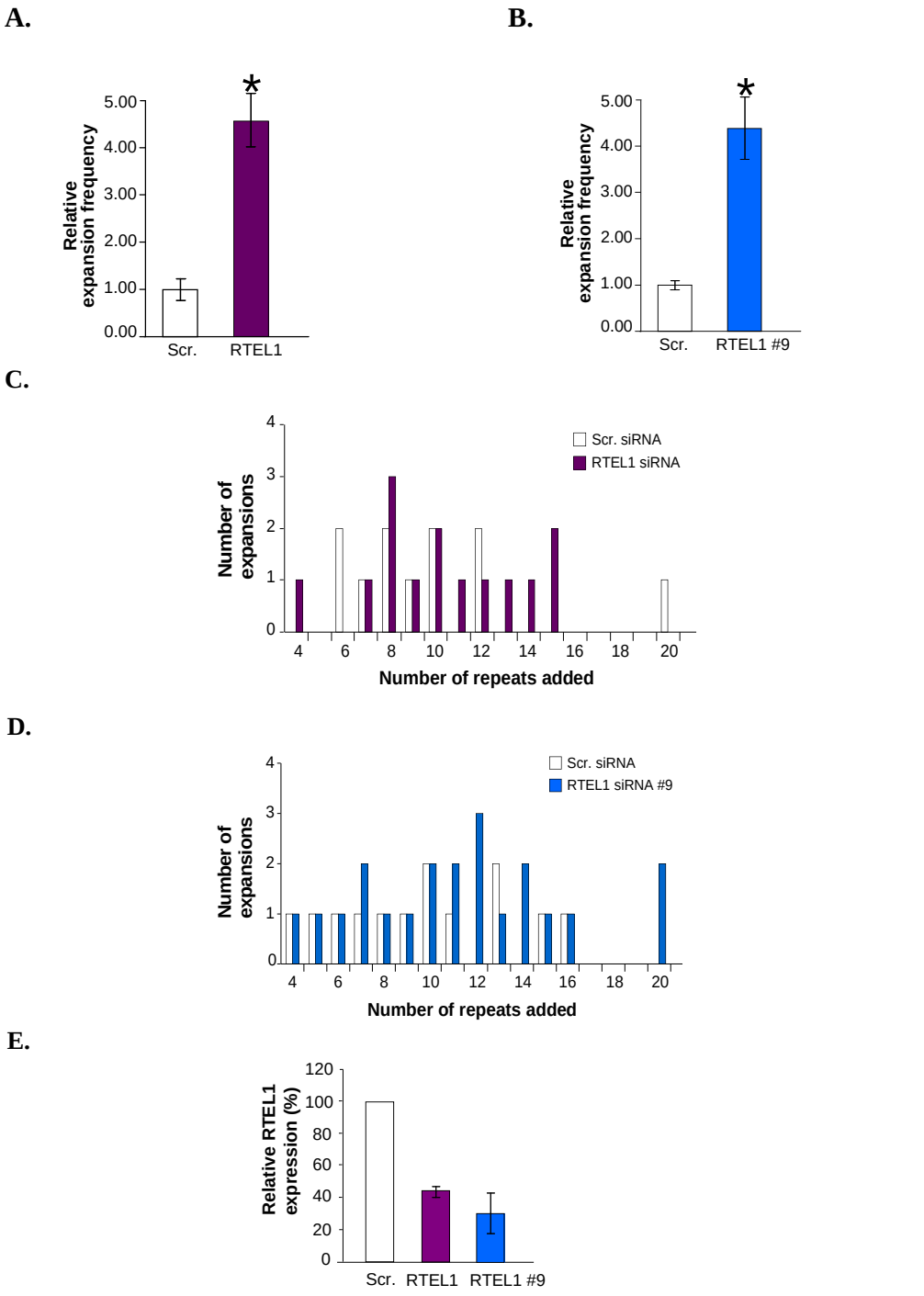

Figure 5.4 Expansions in SVG-A cells treated with siRNA against RTEL1. Expansion frequencies subsequent to treatment with **A.** RTEL1 SMARTpool siRNA n=4 and **B.** individual siRNAs denoted #9. n=3 *, $P<0.05$ compared to scrambled siRNA control. Expansion sizes for **C.** RTEL1 SMARTpool siRNA: 11 genetically independent expansions for scrambled siRNA, 14 for RTEL1 SMARTpool siRNA. and for **D.** RTEL1 siRNA #9: 13 genetically independent expansions for scrambled siRNA, 21 for RTEL1 siRNA #9 **E.** Expression levels of RTEL1 determined by real-time RT-PCR normalised to scrambled siRNA and HPRT. n= 3 for RTEL1 SMARTpool and RTEL1 siRNA #9.

5.3.3 Role of post-replication repair proteins in TNR expansions

Previous studies in yeast demonstrated that Srs2 inhibits CAG•CTG expansions together with the error-free branch of PRR (Daee et al., 2007). Expansions were elevated in *rad18*, *rad5* and *ubc13* mutants, while inhibition of the error-prone TLS polymerase Pol ζ did not affect expansions, leading the authors to suggest that error-free bypass is involved in inhibiting expansions (Collins et al., 2007; Daee et al., 2007). In light of these findings, the role of PRR in TNR expansions in human cells was evaluated specifically by knocking down RAD18 and the proposed Rad5 human homologues, HLTF and SHPRH. Human RAD18 exhibits 62% overall similarity to yeast Rad18 and has been shown to have a similar function in PRR as its yeast counterpart (Tateishi et al., 2000; Watanabe et al., 2004). Until relatively recently, no human Rad5 orthologue had been identified casting doubt over the presence of such a PRR pathway. HLTF and SHPRH, which like Rad5 are members of the SWI/SNF family of ATPases, were posited as homologues based on sequence similarity and domain structure; HLTF and SHPRH show 39% and 21% similarity to Rad5, respectively (Motegi et al., 2006; Unk et al., 2006; Motegi et al., 2008; Unk et al., 2008). Both have been shown to associate *in vivo* in HEK 293T cells with RAD18 and UBC13, and *in vitro*, HLTF and SHPRH function as ubiquitin ligases to promote PCNA polyubiquitination (Motegi et al., 2006; Unk et al., 2006; Motegi et al., 2008; Unk et al., 2008). Additionally, loss of either HLTF or SHPRH enhanced MMS-induced chromosome breaks (Motegi et al., 2006; Motegi et al., 2008). Because human cells possess these two apparent orthologs of Rad5, it was decided to investigate both of these proteins for a role in expansions to determine if they are interchangeable with regard to expansions.

RAD18 siRNA-treated cells exhibited a 5.3-fold increase in expansions compared to scrambled siRNA-treated cells (Fig. 5.5A). This data establishes a role for human RAD18 in preventing the occurrence of expansions. Because the similar phenotype observed in *rad18* yeast was attributed to the post-replicative repair function of Rad18, we can speculate that PRR might be playing an analogous role in mediating TNR stability in human cells (Daee et al., 2007). If the situation in yeast holds for human cells, then it would be expected that depletion of enzymes that promote the catalysis of PCNA polyubiquitination, such as the Rad5 homologues HLTF and/or SHPRH, would also result in an augmentation of expansions. Indeed, knockdown of HLTF resulted in a 3.1-fold increase in expansions relative to scrambled siRNA control ($P = 0.04$) (Fig. 5.5A). Interestingly, depletion of the other mammalian Rad5 homologue, SHPRH, did not have any significant impact on the frequency of expansions, with a minor decrease (30%) in expansions observed ($P = 0.5$). This implies that these proteins have non-redundant functions, which will be considered in section 5.4. The observation that HLTF seems to normally act to inhibit expansions in SVG-

A cells is in line with yeast data whereby *rad5* mutants displayed elevated expansion rates (Daee et al., 2007). Comparing the fold increases in instability in SVG-A cells depleted for PRR factors with the corresponding yeast mutants underscores commonalities with regard to the extent of the elevation in expansions. RAD18 knockdown in SVG-A cells stimulated expansions by ~3.5-5-fold (see also Fig. 5.6A), while in *rad18* yeast expansions were increased by 8-9 fold for starting tracts of $(CTG)_{13}$ and $(CAG)_{25}$ (Daee et al., 2007). Expansion rates of $(CTG)_{13}$ and $(CAG)_{25}$ in *rad5* yeast were 4-6-fold higher than wildtype, no more than twice the fold increase in expansions observed for HLTF siRNA-treated cells (Daee et al., 2007). The relative congruence between the magnitudes of expansion stimulation reported for defects in RTEL1/Srs2 and the PRR proteins in yeast and human cells might be merely coincidental, but the similarity is interesting and may reflect a high degree of conservation for the capacity of this mechanism to prevent expansions.

The sizes of the expansions in cells knocked down for PRR factors were not altered relative to those from control cells with the weighted average size change of expansion alleles determined as +10.6, +11.1, +9.5 and +11 for scrambled, RAD18, HLTF and SHPRH siRNA-treated cells, respectively (Fig. 5.5B). This situation is similar to that of yeast whereby expansion spectra of PRR mutants and wild-type cells overlapped, implying similar types of expansion events are occurring but they are of a greater frequency in mutant cells (Daee et al., 2007)

Knockdown of HLTF, SHPRH and RAD18 was confirmed by western blotting (Fig. 5.5C). Following treatment with the cognate siRNA, efficient levels of knockdown were achieved with HLTF, SHPRH and RAD18 protein levels being depleted by 87% (± 5), 75% (± 5) and 86% (± 9) respectively (Fig. 5.5D). Silencing of each protein only occurred in cells transfected with siRNA directed against the corresponding protein verifying that siRNA treatments were specific (Fig. 5.5C and 5.5D). The possibility that remaining levels of SHPRH present after siRNA treatment are adequate to mask expansion phenotype cannot be eliminated. A visually comparable level of SHPRH depletion was sufficient to reduce polyubiquitination in SW480 cells following MMS treatment (Motegi et al., 2008), suggesting it is unlikely that the absence of an expansion phenotype in our system is attributable to residual levels of expression following siRNA knockdown.

A.

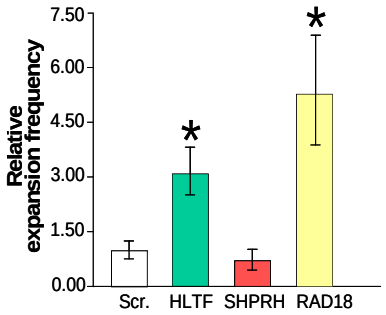

B.

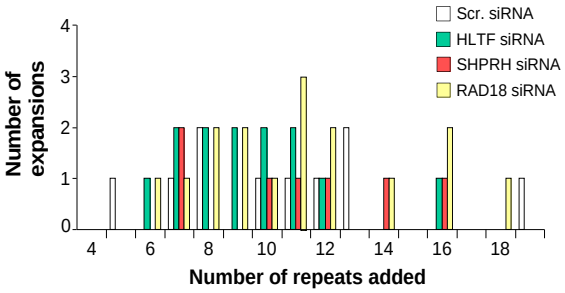

C.

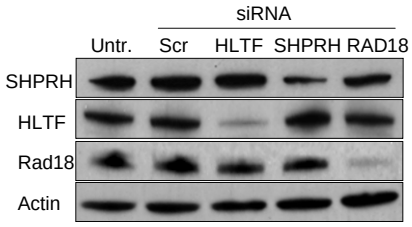

D.

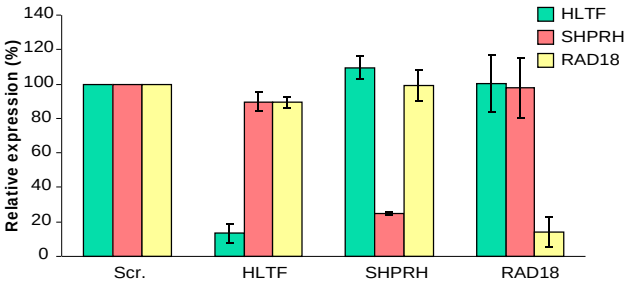

Figure 5.5 Effect of HLTF, SHPRH and RAD18 siRNA on TNR expansions.
A. Expansion frequencies for SVG-A cells treated with HLTF, SHPRH and RAD18 siRNA n=4, except SHPRH siRNA (n= 3) *, $P<0.05$ compared to scrambled siRNA control, for SHPRH siRNA performed T-Test using the corresponding 3 scrambled siRNA control values. **B.** Expansion sizes for HLTF, SHPRH and RAD18 siRNA, 10 genetically independent expansions for scrambled siRNA, 13 for HLTF siRNA, 7 for SHPRH and 16 for RAD18. **C.** Representative western blots showing expression of HLTF, SHPRH and RAD18 following siRNA transfection. **D.** Expression levels of HLTF, SHPRH and RAD18 normalized to β-actin and to scrambled siRNA. n=3. Error bars denote ± one SEM.

5.3.4 Double knockdowns of RTEL1 and PRR factors

The observation that RTEL1 and the PRR factors, HLTF and RAD18, appear to have functions in maintaining TNR stability in SVG-A cells is reminiscent of the situation in yeast whereby Srs2 and the error-free branch of PRR act together to prevent expansions. Further encouraged by the similar level of expansion frequency augmentation observed when RTEL1 and the PRR factors were knocked down, this prompted us to investigate if a similar mechanism is involved in preventing TNR expansions in human cells (Bhattacharyya and Lahue, 2004; Daee et al., 2007). To this end, double knockdowns of RTEL1 in combination with HLTF or RAD18 were performed and the effect on expansion frequency determined. The rationale behind this approach is derived from the prediction that if RTEL1 and PRR act in the same pathway to protect against TNR expansions, then one would expect a similar magnitude of change in expansion frequencies following either single or double knockdowns of the relevant factors. Because a potential involvement of SHPRH in expansions had been ruled out (section 5.3.3), this protein was eliminated from the investigation.

Single knockdowns of RTEL1, HLTF and RAD18 were performed simultaneously alongside the aforementioned double knockdowns. Similarly to the previous experiments, expansion frequencies were elevated 3.5-4.4 when the factors were knocked down individually, all being significantly different than that of scrambled siRNA (P = 0.01-0.002) (Fig. 5.6A). Depletion of RTEL1 (using pooled siRNA) in combination with HLTF or RAD18 resulted in 6.1- and 5.8-fold increases in the frequency of expansions, respectively. While this observed augmentation in expansion frequency was significantly different than for scrambled siRNA-treated cells (P = 0.02 for RTEL1+HLTF siRNA and 0.03 for RTEL1+RAD18 siRNA), there was no significant difference between the individual siRNA and double siRNA experiments. Specifically, P values for RTEL1+HLTF siRNA versus RTEL1 siRNA and HLTF siRNA were 0.28 and 0.21, respectively, while for RTEL1+RAD18 siRNA compared with RTEL1 siRNA and RAD18 siRNA, P values were 0.41 and 0.19, respectively. This observation indicates that RTEL1 is acting in the same pathway as HLTF and RAD18 to prevent expansions, although additive effects cannot be completely excluded.

Measurement of expansion sizes revealed largely overlapping mutation spectra among the different siRNA treatment regimes (Fig. 5.6B). Curiously, for RAD18 siRNA-treated cells, the average weighted increase in expansion size was +8.9 compared with +13.8 for scrambled siRNA (Table 5.1). However, when the size data was combined with that from the corresponding original single siRNA knockdown experiments (sections 5.5.2. and

5.3.3.), these values shifted to +10 and +10.1 respectively, suggesting the dual action of RTEL1 and PRR in preventing expansions is not effected through size changes. The overlapping expansion spectra for all single and double knockdown combinations are consistent with RTEL1, HLTF and RAD18 working in a common pathway.

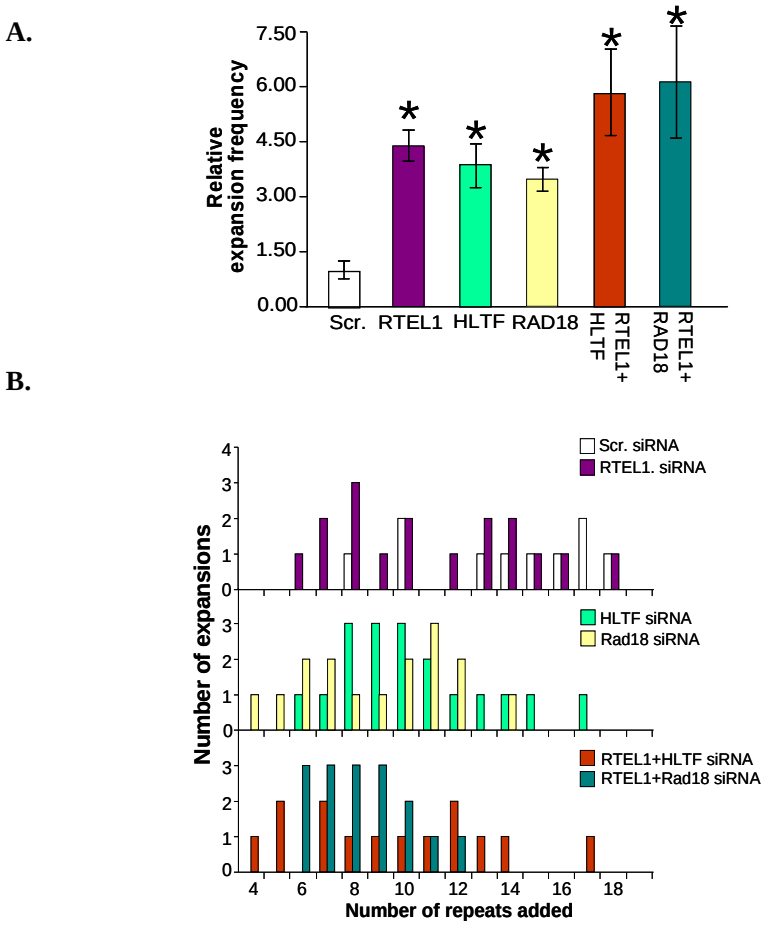

Figure 5.6 Expansion data following double knockdowns of RTEL1 with HLTF or RAD18. A. Expansion frequencies following single or combinatorial siRNA treatment against RTEL1, HLTF and RAD18. All frequencies were normalized to scrambled siRNA. n = 3. (**P*<0.05) Error bars denote ± one SEM. **B.** Expansion sizes for siRNA treatments; 10 genetically independent expansions for scrambled siRNA, 17 for RTEL1 siRNA, 18 for HLTF siRNA, 16 for RAD18 siRNA, 14 for RTEL1+HLTF siRNA.

Table 5.1 Expansion sizes from double RTEL1/PRR siRNA experiments

Treatment	N	Range	Weighted average expansion size
Scr. siRNA	10	+8 to +18	+13.8
RTEL1 siRNA	17	+6 to +18	+11
HLTF siRNA	18	+6 to +17	+10.4
RAD18 siRNA	16	+4 to +14	+8.9
RTEL1+HLTF siRNA	14	+4 to +17	+9.6
RTEL1+RAD18 siRNA	16	+6 to +12	+8.3

Western blotting was performed to confirm successful knockdown of HLTF and RAD18 and to determine any potential cross-reactivity of siRNAs (Fig. 5.7A). HLTF protein levels were decreased by 85% (± 3) and 84% (± 3), for single and combinatorial knockdowns, respectively. RAD18 was also robustly knocked down when treated with RAD18 siRNA alone (84% ± 4) or simultaneously with RTEL1 siRNA (81% ± 3) (Fig. 5.7B). Measurement of RTEL1 knockdown was performed by real-time RT-PCR. RTEL1 mRNA levels were reduced by 56% (± 7), 71% (± 10) and 59% (± 7), following treatment with RTEL1 siRNA, RTEL1+HLTF siRNA and RTEL1+RAD18 siRNA (Fig. 5.7C).

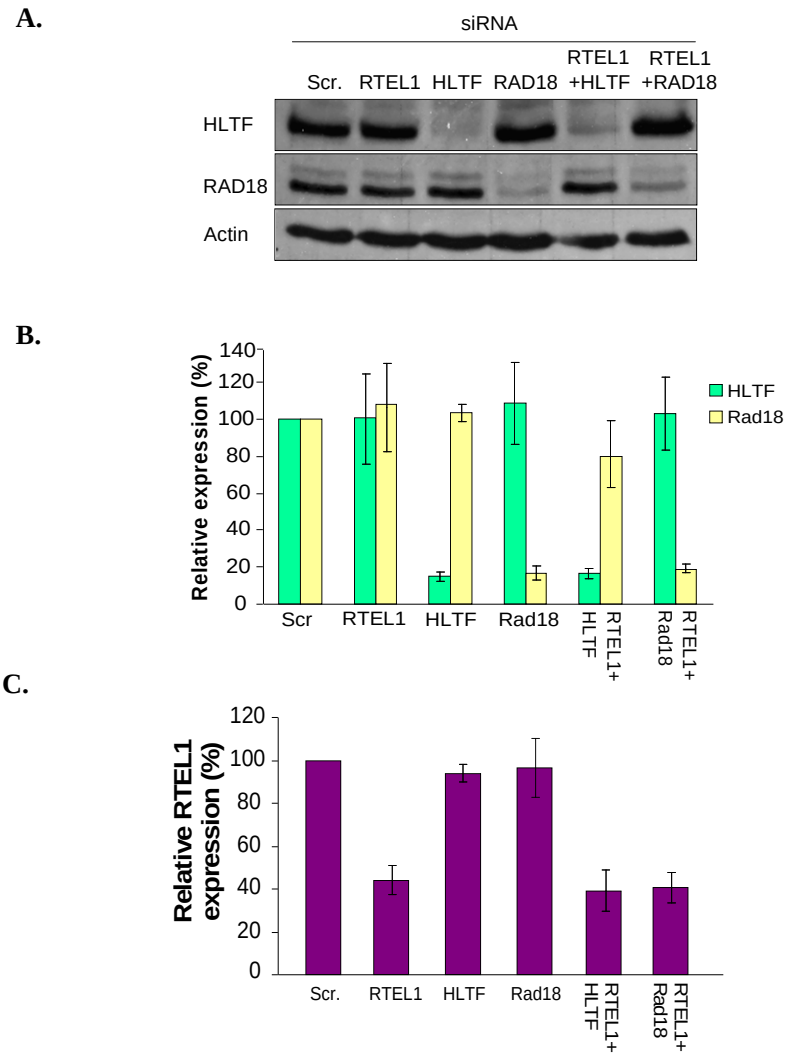

Figure 5.7 Knockdown analysis of RTEL1, HLTF and RAD18. A. Representative western blot of WCEs from cells treated with single or combinatorial siRNA treatment against RTEL1, HLTF and RAD18. **B.** Expression levels of HLTF, SHPRH and RAD18 normalized to Actin and to scrambled siRNA determined by western blotting analysis. n=3. **C.** Expression levels of RTEL1 determined by real-time RT-PCR following single or combinatorial siRNA treatment against RTEL1, HLTF and RAD18 siRNA normalised to scrambled siRNA and HPRT levels. n = 3 for all except HLTF siRNA (n = 2) Error bars denote ± one SEM.

5.3.5 Effect of FEN1 depletion on TNR expansions in SVG-A cells

Given the variable findings for different organisms regarding a role for FEN1 in TNR expansions, further investigations were deemed important to clarify its involvement. Accordingly, SVG-A cells were treated with FEN1 siRNA and expansion frequencies were measured thereafter. This loss of FEN1 did not exert any significant effect on expansion frequency compared with that of scrambled siRNA-treated cells ($P = 0.76$, Fig. 5.8A). This indicates that FEN1 is not a relevant modulator of expansions under these conditions.

*rad27*Δ yeast strains have been reported to accumulate extremely large expansions. One study observed that almost half of all expansions of CTG, CAG, GAC (structure-prone) and CTA (structure-incapable) had at least doubled in size from an original starting length of 25 repeats (Spiro and McMurray, 2003). A similar occurrence was found for *rad27*Δ yeast bearing $(CAG)_{70}$ tracts (Callahan et al., 2003). Therefore, one possibility is that knockdown of FEN1 in SVG-A cells would induce an increase in the sizes of some of the expansions but not affect the frequency with which these expansion events occur. However, analysis of CTG expansion sizes did not show any discernible differences in the expansion spectra for FEN1 knockdown cells and scrambled siRNA-treated cells (Fig. 5.8B). The weighted average increase in expansion sizes were determined to be +11.3 and +10.7, for scrambled siRNA and FEN1, respectively. Taken together with the lack of effect of FEN1 knockdown on the frequency of expansions, this data implies that FEN1 does not impact on expansions in this system.

Transfection of SVG-A cells with FEN1 siRNA reduced FEN1 protein levels by 80% (± 0.8%) compared with scrambled siRNA-treated cells as determined by western blotting (Fig. 5.8C and D). The possibility that residual levels of FEN1 can repress repeat expansions efficiently cannot be ruled out but seems unlikely based on the sensitivity of other FEN1-dependent processes to reduced levels e.g. removal of mitochondrial oxidative DNA damage by long-patch BER in HeLa cells was impaired when FEN1 levels were reduced to 15% (Liu et al., 2008). Furthermore, knockdown of FEN1 in glioblastoma cells by ~75% increased sensitivity to methylating agents and to cisplatin (Nikolova et al., 2009). Extrapolating from these examples, if FEN1 had an effect on expansions in our experiments, it is reasonable to suggest that 80% knockdown would have revealed it.

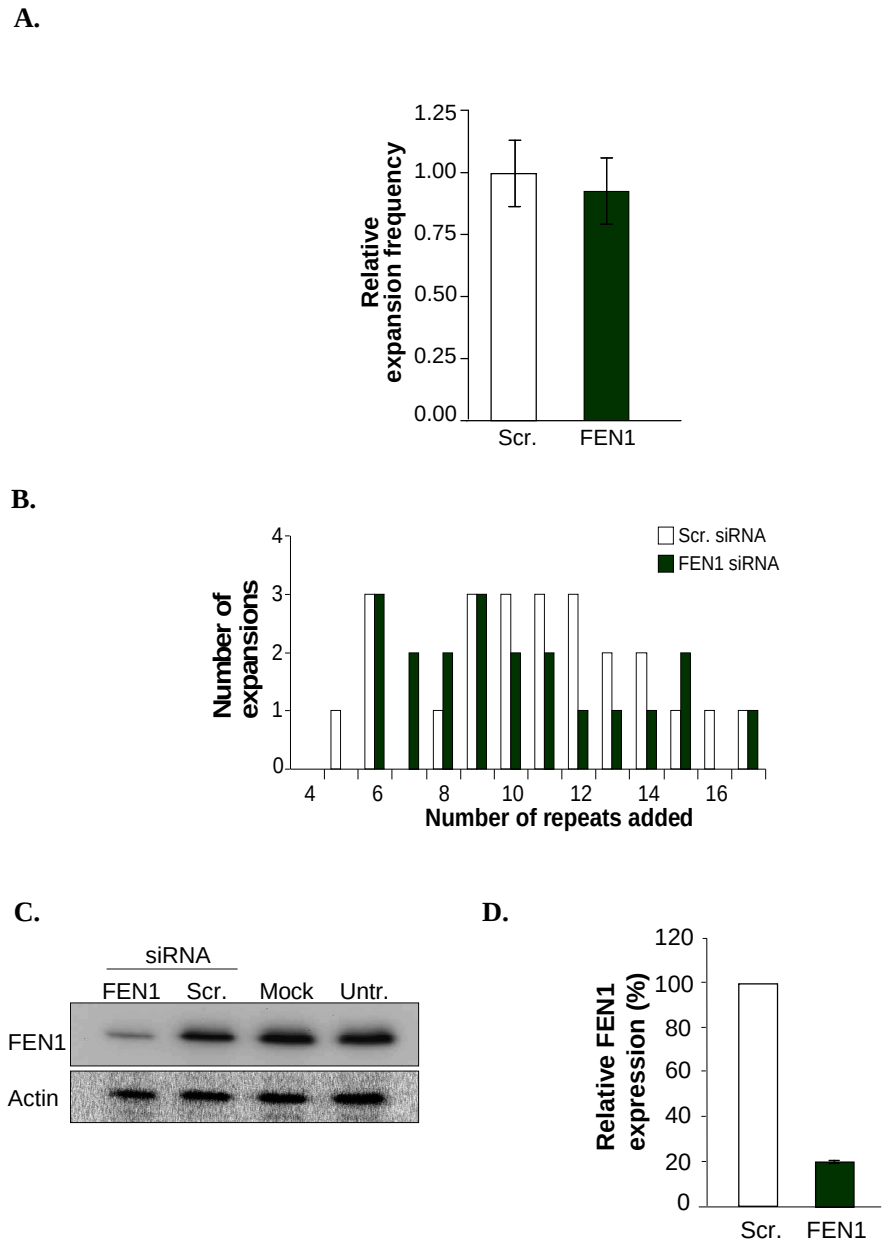

Figure 5.8. Effect of siRNA depletion of FEN1 on TNR expansions in SVG-A cells A. Expansion frequency of FEN1 siRNA-treated cells relative to scrambled siRNA control. n = 3. (**P*<0.05). **B.** Expansion sizes for FEN1 siRNA: 23 genetically independent expansions for scrambled siRNA, 19 for FEN1 siRNA. **C.** Representative western blot of FEN1. Actin was used as a loading control. **D.** Expression levels of FEN1 normalized to Actin and to scrambled siRNA. n=3. Error bars denote ± one SEM

5.4 Discussion

A novel finding derived from this investigation is the identification of a role for RTEL1 in inhibiting TNR expansions in human cells, implying that it acts as a functional analogue of Srs2 with regard to its role in preventing expansions. Furthermore, members of the PRR pathway namely RAD18 and HLTF were also shown to be involved in inhibiting the occurrence of expansions. Support for PRR mechanisms being responsive to spontaneous mutations, such as replication stresses owing to the repetitive nature of TNRs, in addition to induced damage such as UV exposure, comes from the observation that yeast deficient in *POL32*, the non-essential subunit of Polδ, exhibit increased PCNA mono- and polyubiquitination (Karras and Jentsch, 2010). The involvement of HLTF in inhibition of expansions in SVG-A cells suggests that error-free PRR is mediating repeat stability similarly to the situation in yeast. Combinatorial knockdown of RTEL1 with the aforementioned PRR factors inferred that they are working in the same pathway to limit TNR expansions. This work indicates a similar involvement of RTEL1 acting with PRR to assuage expansions in line with observations in yeast cells (Daee et al., 2007). That this conservation of action to stabilise repeats holds between yeast and human cells further consolidates support for a novel protective mechanism acting to resolve mutagenic hairpin intermediates. The results presented in this study exclude a role for FEN1 involvement in TNR expansions in human cells.

Daee et al., 2007 put forward a model to describe a protective mechanism involving PRR and Srs2 to restrain replication-mediated TNR expansions arising from the 3' end of Okazaki fragments. The model envisages that DNA synthesis through the repeat tract results in fork stalling and/or hairpin formation, which directs recruitment of Srs2 and the PRR proteins in order to overcome this replicative stress in a manner dependent on PCNA mono- and polyubiquitination. In addition, Srs2 was posited to mediate the instability by unwinding the hairpin intermediate, likely by recruitment through modification of PCNA (Bhattacharyya and Lahue, 2005; Dhar and Lahue, 2008). Extrapolating from this model seems to be quite reasonable as the basic elements appear to be conserved between yeast and SVG-A cells. It can be postulated that mono-and polyubiquitination of PCNA mediated by RAD18 and HLTF, directs RTEL1 to the hairpin, where it unwinds the TNR substrate. In support of this, very recent data from our colloborators suggests that RTEL1 can unwind TNR hairpin substrates that Srs2 also resolved (Mark Petalcorin and Simon Boulton, personal communication).

Another potential mode of action is through error-free resolution of the TNR replication stress by HLTF. HLTF, like Rad5, has been shown to mediate fork reversal of model stalled

replication fork substrates through unwinding of the leading and lagging strands of the fork followed by annealing of the nascent and parental strands forming a cruciform intermediate, called the "chicken-foot" structure (Blastyak et al., 2007; Blastyak et al., 2010). This raises the possibility that replication fork reversal by HLTF could provide a means for stabilizing TNR tracts. In this case, RTEL1 might somehow be acting to direct correct maintenance of the TNR tract through PRR action. The role played by RTEL1 here is unclear; it might be the case that it acts like Srs2 to direct damaged replication intermediates (in this case, stalled replication fork and/or hairpin formation) from recombination pathways towards PRR. If this were the case, then it is likely that the expansions arising in the absence of RTEL1, RAD18 and HLTF are derived from aberrant recombination. However, RTEL1 has been shown to antagonize recombination at a later stage than Srs2 (Barber et al., 2008), with no evidence that it directs PRR. Furthermore, genetic evidence indicated that most of the inhibitory action for expansions of Srs2 was independent of its role in homologous recombination (Bhattacharyya and Lahue, 2004). Alternatively, RTEL1 could act to directly recruit HLTF to the TNR. Further investigations are warranted to decipher the precise roles of the respective proteins in preventing expansions. Although in light of the biochemical unwinding data, it seems more likely that RTEL1 is directed to the TNR region by action of the PRR pathway. Future efforts to address the mode of action are discussed in Chapter 6.

Intriguingly, knockdown of HLTF resulted in an increase in expansions, while depletion of SHPRH did not impact on the expansion phenotype indicative of a non-redundant function of these proteins in maintaining TNR stability. The presence of two apparent orthologues of Rad5 in humans has been investigated with respect to ubiquitination functions. PCNA polyubiquitination has been shown to be mediated by either SHPRH or HLTF *in vitro* (Unk et al., 2006; Unk et al., 2008). Overexpression of either protein elevates PCNA polyubiquitination *in vivo* (Unk et al., 2006; Unk et al., 2008). Although these observations imply redundancy between these proteins, mounting evidence suggests they cannot compensate for each other for certain functions. SHPRH and HLTF have been shown to mediate specific responses by promoting recruitment of various TLS polymerases to stalled replication forks depending on the type of induced DNA damage: HLTF favours recruitment of Polη following UV damage by acting with RAD18 to monoubiquitinate PCNA (a previously unknown function of HLTF) and inhibiting SHPRH, while SHPRH promotes Polκ recruitment after MMS-induced damage perhaps by PCNA polyubiquitination or through a direct interaction with Polκ (Lin et al., 2011). A similar damage-specific response mechanism might be at play for the case of the spontaneous damage elicited by TNRs. Perhaps HLTF primarily deals with the replication-impairing hairpins and/or polymerase

stalling proposed to arise during replication at TNR tracts, whereas SHPRH is required for different forms of damage. The possibility that residual levels of SHPRH following knockdown could be adequate to contribute to a role in promoting TNR stability cannot be ruled out. Interestingly, it has been demonstrated that mouse cells lacking these two enzymes do not exhibit major defects in polyubiquitination of PCNA inferring the presence of other unidentified E3 ligases acting on PCNA (Krijger et al., 2011). Whether ubiquitination of PCNA is important for the concerted action of RTEL1 and PRR factors in preventing expansions is unknown, but rather assumed based on yeast data and the observation that RAD18 and HLTF knockdown results in increased expansions (Daee et al., 2007). Western blotting is used to monitor polyubiquitination of PCNA and by its nature, is quite a crude and nondiscriminate method; it might be the case that HLTF and SHPRH generate different polyubiquitin chains and these disparities elicit different functions (Chang and Cimprich, 2009). Perhaps, PCNA polyubiquitination by HLTF is required for mediating TNR stability, while the modifications produced by SHPRH do not elicit a similar response. HLTF, like RAD18, is capable of promoting monoubiquitination of PCNA, whereas SHPRH cannot (Lin et al., 2011). PCNA monoubiquitination might be the relevant modification involved in preventing TNR expansions.

The hyperrecombination phenotypes observed in RTEL1-deficient cells in other studies confirms its role as an antirecombinase. This raises the possibility that homologous recombination might be the cause of the increase in TNR expansions in RTEL1 knockdown cells. In yeast, sumoylation of PCNA at K164 enhances the recruitment of Srs2 to stalled replication forks presumably to eliminate Rad51 nucleofilaments, thereby channelling damaged replication intermediates away from a recombination pathway and towards PRR (Papouli et al., 2005; Pfander et al., 2005). In yeast, *srs2Δ rad51Δ* and *srs2Δ rad52Δ* double mutants still exhibited much of the instability of the single *srs2Δ* mutant indicating that erroneous recombination in the absence of Srs2 is not responsible for the phenotype (Bhattacharyya and Lahue, 2004). Contrastingly, another group which performed a similar analysis using longer repeat tracts $(CAG•CTG)_{55/70}$ reported that *srs2Δ rad51Δ* and *srs2Δ rad52Δ* double mutants had expansion frequencies comparable to wild-type cells suggesting that the expansions in *srs2Δ* single mutants were mediated largely by Rad51-induced recombination (Kerrest et al., 2009). The authors propose that the HR-mediated expansions that occur in *srs2Δ* yeast only arise when the repeat reaches a certain length, likely pertaining to the TNR tract's ability to undergo breakage in a length-dependent manner (Napierala et al., 2002; Callahan et al., 2003). Corresponding analysis has not been performed in the SVG-A cells to determine if aberrant homologous recombination is contributing to expansions near the threshold when RTEL1 levels are depleted.

Of the PRR proteins tested in this study, a role for RAD18 in homologous recombination has been demonstrated. RAD18 is recruited to IR-induced DSBs through its zinc finger domain by UBC13 (also involved in PRR) and the E3 ligase RNF8, where it interacts with the recombinase RAD51C to elicit homologous recombination (Huang et al., 2009). This participation in HR is thought to be independent of the contribution of RAD18 to PRR as PCNA mono-ubiquitination is not required for its role in HR (Huang et al., 2009). It is unlikely that the increased expansion phenotype observed in RAD18-depleted SVG-A cells is attributable to DSB repair impairment as the incidence of DSB breaks for the short repeat alleles utilised in this study is expected to be infrequent in the absence of exogenous damaging agents, although a role for recombination has not been directly assessed. siRNA knockdown of HLTF and SHPRH did not result in any increases in DSB-induced HR frequency using a recombination reporter assay implying that they are not involved in HR (Motegi et al., 2008). Taken in combination with the finding that SVG-A cells with reduced levels of RAD18 and HLTF had similar expansion phenotypes, it is likely that the mode of action of these proteins in mediating TNR stability is through the same pathway i.e. PRR rather than HR.

Two studies from the same group examined the role of Rad5 in modulating expansions of longer repeat tracts specifically GAA_{100} repeats and the SCA10 pentanucleotide tract $ATTCT_{81/132}$ (Shishkin et al., 2009; Cherng et al., 2011). Both studies found that *rad5* mutants had decreased levels of expansions, in contrast to the elevated expansion phenotype observed for CTG repeats near the threshold in *rad5* mutants and in HLTF-depleted SVG-A cells. A possible explanation for these disparities is that Rad5 plays differential roles in modulating expansions depending on length of the repeat tract. Longer tracts may engage Rad5 to promote expansions, whereas shorter tracts may employ a separate Rad5 mechanism to prevent their expansion. Alternatively, although not mutually exclusive to the length dependence scenario, the different structural features of the three repeat sequences might dictate whether Rad5 is utilised to promote or inhibit expansion (Shishkin et al., 2009). Of note, for all three yeast studies, contractions were unaffected by a non-functional Rad5 gene implying strong expansion-specificity. It would be interesting to determine the effect of HLTF knockdown of different repeat sequences and lengths to ascertain if the outcome of HLTF activity in modulating instability depends on length and/or sequence.

The data presented here suggests that FEN1 does not play a role in inhibiting expansions at the threshold in SVG-A cells. Given the importance of this protein in preventing expansions in other systems, it is worth considering why it is not implicated. One possible trivial

explanation for the apparent contradictory effect of FEN1 in this system and in yeast is the potential for the remaining FEN1 expression after siRNA treatment to be sufficient for hairpin removal. FEN1 levels were reduced to ~20% following siRNA. In yeast haploinsufficient for Rad27, CAG• CTG repeats do not undergo instability when the tract length is 70, while $(CAG)_{155}$ tracts exhibit significantly increased expansions suggesting that shorter alleles require less FEN1 for preventing expansion than longer tracts (Yang and Freudenreich, 2007). Directly extrapolating from this observation, perhaps the residual FEN1 expression following siRNA treatment can mediate adequate endonuclease activity to maintain stability of $(CTG)_{22}$ repeats. This would also provide an explanation for why no instability was observed in a cell line with short CAG repeats (13-27 repeats) at the HD locus, whereby FEN1 expression was reduced by 10-fold (Moe et al., 2008). Another possible reason for the absence of a phenotype in the SVG-A experiments and other studies in mice and humans is the prospect that there might exist compensatory activities that prevent the exacerbation of expansions in the absence of FEN1. It may be the case that loss of FEN1 alone might not contribute to expansions due to potential redundant pathways in preservation of TNR stability, but combined with loss of some other factors may invoke expansions in higher organisms (Zheng et al., 2011). Evidence for such a scenario comes from the observation that mice heterozygous for FEN1 did not display altered dinucleotide instability but when combined with a mutation in the adenomatous polyposis coli (APC) gene, exhibited increased instability (Kucherlapati et al., 2002).

The major finding identified through this work is the presence of a similar protective mechanism against expansions for yeast and humans. The precise mechanism underlying the concerted action of RTEL1 and PRR in preventing expansions will be an interesting future prospect.

5.5 References

Barber, L. J., J. L. Youds, J. D. Ward, M. J. McIlwraith, N. J. O'Neil, M. I. Petalcorin, J. S. Martin, S. J. Collis, S. B. Cantor, M. Auclair, H. Tissenbaum, S. C. West, A. M. Rose and S. J. Boulton (2008). RTEL1 maintains genomic stability by suppressing homologous recombination. *Cell* **135**(2): 261-71.

Bhattacharyya, S. and R. S. Lahue (2004). Saccharomyces cerevisiae Srs2 DNA helicase selectively blocks expansions of trinucleotide repeats. *Mol Cell Biol* **24**(17): 7324-30.

Bhattacharyya, S. and R. S. Lahue (2005). Srs2 helicase of Saccharomyces cerevisiae selectively unwinds triplet repeat DNA. *J Biol Chem* **280**(39): 33311-7.

Blastyak, A., I. Hajdu, I. Unk and L. Haracska (2010). Role of double-stranded DNA translocase activity of human HLTF in replication of damaged DNA. *Mol Cell Biol* **30**(3): 684-93.

Blastyak, A., L. Pinter, I. Unk, L. Prakash, S. Prakash and L. Haracska (2007). Yeast Rad5 protein required for postreplication repair has a DNA helicase activity specific for replication fork regression. *Mol Cell* **28**(1): 167-75.

Callahan, J. L., K. J. Andrews, V. A. Zakian and C. H. Freudenreich (2003). Mutations in yeast replication proteins that increase CAG/CTG expansions also increase repeat fragility. *Mol Cell Biol* **23**(21): 7849-60.

Chang, D. J. and K. A. Cimprich (2009). DNA damage tolerance: when it's OK to make mistakes. *Nat Chem Biol* **5**(2): 82-90.

Cherng, N., A. A. Shishkin, L. I. Schlager, R. H. Tuck, L. Sloan, R. Matera, P. S. Sarkar, T. Ashizawa, C. H. Freudenreich and S. M. Mirkin (2011). Expansions, contractions, and fragility of the spinocerebellar ataxia type 10 pentanucleotide repeat in yeast. *Proc Natl Acad Sci U S A* **108**(7): 2843-8.

Chiolo, I., M. Saponaro, A. Baryshnikova, J. H. Kim, Y. S. Seo and G. Liberi (2007). The human F-Box DNA helicase FBH1 faces Saccharomyces cerevisiae Srs2 and postreplication repair pathway roles. *Mol Cell Biol* **27**(21): 7439-50.

Claassen, D. A. (2009). Advances in the in vitro study of Huntington's disease mutagenesis and pathogenesis. (University of Nebraska Medical Center): Ref Type: Thesis/Dissertation.

Collins, N. S., S. Bhattacharyya and R. S. Lahue (2007). Rev1 enhances CAG.CTG repeat stability in Saccharomyces cerevisiae. *DNA Repair (Amst)* **6**(1): 38-44.

Daee, D. L., T. Mertz and R. S. Lahue (2007). Postreplication repair inhibits CAG.CTG repeat expansions in Saccharomyces cerevisiae. *Mol Cell Biol* **27**(1): 102-10.

Dhar, A. and R. S. Lahue (2008). Rapid unwinding of triplet repeat hairpins by Srs2 helicase of Saccharomyces cerevisiae. *Nucleic Acids Res* **36**(10): 3366-73.

Ding, H., M. Schertzer, X. Wu, M. Gertsenstein, S. Selig, M. Kammori, R. Pourvali, S. Poon, I. Vulto, E. Chavez, P. P. Tam, A. Nagy and P. M. Lansdorp (2004). Regulation of murine telomere length by Rtel: an essential gene encoding a helicase-like protein. *Cell* **117**(7): 873-86.

Entezam, A., A. R. Lokanga, W. Le, G. Hoffman and K. Usdin (2010). Potassium bromate, a potent DNA oxidizing agent, exacerbates germline repeat expansion in a fragile X premutation mouse model. *Hum Mutat* **31**(5): 611-6.

Freudenreich, C. H., S. M. Kantrow and V. A. Zakian (1998). Expansion and length-dependent fragility of CTG repeats in yeast. *Science* **279**(5352): 853-6.

Fugger, K., M. Mistrik, J. R. Danielsen, C. Dinant, J. Falck, J. Bartek, J. Lukas and N. Mailand (2009). Human Fbh1 helicase contributes to genome maintenance via pro- and anti-recombinase activities. *J Cell Biol* **186**(5): 655-63.

Gordenin, D. A., T. A. Kunkel and M. A. Resnick (1997). Repeat expansion--all in a flap? *Nat Genet* **16**(2): 116-8.

Henricksen, L. A., S. Tom, Y. Liu and R. A. Bambara (2000). Inhibition of flap endonuclease 1 by flap secondary structure and relevance to repeat sequence expansion. *J Biol Chem* **275**(22): 16420-7.

Huang, J., M. S. Huen, H. Kim, C. C. Leung, J. N. Glover, X. Yu and J. Chen (2009). RAD18 transmits DNA damage signalling to elicit homologous recombination repair. *Nat Cell Biol* **11**(5): 592-603.

Karras, G. I. and S. Jentsch (2010). The RAD6 DNA damage tolerance pathway operates uncoupled from the replication fork and is functional beyond S phase. *Cell* **141**(2): 255-67.

Kerrest, A., R. P. Anand, R. Sundararajan, R. Bermejo, G. Liberi, B. Dujon, C. H. Freudenreich and G. F. Richard (2009). SRS2 and SGS1 prevent chromosomal breaks and stabilize triplet repeats by restraining recombination. *Nat Struct Mol Biol* **16**(2): 159-67.

Kohzaki, M., A. Hatanaka, E. Sonoda, M. Yamazoe, K. Kikuchi, N. Vu Trung, D. Szuts, J. E. Sale, H. Shinagawa, M. Watanabe and S. Takeda (2007). Cooperative roles of vertebrate Fbh1 and Blm DNA helicases in avoidance of crossovers during recombination initiated by replication fork collapse. *Mol Cell Biol* **27**(8): 2812-20.

Krijger, P. H., K. Y. Lee, N. Wit, P. C. van den Berk, X. Wu, H. P. Roest, A. Maas, H. Ding, J. H. Hoeijmakers, K. Myung and H. Jacobs (2011). HLTF and SHPRH are not essential for PCNA polyubiquitination, survival and somatic hypermutation: existence of an alternative E3 ligase. *DNA Repair (Amst)* **10**(4): 438-44.

Kucherlapati, M., K. Yang, M. Kuraguchi, J. Zhao, M. Lia, J. Heyer, M. F. Kane, K. Fan, R. Russell, A. M. Brown, B. Kneitz, W. Edelmann, R. D. Kolodner, M. Lipkin and R. Kucherlapati (2002). Haploinsufficiency of Flap endonuclease (Fen1) leads to rapid tumor progression. *Proc Natl Acad Sci U S A* **99**(15): 9924-9.

Laulier, C., A. Cheng, N. Huang and J. M. Stark (2010). Mammalian Fbh1 is important to restore normal mitotic progression following decatenation stress. *DNA Repair (Amst)* **9**(6): 708-17.

Lin, J. R., M. K. Zeman, J. Y. Chen, M. C. Yee and K. A. Cimprich (2011). SHPRH and HLTF act in a damage-specific manner to coordinate different forms of postreplication repair and prevent mutagenesis. *Mol Cell* **42**(2): 237-49.

Liu, P., L. Qian, J. S. Sung, N. C. de Souza-Pinto, L. Zheng, D. F. Bogenhagen, V. A. Bohr, D. M. Wilson, 3rd, B. Shen and B. Demple (2008). Removal of oxidative DNA damage via FEN1-dependent long-patch base excision repair in human cell mitochondria. *Mol Cell Biol* **28**(16): 4975-87.

Liu, Y. and R. A. Bambara (2003). Analysis of human flap endonuclease 1 mutants reveals a mechanism to prevent triplet repeat expansion. *J Biol Chem* **278**(16): 13728-39.

Liu, Y., H. Zhang, J. Veeraraghavan, R. A. Bambara and C. H. Freudenreich (2004). Saccharomyces cerevisiae flap endonuclease 1 uses flap equilibration to maintain triplet repeat stability. *Mol Cell Biol* **24**(9): 4049-64.

Moe, S. E., J. G. Sorbo and T. Holen (2008). Huntingtin triplet-repeat locus is stable under long-term Fen1 knockdown in human cells. *J Neurosci Methods* **171**(2): 233-8.

Motegi, A., H. J. Liaw, K. Y. Lee, H. P. Roest, A. Maas, X. Wu, H. Moinova, S. D. Markowitz, H. Ding, J. H. Hoeijmakers and K. Myung (2008). Polyubiquitination of proliferating cell nuclear antigen by HLTF and SHPRH prevents genomic instability from stalled replication forks. *Proc Natl Acad Sci U S A* **105**(34): 12411-6.

Motegi, A., R. Sood, H. Moinova, S. D. Markowitz, P. P. Liu and K. Myung (2006). Human SHPRH suppresses genomic instability through proliferating cell nuclear antigen polyubiquitination. *J Cell Biol* **175**(5): 703-8.

Napierala, M., P. Parniewski, A. Pluciennik and R. D. Wells (2002). Long CTG.CAG repeat sequences markedly stimulate intramolecular recombination. *J Biol Chem* **277**(37): 34087-100.

Nikolova, T., M. Christmann and B. Kaina (2009). FEN1 is overexpressed in testis, lung and brain tumors. *Anticancer Res* **29**(7): 2453-9.

Papouli, E., S. Chen, A. A. Davies, D. Huttner, L. Krejci, P. Sung and H. D. Ulrich (2005). Crosstalk between SUMO and ubiquitin on PCNA is mediated by recruitment of the helicase Srs2p. *Mol Cell* **19**(1): 123-33.

Pfander, B., G. L. Moldovan, M. Sacher, C. Hoege and S. Jentsch (2005). SUMO-modified PCNA recruits Srs2 to prevent recombination during S phase. *Nature* **436**(7049): 428-33.

Shishkin, A. A., I. Voineagu, R. Matera, N. Cherng, B. T. Chernet, M. M. Krasilnikova, V. Narayanan, K. S. Lobachev and S. M. Mirkin (2009). Large-scale expansions of Friedreich's ataxia GAA repeats in yeast. *Mol Cell* **35**(1): 82-92.

Spiro, C. and C. T. McMurray (2003). Nuclease-deficient FEN-1 blocks Rad51/BRCA1-mediated repair and causes trinucleotide repeat instability. *Mol Cell Biol* **23**(17): 6063-74.

Tateishi, S., Y. Sakuraba, S. Masuyama, H. Inoue and M. Yamaizumi (2000). Dysfunction of human Rad18 results in defective postreplication repair and hypersensitivity to multiple mutagens. *Proc Natl Acad Sci U S A* **97**(14): 7927-32.

Ulrich, H. D. (2005). The RAD6 pathway: control of DNA damage bypass and mutagenesis by ubiquitin and SUMO. *Chembiochem* **6**(10): 1735-43.

Unk, I., I. Hajdu, K. Fatyol, J. Hurwitz, J. H. Yoon, L. Prakash, S. Prakash and L. Haracska (2008). Human HLTF functions as a ubiquitin ligase for proliferating cell nuclear antigen polyubiquitination. *Proc Natl Acad Sci U S A* **105**(10): 3768-73.

Unk, I., I. Hajdu, K. Fatyol, B. Szakal, A. Blastyak, V. Bermudez, J. Hurwitz, L. Prakash, S. Prakash and L. Haracska (2006). Human SHPRH is a ubiquitin ligase for Mms2-Ubc13-dependent polyubiquitylation of proliferating cell nuclear antigen. *Proc Natl Acad Sci U S A* **103**(48): 18107-12.

van den Broek, W. J., M. R. Nelen, G. W. van der Heijden, D. G. Wansink and B. Wieringa (2006). Fen1 does not control somatic hypermutability of the (CTG)(n)*(CAG)(n) repeat in a knock-in mouse model for DM1. *FEBS Lett* **580**(22): 5208-14.

Watanabe, K., S. Tateishi, M. Kawasuji, T. Tsurimoto, H. Inoue and M. Yamaizumi (2004). Rad18 guides poleta to replication stalling sites through physical interaction and PCNA monoubiquitination. *Embo J* **23**(19): 3886-96.

Waters, L. S., B. K. Minesinger, M. E. Wiltrout, S. D'Souza, R. V. Woodruff and G. C. Walker (2009). Eukaryotic translesion polymerases and their roles and regulation in DNA damage tolerance. *Microbiol Mol Biol Rev* **73**(1): 134-54.

Yang, J. and C. H. Freudenreich (2007). Haploinsufficiency of yeast FEN1 causes instability of expanded CAG/CTG tracts in a length-dependent manner. *Gene* **393**(1-2): 110-5.

Zheng, L., J. Jia, L. D. Finger, Z. Guo, C. Zer and B. Shen (2011). Functional regulation of FEN1 nuclease and its link to cancer. *Nucleic Acids Res* **39**(3): 781-94.

CHAPTER 6

Conclusions and future perspectives

6.1 Conclusions

This thesis identifies specific human proteins that modulate expansions of triplet repeat tracts near the threshold, the crucial allele length where genetic instability and human polyglutamine disease are initiated. While numerous modulators of expansions near the threshold have been reported in yeast, very little was known about what factors contribute to these events in human cells. Using SVG-A astrocytes, I discovered five proteins that inhibit expansions (p300, HDAC9, RTEL1, HLTF and RAD18), plus I verified a protective role for CBP. The same approach provided the novel finding that HDAC3 and HDAC5 have the opposite role, namely to promote expansions. Experiments with MSH2 and MSH3 verified that MutSβ also promotes expansions of threshold length repeats, in addition to its role at longer tracts. Moreover, I found evidence that HDAC3, HDAC5 and MutSβ function in a common pathway to promote expansions. Finally, my experiments showed no change in expansion frequencies when six proteins were knocked down or chemically inhibited (HDAC1, HDAC2, MSH6, CtIP, MRE11 and SHPRH), providing the first suggestion that these factors are unlikely to be important for expansions. My results therefore shed significant new light on some of the mechanisms of instability. Although the focus was on shorter repeats, it is clear that at least some mechanistic aspects highlight commonalities between expansion of these and pathogenic-length tracts.

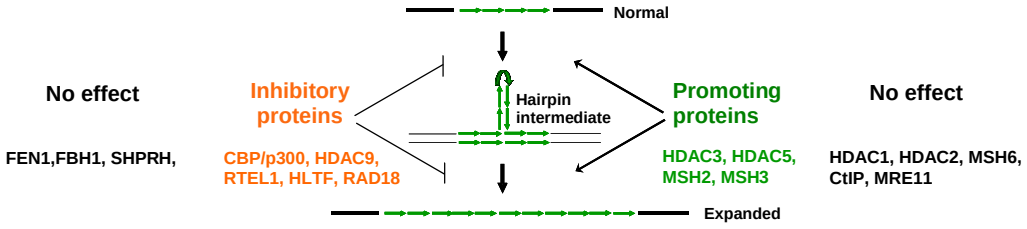

Figure 6.1 Summary of proteins identified in this study to be involved in expansion mutagenesis, both inhibitory and promoting. Also shown are proteins that were found to have no effect on expansions in this system.

Support for a contribution by specific HDACs to TNR instability is described in Chapter 3. In this chapter, evidence is provided to suggest that HDAC3 and 5 promote expansions, the first depiction of human trans-acting factors that promote expansions near the crucial threshold length where genetic instability and human polyglutamine disease are initiated. HDAC1 and 2 do not seem to be implicated in expansions, while data support a role for HDAC9 in inhibiting instability. In further support for acetylation playing an important role in instability, knockdown of the HATs, CBP and p300, increased the frequency of expansions, implying that specific HDACs and HATs have opposing effects on expansions. This data complements earlier observations in Drosophila, whereby loss of one copy of CBP

increased instability of long, disease-lengths repeats (Jung and Bonini, 2007), hinting at shared mechanisms of instability for short and longer repeats. The findings regarding HDACs and HATs modulating expansions further contributes to the growing body of evidence for chromatin remodeling/epigenetic factors being implicated in TNR expansion (Jung and Bonini, 2007; Dion et al., 2008; Libby et al., 2008). The causal relationship between HDAC3 and expansions raises the intriguing possibility that HDAC3 inhibitors being tested for relief of expansion-associated gene silencing may also suppress somatic expansions that contribute to disease progression.

In Chapter 4, I provide evidence to suggest that the MMR complex MutSβ is responsible for promoting the expansion of threshold length repeats into the disease-causing range. This novel finding is supported by ChIP data showing MutSβ is selectively recruited to the TNR (Gannon et al., Submitted). These data advocate similar trans-acting factors promoting expansion of long repeat tracts and short, threshold-length alleles. This inference is incongruent with studies in yeast that determined MMR factors to have little consequence on expansion of $(CAG)_{25}$ or $(CTG)_{25}$ tracts (Schweitzer and Livingston, 1997; Freudenreich et al., 1998; Miret et al., 1998; Rolfsmeier et al., 2000). Further investigation suggests that HDAC3, HDAC5 and MutSβ all function in the same pathway to help cause expansions of threshold-length repeats. How these factors might function in the expansion process was addressed. I could find no compelling evidence in SVG-A cells to suggest that HDAC3 promotes CTG•CAG expansions by regulating MSH2 or MSH3 protein levels. Another potential mechanism for functional interaction has been ruled out with the finding that HDAC3 depletion does not alter MutSβ occupancy at the repeat tract (Gannon et al., Submitted). I discuss this in section 6.2.2.

The work presented in Chapter 5 arose from the findings in yeast that Srs2 works together with members of the PRR pathway to inhibit expansions. Knockdown experiments determined that RTEL1, but not the other proposed orthologue of Srs2 FBH1, acts to prevent expansions in SVG-A cells, reminiscent of Srs2 in yeast. Additionally, members of the PRR pathway in human, HLTF and RAD18, were also shown to protect against the occurrence of expansions. A role for RTEL1 and the PRR factors in preventing expansions in a shared pathway was illustrated by double knockdown experiments. The nature of this protective mechanism remains undetermined. Collectively, the data presented in this thesis are reflective of mechanistic insights into the process of expansions (Fig. 6.1).

6.2 Future studies

6.2.1 Will pharmacologically targeting HDAC3 affect somatic expansions in a TNR disease mouse model?

One exciting prospect stemming from the finding that HDAC3 promotes expansions is the possibility that HDAC3 inhibitors already being tested to alleviate symptoms of TNR diseases might have further advantageous effects in curtailing the expansion mutation that contributes to disease. HDAC3 has been implicated as a potential therapeutic target in FRDA and HD. In a *C.elegans* HD model, it has been shown that HDA-3 (HDAC3 homologue) potentiates neurotoxicity while HDA-1 (HDAC1 and HDAC2 homologue) suppresses it (Bates et al., 2006). In fact, in this model neurotoxicity was primarily controlled by the counteracting effects of HDAC3 and CBP, which were shown in SVG-A cells to have opposing effects on TNR expansions (Chapter 3). Specific inhibition of HDAC3 by small molecule inhibitors including 4b has been shown to relieve frataxin gene silencing in FRDA patient cells and disease mouse models (Herman et al., 2006; Xu et al., 2009; Rai et al., 2010). In addition, treatment of R6/2 HD mice with 4b alleviated the disease phenotype and reduced transcriptional abnormalities (Thomas et al., 2008). Moreover, 4b and other HDAC3-specific inhibitors showed beneficial effects in a *Drosophila* model of HD and in immortalized cells from striatal tissue of *HdhQ111* knock-in mice (Jia et al., 2012). In contrast to these collective findings, a recent study reported that genetic knock-down of HDAC3 in R6/2 mice did not show any marked improvement in R6/2 behavioural and molecular phenotypes (Moumne et al., 2012). However, since complete ablation of HDAC3 in mice is embryonic lethal (Bhaskara et al., 2008), $HDAC3^{+/-}$ heterozygotes were used to for the purpose of determining a role for HDAC3 in HD. HDAC3 was reduced to ~60% of the WT level in the brain (Moumne et al., 2012), which might not be sufficient to reveal HDAC3-dependent effects, especially since HDAC3 is abundantly expressed. 60% residual protein may be enough to mask any phenotype.

The finding that HDAC3 and HDAC5 promote expansions is coincidental with their reported abundant expression in the brain. In situ hybridisation analysis of HDAC expression patterns throughout the rat brain revealed that HDAC3 and HDAC5, along with HDAC11 exhibited the most abundant levels overall in the brain (Broide et al., 2007). Of note, HDAC3 and HDAC5 were shown to be highly expressed in the striatum (Hoshino et al., 2003; Broide et al., 2007), where expansion is particularly frequent in HD (Hoshino et al., 2003; Broide et al., 2007; Gonitel et al., 2008). Furthermore, both HDAC3 and HDAC5 were present in striatal tissue from R6/2 HD mice at early and terminal disease stages (Quinti et al., 2010). Western blot analysis of HDAC3 localisation in N171-82Q transgenic HD mice showed increased nuclear accumulation and decreased cytoplasmic accumulation

implying that it is localised to the nucleus in the presence of mHTT (Jia et al., 2012). These data may serve to strengthen evidence for HDAC3 and/or HDAC5 as relevant pharmacological targets in alleviation of disease symptoms but also strengthens the importance of their potential as modifiers of instability in a disease context.

In light of the key links between HDAC3 being a potential target in TNR disease pathogenesis (Thomas et al., 2008; Xu et al., 2009) and causal for TNR expansions, I feel that determination of the effects of inhibition of HDAC3 using small molecule inhibitors on somatic expansions in the brain of a TNR disease mouse model is warranted. Because the striatum is a source of frequent somatic instability in HD patients and this region of the brain is a target of pathogenesis, exploring the effects of HDAC3 inhibition on expansions in a mouse model would be highly informative. Alternatively to the inhibitor approach, HDAC3 knockout mice could be employed. However, HDAC3 knockout mice are embryonic lethal (Bhaskara et al., 2008) so creating HDAC3 null mice in a model of HD such as R6/2 is not a viable option. Conditional tissue-specific HDAC3 knockout mice lines could be generated in an R6/2 background to evaluate the effect of loss of HDAC3 expression on expansions in the striatum. A similar experimental approach was successfully used to generate mice with HDAC3 deleted in regions of the hippocampus using the Cre/lox system to examine the role of HDAC3 in long-term memory (McQuown et al., 2011). Such experiments are beyond the scope of our laboratory but would provide useful insights. CAG-repeat antisense oligonucleotides (ASOs), which are currently being evaluated for their ability to circumvent the RNA pathogenesis associated with DM1, were recently found to suppress somatic instability in HT1080 cells expressing 800 CTG repeats in the *DMPK* 3' UTR (Nakamori et al., 2011). Direct injection of ASOs into DM1 mice also stabilised the expanded repeat supporting the inference that early intervention with ASOs might stabilise the repeat at subpathogenic lengths (Nakamori et al., 2011). This study serves to highlight the exciting prospect of compounds that have dual functions in reducing disease pathogenesis and suppressing somatic instability.

While HDAC3 and HDAC5 were shown to promote expansions in SVG-A cells, evidence suggests that HDAC9 actually acts antagonistically to inhibit expansions. The differential functions among specific HDACs in controlling expansions, serves to underscore the importance of indentifying which of the untested HDACs are involved, if any. In light of the opposing roles reported for certain HDACs in other biological processes such as neurodegeneration (Majdzadeh et al., 2008), this is a worthwhile pursuit. To address this, siRNA knockdown of the other HDACs could be performed to determine the relevant targets.

6.2.2 Nature of the functional interaction between HDACs and MMR for promoting expansions

The findings presented in Chapter 3 imply that HDAC3 and HDAC5 work in the same pathway to promote expansions. How this functional interaction is borne out might be explained by *in vitro* analysis of HDAC activity. Evidence points towards class IIa HDACs having an inherent low-level enzymatic activity for acetyllysine substrates due to the substitution of a Tyr residue in class I HDACs to a His residue in class IIa HDACs (Lahm et al., 2007; Bottomley et al., 2008). Coupled with the observation that HDAC3 interacts with HDAC5 (Fischle et al., 2002), a developing hypothesis is that class IIa HDACs act as recognition units for acetylated lysines (Bradner et al., 2010) and might recruit HDAC3 to supply deacetylase activity. Perhaps in the case of TNR repeats, HDAC5 recognises the relevant acetylated residue(s) and binds HDAC3 to remove the modification (Fig 6.2). This would provide an explanation for why double HDAC3/HDAC5 knockdowns resulted in similar decreases in expansions as the single knockdowns. To add weight to this proposal, double knockdown of HDAC5 and MSH2 should give a similar reduced expansion phenotype to that of individual knockdowns, as was the case for HDAC3/MSH2 double knockdown. Additionally triple knockdowns of HDAC3, HDAC5 and MSH2 should result in a suppression of expansions comparable to the single knockdowns.

The mechanism by which HDAC3 and MSH2/3 promote expansions remains elusive. Two models were tested. A 'gatekeeper' hypothesis posits that HDAC3/5 modify histones near the TNR and thereby regulate access of MutSβ. Thus far, we have found no evidence that HDAC3 promotes CTG•CAG expansions by controlling access of MutSβ to the repeat tract suggesting that this mechanism may not be applicable. Another potential model is a 'caretaker' model, where HDACs influence proteins or genes at a distance, which then travel to the TNR to exert their effects. We have eliminated the possibilities that HDAC3 promotes CTG•CAG expansions by regulating MSH2 or MSH3 protein levels. Another facet to the caretaker model is that HDAC deacetylation of MSH2 might influence its activity and this promotes expansions. As described in chapter 4, acetylation sites have been identified on MSH2 (Choudhary et al., 2009). Perhaps, MSH2 acetylation negatively impacts on MSH2's ability to destabilise TNRs by affecting the ATPase activity of the MutSβ complex, assuming functional MMR is required for expansions in the SVG-A system. The HDAC(s) and HAT(s) responsible for maintaining the acetylation status of MSH2 are currently unknown. My prediction is that HDAC3/5 are requisite HDACs, while CBP/p300 might be involved in catalysing MSH2 acetylation. This is based on the finding reported in Chapter 3 that HDAC3 and HDAC5 to be key players in expansion causation, whereas the HATs

CBP/p300 were found have the opposing effect of suppressing expansions, consistent with their opposing roles in controlling acetylation status. Furthermore, CBP/p300 and these HDACs share many of the same non-histone substrates.

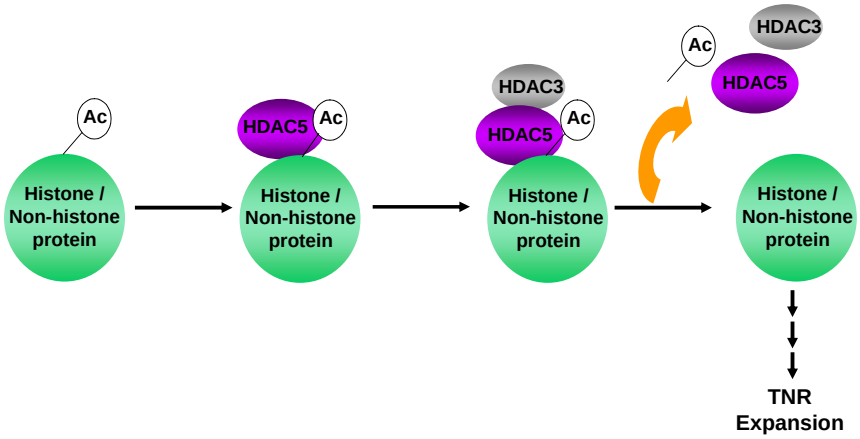

Figure 6.2 Proposed mechanism for HDAC3/5 and MMR factors in promoting expansions. A non-histone (e.g. MSH2) or histone protein is acetylated, perhaps by CBP/p300. HDAC5 recognises the acetyllysine residue and recruits HDAC3 to catalyse deacetylation. This leads to expansion of the TNR tract.

In order to determine how HDAC3/5 and MutSβ are acting to promote expansions, useful insight would be provided by elucidation of the mechanism by which MutSβ acts to mediate expansion of subthreshold-length repeats. An interesting experiment would be investigation of the downstream repair proteins. If MMR proteins downstream of MutSβ are important for facilitating, then knockdown of such factors by siRNA should reveal a similar decrease in expansions as for MSH2- and MSH3-depleted SVG-A cells.

One method of determining whether the ATPase function of MSH2 is required for expansions is to create an ATPase mutant version of the protein using site-directed mutagenesis. The rationale for this experiment is based on the observation that mice expressing ATPase-deficient MSH2 had a similar suppression of expansions as for MSH2-deficient mice (Tome et al., 2009). Mutation of the two putative acetylation sites on MSH2 (lysine 555 and lysine 635) to prevent modification by acetylation would reveal the relevance of these in TNR instability. If mutation of one or both residues resulted in an increase in expansions, then this would lend support to a model requiring that the ATPase function of MSH2 is important in promoting expansions. This would also further address whether the involvement of MMR factors exacts similar. Acetylation of MSH2 might affect

some other important aspect of MSH2 function, which is required for driving expansion but is currently unidentified.

If acetylation of MSH2 turns out to be important for expansions, a key follow-up experiment is to test whether MSH2 deacetylation is catalysed in a HDAC3-dependent manner. In order to test if HDAC3 is responsible for MSH2 deacetylation, purification of MSH2 from SVG-A cells could be performed. A pan-acetyl-lysine antibody would then be utilised to confirm acetylation of MSH2. If HDAC3 is responsible for its deacetylation of MSH2, then addition of purified HDAC3 to purified MSH2 should abrogate acetylation levels. A caveat with this experiment is that MSH2 acetylation levels must be high enough to enable detection.

6.2.3 Characterising the mechanism of RTEL1 and PRR in preventing expansions

One key finding in yeast was that expansion rates are elevated when PCNA ubiquitination is blocked (Daee et al., 2007). The importance of this modification in preventing expansions in SVG-A cells is implied by the observation that loss of the ubiquitin ligases RAD18 and HLTF, proposed to mediate PCNA ubiquitination, resulted in increased expansions. Analysis of levels of ubiquitinated PCNA by western blotting in cells depleted of RAD18 and HLTF might reveal a decrease in polyubiquitinated PCNA, which would shore up the supposition that it is relevant to the mechanism of protection against expansions. Based on our hypothesis, ubiquitination of PCNA occurs in response to replication being hampered by the repeats on the shuttle vector. It has been shown that MMS-induced PCNA polyubiquitination is reduced following knockdown of HLTF in HEK293T cells (Motegi et al., 2008). Whether or not polyubiquitin levels are high enough to be detected following transfection with the shuttle will have to be established in order to identify any decreases in knockdown cells. This proposed experiment is further complicated by the recent finding that HLTF and SHPRH are not essential for PCNA polyubiquination as mouse cells lacking these enzymes still retained some modified PCNA (Krijger et al., 2011).

The nature of the working relationship between RTEL1 and PRR in protecting against expansions is uncharacterised. In order to clarify the mechanism of their concerted action, some relatively straightforward experiments can be done. It would be useful to determine that these proteins are actually present at TNR sequences to validate our assumption that they are directly involved in TNR stability. ChIP experiments have been successfully performed using the SVG-A shuttle vector system to detect enriched signals of MSH2 and MSH3 at the TNR relative to a randomized TNR sequence (Gannon et al., Submitted). Although the technique has been established, other technical issues may persist. For RTEL1, the lack of available antibodies precludes direct assessment in SVG-A cells as was

performed for MSH2 and MSH3. In addition, the residency time of these proteins at the TNR tract is likely to be transient, which may cause problems in detecting a signal. If RTEL1 is efficiently detected and enriched at the TNR tract compared with the control, as would be expected based on biochemical unwinding experiments (Mark Petalcorin and Simon Boulton, personal communication), this would further bolster the proposed mechanism whereby RTEL1 is recruited to the hairpin and unwinds it. Based on the premise that RTEL1 is acting to unwind the proposed hairpin, similar to Srs2 in yeast, an informative experiment to decipher the mechanism of RTEL1 and PRR action would be to assess RTEL1 occupancy in RAD18 or HLTF knockdown cells. The prediction here is that RTEL1 occupancy at the repeat would result due to lack of recruitment signaling by HLTF and RAD18.

The instability phenotype observed in yeast following mutation of Srs2 and PRR components was specific to an exacerbation of expansions, with no effect observed for contractions, dinucleotide repeats or forward mutations (Bhattacharyya and Lahue, 2004; Daee et al., 2007). This is suggestive of the concerted action of Srs2 and PRR being directed towards the nascent lagging strand, where expansions arise rather than the lagging-strand template, where contractions predominate. It would be interesting to test if the selectivity for expansions extends to human cells. To achieve this, RTEL1, HLTF and/or RAD18 could be knocked down and the contraction phenotype measured by comparison to cells treated with scrambled siRNA. In light of the findings in yeast, the predicted outcome is that contractions would be unaffected.

Studies in yeast have implicated a role for the replication protein Mrc1 in maintaining TNR instability for sub-threshold and disease-length alleles (Freudenreich and Lahiri, 2004; Razidlo and Lahue, 2008). Mrc1 interacts with Tof1 and Csm3 to mediate the intra-S-phase checkpoint, which responds to stalled replication forks (Alcasabas et al., 2001; Tourriere and Pasero, 2007). The evidence for Mrc1 acting to prevent expansions has been shown to be dependent on checkpoint function (Razidlo and Lahue, 2008). Additionally, Mrc1 associates with Tof1 and Csm3 to co-ordinate DNA polymerase and replicative helicase activities, independently of its checkpoint function (Nedelcheva et al., 2005; Tourriere and Pasero, 2007). Based on findings in yeast that increased expansion rates in single *mrc1* mutants were not significantly different from double *pol30-K164R mrc1* mutants, it has been hypothesised that the intra-S checkpoint is activated by polymerase slippage and/or stalling at the TNR, which triggers PRR by permitting or recruiting PRR to the site, thereby inhibiting expansions (Daee, 2006). These preliminary findings did not establish if this functional relationship is due to a checkpoint-dependent role for Mrc1.

Recently, it has been shown that siRNA depletion of the human homologues of Mrc1, Tof1 and Csm3 (Claspin, Timeless and Tipin, respectively) enhances both contraction and expansion of $(CTG\bullet CAG)_{102}$ in HeLa cells and $(CTG\bullet CAG)_{13}$ in DM1 cells, although the source of instability in the DM1 line is unclear due to the presence of a $(CTG\bullet CAG)_{1000}$ allele also (Liu et al., 2012). This raises the question is Claspin involved in modulating expansions in conjunction with the PRR machinery? In order to test this, a role for Claspin in mediating TNR expansions could be determined by siRNA-mediated depletion and the effect on expansions measured by the shuttle vector assay. If Claspin plays a similar role to that described for yeast and human cells, then the prediction is that knocking it down would result in an elevation of expansions. If this prediction is borne out experimentally, then double knockdowns of Claspin with RTEL1, RAD18 and HLTF could be performed to determine if they are working through a common pathway.

Interestingly, Claspin and Timeless have been shown to promote ubiquitination of PCNA in a manner dependent on Chk1 but independent of the checkpoint response (Yang et al., 2008). Loss of Claspin in human cells was accompanied by reduction in Rad18 chromatin, while both Claspin and Timeless were found to interact with PCNA (Yang et al., 2008). This might envisage a model involving Claspin and PRR promoting RTEL1 recruitment to the TNR tract by PCNA ubiquitination, whereupon expansions are prevented. In order to determine if checkpoint activity is involved, knockdown of ATR could be performed. If expansion-prevention is dependent on checkpoint function, then a similar increase in expansions as predicted for Claspin knockdown would be expected. Compiling the observations that (i) Mrc1 and PRR act together in yeast to inhibit expansions, (ii) Claspin, Timeless and Tipin were found to protect against instability in human cells and (iii) Claspin and Timeless act to promote PCNA ubiquitnation, raises the interesting possibility that Claspin and Timeless might be central components in RTEL1/PRR-mediated maintenance of TNR stability.

6.2.4 Alternative approach to shuttle vector assay

The approach used to determine potential trans-acting factors involved in controlling expansions throughout this study was candidate-based rather than using unbiased, random screens. While this has proved useful for indentifying the specific trans-acting factors described throughout the main body of the thesis, the approach relies on information from other model organisms, such as yeast and mice to provide testable candidates. Thus the scope of investigation is limited and important pathways in instability may remain undiscovered. The shuttle vector assay is not amenable to the required high-throughput

screening that would facilitate discovery of novel protein or chemical modulators of instability, due to the labour-intensive nature of the assay and the intrinsic variability rooted in its numerous moving parts. In order to conquer these shortcomings and perform such screens, a different system is warranted. A reporter system with a read-out such as fluorescence being turned on or off upon changes in repeat length would be useful. Quantitation of changes in expansion frequency could be determined using FACS analysis. Development of such a system would likely be time-consuming but if successful, would provide a streamlined approach more suited for high-throughput analyses.

6.3 References

Alcasabas, A. A., A. J. Osborn, J. Bachant, F. Hu, P. J. Werler, K. Bousset, K. Furuya, J. F. Diffley, A. M. Carr and S. J. Elledge (2001). Mrc1 transduces signals of DNA replication stress to activate Rad53. *Nat Cell Biol* **3**(11): 958-65.

Bates, E. A., M. Victor, A. K. Jones, Y. Shi and A. C. Hart (2006). Differential contributions of Caenorhabditis elegans histone deacetylases to huntingtin polyglutamine toxicity. *J Neurosci* **26**(10): 2830-8.

Bhaskara, S., B. J. Chyla, J. M. Amann, S. K. Knutson, D. Cortez, Z. W. Sun and S. W. Hiebert (2008). Deletion of histone deacetylase 3 reveals critical roles in S phase progression and DNA damage control. *Mol Cell* **30**(1): 61-72.

Bhattacharyya, S. and R. S. Lahue (2004). Saccharomyces cerevisiae Srs2 DNA helicase selectively blocks expansions of trinucleotide repeats. *Mol Cell Biol* **24**(17): 7324-30.

Bottomley, M. J., P. Lo Surdo, P. Di Giovine, A. Cirillo, R. Scarpelli, F. Ferrigno, P. Jones, P. Neddermann, R. De Francesco, C. Steinkuhler, P. Gallinari and A. Carfi (2008). Structural and functional analysis of the human HDAC4 catalytic domain reveals a regulatory structural zinc-binding domain. *J Biol Chem* **283**(39): 26694-704.

Bradner, J. E., N. West, M. L. Grachan, E. F. Greenberg, S. J. Haggarty, T. Warnow and R. Mazitschek (2010). Chemical phylogenetics of histone deacetylases. *Nat Chem Biol* **6**(3): 238-243.

Broide, R. S., J. M. Redwine, N. Aftahi, W. Young, F. E. Bloom and C. J. Winrow (2007). Distribution of histone deacetylases 1-11 in the rat brain. *J Mol Neurosci* **31**(1): 47-58.

Choudhary, C., C. Kumar, F. Gnad, M. L. Nielsen, M. Rehman, T. C. Walther, J. V. Olsen and M. Mann (2009). Lysine acetylation targets protein complexes and co-regulates major cellular functions. *Science* **325**(5942): 834-40.

Daee, D. L. (2006). Trans-factors influencing trinucleotide repeat instability in Saccharomyces cerevisiae. (University of Nebraska Medical Center): Ref Type: Thesis/Dissertation.

Daee, D. L., T. Mertz and R. S. Lahue (2007). Postreplication repair inhibits CAG.CTG repeat expansions in Saccharomyces cerevisiae. *Mol Cell Biol* **27**(1): 102-10.

Dion, V., Y. Lin, L. Hubert, Jr., R. A. Waterland and J. H. Wilson (2008). Dnmt1 deficiency promotes CAG repeat expansion in the mouse germline. *Hum Mol Genet* **17**(9): 1306-17.

Fischle, W., F. Dequiedt, M. J. Hendzel, M. G. Guenther, M. A. Lazar, W. Voelter and E. Verdin (2002). Enzymatic activity associated with class II HDACs is dependent on a multiprotein complex containing HDAC3 and SMRT/N-CoR. *Mol Cell* **9**(1): 45-57.

Freudenreich, C. H., S. M. Kantrow and V. A. Zakian (1998). Expansion and length-dependent fragility of CTG repeats in yeast. *Science* **279**(5352): 853-6.

Freudenreich, C. H. and M. Lahiri (2004). Structure-forming CAG/CTG repeat sequences are sensitive to breakage in the absence of Mrc1 checkpoint function and S-phase checkpoint signaling: implications for trinucleotide repeat expansion diseases. *Cell Cycle* **3**(11): 1370-4.

Gannon, A., A. Frizzell, E. Healy and R. S. Lahue (Submitted). MutSβ and histone deacetylase complexes promote expansions of trinucleotide repeats in human cells.

Gonitel, R., H. Moffitt, K. Sathasivam, B. Woodman, P. J. Detloff, R. L. Faull and G. P. Bates (2008). DNA instability in postmitotic neurons. *Proc Natl Acad Sci U S A* **105**(9): 3467-72.

Herman, D., K. Jenssen, R. Burnett, E. Soragni, S. L. Perlman and J. M. Gottesfeld (2006). Histone deacetylase inhibitors reverse gene silencing in Friedreich's ataxia. *Nat Chem Biol* **2**(10): 551-8.

Hoshino, M., K. Tagawa, T. Okuda, M. Murata, K. Oyanagi, N. Arai, T. Mizutani, I. Kanazawa, E. E. Wanker and H. Okazawa (2003). Histone deacetylase activity is

retained in primary neurons expressing mutant huntingtin protein. *J Neurochem* **87**(1): 257-67.

Jia, H., J. Pallos, V. Jacques, A. Lau, B. Tang, A. Cooper, A. Syed, J. Purcell, Y. Chen, S. Sharma, G. R. Sangrey, S. B. Darnell, H. Plasterer, G. Sadri-Vakili, J. M. Gottesfeld, L. M. Thompson, J. R. Rusche, J. L. Marsh and E. A. Thomas (2012). Histone deacetylase (HDAC) inhibitors targeting HDAC3 and HDAC1 ameliorate polyglutamine-elicited phenotypes in model systems of Huntington's disease. *Neurobiology of Disease* **46**(2): 351-361.

Jung, J. and N. Bonini (2007). CREB-binding protein modulates repeat instability in a Drosophila model for polyQ disease. *Science* **315**(5820): 1857-9.

Krijger, P. H., K. Y. Lee, N. Wit, P. C. van den Berk, X. Wu, H. P. Roest, A. Maas, H. Ding, J. H. Hoeijmakers, K. Myung and H. Jacobs (2011). HLTF and SHPRH are not essential for PCNA polyubiquitination, survival and somatic hypermutation: existence of an alternative E3 ligase. *DNA Repair (Amst)* **10**(4): 438-44.

Lahm, A., C. Paolini, M. Pallaoro, M. C. Nardi, P. Jones, P. Neddermann, S. Sambucini, M. J. Bottomley, P. Lo Surdo, A. Carfi, U. Koch, R. De Francesco, C. Steinkuhler and P. Gallinari (2007). Unraveling the hidden catalytic activity of vertebrate class IIa histone deacetylases. *Proc Natl Acad Sci U S A* **104**(44): 17335-40.

Libby, R. T., K. A. Hagerman, V. V. Pineda, R. Lau, D. H. Cho, S. L. Baccam, M. M. Axford, J. D. Cleary, J. M. Moore, B. L. Sopher, S. J. Tapscott, G. N. Filippova, C. E. Pearson and A. R. La Spada (2008). CTCF cis-regulates trinucleotide repeat instability in an epigenetic manner: a novel basis for mutational hot spot determination. *PLoS Genet* **4**(11): e1000257.

Liu, G., X. Chen, Y. Gao, T. Lewis, J. Barthelemy and M. Leffak (2012). Altered Replication in Human Cells Promotes DMPK (CTG)n {middle dot} (CAG)n Repeat Instability. *Mol Cell Biol* **32**(9): 1618-32.

Majdzadeh, N., B. E. Morrison and S. R. D'Mello (2008). Class IIA HDACs in the regulation of neurodegeneration. *Front Biosci* **13**: 1072-82.

McQuown, S. C., R. M. Barrett, D. P. Matheos, R. J. Post, G. A. Rogge, T. Alenghat, S. E. Mullican, S. Jones, J. R. Rusche, M. A. Lazar and M. A. Wood (2011). HDAC3 is a critical negative regulator of long-term memory formation. *J Neurosci* **31**(2): 764-74.

Miret, J. J., L. Pessoa-Brandao and R. S. Lahue (1998). Orientation-dependent and sequence-specific expansions of CTG/CAG trinucleotide repeats in Saccharomyces cerevisiae. *Proc Natl Acad Sci U S A* **95**(21): 12438-43.

Motegi, A., H. J. Liaw, K. Y. Lee, H. P. Roest, A. Maas, X. Wu, H. Moinova, S. D. Markowitz, H. Ding, J. H. Hoeijmakers and K. Myung (2008). Polyubiquitination of proliferating cell nuclear antigen by HLTF and SHPRH prevents genomic instability from stalled replication forks. *Proc Natl Acad Sci U S A* **105**(34): 12411-6.

Moumne, L., K. Campbell, D. Howland, Y. Ouyang and G. P. Bates (2012). Genetic knock-down of HDAC3 does not modify disease-related phenotypes in a mouse model of Huntington's disease. *PLoS One* **7**(2): e31080.

Nakamori, M., G. Gourdon and C. A. Thornton (2011). Stabilization of expanded (CTG)*(CAG) repeats by antisense oligonucleotides. *Mol Ther* **19**(12): 2222-7.

Nedelcheva, M. N., A. Roguev, L. B. Dolapchiev, A. Shevchenko, H. B. Taskov, A. Shevchenko, A. F. Stewart and S. S. Stoynov (2005). Uncoupling of unwinding from DNA synthesis implies regulation of MCM helicase by Tof1/Mrc1/Csm3 checkpoint complex. *J Mol Biol* **347**(3): 509-21.

Quinti, L., V. Chopra, D. Rotili, S. Valente, A. Amore, G. Franci, S. Meade, M. Valenza, L. Altucci, M. M. Maxwell, E. Cattaneo, S. Hersch, A. Mai and A. Kazantsev (2010). Evaluation of histone deacetylases as drug targets in Huntington's disease models. Study of HDACs in brain tissues from R6/2 and CAG140 knock-in HD mouse models and human patients and in a neuronal HD cell model. *PLoS Curr* **2**.

Rai, M., E. Soragni, C. J. Chou, G. Barnes, S. Jones, J. R. Rusche, J. M. Gottesfeld and M. Pandolfo (2010). Two new pimelic diphenylamide HDAC inhibitors induce

sustained frataxin upregulation in cells from Friedreich's ataxia patients and in a mouse model. *PLoS One* **5**(1): e8825.

Razidlo, D. F. and R. S. Lahue (2008). Mrc1, Tof1 and Csm3 inhibit CAG.CTG repeat instability by at least two mechanisms. *DNA Repair (Amst)* **7**(4): 633-40.

Rolfsmeier, M. L., M. J. Dixon and R. S. Lahue (2000). Mismatch repair blocks expansions of interrupted trinucleotide repeats in yeast. *Mol Cell* **6**(6): 1501-7.

Schweitzer, J. K. and D. M. Livingston (1997). Destabilization of CAG trinucleotide repeat tracts by mismatch repair mutations in yeast. *Hum Mol Genet* **6**(3): 349-55.

Thomas, E. A., G. Coppola, P. A. Desplats, B. Tang, E. Soragni, R. Burnett, F. Gao, K. M. Fitzgerald, J. F. Borok, D. Herman, D. H. Geschwind and J. M. Gottesfeld (2008). The HDAC inhibitor 4b ameliorates the disease phenotype and transcriptional abnormalities in Huntington's disease transgenic mice. *Proc Natl Acad Sci U S A* **105**(40): 15564-9.

Tome, S., I. Holt, W. Edelmann, G. E. Morris, A. Munnich, C. E. Pearson and G. Gourdon (2009). MSH2 ATPase domain mutation affects CTG*CAG repeat instability in transgenic mice. *PLoS Genet* **5**(5): e1000482.

Tourriere, H. and P. Pasero (2007). Maintenance of fork integrity at damaged DNA and natural pause sites. *DNA Repair (Amst)* **6**(7): 900-13.

Xu, C., E. Soragni, C. J. Chou, D. Herman, H. L. Plasterer, J. R. Rusche and J. M. Gottesfeld (2009). Chemical probes identify a role for histone deacetylase 3 in Friedreich's ataxia gene silencing. *Chem Biol* **16**(9): 980-9.

Yang, X. H., B. Shiotani, M. Classon and L. Zou (2008). Chk1 and Claspin potentiate PCNA ubiquitination. *Genes Dev* **22**(9): 1147-52.

APPENDIX 1

Role of DNA polβ in TNR expansions in human cells

A1.1 Introduction

A causative role for BER in expansions has been postulated (Kovtun et al., 2007; Liu and Wilson, 2012). It has been hypothesised that there may be crosstalk between MMR and BER with respect to promoting expansions (McMurray, 2010). It has been shown that MutSα (MSH2-MSH6) interacts with the BER glycosylase, MUTYH (Gu et al., 2002). McMurray, 2010 speculates that MutSβ might interact with OGG1 based on the involvement of both of these pathways in TNR instability. With this in mind, I decided to investigate the effects of knocking down the BER polymerase polβ on expansions in SVG-A cells.

A1.2 Results

Knockdown of polβ was accomplished by transfection of SVG-A cells with polβ siRNA and expansions frequencies in scrambled siRNA control cells and polβ siRNA cells were determined. Loss of polβ resulted in a 2.2-fold decrease in expansion frequency compared with scrambled siRNA (Fig. A1A). This was not found to be statistically significant compared with scrambled siRNA ($P = 0.45$). However, the variation was quite high between scrambled siRNA data sets as confirmed by the large error bars in figure A1A. Due to this issue, the effect of knocking down polβ on expansions cannot be concluded with confidence. No difference in the sizes of expansions was observed between scrambled siRNA and polβ siRNA (Fig. A1B). Efficient knockdown was achieved as confirmed by western blotting (Fig. A1C). Densitometric analysis was performed and knockdown efficiency for polβ was determined to be 83% (± 6) (Fig. A1D).

Interestingly, ChIP experiments investigating the recruitment of polβ also proved inconclusive (Anne-Marie Gannon, personal communication). In line with the expansion data, a general trend for enhanced polβ occupancy at the repeat compared with a randomised sequence was observed in SVG-A cells but this was variable and no statistically significant effects were recorded. Unfortunately, these experiments were unable to reveal the role of polβ in this system.

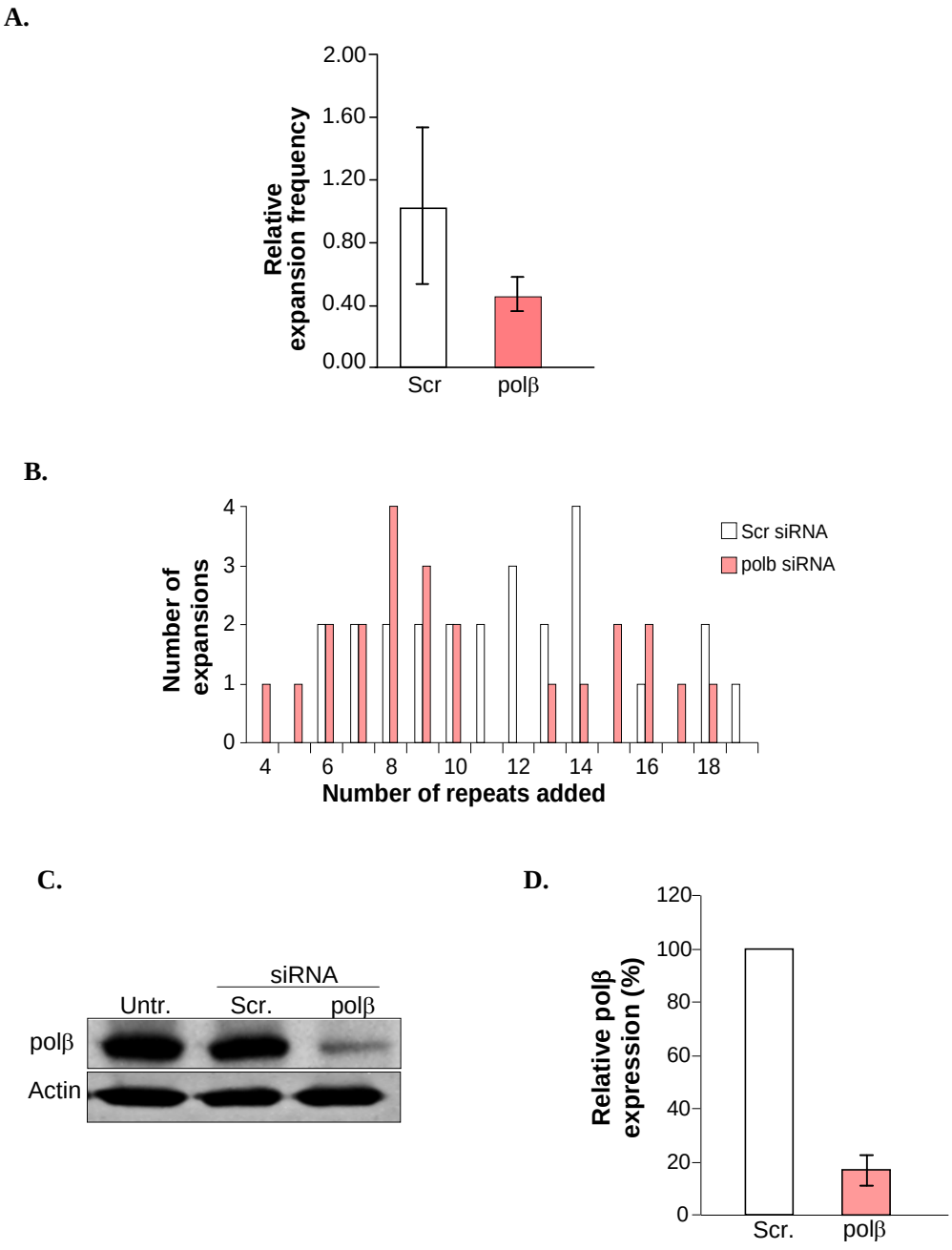

Figure A.1. Expansions in SVG-A cells treated with siRNA against polβ. A. Expansion frequencies subsequent to treatment with polβ siRNA. n=4. **B.** Expansion sizes for polβ siRNA: 25 genetically independent expansions for scrambled siRNA, 23 for polβ siRNA. **C.** Representative western blot of polβ expression in SVG-A cells treated with polβ siRNA **D.** Quantification of polβ protein levels after knockdown, normalised to actin and to the scrambled siRNA control. Error bars denote ± one SEM; n= 4.

A1.3 References

Gu, L., B. Cline-Brown, F. Zhang, L. Qiu and G. M. Li (2002). Mismatch repair deficiency in hematological malignancies with microsatellite instability. *Oncogene* **21**(37): 5758-64.

Kovtun, I. V., Y. Liu, M. Bjoras, A. Klungland, S. H. Wilson and C. T. McMurray (2007). OGG1 initiates age-dependent CAG trinucleotide expansion in somatic cells. *Nature* **447**(7143): 447-52.

Liu, Y. and S. H. Wilson (2012). DNA base excision repair: a mechanism of trinucleotide repeat expansion. *Trends Biochem Sci* **37**(4): 162-72.

McMurray, C. T. (2010). Mechanisms of trinucleotide repeat instability during human development. *Nat Rev Genet* **11**(11): 786-99.

APPENDIX 2

Author publications

OPEN ACCESS Freely available online

Histone Deacetylase Complexes Promote Trinucleotide Repeat Expansions

Kim Debacker[◔], Aisling Frizzell[◔], Olive Gleeson, Lucy Kirkham-McCarthy, Tony Mertz, Robert S. Lahue*

Centre for Chromosome Biology, School of Natural Sciences, National University of Ireland Galway, Galway, Ireland

Abstract

Expansions of DNA trinucleotide repeats cause at least 17 inherited neurodegenerative diseases, such as Huntington's disease. Expansions can occur at frequencies approaching 100% in affected families and in transgenic mice, suggesting that specific cellular proteins actively promote (favor) expansions. The inference is that expansions arise due to the presence of these promoting proteins, not their absence, and that interfering with these proteins can suppress expansions. The goal of this study was to identify novel factors that promote expansions. We discovered that specific histone deacetylase complexes (HDACs) promote CTG•CAG repeat expansions in budding yeast and human cells. Mutation or inhibition of yeast Rpd3L or Hda1 suppressed up to 90% of expansions. In cultured human astrocytes, expansions were suppressed by 75% upon inhibition or knockdown of HDAC3, whereas siRNA against the histone acetyltransferases CBP/p300 stimulated expansions. Genetic and molecular analysis both indicated that HDACs act at a distance from the triplet repeat to promote expansions. Expansion assays with nuclease mutants indicated that Sae2 is one of the relevant factors regulated by Rpd3L and Hda1. The causal relationship between HDACs and expansions indicates that HDACs can promote mutagenesis at some DNA sequences. This relationship further implies that HDAC3 inhibitors being tested for relief of expansion-associated gene silencing may also suppress somatic expansions that contribute to disease progression.

Citation: Debacker K, Frizzell A, Gleeson O, Kirkham-McCarthy L, Mertz T, et al. (2012) Histone Deacetylase Complexes Promote Trinucleotide Repeat Expansions. PLoS Biol 10(2): e1001257. doi:10.1371/journal.pbio.1001257

Academic Editor: Nancy Maizels, University of Washington, United States of America

Received July 28, 2011; **Accepted** December 20, 2011; **Published** February 21, 2012

Funding: This work was supported by Science Foundation Ireland (SFI; www.sfi.ie) grants 06/IN.1/B73 and 10/IN.1/B2973, by an SFI equipment award, and by the Millenium Fund of National University of Ireland, Galway (www.nuigalway.ie) (all to R.S.L.); by a postdoctoral fellowship from the Irish Research Council for Science Engineering and Technology (IRCSET, www.ircset.ie; to K.D.); and by an IRCSET postgraduate scholarship and by the Thomas Crawford Hayes Fund www.nuigalway.ie (both to A.F.). The funders had no role in study design, data collection and analysis, decision to publish, or preparation of the manuscript.

Competing Interests: The authors have declared that no competing interests exist.

Abbreviations: DM1, myotonic dystrophy type 1; HAT, histone acetyltransferase; HD, Huntington's disease; HDAC, histone deacetylase complex; TNR, trinucleotide repeat; TSA, trichostatin A

* E-mail: Bob.Lahue@nuigalway.ie

◔ These authors contributed equally to this work.

Introduction

The relentless expansion of trinucleotide repeats (TNRs) causes Huntington's disease (HD), myotonic dystrophy type 1 (DM1), and at least 15 other inherited neurological disorders [1]. It is thought that expansions are actively promoted by the presence of key proteins, not their absence, probably due to the "corruption" of their normal biochemical activities by TNR DNA [2–4]. Evidence for promoting factors includes the fact that disease alleles expand at high frequencies, sometimes approaching 100% [5], in otherwise normal individuals and in a number of transgenic and knockin mouse models of HD and DM1 [6–12]. Using candidate gene approaches, the DNA repair factors Msh2, Msh3, Pms2, Ogg1, and Xpa were identified as promoting proteins in mice, based on the fact that somatic expansions are suppressed ~50%–90% by homozygous knockout of *Msh2*, *Msh3*, *Pms2*, *Ogg1*, or *Xpa* [6–13]. Knockout of *Msh2* or *Msh3* also largely eliminates intergenerational expansions [7,9,10,14]. Thus, key DNA repair components promote expansions in certain mouse models.

The transgenic mice studies described above monitor long, disease-causing TNRs becoming even longer. For example, commonly used HD mouse models carry CAG tracts of 110–120 repeats [10,12]. A human inheriting an HD allele in this length range would develop the disease as a young child [15]. As an alternative approach, we focus on expansions near the crucial threshold, a narrow range of allele lengths (~30–40 uninterrupted repeats in humans [2,4,16]) that demarcates stable shorter repeats from unstable longer tracts. Expansion risk in humans and in yeast increases sharply once the threshold is crossed [17,18]. Expansions crossing the threshold are critical initiating mutations leading to enhanced instability and disease [2–4]. It is not known whether the mechanism of expansion is the same for threshold-length alleles and long, disease-causing tracts. In this study, we find that yeast mutants lacking the nucleases Sae2 or Mre11 reduce expansion rates for $(CTG)_{20}$ alleles, whereas *sae2* or *mre11* mutants show increased expansion frequencies for long $(CAG)_{70}$ repeats [19]. This new evidence suggests that triplet repeat length helps determine expansion mechanism.

The goal of this study was to identify novel factors in yeast and human cells that promote expansions of TNR alleles near the threshold. We found specific histone deacetylase complexes (HDACs) that promote expansions, plus one human histone acetyltransferase (HAT) that inhibits expansions, and we suggest a mechanistic link between HDACs and DNA repair. These results indicate a causal relationship between HDACs and expansions, and they show that protein acetylation and deacetylation are key modulators of TNR instability.

Author Summary

The human genome contains numerous DNA trinucleotide repeats, which mutate infrequently in most situations. However, in families affected by certain inherited neurological diseases such as Huntington's, a trinucleotide repeat has undergone an expansion mutation that lengthens the repeat tract. This expansion is generally sufficient to cause disease. Further germline and somatic expansions in affected families occur at very high frequencies—approaching 100% in some cases—suggesting that mutation of the trinucleotide repeat becomes the norm rather than the exception, while the rest of the genome remains genetically stable. These observations indicate that trinucleotide repeat expansions are localized in the genome and occur by novel mutational mechanisms. We searched for proteins that favor expansions and identified specific histone deacetylase complexes (HDACs)—comprising enzymes that remove acetyl groups from histones—in budding yeast and in human astrocytes. Interfering with these HDACs by mutation, RNA interference, or small molecule inhibitors blocked 50%–90% of expansion events. We also found that yeast HDACs promote expansions via a downstream deacetylation target, the nuclease Sae2. These results indicate that HDACs promote trinucleotide repeat expansions by modulating key proteins, which in turn catalyze the expansion. We postulate that HDAC inhibitors, currently being tested for relief of the transcription-related consequences of expansions, may have the beneficial side effect of reducing the risk of further somatic expansion.

Results

Yeast HDACs Rpd3L and Hda1 Promote CTG•CAG Repeat Expansions

If specific proteins promote TNR expansions, then mutants deficient in these proteins will have fewer expansions. A large-scale yeast mutant screen was performed to identify mutants with reduced expansion rates. Cells with a $(CTG)_{20}$-*CAN1* reporter (Figure 1A) were randomly mutagenized with a disruption library. A $(CTG)_{20}$ repeat tract was utilized, as this allele length is near the apparent threshold in yeast [18]. Reduced expansion rates are manifested as fewer canavanine resistant cells (Figure S1). Nine thousand disruptants, covering approximately 50% of non-essential genes, were subjected to several rounds of screening with increasing stringency. Eleven mutant genes were identified that consistently suppressed TNR expansions (Figure S1). Three of the 11 genes were *SIN3*, *PHO23*, and *HDA3*. *SIN3* encodes a subunit of histone deacetylases Rpd3L and Rpd3S, whereas the subunit encoded by *PHO23* is unique to Rpd3L. *HDA3* encodes a subunit of another HDAC, Hda1. The *hda3* mutant was found twice, along with single isolates of *sin3* and *pho23*. Thus, a blind screen pulled out three genes encoding components of Rpd3L and Hda1, an enrichment of ~100-fold compared to random chance. This clustering of mutations in related enzymes suggested a causal relationship between specific HDACs and TNR expansion.

Targeted knockouts of *sin3*, *pho23*, and *hda3* confirmed the gene assignments and allowed further analysis of expansions. Expansion rates were quantified using two reporters, *CAN1* (Figure 1A) and *URA3* [18], and all expansions were confirmed by PCR (Figure 1B). If an HDAC mutant primarily affects the instability at the triplet repeat, independently of the readout gene, then similar phenotypes would be expected for assays with *CAN1* and *URA3*. This outcome was observed (Figure 1C and Table S1). Single mutants of *sin3*, *pho23*, and *hda3* showed 9- to 18-fold reductions in expansion rates for the *CAN1* reporter integrated into chromosome II (Figure 1C, left panel). Expansion rates were reduced >1,000-fold in the double mutants *pho23 hda3* and *sin3 hda3*, which are simultaneously deficient in both Rpd3L and Hda1. When the reporter gene was *URA3*, a similar pattern of suppressed expansion rates occurred (Figure 1C, middle panel). The magnitude of the phenotype was somewhat smaller: 2- to 4-fold suppression in expansion rates for single HDAC mutants, and 10- to 18-fold for the double mutants. Thus, both *CAN1* and *URA3* reporters integrated at the same locus yielded similar outcomes, suggesting that Rpd3L and Hda1 affect instability of the TNR. To exclude a position effect, the *CAN1* reporter was relocated to an integration site on chromosome V. Suppression of expansions was again seen for the HDAC mutants (Figure 1C, right panel). Single mutants reduced expansion rates by 2- to 3-fold, while the *pho23 hda3* and *sin3 hda3* double mutants yielded 12- to 340-fold effects. In total (Figure 1C), the single mutants *sin3*, *pho23*, or *hda3* showed significant reduction in CTG expansion rates in seven of nine assays. All six assays using the double mutants, *pho23 hda3* or *sin3 hda3*, consistently gave lower expansion rates, and the double mutant effect was always stronger than for the single mutants. HDAC mutants in a common commercial strain, BY4741, also displayed reduced expansion rates for *CAN1* integrated at *LYS2*. Relative to wild type, expansion rates in the *sin3* mutant were strongly suppressed (>100-fold), with a milder phenotype for *pho23* (3-fold reduced), and a small but not statistically significant reduction of 1.7-fold for *hda3*. Overall, targeted knockout of Rpd3L and/or Hda1 suppressed expansion rates in most assays, and expansions were almost completely eliminated in some cases.

Expansion suppression could be phenocopied by treating wild type cells with trichostatin A (TSA), which inhibits many but not all HDACs [20]. TSA reduced expansion frequencies by 2.6-fold (Figure 1D) at a concentration that inhibits most HDAC activity of Rpd3 and Hda1 in vitro [21]. This finding is consistent with a published report showing that TSA-treated *Drosophila* had ~3-fold fewer expansions of a $(CAG)_{78}$ transgene, with preferential modulation of +1 repeat changes relative to other sizes [22]. In yeast, expansion sizes were similar with or without TSA, ranging from +6 to +19 repeats (Figure S2). Cells with impaired HDAC function showed the anticipated accumulation of acetylated histone H3, by nearly 5-fold in the *sin3 hda3* mutant and about 2.4-fold in wild type cells treated with TSA (Figure 1E). Compared to the HDAC mutants, TSA gave smaller effects on both expansion levels and the accumulation of acetylated histone H3, presumably due to incomplete inhibition by the drug.

Several control experiments eliminated trivial explanations of the HDAC effect on expansions. The range of expansion sizes was similar in wild type cells, HDAC mutants, and TSA-treated cells (Figures 1F and S2), indicating that HDAC status did not affect the genetic selection for expansions. Rather, the expansion size data suggest that HDACs likely govern initiation of expansions; there are fewer initiation events when HDACs are mutated or inhibited, but once the process is started the final size of the expansion is similar. There was no growth disadvantage of the HDAC mutants, with or without an expanded TNR, under conditions that select for expansions (Figures S3 and S4). *CAN1* transcript levels varied by 2-fold or less in the HDAC mutants (Table S2), showing no correlation with changes in expansion rates. Finally, suppression of expansions was primarily attributable to Rpd3L and Hda1, because only modest expansion phenotypes occurred in mutants defective in the alternative HDACs Rpd3S, Hos1, Hos2, Hos3, or Sir2 (Figure S5). In summary, mutation or chemical inhibition of yeast Rpd3L and Hda1 suppresses CTG repeat expansions by

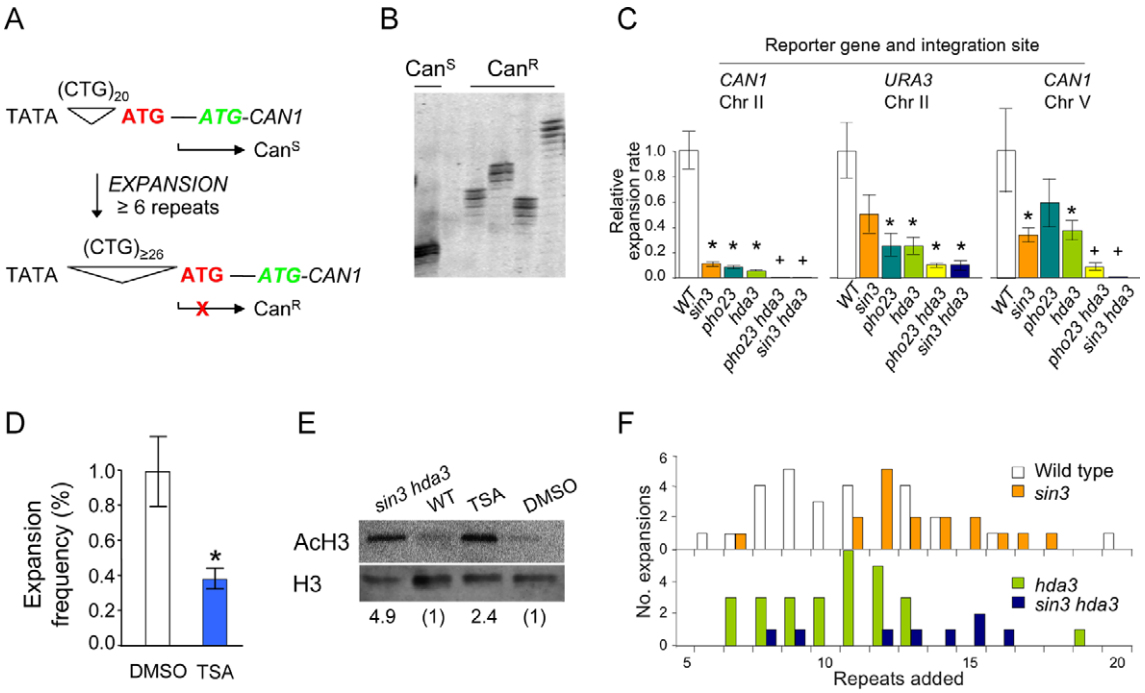

Figure 1. Mutation or chemical inhibition of yeast HDACs suppresses TNR expansions. (A) Reporter with $(CTG)_{20}$ permits expression of the reporter gene *CAN1*, and results in canavanine sensitivity. Expansions of ≥6 repeats alter transcription initiation, incorporating the out-of-frame ATG codon that blocks expression of *CAN1* (X). Canavanine resistance ensues. (B) PCR products displayed on a high-resolution polyacrylamide gel. All expansion results reported here include PCR validation. (C) Expansion rates in mutants of Rpd3L (*sin3* or *pho23*), Hda1 (*hda3*), or both (*pho23 hda3* or *sin3 hda3*). TNR reporter integration sites are indicated in the figure. Error bars, ±SEM; * $p<0.05$ compared to wild type; + $p<0.05$ compared to wild type and to each single mutant (details in Table S1). (D) Cells were grown 13–14 generations in liquid culture ±30 μg/ml TSA, followed by expansion analysis. Error bar, ± SEM; * $p=0.02$ compared to DMSO-only control, $n=5$ independent measurements. (E) Accumulation of acetylated histone H3 in yeast cells with impaired HDAC activity. Immunoblot results of 15 μg protein from whole cell lysates. Top, acetylated H3; bottom, total H3. Values below the blot show the ratio of acetylated H3/total H3. (F) Expansion sizes, derived from PCR analysis. 26 genetically independent expansions for wild type, 17 for *sin3*, 25 for *hda3*, and 8 for *hda3 sin3*.
doi:10.1371/journal.pbio.1001257.g001

50%–90%, with even greater effects in some mutant strains. These data support a mechanistic link between triplet repeat expansions and the yeast HDACs Rpd3L and Hda1.

Human HDAC3, a Homolog of Yeast Rpd3L, Promotes Expansions in Cultured Human Astrocytes

To address whether HDACs promote expansions in human cells, we focused on class I human HDACs, the homologs of yeast Rpd3 [23]. The small molecule inhibitor **4b** is selective for the class I enzyme HDAC3 but with some activity against HDAC1 [24]. **4b** treatment reverses *FXN* gene silencing in primary cells from Friedreich's ataxia patients [24] and relieves disease phenotype and transcriptional abnormalities in HD transgenic mice [25]. In light of the yeast experiments presented above, we posited that HDAC inhibition by **4b** might have the added benefit of suppressing expansions in human cells. To test this idea, CTG repeat expansions were measured in a cultured human astrocyte cell line, SVG-A. Glial cells such as astrocytes show somatic expansions in HD patients [26], and SVG-A cells support expansions in culture, as measured by the assay shown in Figure 2A [27].

4b efficiently suppresses TNR expansions in SVG-A cells at doses that are well tolerated. Treatment with **4b** reduced expansion frequencies in a dose-dependent manner (Figure 2B and Table S3). Compared to the DMSO-only control, expansion frequencies were suppressed 70% and 77% by **4b** at 10 μM and 20 μM, respectively. In contrast, treatment of SVG-A cells with an HDAC1- and HDAC2-selective inhibitor called compound **3** [28] did not suppress expansion frequencies (Figure 2B; small increases were not significant). Together, the inhibitor results suggest HDAC3 is the relevant target. Confirmation came from RNAi knockdowns. Knockdown of HDAC3 resulted in 76% reduction in expansion frequencies (Figure 2C), the same extent seen at the highest doses of **4b**, whereas knockdown of HDAC1 elevated the expansion frequency slightly but not to a statistically significant level. Inhibiting HDAC3 with **4b** or knocking it down changed the frequency of expansions, not their sizes (Figure 2D). Expansions added as many as 18 repeats to a starting tract of 22 repeats; thus, some expansions regulated by HDAC3 in SVG-A cells cross the threshold of 30–40 repeats observed in humans [2,4,16]. The reduced number of expansions upon **4b** treatment could not be attributed to increased cell death, because the SVG-A cells retained ≥83% viability, relative to DMSO-only control, even at the highest dose of inhibitor (Figure 2E). Molecular analysis of global histone H4 acetylation showed the anticipated increase in acetylated H4, up to about 10-fold, when cells were treated with **4b** (Figures 2F and S6). The opposite phenotype—increased expansions—was seen with RNAi knockdown of the histone acetyltransferases CREB-binding protein (CBP) and p300 (Figure 2G), consistent with observations in *Drosophila* [22]. We conclude that HDAC3 and CBP/p300 have opposing effects on expansions in SVG-A cells, with HDAC3 promoting TNR expansions.

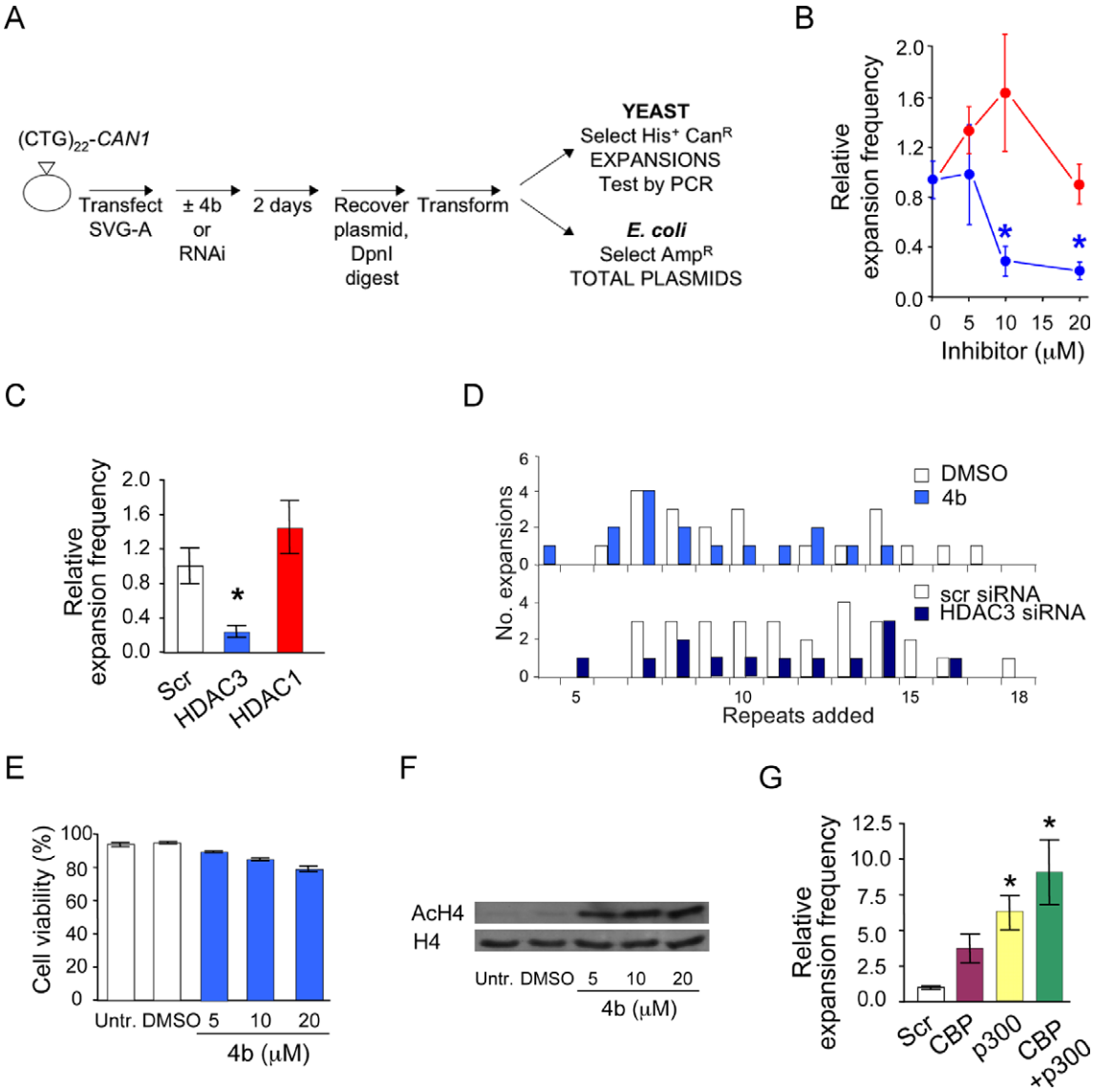

Figure 2. Chemical inhibition or RNAi knockdown of HDAC3 in human SVG-A cells suppresses expansions. (A) The genetic assay is essentially as described [27]. Cells were treated with either HDAC inhibitor **4b**, compound **3**, or DMSO only. Alternatively, siRNA was used with scrambled siRNA as a control. Expansions are scored using yeast as a biosensor, and total plasmid counts are monitored by bacterial transformation for enhanced sensitivity. (B) Expansion frequencies as a function of inhibitor dose, compared to DMSO-treated control cells. Blue, **4b**-treated; red, compound **3**-treated. Error bar, ±SEM; * $p<0.05$ compared to DMSO-treated cells. Details in Table S3. (C) Expansion frequency after RNAi. Knockdown efficiency, judged by three independent immunoblots, averaged 76(±8)% for HDAC3 and 76(±2)% for HDAC1. Error bars, ±SEM; * $p<0.05$ compared to scrambled control. Details in Table S3. (D) Expansion sizes, derived from PCR analysis. 21 genetically independent expansions for DMSO, 16 for **4b** (combined data from 10 μM and 20 μM treatments), 28 for scrambled siRNA, and 13 for HDAC3 siRNA. (E) Cell viability measured by nigrosin staining just prior to cell harvest. (F) Representative immunoblot of acetylated histone H4 and total histone H4 upon treatment with **4b**; data summary in Figure S6. (G) Expansion frequencies after RNAi against histone acetyltransferases. Error bars, ±SEM; * $p<0.05$ compared to scrambled control.
doi:10.1371/journal.pbio.1001257.g002

Rpd3L and Hda1 Promote Expansions in Trans, Partly through Sae2

We first tested the idea that expansion rates are suppressed in cis by hyperacetylation of histones near the repeat tract, as might occur in HDAC mutants. The approach took advantage of previous studies showing that transcription and histone acetylation at some yeast genes are particularly sensitive to the absence of *SIN3*. One such locus is the *INO1* gene, which we refer to as a "hot" zone. In *sin3* mutants compared to wild type, transcript levels increase about 30-fold [20,29] and histone acetylation increases 3.6- to 5-fold [30,31] at *INO1*. If expansions are sensitive to local histone acetylation, then integration of the TNR reporter at *INO1* should give an enhanced *sin3* phenotype, i.e. show greater suppression of expansions. Similarly, there should be less *sin3* phenotype on expansions at a "cold" zone like *SPS2* whose expression and histone acetylation is nearly unaffected in a *sin3* mutant [20,29,30]. The results indicate otherwise (Figure 3A). For both integration sites, hot and cold, the effect of *sin3* on expansions was similar (6.4-fold suppression at *INO1*, 5.7-fold at *SPS2*). Nearly identical suppression effects were seen when the reporter was integrated at another relatively cold locus, *LYS2* (8.8-fold; Figure 1C, left panel), or at another hot zone locus, *IME2* (8.8-fold; unpublished data).

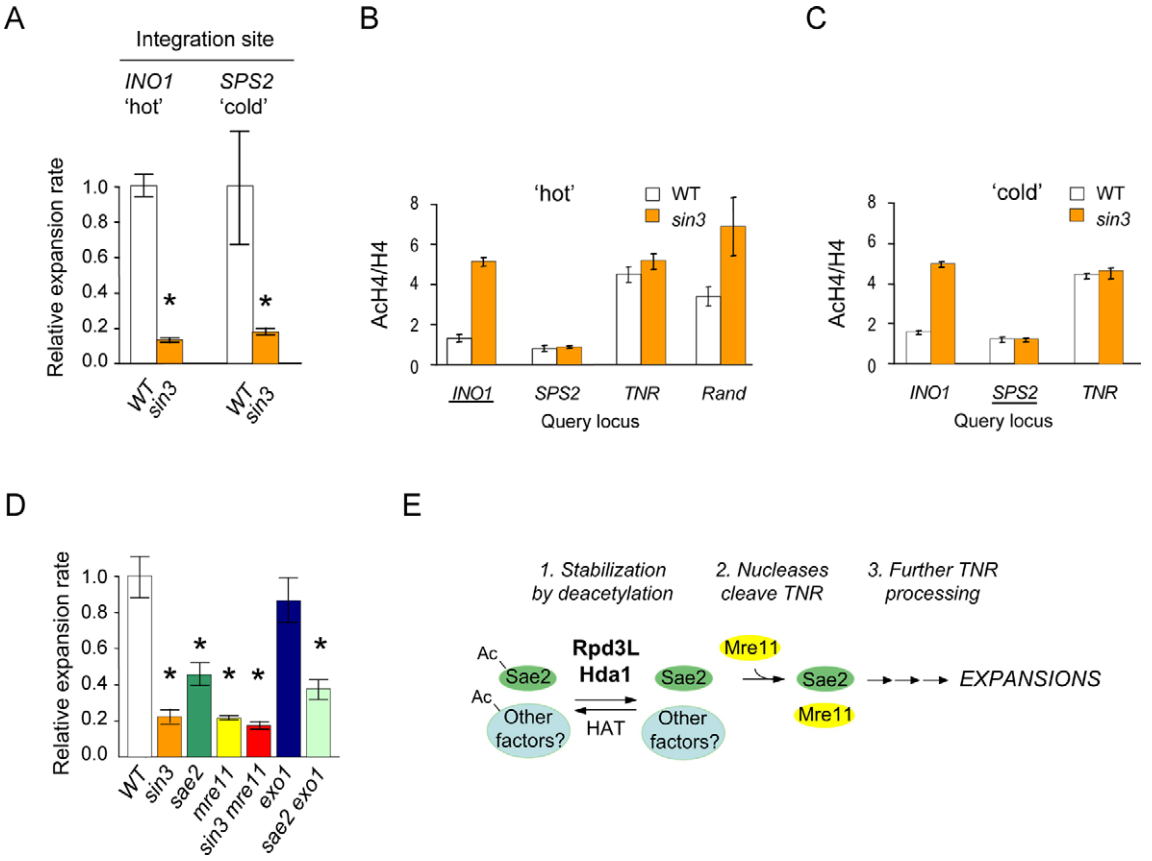

Figure 3. Evidence that Rpd3L acts in trans to promote expansions. (A) *sin3* mutants suppress expansion rates when the TNR reporter is integrated at "hot" zone, *INO1* on chromosome X and a "cold" zone, *SPS2* on chromosome IV. Error bars, ±SEM; * $p<0.05$ compared to wild type. (B, C) Chromatin immunoprecipitation using antibodies against pan-acetylated histone H4 or total H4. Underline indicates the TNR reporter integration site at *INO1* (B) or *SPS2* (C). Rand, control reporter with randomized sequence in place of triplet repeat. Error bars, ±SEM. Primer site details are provided in Figure S8. (D) Expansion rates in single or double mutants of *sae2*, *mre11*, *exo1*, and/or *sin3*. The reporter was $(CTG)_{20}$-*CAN1* integrated on chromosome II. Error bars, ±SEM; * $p<0.05$ compared to wild type. Details for panels (A–D) are in Table S4. (E) Model for HDAC promotion of expansions in yeast. 1. Acetylated Sae2 (Ac-Sae2) is marked for degradation, but it is stabilized by deacetylation in an Rpd3L- and Hda1-dependent manner [32]. The same HDACs may deacetylate other factors relevant to expansions, thereby stabilizing them or influencing their activities. The action of Rpd3L and Hda1 is counterbalanced by one or more HATs that await identification. 2. Sae2 along with another nuclease, Mre11, cleaves TNR DNA, possibly in a hairpin structure, to initiate the expansion pathway. 3. The cleaved TNR undergoes additional processing steps to complete the expansion.
doi:10.1371/journal.pbio.1001257.g003

Confirmation studies of chromatin acetylation at the TNR locus led to an unanticipated result. Chromatin immunoprecipitation (ChIP) was used to evaluate pan-acetylation of histone H4 compared to total H4 at *INO1*, *SPS2*, and the TNR reporter (Figure 3B and C). H4 acetylation at *INO1* was increased 3- to 5-fold in the *sin3* mutant as expected for a hot zone, while H4 acetylation at *SPS2* was low in both the wild type and *sin3* strains, typical of a cold zone. These findings are independent of the integration site of the TNR reporter (compare Figure 3B and 3C), indicating that insertion of the reporter does not alter acetylation levels at either integration locus. Unexpectedly, we found that histones near the TNR are hyperacetylated, regardless of *SIN3* status, to about the same level as *INO1* in the *sin3* mutant (Figure 3B and C). Hyperacetylation seems to be conferred in part by the trinucleotide repeat, because a control reporter with a randomized sequence in lieu of the TNR yielded a greater dependence of histone acetylation on *SIN3* status ("Rand," Figure 3B). Although the TNR is not uniquely responsible for hyperacetylation of nearby histones (Figure S7), it does contribute.

We concluded from the results in Figure 3A–C that HDACs most likely promote expansions in trans, perhaps by controlling the expression or stability of factors that expand the TNR. The nuclease Sae2 was investigated because a recent study showed Sae2 is stabilized by deacetylation in an Rpd3- and Hda1-dependent manner [32]. Furthermore, Sae2, along with the Mre11/Rad50/Xrs2 complex, is known to process hairpin DNA in vivo and in vitro [33,34]. Since TNR expansions are thought to involve structured intermediates such as a hairpin [2–4], we tested the idea that an *sae2* mutant would suppress expansions. The *sae2* mutant partially suppressed expansions when compared side-by-side with a *sin3* mutant (Figure 3D), consistent with the idea that Sae2 is one (but not the sole) relevant target of Rpd3. Mutation of the nuclease encoded by *MRE11* suppressed expansions as much as the *sin3* mutant (Figure 3D). Although Rpd3 is not known to directly regulate Mre11, the expansion phenotype of the *mre11* mutant is consistent with the possibility that HDACs stabilize Sae2, which then works together with Mre11 to promote expansions. In support of this idea, the expansion phenotype of the *sin3 mre11* double mutant was indistinguishable from those of the *sin3* and *mre11* single mutants (Figure 3D). In contrast, loss of the Exo1 exonuclease showed no effect on expansions, and the *sae2 exo1* double mutant was no more defective than the *sae2* single

mutant (Figure 3D). Together, the results of Figure 3 suggest that yeast Rpd3L and Hda1 promote expansions in trans through the nucleases Sae2 and Mre11.

Discussion

This study reveals that yeast Rpd3L and Hda1 and human HDAC3 promote expansions of threshold-length triplet repeats in budding yeast and human astrocytes. Interfering with HDAC function through mutation, RNAi knockdown, or small molecule inhibitors eliminates most expansions. It is striking that yeast Rpd3 and Hda1 elicit opposite effects on genetic stability depending on the genomic context; these HDACs accelerate mutagenesis at triplet repeats, whereas they favor chromosome stability via the DNA damage response and processing of double strand breaks [32]. We also found that the human HATs encoded by CBP and p300 have the contravening effect of stabilizing triplet repeats. The latter finding complements an earlier report that CBP modulates instability of long repeats in *Drosophila* [22]. The relevant yeast HAT remains to be identified. The identification of HDACs as promoting factors and the protective action of HATs emphasizes the importance of protein acetylation/deacetylation to expansions. The mechanistic and therapeutic implications of these findings are considered below.

As in double strand break processing [32], one downstream target of Rpd3L and Hda1 is likely to be the nuclease Sae2. We propose a model where Rpd3L and Hda1 positively regulate Sae2 by stabilizing it. Sae2 and Mre11 then function together as nucleases to promote expansions (Figure 3E). This model is based in part on the study of Robert et al., who found that acetylated Sae2 is degraded by autophagy, but that Sae2 is stabilized by deacetylation in an Rpd3- and Hda1-dependent manner [32]. Also consistent with the Robert et al. work, we infer that Sae2 is not the only relevant target of these HDACs because the expansion phenotype of a *sae2* mutant is not as strong as for *sin3* (Figure 3D). Other factors, currently unknown, are also proposed to be regulated by Rpd3 and Hda1 and to contribute to expansions by mechanisms that remain to be elucidated (Figure 3E). Sae2 and Mre11 (acting in the Mre11/Rad50/Xrs2 complex) are known to process hairpin DNA in vivo and in vitro [33,34]. It remains to be determined whether these enzymes actually process a TNR hairpin intermediate to accelerate expansions. The effects of Sae2 and Mre11 have also been examined for expansions of long $(CAG)_{70}$ repeats [19]. In this study, expansion frequencies increased in *sae2* or *mre11* mutants. One likely explanation is that long alleles in yeast break more frequently than do the shorter alleles we utilize; thus, long repeats in yeast rely on double strand break repair to prevent expansions [19]. In support of this possibility, expansions of $(CAG)_{70}$ are also enhanced by loss of the recombination proteins Rad51 and Rad52 [19], whereas *rad51* or *rad52* mutants do not affect expansion rates of CTG alleles between 13 and 25 repeats [35,36]. The outcomes of Sae2 and Mre11 activity could be different in break repair than in putative hairpin processing described above.

We found that yeast HDAC mutants suppress expansions in nearly all assays (Figure 1C), but quantitative differences in phenotype illustrate that some aspects of HDAC regulation of expansions remain unknown. What other factors regulated by yeast Rpd3L and Hda1 or human HDAC3 might contribute to expansions? One possibility is chromatin structure near but not immediately adjacent to the repeat. The triplet repeat literature contains several connections between expansions and proteins that modulate chromatin structure, including *Drosophila* CBP [22] mentioned above, the insulator protein CTCF [37,38], and the DNA methyltransferase Dnmt1 [39]. A second possibility is that HDACs promote expansions by controlling the firing of DNA replication origins [40–43]. The major finding against the origin firing model is that similar *SIN3*-dependent promotion of expansions was seen when our yeast reporter was integrated at four different loci (*LYS2*, *INO1*, *SPS2*, and *IME2*; Figures 1 and 3), which are 21–130 kb away from the nearest origins that become deregulated in *rpd3Δ* cells [42]. We feel it is unlikely that Rpd3-dependent origin firing explains suppression of expansions, although HDAC effects on fork progression or fork stalling cannot be ruled out at this time.

HDAC inhibitors are currently being evaluated as therapies to treat the transcriptional defects in several TNR expansion diseases [44,45]. For example, **4b** treatment reverses *FXN* gene silencing in primary cells from Friedreich's ataxia patients [24] and relieves disease phenotype and transcriptional abnormalities in HD transgenic mice [25]. Our work implies these inhibitors may have a second, beneficial effect of suppressing somatic expansions that contribute to disease progression.

Materials and Methods

Genetic Assays and Analysis of Expanded TNR Alleles

Triplet repeat expansion assays using the *URA3* reporter have been described previously [18,27]. Assays using the *CAN1* reporter (Figure 1A) utilized canavanine at 60 μg/ml to select for resistance. All expansions were verified by single-colony PCR across the repeat tract followed by analysis on high-resolution polyacrylamide gels [18]. Details of statistical analysis are provided in Tables S1 and S4.

Western Blot Analysis

Whole cell lysates (yeast and SVG-A astrocytes) or histone acid extracts (SVG-A astrocytes) were separated electrophoretically and transferred to PVDF membranes. Primary rabbit antibodies were against histone H3 (A300-823A, Bethyl Laboratories), acetyl-histone H3 (#17-615, Millipore), acetyl-histone H4 (#06-866, Millipore), β-actin (A2066, Sigma-Aldrich), HDAC3 (sc-11417, Santa Cruz Biotechnology), and HDAC1 (CH00218, Coriell Institute for Medical Research). Assessment of HDAC3 expression via Western blot analysis resulted in two bands around 50 kDa, the predicted size of the protein, presumably representing the two reported isoforms of HDAC3 [46]. Throughout all experiments, consistent knockdown of the top band was observed following HDAC3 siRNA treatment, however levels of the bottom band varied between experiments. Quantitation of HDAC3 knockdown was performed by densitometric analysis of the top band only. A mouse antibody was used against histone H4 (ab31830, Abcam). Secondary antibodies conjugated to horseradish peroxidase were 711-035-152 and 115-035-003 from Jackson ImmunoResearch Laboratories. Visualization was by chemilluminescence (Western Lightning Plus-ECL, PerkinElmer).

Chromatin Immunoprecipitation

250 ml yeast cell cultures were grown to A_{600}~0.8 at 30° in yeast extract/peptone/dextrose. Following cross-linking with 1% formaldehyde (15 min, 22°), cross-linked chromatin was isolated in lysis buffer containing 50 mM HEPES/KOH pH 7.5, 140 mM NaCl, 1 mM EDTA, 1% Triton X-100%, 0.1% sodium deoxycholate and the protease inhibitors 1 mM PMSF, 1 mM benzamidine, 1 μg/ml leupeptin, and 1 μg/ml pepstatin. After sonication (40% duty cycle for seven cycles of 5 s each with

50 s cooling in between; Digital Sonifier EDP 100-214-239, Branson), chromatin fragments were immunoprecipitated with antibodies specific for total histone H4 (5 μg, A300-646A, Bethyl Laboratories) or pan-acetylated H4 (7 μl, # 06-866, Millipore) at 4°C overnight. Immune complexes were captured by incubating with Protein G magnetic beads (S1430S, New England BioLabs) for 4 h at 4°C. After a series of washes, DNA was eluted in 250 μl elution buffer (50 mM Tris-HCl pH 8, 10 mM EDTA, and 1% SDS) and crosslinks were reversed by incubating overnight at 65°C. DNA was purified by phenol-chloroform extraction followed by an ethanol precipitation and analyzed by quantitative PCR (Applied Biosystems, 7500 FAST). Primer sequences used for quantitative PCR are provided in the Supporting Information section. Signals for total H4 and acetylated H4 were quantified by the method of $2^{-\Delta\Delta Ct}$ and normalized using the following calculation: (C_t immunoprecipitate$-C_t$ input)$-$(C_t background$-C_t$ input). Amplification of the chromosome VI telomere region was chosen as a measurement for background [31,47]. The normalized IP values obtained for acetylated H4 were divided by the normalized IP values for total H4.

Reverse Transcription-PCR

Cells were grown to mid-log phase and then extracted with hot acidic phenol. Following clean-up of the RNA, reverse transcription was performed in triplicate. cDNA levels were analyzed in triplicate by quantitative real-time PCR and normalized to *ALG9* levels. Details and primer sequences are provided in Table S2.

Shuttle Vector Assays and Molecular Analysis of Protein Components

SVG-A astrocytes were seeded in 60 mm tissue culture dishes and transfected with 5 μg shuttle vector DNA using Lipofectamine 2000 (Invitrogen Corporation). After 6 h, the DMEM transfection media was replaced by DMEM supplement with 10% fetal bovine serum, plus one of the HDAC inhibitors **4b** or compound **3** (kindly provided by Joel Gottesfeld, The Scripps Research Institute) or DMSO only. Cells were incubated for an additional 48 hours, then samples were taken for either expansion assay or histone analysis. To measure expansions, plasmid DNA was extracted and concentrated by using Hirt's alkaline lysis [48] and Amicon Ultra 50 K centrifugal filter units (Millipore). Purified plasmid DNA was digested by DpnI (New England Biolabs) and then transformed into *S. cerevisiae* for measurement of canavanine resistance or into *E. coli* for analysis of total plasmid numbers as measured by ampicillin-resistant colonies. Histone extracts were prepared by acid extraction (protocol provided by Abcam).

RNA interference experiments were performed with minor variations. SVG-A cells were seeded and transfected with ON-TARGET plus or siGenome SMARTpool siRNAs (100 nM) against HDAC3 (L-003496, M-003496), HDAC1 (M-003493), or scrambled non-targeting siRNA (D-001810) from Dharmacon using DharmaFECT 1. After 48 h, cells were transfected with 7 μg of shuttle vector and also re-transfected with siRNAs using Lipofectamine 2000. After another 2 d, expansion frequencies were prepared as above, in parallel with immunoblot analysis of whole cell lysates.

Statistical Analyses

All p values were determined by two-tailed Student's t test. p and n values for each data set are specified in Tables S1, S2, S3, S4 unless stated in the figure legend.

Supporting Information

Figure S1 Identification of mutants with reduced expansion rates. (A) Overview of screen and results. (B) Schematic of replica plating strategy to identify relevant mutants.
(TIF)

Figure S2 Expansion sizes in yeast ± TSA. Expansion sizes were measured by PCR and high-resolution gel electrophoresis to within ±2 repeats. All expansions are genetically independent. The histogram shows the spectra from 42 expansions seen in cells treated with DMSO (unfilled bars), or from 39 expansions from cells treated with 30 μg/ml TSA (blue-filled bars).
(TIF)

Figure S3 Survival of *sin3*, *pho23*, and *hda3* mutants on canavanine- or 5FOA-containing media. This experiment tests whether HDAC mutants without a triplet repeat reporter show any innate sensitivity to canavanine or 5FOA, the compounds used to select expansions from the *CAN1* and *URA3* reporters, respectively. If there were any innate sensitivity, then expansion assays with the HDAC mutants might give low apparent expansion rates for reasons unrelated to the triplet repeats themselves. For each strain, spontaneous deletion of the reporter ("pop-out") was identified genetically. Cells from each reporter-less strain were grown in YPD medium to mid-log phase, and serial 10-fold dilutions were spotted onto control media (SC-Ura, left) or selective media (center and right). The plates were incubated at 30° for 6 d and then photographed. Selection was for canavanine resistance (top) or 5FOA resistance (bottom). Low concentrations of Can or 5FOA were used to magnify any difference in sensitivities of wild type controls versus HDAC mutants. The results indicate similar growth rates for wild type and HDAC mutants on the control media (left) and plates with low (center) or high drug concentrations (center). Based on these experiments, we conclude there is no evidence for innate sensitivity of the HDAC mutants to canavanine or 5FOA. Therefore, low expansion rates in the HDAC mutants cannot be attributed to the selection method.
(TIF)

Figure S4 Growth tests of *sin3*, *pho23*, and *hda3* mutants containing an expanded repeat on canavanine-containing media. This experiment tests whether HDAC mutants with an expanded CTG repeat grow similarly to wild type on selective media. The result will tell whether a hypothetical slow-growth phenotype in HDAC mutants on selective media could lead to undercounting of Can resistant colonies, thus imitating low expansion rates. For each strain, a spontaneous expansion was identified that contained circa 33 CTG repeats, based on PCR analysis (Figure 1B). The cells were then resuspended in water, and serial 10-fold dilutions were spotted onto complete media (top panel) or canavanine-containing media. The cells were incubated at 30° for 2 d (top panel) or 6 d (bottom panel). The time, temperature, and selective media are all the same as used when measuring expansion rates. The results indicate similar growth rates, and clearly visible colonies, for all the HDAC mutants and the wild type control strain. We conclude that the reduced expansion rates in the HDAC mutants cannot be attributed to slow growth on canavanine-containing media.
(TIF)

Figure S5 Expansion rate data for alternative HDACs. This experiment tests whether mutation of any HDAC besides Rpd3L or Hda1 gives reduced rates of expansion for the (CTG)20-*CAN1* reporter integrated on chromosome II. For each strain, expansion rates were measured as described in Materials and Methods. Data

for *sin3*, *pho23*, and *hda3* strains are reproduced from Figure 1C for comparison. Error bars represent ±1 SEM. The results indicate that the additional HDAC mutants tested yielded small expansion phenotypes compared to *sin3*, *pho23*, or *hda3*.
(TIF)

Figure S6 Accumulation of acetylated histone H4 upon treatment of SVG-A cells with the HDAC inhibitor 4b. These results are from four independent measurements of acetylated histone H4 (AcH4) and total H4 by immunoblot. One representative blot is shown in Figure 2E. The graph below shows the AcH4/Total H4 ratio normalized to the DMSO-only control. Error bars denote ±1 SEM. * $p<0.05$ compared to untreated.
(TIF)

Figure S7 Histone acetylation levels at *LYS2*. Chromatin immunoprecipitation (ChIP) was used to measure acetylated histone H4 (AcH4) and total H4 levels. Results were measured by real-time PCR of the *LYS2* promoter. Primer positions for each gene are shown in Figure S8. The *x*-axis indicates strains with the TNR reporter integrated at different genomic loci. Bars are average of three measurements. Error bars reflect ±1 SEM.
(TIF)

Figure S8 Position of ChIP primers. Real-time PCR was used to quantify the ChIP signals in Figure 3 and Figure S7. Shown below are the primer positions (not to scale) when the TNR reporter was integrated at the query loci. The 4.3–6 kb distance between the query site primers and the TNR primers make it likely that the two amplicons were derived from independent template fragments. In each case the target locus was disrupted by the reporter; for example *IN…O1* indicates disruption of the *INO1* gene.
(TIF)

Table S1 Expansion rate analysis in yeast HDAC mutants. All rate data are expressed as expansions per cell generation. *n*, number of independent rate measurements; SEM, standard error of the mean; *p* values calculated by Student's *t* test.
(TIF)

Table S2 Expansion suppression and transcript levels in HDAC mutants. Expansion suppression values are from Table S1. Transcript levels were measured in triplicate from three independent cDNA preparations. For RNA preparation, yeast cells from overnight cultures were grown in YPD to an A600 of 0.6. Cultures were then centrifuged at room temperature for 5 min at 4,000 rpm, washed in sterile water, and centrifuged again. RNA extraction was performed using hot acidic phenol as described previously (http://www.transcriptome.ens.fr/sgdb/protocols/preparation_yeast.php). A maximum of 100 µg of RNA was used for clean-up. The RNeasy Mini Kit (Qiagen) was used for the RNA clean up, which included the on-column DNase digestion. 1 µg of total RNA was reverse-transcribed in triplicate into cDNA using random nonamer primers in a 20 µl reaction mixture using the Primerdesign Precision qScript Reverse Transcription kit. The cDNA levels were then analyzed using the Applied Biosystems 7500 FAST. Each cDNA sample replicate was tested in triplicate in a 96-well plate, and values were normalized to *ALG9* expression. The reaction mix consisted of 10 µl of Fast SYBR Green Master Mix (Applied Biosystems) in final volume of 20 µl. A blank (no template control) was also incorporated into each assay. Relative expression levels were determined using the method of $2^{-\Delta\Delta Ct}$. Primer sequences were: rtCAN1F, CGA ATG GCT ATT AAA TAT CAC TGG TGT TGC; rtCAN1R, GAA TTT TGG TGC AAA AGC CGT GAA ACC TTG; rtALG9F, CAC GGA TAG TGG CTT TGG TGA ACA ATT AC; rtALG9R, TAT GAT TAT CTG GCA GCA GGA AAG AAC TTG GG.
(TIF)

Table S3 Expansion frequencies in SVG-A cells. Expansion frequencies (defined in Materials and Methods and in the legend to Figure 2) were normalized to frequencies from control cells, as indicated. *n*, number of independent experiments; SEM, standard error of the mean. *p* values were calculated by two-tailed Student's *t* test. Background expansions were estimated at 0.06±0.04 relative expansion frequency. Absolute frequencies of expansions, expressed as verified expansions per 100,000 *E. coli* transformants, were: 44±22 for HDAC inhibitor 4b experiments; 220±24 for HDAC3 and HDAC1 knockdown experiments; and 120±76 for CBP, p300, and CBP+p300 knockdowns. Knockdown efficiencies were estimated by immunoblot at 75%–80% for single knockdowns of CBP or p300, and 80%–85% each for the double knockdown.
(TIF)

Table S4 Data for expansions and ChIP at *INO1* and *SPS2*, and expansion rate analysis in yeast nuclease mutants. *n*, number of independent experiments; SEM, standard error of the mean; *p* values calculated by two-tailed Student's *t* test.
(TIF)

Acknowledgments

We thank Joel Gottesfeld (The Scripps Research Institute) for providing the HDAC inhibitors **4b** and compound **3**.

Author Contributions

The author(s) have made the following declarations about their contributions: Conceived and designed the experiments: KD AF TM RSL. Performed the experiments: KD AF OG LK-M. Analyzed the data: KD AF OG LK-M RSL. Contributed reagents/materials/analysis tools: KD AF OG LK-M TM. Wrote the paper: KD AF RSL.

References

1. Orr HT, Zoghbi HY (2007) Trinucleotide repeat disorders. Annu Rev Neurosci 30: 575–621.
2. Mirkin SM (2007) Expandable DNA repeats and human disease. Nature 447: 932–940.
3. Castel AL, Cleary JD, Pearson CE (2010) Repeat instability as the basis for human diseases and as a potential target for therapy. Nat Rev Mol Cell Biol 11: 165–170.
4. McMurray CT (2010) Mechanisms of trinucleotide repeat instability during human development. Nat Rev Genet 11: 786–799.
5. Fu Y-H, Kuhl DPA, Pizzuti A, Pieretti M, Sutcliffe JS, et al. (1991) Variation of the CGG repeat at the fragile X site results in genetic instability: resolution of the Sherman paradox. Cell 67: 1047–1058.
6. Manley K, Shirley TL, Flaherty L, Messer A (1999) *Msh2* deficiency prevents *in vivo* somatic instability of the CAG repeat in Huntington disease transgenic mice. Nat Genet 23: 471–473.
7. Kovtun IV, McMurray CT (2001) Trinucleotide expansion in haploid germ cells by gap repair. Nat Genet 27: 407–411.
8. van den Broek WJAA, Nelen MR, Wansink DG, Coerwinkel MM, te Riele H, et al. (2002) Somatic expansion behaviour of the (CTG)n repeat in myotonic dystrophy knock-in mice is differentially affected by Msh3 and Msh6 mismatch-repair proteins. Hum Mol Genet 11: 191–198.
9. Savouret C, Brisson E, Essers J, Kanaar R, Pastink A, et al. (2003) CTG repeat instability and size variation timing in DNA repair-deficient mice. EMBO J 22: 2264–2273.
10. Wheeler VC, Lebel L-A, Vrbanac V, Teed A, te Riele H, et al. (2003) Mismatch repair gene *Msh2* modifies the timing of early disease in HdhQ111 striatum. Hum Mol Genet 12: 273–281.
11. Gomes-Pereira M, Fortune MT, Ingram L, McAbney JP, Monckton DG (2004) Pms2 is a genetic enhancer of trinucleotide CAG•CTG repeat somatic

mosaicism: implications for the mechanism of triplet repeat expansion. Hum Mol Genet 13: 1815–1825.
12. Kovtun IV, Liu Y, Bjoras M, Klungland A, Wilson SH, et al. (2007) OGG1 initiates age-dependent CAG trinucleotide expansion in somatic cells. Nature 447: 447–452.
13. Hubert L, Jr., Lin Y, Dion V, Wilson JH (2011) Xpa deficiency reduces CAG trinucleotide repeat instability in neuronal tissues in a mouse model of SCA1. Hum Mol Genet 20: 4822–4830.
14. Owen BAL, Yang Z, Lai M, Gajek M, Badger JD, II, et al. (2005) (CAG)n-hairpin DNA binds to Msh2-Msh3 and changes properties of mismatch recognition. Nat Struct Mol Biol 12: 663–670.
15. Brinkmann RR, Mezei MM, Theilmann J, Almqvist E, Hayden MR (1997) The likelihood of being affected with Huntington disease by a particular age, for a specific CAG size. Am J Hum Genet 60: 1202–1210.
16. Paulson HL, Fischbeck KH (1996) Trinucleotide repeats in neurogenetic disorders. Annu Rev Neurosci 19: 79–107.
17. Leeflang EP, Zhang L, Tavare S, Hubert R, Srinidhi J, et al. (1995) Single sperm analysis of the trinucleotide repeats in the Huntington's disease gene: quantification of the mutation frequency spectrum. Hum Mol Genet 4: 1519–1526.
18. Rolfsmeier ML, Dixon MJ, Pessoa-Brandao L, Pelletier R, Miret JJ, et al. (2001) Cis-elements governing trinucleotide repeat instability in *Saccharomyces cerevisiae*. Genetics 157: 1569–1579.
19. Sundararajan R, Gellon L, Zunder RM, Freudenreich CH (2010) Double-strand break repair pathways protect against CAG/CTG repeat expansions, contractions and repeat-mediated chromosomal fragility in *Saccharomyces cerevisiae*. Genetics 184: 65–77.
20. Bernstein BE, Tong JK, Schreiber SL (2000) Genomewide studies of histone deacetylase function in yeast. Proc Natl Acad Sci U S A 97: 13708–13713.
21. Lin Y-Y, Qi Y, Lu J-Y, Pan X, Yuan DS, et al. (2008) A comprehensive synthetic genetic interaction network governing yeast histone acetylation and deacetylation. Genes Dev 22: 2062–2074.
22. Jung J, Bonini N (2007) CREB-binding protein modulates repeat instability in a Drosophila model for polyQ disease. Science 315: 1857–1859.
23. Yang X-J, Seto E (2008) The Rpd3/Hda1 family of lysine deacetylases: from bacteria and yeast to mice and men. Nat Rev Mol Cell Biol 9: 206–218.
24. Herman D, Jenssen K, Burnett R, Soragni E, Perlman SL, et al. (2006) Histone deacetylase inhibitors reverse gene silencing in Friedreich's ataxia. Nat Chem Biol 2: 551–558.
25. Thomas EA, Coppola G, Desplats PA, Tang B, Soragni E, et al. (2008) The HDAC inhibitor 4b ameliorates the disease phenotype and transcriptional abnormalities in Huntington's disease transgenic mice. Proc Natl Acad Sci U S A 105: 15564–15569.
26. Shelbourne PF, Keller-McGandy C, Bi WL, Yoon SR, Dubeau L, et al. (2007) Triplet repeat mutation length gains correlate with cell-type specific vulnerability in Huntington disease brain. Hum Mol Genet 16: 1133–1142.
27. Claassen DA, Lahue RS (2007) Expansions of CAG•CTG repeats in immortalized human astrocytes. Hum Mol Genet 16: 3088–3096.
28. Xu C, Soragni E, Chou CJ, Herman D, Plasterer HL, et al. (2009) Chemical probes identify a role for histone deacetylase 3 in Friedreich's ataxia gene silencing. Chem Biol 16: 980–989.
29. Fazzio TG, Kooperberg C, Goldmark JP, Neal C, Basom R, et al. (2001) Widespread collaboration of Isw2 and Sin3-Rpd3 chromatin remodeling complexes in transcriptional repression. Mol Cell Biol 21: 6450–6460.
30. Rundlett SE, Carmen AA, Suka N, Turner BM, Grunstein M (1998) Transcriptional repression by UME6 involves deacetylation of lysine 5 of histone H4 by RPD3. Nature 392: 831–835.
31. Carrozza MJ, Li B, Florens L, Suganuma T, Swanson SK, et al. (2005) Histone H3 methylation by Set2 directs deacetylation of coding regions by Rpd3S to suppress spurious intragenic transcription. Cell 123: 581–592.
32. Robert T, Vanoli F, Chiolo I, Shubassi G, Bernstein KA, et al. (2011) HDACs link the DNA damage response, processing of double-strand breaks and autophagy. Nature 471: 74–79.
33. Lobachev KS, Gordenin DA, Resnick MA (2002) The Mre11 complex is required for repair of hairpin-capped double-strand breaks and prevention of chromosome rearrangements. Cell 108: 183–193.
34. Lengsfeld BM, Rattray AJ, Bhaskara V, Ghirlando R, Paull TT (2007) Sae2 is an endonuclease that processes hairpin DNA cooperatively with the Mre11/Rad50/Xrs2 complex. Mol Cell 28: 638–651.
35. Miret JJ, Pessoa-Brandao L, Lahue RS (1998) Orientation-dependent and sequence-specific expansions of CTG/CAG trinucleotide repeats in *Saccharomyces cerevisiae*. Proc Natl Acad Sci U S A 95: 12438–12443.
36. Bhattacharyya S, Lahue RS (2004) Yeast Srs2 DNA helicase selectively blocks expansions of trinucleotide repeats. Mol Cell Biol 24: 7324–7330.
37. Filippova GN, Thienes CP, Penn BH, Cho DH, Hu YJ, et al. (2001) CTCF-binding sites flank CTG/CAG repeats and form a methylation-sensitive insulator at the DM1 locus. Nat Genet 28: 335–343.
38. Libby RT, Hagerman KA, Pineda VV, Lau R, Cho DH, et al. (2008) CTCF cis-regulates trinucleotide repeat instability in an epigenetic manner: a novel basis for mutational hot spot determination. PLoS Genet 4: e1000257. doi:10.1371/journal.pgen.1000257.
39. Dion V, Lin Y, Hubert Jr. L, Waterland RA, Wilson JH (2008) Dnmt1 deficiency promotes CAG repeat expansion in the mouse germline. Hum Mol Genet 17: 1306–1317.
40. Vogelauer M, Rubbi L, Lucas I, Brewer BJ, Grunstein M (2002) Histone acetylation regulates the time of replication origin firing. Mol Cell 10: 1223–1233.
41. Aparicio JG, Viggiani CJ, Gibson DG, Aparicio OM (2004) The Rpd3-Sin3 histone deacetylase regulates replication timing and enables intra-S origin control in *Saccharomyces cerevisiae*. Mol Cell Biol 24: 4769–4780.
42. Knott SRV, Viggiani CJ, Tavare S, Aparicio OM (2009) Genome-wide replication profiles indicate an expansive role for Rpd3L in regulating replication initiation timing or efficiency, and reveal genomic loci of Rpd3 function in *Saccharomyces cerevisiae*. Genes Dev 23: 1077–1090.
43. Unnikrishnan A, Gafken PR, Tsukiyama T (2010) Dynamic changes in histone acetylation regulate origins of DNA replication. Nat Struct Mol Biol 17: 430–437.
44. Butler R, Bates GP (2006) Histone deacetylase inhibitors as therapeutics for polyglutamine disorders. Nat Rev Neurosci 7: 784–796.
45. Kazantsev AG, Thompson LM (2008) Therapeutic application of histone deacetylase inhibitors for central nervous system disorders. Nat Rev Drug Disc 7: 854–868.
46. Yang W-M, Yao Y-L, Sun J-M, Davie JR, Seto E (1997) Isolation and characterization of cDNAs corresponding to an additional member of the human histone deacetylase gene family. J Biol Chem 272: 28001–28007.
47. Suka N, Suka Y, Carmen AA, Wu J, Grunstein M (2001) Highly specific antibodies determine histone acetylation site usage in yeast heterochromatin and euchromatin. Mol Cell 8: 473–479.
48. Hirt B (1967) Selective extraction of polyoma DNA from infected mouse cell cultures. J Mol Biol 26: 365–369.